Physics at the edge

Kruthoff, J.

Jorrit Kruthoff (1991) was born in Oldenzaal (the Netherlands) and graduated from the local high-school in 2010. After high-school he studied experimental physics at the University of Twente and obtained his Bachelor degree in 2013. He then moved to the University of Amsterdam to continue his studies. In 2015 he completed the Master's degree program in theoretical physics and worked as a doctoral candidate at the same university afterwards. In september 2019 he will start a postdoc at Stanford University.

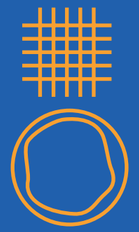

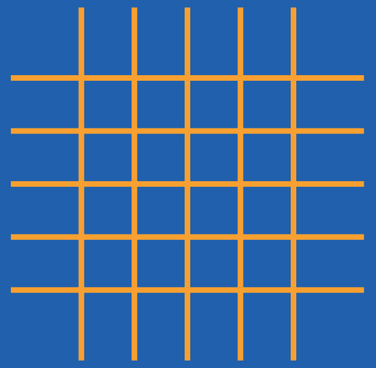

Physics at the Edge

Jorrit Kruthoff

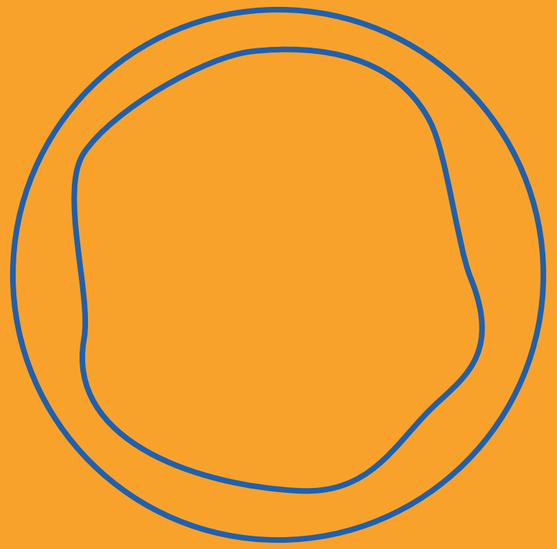

Physics at the Edge

Jorrit Kruthoff

You are cordially invited to attend the public defence of my PhD dissertation, entitled:

Physics at the Edge

From holography to the classification of topological insulators

The defence will take place on Friday 5th of July 2019 at 11:00h in the Oude Lutherse Kerk (Aula der Universiteit), Singel 411 in Amsterdam. After the ceremony there will be a reception.

Paranymphs:
Lars Aalsma
Vincent Min

Invitation

Physics at the Edge

FROM HOLOGRAPHY TO THE CLASSIFICATION OF TOPOLOGICAL INSULATORS

This work has been accomplished at the Institute for Theoretical Physics (ITFA) of the University of Amsterdam (UvA) and is part of the Delta ITP consortium, a program of the Netherlands Organisation for Scientific Research (NWO) that is funded by the Dutch Ministry of Education, Culture and Science (OCW).

UNIVERSITY OF AMSTERDAM

ISBN: 978-94-63236-84-3

Physics at the Edge

FROM HOLOGRAPHY TO THE CLASSIFICATION OF TOPOLOGICAL INSULATORS

Academisch Proefschrift

ter verkrijging van de graad van doctor

aan de Universiteit van Amsterdam

op gezag van de Rector Magnificus

prof. dr. ir. K.I.J. Maex

ten overstaan van een door het College voor Promoties

ingestelde commissie,

in het openbaar te verdedigen in de Aula der Universiteit

op vrijdag 5 juli 2019, te 11:00 uur

door

Jorrit Kruthoff

geboren te Oldenzaal

Promotiecommissie

Promotor

prof. dr. J. de Boer	Universiteit van Amsterdam

Co-Promotor

dr. J. van Wezel	Universiteit van Amsterdam

Overige leden

prof. dr. J. Zaanen	Universiteit Leiden
prof. dr. H.L. Verlinde	Princeton University
prof. dr. E.P. Verlinde	Universiteit van Amsterdam
prof. dr. C.J.M. Schoutens	Universiteit van Amsterdam
dr. D.M. Hofman	Universiteit van Amsterdam
dr. A. Castro Anich	Universiteit van Amsterdam

Faculteit der Natuurwetenschappen, Wiskunde en Informatica

Preface

I never wanted to be a theoretical physicist. In 2010, when I finshed high-school, I always wanted to do something with physics, but no way I wanted to do theoretical physics. I found it interesting, but there should always be a practical side to it in the form of building a machine that could fly off to Mars or help cure diseases, I thought. Now, almost 10 years later, this mindset is completely gone. I did start with experimental physics at the University of Twente, but after two years I realised that I wanted to know how it all really worked. I became more and more theoretically inclined and moved to Amsterdam for a master in theoretical physics and eventually joined the string theory group at the UvA as a PhD student.

The end result of that PhD period now lies before you. It is a composition of the the work I did not only in the string theory group, but also in the group of Jasper van Wezel, where I focussed more on condensed matter theory. This symbiosis is not a complete coincidence, I guess, but rather the result of part of me still wanting to also do theoretical work that is closely related to experiment. After four years, I can also say that it is very illuminating to have been exposed to both high-energy and condensed matter theory as they complement each other beautifully. Nevertheless, I decided to split the dissertation in two parts, one concerning high-energy theory and one on the classification of topological insulators, highlighting the overlap in the summary and outlook section.

The first part is based on work my collaborators and I did on the holographic principle that relates gravitational to non-gravitational physics and could provide a route to understanding the holy grail of high-energy theory: *quantum* gravity. The two chapters 2 and 3 in this part are largely unrelated, but both explore the possibility of extending the usual AdS/CFT logic outside the realm of string theory and spacetimes with infinite spatial volume. In principle they can be read independently.

The second part of the dissertation is a complete and self-contained story on the classification of topological insulators. In chapter 4, we set the stage for chapters 5

and 6 by discussing the quantum Hall effect in detail and will serve as a prototype for all the physics that is to come. We then apply in chapter 5 the symmetry properties of the crystal to discuss a heuristic algorithm to classify topological insulators given a certain crystal symmetry group in the presence or absence of time-reversal symmetry. Chapter 6 is then a rather mathematical chapter that verifies the claims made in the previous chapter for certain simple crystals.

After the bulk of the dissertation, we contemplate in the summary and outlook on what would be next and what we have learned from the studies comprised in this dissertation. We finish with a summary in both English and Dutch and an acknowledgement.

Jorrit Kruthoff
May 20, 2019

Publications

This dissertation is based on the following publications:

[1] A. Belin, J. de Boer, J. Kruthoff, Ben Michel, E. Shaghoulian and M. Shyani, *"Universality of sparse $d > 2$ conformal field theory at large N"*, JHEP **03** (2017), 067, arXiv:1610.06186 [hep-th].

Presented in Chapter **2**.

[2] T. Hartman, J. Kruthoff, E. Shaghoulian and A. Tajdini, *"Holography at finite cutoff with a T^2 deformation"*, JHEP **03** (2019), 004, arXiv:1807.11401 [hep-th].

Presented in Chapter **3**.

[3] J. Kruthoff, J. de Boer, J. van Wezel, C. L. Kane and R-J. Slager, *"Topological Classification of Crystalline Insulators through Band Structure Combinatorics"*, Phys. Rev. X **7** (2017) 4, 041069, arXiv:1612.02007 [cond-mat.mes-hall].

[4] J. Kruthoff, J. de Boer and J. van Wezel, *"Topology in time-reversal symmetric crystals"*, Submitted to Scipost, arXiv:1711.04769 [cond-mat.str-el].

Presented in Chapter **5**.

[5] L. Stehouwer, J. de Boer, J. Kruthoff and H. Posthuma,
"Classification of crystalline topological insulators through K-theory",
Submitted to Advances in Theoretical and Mathematical Physics,
`arXiv:1811.02592 [cond-mat.mes-hall]`.

Presented in Chapter **6**.

Other publications by the author:

[6] A. Belin, J. de Boer and J. Kruthoff
"Comments on a state-operator correspondence for the torus",
SciPost Phys. **5** (2018) 060, `arXiv:1802.00006 [hep-th]`.

Contribution of the author to the publications:

The author contributed to all conceptual discussions in all publications present in this dissertation. In [1], the author did most of the computations in section 2.5 and also considered a special torus to prove sparsness in section 2.4.4. In [2], the author found the deforming operator for curved backgrounds via both the trace relation and the Wheeler-DeWitt method. Moreover, the author suggested studying the correlators in momentum space, which lead to a simplified analysis of the correlators in the deformed theory. In [3, 4], the author was responsible for most of the computations and wrote a first draft of the papers. In [5], the author helped writing many parts of the paper so that they became accessible not only to mathematicians, but also physicists. Furthermore, the author suggested a simplified way of computing the twisted representation rings.

Contents

Preface **v**

I Holography at Infinite and Finite Cutoff **1**

1 Holography **5**
1.1 The AdS/CFT correspondence 7
1.2 Constraints on 2d holographic CFTs 10
1.3 Irrelevant deformations of field theories 15
1.3.1 Irrelevant deformations in quantum mechanics 17

2 Universality of Sparse $d > 2$ Conformal Field Theory at Large N **21**
2.1 Introduction 21
2.2 Generalities of CFT$_d$ 24
2.2.1 Review of higher-dimensional Cardy formulas 25
2.2.2 Review of vacuum energies in CFT 28
2.3 Phase structure of toroidally compactified AdS gravity 29
2.3.1 Thermal phase structure 31
2.3.2 Quantum phase structure 31
2.4 Necessary and sufficient conditions for universality 31
2.4.1 Modular constraints on vacuum energy 32
2.4.2 Necessary and sufficient conditions 34
2.4.3 Sparseness constraints without assuming $\tilde{f}(\psi) = 0$ 35
2.4.4 Sparseness constraints assuming $\tilde{f}(\psi) = 0$ 37
2.5 Symmetric Product Orbifolds in $d > 2$ 39
2.5.1 A review of permutation orbifolds in two dimensions 39
2.5.2 Symmetric product orbifolds in higher dimensions 41
2.5.3 Spectrum of the theory 42
2.5.4 Vacuum energy of the orbifold theory 48
2.5.5 Universality for $\tilde{f}(\psi) = 0$ and free energy at large N 51

2.6 Discussion . . . 55
2.6.1 Modular invariance . . . 55
2.6.2 State-operator correspondence . . . 56
2.6.3 Defining the orbifold theory . . . 57
2.6.4 Orbifold theories on other manifolds . . . 58
2.6.5 Outlook . . . 58

3 Holography at Finite Cutoff with a T^2 Deformation 59
3.1 Introduction . . . 59
3.1.1 The dictionary at finite cutoff . . . 61
3.2 Scalar example . . . 63
3.2.1 Flow equation of the dual EFT . . . 64
3.2.2 Free massive scalar . . . 65
3.2.3 Scalar correlators . . . 66
3.3 Deriving the deformation with gravity . . . 67
3.3.1 Trace equation . . . 67
3.3.2 Wheeler-DeWitt method . . . 71
3.3.3 The final prescription . . . 73
3.3.4 Matter contributions and the $U(1)$ case . . . 73
3.4 Random metrics via Hubbard-Stratonovich . . . 75
3.5 Spectrum . . . 76
3.5.1 Field theory analysis . . . 76
3.5.2 Bulk analysis . . . 79
3.6 Thermodynamics . . . 81
3.6.1 Entropy density . . . 81
3.6.2 Speed of sound . . . 82
3.7 Two-point functions . . . 83
3.7.1 $U(1)$ current correlators . . . 83
3.7.2 Stress-tensor correlators . . . 85
3.8 Discussion . . . 87

II Classification of Topological Insulators 89

4 Topological Insulators 93
4.1 The quantum Hall state . . . 94
4.2 Anybody out there? . . . 101

5 Combinatorial Classification of Crystalline Topological Insulators 105
5.1 Introduction . . . 105
5.2 Some examples . . . 108
5.2.1 $p4mm$ in class A as an example . . . 109

5.2.2 $p4$ with $T^2 = -1$ . . . 116
5.3 Torsion invariants in class AII . . . 117
5.3.1 Line invariants . . . 120
5.3.2 A new invariant . . . 122
5.4 General wallpaper group . . . 125
5.5 Three dimensions . . . 127
5.6 Conclusions . . . 131

6 K-theory Classification of Crystalline Topological Insulators 133
6.1 Introduction . . . 133
6.2 Time-reversal only . . . 135
6.3 The spectral sequence and applications . . . 139
6.3.1 A general method: the Atiyah-Hirzebruch spectral sequence 141
6.3.2 Time-reversal only: revisited . . . 145
6.3.3 Time-reversal and a twofold rotation symmetry . . . 150
6.4 Generalizations . . . 154
6.4.1 Other crystal symmetries . . . 154
6.4.2 Class AI . . . 159
6.4.3 Class A . . . 161
6.5 Discussion . . . 162

A Appendices 167
A.1 Alternate proof without assuming $\tilde{f}(\psi) = 0$ . . . 167
A.2 Conventions . . . 168
A.3 Time-reversal and crystal symmetries . . . 169
A.4 A brief introduction to K-theory . . . 179
A.4.1 Set-up . . . 179
A.4.2 Equivariant K-theory . . . 182
A.5 Freed & Moore K-theory and twists . . . 189
A.5.1 Higher twisted representation rings and the K-theory of a point . . . 193
A.5.2 Construction of the spectral sequence . . . 195

Summary & Outlook 199

Bibliography 207

Samenvatting 229

Acknowledgements 235

Part I:
Holography at Infinite and Finite Cutoff

Ait vedan

1 Holography

In theoretical high-energy physics, there are two very successful theories. On the one hand, we have quantum mechanics accounting for the physics at very small distances, for example within an atom or even within the core of an atom. It can be used to predict the energy levels of an electron orbiting the atom's nucleus or by incorporating the effects of special relativity we can make very precise predictions of the scattering amplitude of two colliding particles. On the other hand, Einstein's theory of general relativity is very successful in explaining physics at very large distances. It super-seeds the laws of Newton and can account not only for various subtle effects, such as the precession of Mercury's orbit, but also very violent objects in our Universe, such as black holes. At the time of Einstein, many of these effects were predictions awaiting experimental verification and it was only recently that some of these, such as the existence of gravitation waves was confirmed [7].

These two pillars of theoretical physics are around for more than 100 years and are still an integral part of current research. One of the biggest questions scientists are interested in right now is whether there exist a merger of the two; a combined theory that can both account for the very small and the very large. Since the time of Einstein, people have been wondering about such a theory of quantum gravity, but as of today, no such theory that makes predictions in our own Universe has been found. There is, however, a very promising candidate theory: string theory.

String theory is an attempt to describe quantum gravitational physics, not by using point particles and their excitations, but by the wiggles of a string. Every wiggle or rather every vibration of the string corresponds not only to a different degree of freedom that we are more familiar with, like the photon or gluon, but also a quantum mechanical excitation responsible for gravity: the graviton! That is great news; we have found our theory of quantum gravity! We should start using

it to reproduce known results and make predictions about quantum gravitational effects. It is precisely here where many challenges lie and one of the prime reasons why physicists are still trying to unravel the mysteries of string theory.

In trying to do such computations, one almost immediately runs in to the well-known fact that string theory is not consistent in four spacetime dimensions, but needs a ten dimensional spacetime or sometimes even eleven dimensional! Accordingly, if we believe that string theory is really a theory of our Universe, there should be a way to get rid of most of these dimensions so that we are left with the four we observe. This process is known as compactification and makes some dimensions very small in much the same way as a thin wire is one-dimensional when viewed from far away but remains three dimensional up close. Nowadays, compactifications in string theory are very common and can give rise to a whole range of different theories (of quantum gravity) in four dimensions. This is known in string theory as the *landscape* and it is believed that one of these theories, or vacua as they are usually called, describes our Universe.

At the time of writing, much research is devoted to studying what type of theories live in the landscape and which ones do not. A little over a decade ago, a set of conjectures, mostly motivated by string theory, was proposed to indicate which theories that appear to be consistent theories of quantum gravity at first sight, are actually inconsistent [8]. This rules out a large portion of possible theories of quantum gravity, possibly also ones that could potentially be used to describe our Universe. It is therefore not entirely clear what the precise status is of these conjectures and whether they should hold or not. Nevertheless, they have triggered a very exciting discussion in the string theory community and has revived a renewed interest in finding string theory vacua that look like our Universe.

In string theory, this is only one of many challenges that we are currently facing. Some of them are more fundamental than others, but every step forward and every resolution that we find, brings us closer to a fuller understanding of quantum gravity, even outside the realm of string theory itself. One particularly interesting idea that was first put forward as a result of studying black holes, but was later found to arise in string theory as well, is the holography principle. Arguably, the holographic principle is one of the most revolutionary ideas ever formulated and completely changed our way of thinking about quantum gravity.

The holographic principle is a concept in theoretical physics, first put forward by Gerard 't Hooft in 1993 [9], which states that quantum gravity theories should somehow be described by a hologram, an object in one lower dimension. This idea was born out of a curious formula, found by Bekenstein in [10], expressing the

entropy S of a black hole in terms of the area A of its event horizon:

$$S = \frac{A}{4G}, \tag{1.1}$$

with G the Newton constant. As was shown by Hawking [11], this entropy can be interpreted as a thermodynamic entropy and as a result, the microscopic degrees of freedom describing black holes appear to live in one dimension less. 't Hooft took this idea a bit further by saying that the degrees of freedom on any surface surrounding the black hole are enough to describe what is going on on the inside.

In ordinary quantum field theories, the entropy is always exponentially growing with volume as its fundamental constituents cover all of spacetime. Quantum gravity theories on the other hand seems to follow a rather different path and have degrees of freedom that behave holographically and repackage themselves on a surface in one lower dimension. In fact, one way to study this idea a bit more is by taking the hologram all the way to spatial infinity and describe the physics inside by an ordinary quantum field theory, i.e. without gravity, at infinity.

At first this might seem like a crazy idea, but in spacetimes where such a limit is well-defined, by which we mean that gravity becomes very weak in that limit, the degrees of freedom of the hologram can indeed be described by a quantum field theory. This is the content of the AdS/CFT correspondence.

1.1 The AdS/CFT correspondence

The AdS/CFT correspondence is an explicit example of holography found in string theory by Juan Maldacena in 1997 [12]. It relates quantum gravitational physics in asymptotically anti-de Sitter (AdS) spacetimes to a conformal field theory (CFT). This conformal field theory is a quantum field theory with an additional symmetry, conformal symmetry that makes it independent of scale and acts in the AdS/CFT correspondence as the hologram. The beauty of this proposal is that on the field theory side, i.e. the hologram, we potentially have a lot of control. It is an ordinary field theory that we know how to deal with in principle and can therefore facilitate the tractability of many computations we would like to do in a quantum gravitational theory. However, the converse is also true, we can learn about questions in conformal field theory by doing computations in the gravity theory. Of course, for that to be useful, there better be no quantumness in the bulk. This will, in fact, be an important point later on.

Since the advent of Maldacena's conjecture, many interesting studies have been conducted to understand it more thoroughly. A huge amount of non-trivial checks

has been made and various interesting results have been established. In particular, other examples of holography have been found, mostly within the context of string theory and in asymptotically anti de-Sitter spacetimes. As a result of all these studies one might start wondering whether there are common features between conformal field theories that can act as a hologram and describe gravitational physics.

One common feature is of course that they are all conformal field theories. This follows from a careful analysis of the symmetries present in the problem. The isometries of AdS, symmetries that leave the anti-de Sitter spacetime unchanged, form a group, $SO(d,2)$, containing not only the Lorentz group in d dimensions, but also a dilatation and an inversion symmetry. To see, this, let us write the metric of Lorentzian AdS in $d+1$ dimensions as

$$ds^2 = \ell_{\text{AdS}}^2 \frac{dz^2 + \eta_{\mu\nu} dx^\mu dx^\nu}{z^2}, \tag{1.2}$$

with $z > 0$ and $\eta_{\mu\nu}$ the Minkowski metric with mostly plus signature and $\mu = 0, \ldots, d-1$. Here, ℓ_{AdS}, is the AdS radius characterising the curvature of the spacetime in the sense that the Ricci curvature is given by $-(d+1)d/\ell_{\text{AdS}}^2$. The metric (1.2) covers a part of the full AdS spacetime, the so-called Poincaré patch of AdS_{d+1}. From this parametrisation it is straightforward to see that the dilatation symmetry sending $z \to \lambda z$ and $x^\mu \to \lambda x^\mu$ leaves the metric in (1.2) invariant. With a bit more work, one can also show that

$$z \to \frac{z}{z^2 + \eta_{\mu\nu} x^\mu x^\nu}, \quad x^\mu \to \frac{x^\mu}{z^2 + \eta_{\mu\nu} x^\mu x^\nu}, \tag{1.3}$$

is an isometry as well. On the field theory side, i.e. the hologram, these isometries become symmetries as the physics in the bulk remains unaltered when acting with these isometries. Of course, this is a slight simplification, since in AdS/CFT it is important that the hologram does not experience any gravitational forces. For AdS or asymptotically AdS spacetimes, it turns out that this is the case at the (conformal) boundary of AdS, which for the metric (1.2) is located at $z = 0$.

Conformal symmetry is only one of the features holographic field theories have in common, at least for quantum gravity in AdS. Below and in chapter 2, we will encounter other features as well. They form a set of necessary and sufficient conditions to describe gravitational physics in the AdS bulk. An important aspect of these conditions is that they do not (necessarily) require string theory and could therefore be a first step towards understanding the AdS/CFT correspondence outside the realm of string theory. This might seem like a rather radical step, since besides string theory, we do not really know any consistent theory of quantum gravity and so knowing these constraints might be hopeless. However, they do

teach us a lot about quantum gravity and holography in a more general settings. In fact, we will indeed see that holographic (conformal) field theories are rather special and not at all weakly coupled such as, for example, QED at low energies. On the contrary, these field theories are strongly interacting and only a limited number of explicit examples are known. With the constraints that we present in chapter 2 and below as well (for AdS_3), we will understand a bit better how we can find more of those examples.

Nevertheless, even with these constraints and even if find an explicit example of a holographic conformal field theory, which is already an extremely difficult endeavour, we are still only going to be able to describe quantum gravity in asymptotically AdS spacetimes and not in more general spacetimes. At first sight, this might not sound like an issue, if it were not for the fact that, ironically, around the same time as AdS/CFT was born, there was an observation claiming that our Universe is more de Sitter-like instead of anti-de Sitter-like [13, 14]. These spacetimes only differ in their sign of the Ricci curvature and so, naively, should not differ too much physically. However, due to the expanding nature of de Sitter (dS) and the cosmological horizon that is not quite true; they differ a lot and in fact, de Sitter is much harder to study. Despite this, many believe that holography should still have its incarnations in dS or cosmological spacetimes in general [15, 16]. Findings such incarnations is challenging, but worthwhile as it can teach us something about holography in our own Universe.

In this dissertation we will make a first step in that direction by considering the question whether we can apply the holographic principle to spacetimes with finite spatial volumes, as is the case for de Sitter spacetime. In a controlled setting, this endeavour was first undertaken by McGough et al in [17] in three bulk dimensions. In this rather violent proposal one starts with AdS/CFT and deforms the CFT in a particular way as to explicitly cutoff the UV. In the bulk this then translates to cutting off the asymptotic region of AdS, making the spatial volume manifestly finite. In chapter 3 we will not only generalise this proposal to $d > 2$, but also give a concise dictionary between the field theory and gravitational theory, generalising the usual AdS/CFT dictionary.

To understand not only the constraints on holographic conformal field theories, but also holography at finite spatial volume, we consider baby versions of them below to illustrate the studies conducted in chapters 2 and 3. We will embark on the constraints on two dimensional conformal field theories coming from $3d$ gravity, which sets the stage for the constraints that we will present in chapter 2. After that, we will consider a simple quantum mechanics problem that allows us to understand already what types of deformations we would need to consider in order to cutoff the UV in field theories in chapter 3.

1.2 Constraints on 2d holographic CFTs

Let us start with gravity or more specifically with Einstein gravity in three bulk dimensions. This theory of gravity is special as it has no propagating degrees of freedom and is therefore simpler to study. On the conformal field theory side, this simplification manifests itself by the large amount of symmetry. Instead of the global conformal transformations, encountered above, the CFT is invariant under local conformal transformations. This results in an infinite amount of symmetry generators that together form the Virasoro algebra. They come from the fact that asymptotically, i.e. at the conformal boundary of AdS at $z = 0$ in (1.2), the metric has an infinite number of symmetries that leave it invariant up to a rescaling. The non-trivial part of this observation is that it is not just the algebra of those symmetries, but a central extension of it. The central extended symmetry algebra is called the Virasoro algebra. In this case, the central extension is a quantum mechanical effect, coming from the fact that classically the field theory is conformal but not once quantum effects are taken into account. In other words, the central extension is related to the conformal anomaly of 2d CFTs. The central extension is characterised by a number c, called the central charge. Roughly speaking, the central charge counts the number of degrees of freedom. For instance, a single free boson in two dimensions has central charge one and N free bosons central charge N. For now, this knowledge of the central charge is enough to proceed. What is important is the following. Henneaux and Brown [18] showed that for an AdS_3 bulk, the central charge of the Virasoro algebra at asymptotic infinity is given in terms of gravitational parameters:

$$c = \frac{3\ell_{\text{AdS}}}{2G}. \tag{1.4}$$

This is a curious formula, since c and G are inversely related. When G is large, the central charge c is small and hence the number of degrees of freedom of the CFT at asymptotic infinity is small, but when G is small, c is big. In fact, it is the latter case that concerns us. The reason is that in the bulk there is also classical gravity, which the CFT should know about. Classical gravity is achieved by taking the coupling constant of gravity small, hence G small and therefore the CFT should have a parameter, in this case c, that we can take large so that quantum gravitational effects are supressed[1]. This means that holographic CFTs have a large number of degrees of freedom. Usually, we will consider the extreme limit $c \to \infty$, which effectively turns off gravity in the bulk. Besides conformal symmetry, this forms another constraint that holographic CFTs need to satisfy in

[1] Strictly speaking, we have a family of CFTs labelled by a parameter c and each such CFT, according to the strong version of AdS/CFT, describes quantum gravity in AdS_3. It is only when c is large that the CFT describes just semi-classical bulk physics

order to describe semi-classical bulk gravitational physics in asymptotically AdS spacetimes.

Let us see what else is going on in the bulk. For example, let us consider the bulk thermal phase structure of Einstein gravity in the presence of a cosmological constant $\Lambda = -1/\ell_{\text{AdS}}^2$. To understand the thermal phase structure, we go, as usual, to Euclidean signature with a compact temporal coordinate τ with period $\beta = 1/T$, with T the temperature. Moreover, we will consider the spatial direction at asymptotic infinity to be a circle with period 2π. In three (Euclidean) bulk dimensions, there are two important solutions of Einstein's equations. First of all we have thermal AdS_3,

$$ds^2 = \left(1 + \frac{r^2}{\ell_{\text{AdS}}^2}\right) d\tau^2 + \frac{dr^2}{1 + \frac{r^2}{\ell_{\text{AdS}}^2}} + r^2 d\phi^2. \tag{1.5}$$

The coordinates in this metric have the following range $r \geq 0$, $0 \leq \tau < \beta$ and $0 \leq \phi < 2\pi$. Notice that this geometry does not have a horizon. The conformal boundary of this metric is now at $r \to \infty$. The other solution is a black hole, called the Bañados-Teitelboim-Zanelli (BTZ) black hole [19,20]. This black hole has a metric that looks like

$$ds^2 = \frac{\left(r^2 - r_+^2\right)}{\ell_{\text{AdS}}^2} d\tau^2 + \frac{\ell_{\text{AdS}}^2 dr^2}{r^2 - r_+^2} + r^2 d\phi^2, \tag{1.6}$$

with r_+ related to the black hole mass M. The coordinates take values in $r \geq r_+$, $0 < \phi \leq 2\pi$ and $0 \leq \tau < \beta$. There is also a rotating version of this black hole that has two horizons, an inner and outer one, but for our discussion we will not need this solution. Regularity of the metric at $r = r_+$ requires the temperature to be related to r_+ as well,

$$\beta = \frac{2\pi \ell_{\text{AdS}}^2}{r_+}. \tag{1.7}$$

With these two solutions at hand, we want to study the phase structure in the canonical ensemble, which means that we fix the temperature and whichever solutions has the lowest free energy will then dominate the canonical ensemble at that temperature. The free energies of the BTZ black hole and thermal AdS_3 are computed by computing the on-shell action of the Einstein-Hilbert action, supplemented by the usual Gibbons-York-Hawking boundary term [21,22] $\sim \int d^2x \sqrt{\gamma} K$, as well as the well-known boundary term [23] $\sim \int d^2x \sqrt{\gamma}$ for AdS_3 gravity. The total action is then

$$I = -\frac{1}{16\pi G} \int d^3x \sqrt{g} \left(R + \frac{2}{\ell_{\text{AdS}}^2}\right) + \frac{1}{8\pi G} \int d^2x \sqrt{\gamma} \left(K - \frac{1}{\ell_{\text{AdS}}}\right). \tag{1.8}$$

Plugging in the solutions (1.5) and (1.6), we find that the on-shell action of these solutions is

$$I_{\text{thermal AdS}} = -\frac{\beta}{8G}, \quad I_{\text{BTZ}} = -\frac{\beta r_+^2}{8G}, \tag{1.9}$$

which results in the free energies,

$$F_{\text{thermal AdS}} = -\frac{1}{8G}, \quad F_{\text{BTZ}} = -\frac{\pi^2}{2G\beta^2}. \tag{1.10}$$

Here we used (1.7) and set ℓ_{AdS} to unity, or equivalently, made a dimensionless temperature by absorbing ℓ_{AdS} into β. In this way, we can talk about dimensionless ratios, which is convenient later on and will also be adapted in later chapters. From these expressions it is also straightforward to get the entropy of the BTZ black hole,

$$S = (1 - \beta\partial_\beta) \log Z_{\text{BTZ}} = \frac{\pi r_+^2}{2G} = \frac{A}{4G}, \tag{1.11}$$

indeed obeying the universal area law for the entropy of black holes, equation (1.1).

We see that for $\beta > 2\pi$: $-F_{\text{thermalAdS}} > -F_{\text{BTZ}}$, hence at small temperatures thermal AdS_3 dominates the canonical ensemble. For $\beta < 2\pi$, the situations is exactly reversed and the black hole dominates [2]. At $\beta = 2\pi$ there is a phase transitions, which is known as the Hawking-Page phase transition [25].

The difference between thermal AdS_3 and the BTZ black hole can be understood as which circle, the thermal or spatial one, becomes contractible in the bulk. For the black hole, the thermal circle is contractible, whereas for thermal AdS_3 the spatial circle is contractible and shrinks to zero size at $r = 0$. Thus on either side of the phase transition, the two cycles of the torus are swapped. On the 2d CFT side, something analogous has to happen if it is supposed to describe gravitational physics. In fact, what has to happen is that the CFT partition function needs to be dominated by the vacuum contribution for $\beta < 2\pi$, but for $\beta > 2\pi$ has to have a free energy that is like that of the black hole. More precisely, converting the expressions for the free energies in (1.10) to CFT variables, we see that need the partition function to roughly behave as

$$Z \approx \begin{cases} \exp\left(\frac{c\beta}{12}\right) & \text{if } \beta > 2\pi \\ \exp\left(\frac{\pi^2 c}{3\beta}\right) & \text{if } \beta < 2\pi \end{cases} \tag{1.12}$$

Surprisingly, to get this type of behaviour, the 2d CFT need not to be that special. This particular behaviour of the partition function, namely follows already from

[2] There could also be other saddles point of the partition functions at imaginary angular potential, but for real angular potentials (which we have set to zero here) the two dominant saddles are thermal AdS_3 or the BTZ black hole [24].

a very rather standard symmetry of conformal field theories in two dimensions: modular invariance. Modular invariance is the statement that the partition function is invariant under $\beta \to 4\pi^2/\beta$ and stems from the fact that it does not (in Euclidean signature) matter what we call Euclidean time [3]. Since we also compactified the spatial circle, the 2d CFT lives on a torus and we can understand modular invariance straightforwardly as swapping of the two cycles of the torus, resulting precisely in $\beta \to 4\pi^2/\beta$. Consequently, a modular invariant partition function satisfies

$$Z(\beta) = Z\left(\frac{4\pi^2}{\beta}\right). \tag{1.13}$$

Notice that this is already good news, since again at $\beta = 2\pi$ the partition function is self-dual, similar to the equality of the free energies in the bulk at that temperature. Form this point of view, it is not difficult to get something that looks like (1.12). At very low temperatures or more precisely at asymptotically low temperaturs, so $\beta \to \infty$, the thermal partition function is dominated by the vacuum contribution,

$$Z(\beta) \approx \exp\left(-\beta E_{\text{vac}}\right) + \dots, \tag{1.14}$$

where the dots indicate contributions from excited states. In $2d$ CFTs, the vacuum energy is fixed by the conformal anomaly c that we saw earlier as well. In fact, it is $E_{\text{vac}} = -\frac{c}{12}$. At asymptotically low temperatures, the partition function is thus given by (1.12). With the use of modular invariance we then also find that at asymptotically large temperatures, the partition function is approximately

$$Z(\beta) \approx \exp\left(\frac{\pi^2 c}{3\beta}\right), \tag{1.15}$$

again in agreement with (1.12). This expression for the asymptotic formula of the partition function was first found by Cardy in [26] and is commonly referred to as the Cardy formula. Thus, by using modular invariance, we see that we almost get something that looks like gravity, i.e. is almost the same as (1.12). The problem is that from the CFT point of view, they are only asymptotic formulas and to match with gravity we would like them to be valid in an extended regime. Moreover, for holographic theories with a semi-classical bulk, we also need a large number of degrees of freedom, hence we want to take c to infinity as well and not finite as we have done here.

To see how we can get such an extended regime, it is easier to work in terms of density of states as it will allow us to study corrections a bit more systematically [4]. To go from the thermal partition function to the density of states, one performs

[3] For 2d CFTs that do not admit a Lagrangian description, the statement is still true, but more non-trivial as canonical quantisation is usually unavailable then.

[4] This analysis was is also present in the appendix of [1] and will be presented here for the case with no angular momentum.

a (inverse) Laplace transform:

$$\rho(E) = \frac{1}{2\pi i}\int_{\alpha-i\infty}^{\alpha+i\infty} d\beta\, e^{\beta E} Z(\beta) \tag{1.16}$$

where $\rho(E)$ is the density of states at energy E and $\alpha > 0$. The density of states is a microcanonical density of states and since, a priori, the canonical and microcanonical ensemble are different, trying to derive anything meaningful in this way is rather suspect. However, as discussed carefully for two dimensions in [24], the limit $c \to \infty$ in which we are ultimately interested, is a good thermodynamic limit which allows us to conclude $\rho(\langle E\rangle) \approx e^{S(\langle E\rangle)}$ for $\langle E\rangle = -\partial_\beta \log Z(\beta)$. Large c suppresses the fluctuations in $\langle E\rangle$ and unambiguously defines an energy $E \equiv \langle E\rangle$. Said differently, the existence of a stable saddle point in (1.16) due to large c is the statement that the microcanonical and canonical ensembles are equivalent.

To get an approximate expression for the density of states, we need a stable saddle point, which means that the integral is dominated by a large value of β where the integrand is highly peaked. For the case at hand, this is easily found by modular transforming $Z(\beta)$ and using the fact that it behaves as (1.15) at large energies. The saddle point value of the integral is then located at

$$\beta_\star = \sqrt{\frac{\pi^2 c}{3E}} \tag{1.17}$$

and the density of states behaves as

$$\log \rho(E) = 2\pi\sqrt{\frac{c}{3}E}. \tag{1.18}$$

To ensure a good saddle point approximation, the corrections need to be small. At asymptotically large energies, the excited states contributions in $Z(\beta)$ are indeed supressed exponentially and our approximation is justified. Equation (1.18) is the usual Cardy formula and is valid for $E \to \infty$, but c fixed. For gravity we need (1.18) to hold for $c \to \infty$ and $E \sim c$. To get this, there has to be some constraint on the spectrum.

Let us consider the limit $c \to \infty$ with $E = mc$. We will have the same saddle as before, but we need to check again that the excited states contributions are suppressed. In particular, we need

$$\widetilde{Z}(\beta) = \exp\left(\beta E_{\text{vac}}\right) Z(\beta) \tag{1.19}$$

to not give a big contribution on the saddle. If we take $m \to \infty$, then again all terms except the vacuum contribution are infinitely exponentially suppressed and our saddle is justified. But now we want to see how small we can make m. We

will use the fact that $Z(\beta)$ is dominated by the light states ($E < \epsilon$ with $\epsilon > 0$) as long as $\beta > 2\pi$. This means that $\tilde{Z}(\beta)$ is also dominated by the light states. We can therefore write

$$\widetilde{Z}(4\pi^2/\beta_\star) \approx \sum_{\tilde{E}\leq\epsilon} \rho(\tilde{E}) \exp\left(-\frac{2\pi(\tilde{E}+c/12)}{\sqrt{\frac{c}{12E}}}\right). \tag{1.20}$$

We need all terms on the right-hand-side to contribute exponential suppressions, except for the vacuum, which will contribute $+1$. From gravity, we see that black holes start dominating when [5]

$$E = \frac{c}{12} \tag{1.21}$$

and so we need to push the validity of the saddle down to there. To achieve this, we need to bound the degeneracy as

$$\rho(E \leq \epsilon) \lesssim \exp\left(2\pi(E + c/12)\right). \tag{1.22}$$

This is the same bound on the light states as in [24]. Thus in order to have a holographic CFT in two dimensions, the spectrum should obey (1.22).

Let us summarise what we have seen so far. We have studied three dimensional gravity in AdS_3 and argued that for the CFT to be holographic and describe semi-classical bulk physics, there are two constraints. First of all, it should have a parameter, in this case c, that we can take large so that in the bulk quantum gravity effects are suppressed. Second, the density of states of low-lying states, i.e. states for which the energy satisfies $E < \epsilon$ with $\epsilon > 0$, is bounded from above as in (1.22).

In chapter 2 we will repeat the analysis done here for AdS_{d+1} for $d > 2$ and with a particular (conformal) boundary where all spatial directions are compactified. The analysis is slightly more involved since the vacuum energy is then not fully fixed by conformal symmetry, but contains a rather high degree of arbitrariness. Besides that, the derivation of the constraints for $d > 2$ is similar to the one presented in this section. For this reason, we will not present more introductory material for chapter 2, but rather go on to put chapter 3 into a broader context and explain why it can help understand holography for finite volumes.

1.3 Irrelevant deformations of field theories

In order to do holography at finite volume, we need to do something to the CFT so that it only describes part of the full spacetime. For example one can image

[5] It is true that there are black holes with $E \geq 0$ as well, but those are unstable and hence will never dominate the canonical ensemble [24]

trying to cutoff the spacetime in the radial direction parametrised by r, in for instance the metrics written in (1.5) and (1.6). In AdS/CFT, the radial direction signifies the energy scale in the field theory. In particular, cutting off spacetime in the radial direction is the same as putting a UV cutoff on the energies in the CFT. This is a non-trivial statement that will not be explained here. For details see [27]. Introducing a UV cutoff breaks conformal invariance, so the CFT turns into an effective field theory only valid for energies below the cutoff.

How can we implement such a cutoff in a controllable way starting from a CFT? One way to do that is by deforming the CFT with an irrelevant operator, which leaves the IR unchanged but has a dramatic effect on the UV. Thus to understand holography at finite volume we are prompted to study irrelevant deformations of CFTs.

Deformations of field theories in general are usually studied in the sense of an RG flow. One starts with some initial conformal field theory and studies what happens when relevant or marginal operators are added. This will trigger an RG flow and may result in an interesting, i.e. strongly coupled theory in the IR. For example, the marginal interactions in QCD or close to a Fermi surface cause the formation of bound states in the IR resulting in confinement or superconductivity, respectively. However, the theory could also be gapped in the IR and become topological. This can, for example happen if we start with an action,

$$S = \int d^3x \bar{\Psi}(\gamma^\mu \partial_\mu + iA_\mu)\Psi, \tag{1.23}$$

of free fermions coupled to a background gauge field A_μ and add a mass term,

$$S_{int} = \int d^3x \, m\bar{\Psi}\Psi. \tag{1.24}$$

We can now integrate out the fermion Ψ and look at the field theory at energies below the mass m. This theory is topological and has no propagating degrees of freedom and forms the basis for an effective field theory description of the integer quantum Hall effect. We will come back to this particular system in chapter 4.

However, we do not want to deform by relevant or marginal operators , but by irrelevant operators. In the old days of quantum field theory, these operators were considered very dangerous as they would render the theory non-renormalisable. Nowadays, such theories with irrelevant couplings are considered as effective field theories, valid only up to a certain energy scale. In the RG flow sense adding irrelevant operators can be thought of as flowing upwards, from the IR to the UV, instead of the other way around. A priori, this seems like an odd thing to do, since it is unclear what irrelevant operators need to be added in order to flow to the UV. Or in other words, it is extremely hard to know the UV completion of

some effective field theory if it exists at all. It is like sailing against the wind, one wrong move and you end up somewhere completely different.

The purpose of this section is to study flows of QFTs by deforming with irrelevant operators. Instead of the reversed-RG flow perspective, we will take the perspective of these flows as flows in the space of QFTs and so different points along the flow correspond to different theories. One of the simplest ways to study such irrelevant flows is by going back to plain vanilla quantum mechanics.

1.3.1 Irrelevant deformations in quantum mechanics

Following the Wilsonian logic down to a quantum mechanics theory in zero spatial dimensions, we are confronted with a curious situation. Normally, in higher-dimensions, most interactions that we can write down are irrelevant not only because scalar and spinor fields have high enough mass dimension, but in particular due to the existence of derivatives. Of course, not everything can be added, because there are also constraints coming from causality and unitarity, see for example [28] in the context of Einstein gravity. As a result, the IR of quantum *field* theories is rather robust, i.e it is generically gapped. The UV on the other hand is not universal at all. In zero spatial dimensions this is completely reversed. There, the scalar and spinor fields have mass dimension $-1/2$ and 0, respectively. Thus anything you build with these fields alone is going to be marginal or relevant. The UV instead of the IR is universal, giving rise to a spectacular wealth of interesting physics at low energies.

However, there are still temporal derivatives to make irrelevant operators with. As we mentioned, in higher-dimensions such higher-derivative interactions have the potential to destroy causality and locality, but in quantum mechanics such interactions are less problematic, since there is no space. In quantum mechanics, they have in fact been been considered before, for example, as the relativistic corrections to Schrödinger's equation. To first order in v^2/c^2, such corrections take the form

$$H^{(1)} = -\frac{p^4}{8m^3c^2} = -\frac{1}{2mc^2}\left(\frac{p^2}{2m}\right)^2 , \tag{1.25}$$

which is a deformation of the original Hamiltonian $p^2/(2m)$ by its square. These types of deformations are prototypical for what will be discussed in chapter 3 and in the remainder of this subsection we would like to highlight some of its properties to gain some intuition. Specifically, we want to consider deformations as flow equations, for example:

$$\frac{\partial S}{\partial \lambda} = \int d\tau \; H^2(\lambda) \tag{1.26}$$

or any other power of $H(\lambda)$. Here S the Euclidean action of the deformed theory and $\lambda > 0$. This flow equation should be understood as a flow equation in the space of theories, labelled by λ. From this flow equation of the Euclidean action, it is trivial to get the flow of the deformed spectrum, since $S = \int d\tau H$. The spectrum then flows in the same way and the deformed Hamiltonian takes the form:

$$H(\lambda) = \frac{H}{1 - \lambda H}, \tag{1.27}$$

where we have taken the initial condition $H(\lambda = 0) = H$. This Hamiltonian is a bit strange. Since λ is a continuous parameter, there are points along the flow for which $H(\lambda)$ blows up. This means that we cannot flow past these points. In particular, when $\lambda = 1/E_{\text{max}}$ with E_{max} the maximum eigenvalue of the original Hamiltonian, the flow stops. In most cases E_{max} is infinite and so there won't be any flow at all. There are three ways to deal with this. The first is to truncate the spectrum of H, so that $E_{\text{max}} < \infty$ and there is a non-trivial flow. In quantum mechanics, truncating the spectrum is not as violent as in higher-dimensions, because of the lack of locality and can therefore be implemented straightforwardly. Second, one can complexify λ and excise the region of the poles of $H(\lambda)$. In this way of defining the deformation, one might be forced to allow for a slight breaking of hermiticity. Third, the theory with $\lambda > 0$ does not make sense and one can only consider this deformation for $\lambda < 0$. In that case, there could still be negative energies that are problematic, but since H is bounded from below, the flow will be non-trivial.

Out of these three options, the first one is the most reasonable and most controllable. However, this immediately brings about interesting questions such as: what happens to the high energy states? or is there a way to UV complete the theory? The answers to these questions is not straightforward as there may be many UV completions if they exist at all. In fact, the second proposal, making λ complex, also touches on those same issues. In that case, the slight breaking of hermiticity can be though of as coupling to a bath in some way, which again provides a particular UV completion.

Using the quantum mechanics problems as a warm-up, we see that the irrelevant deformations are not without problems. In fact, these problems are prototypical for what happens in field theories. In particular, in chapter 3, where we deform holographic conformal field theories, we see that the deformed spectrum indeed experiences the same problems as the H^2 deformation in quantum mechanics, but again only for certain signs of the coupling. The precise form of the deformation is discussed at length in chapter 3, but follows rather straightforwardly from demanding finite volume in the bulk. Using this deformation, we match various quantities between the bulk and the field theory, but also find some intriguing

consequences that touch upon the very roots of the AdS/CFT correspondence.

2 Universality of Sparse $d > 2$ Conformal Field Theory at Large N

This chapter is based on the following publication:

A. Belin, J. de Boer, J. Kruthoff, Ben Michel, E. Shaghoulian and M. Shyani, *"Universality of sparse $d > 2$ conformal field theory at large N"*, JHEP **03** (2017), 067, `arXiv:1610.06186 [hep-th]`.

2.1 Introduction

The strongest form of the AdS/CFT correspondence states that every conformal field theory (CFT_d) is dual to a theory of quantum gravity living in a higher-dimensional anti-de Sitter space (AdS_{d+1}). For a generic CFT, the dual theory of quantum gravity at low energies will look nothing like semi-classical Einstein gravity. One of the most interesting questions in the context of holography is then to understand which CFTs – when interpreted as theories of quantum gravity in AdS – have a semi-classical Einstein gravity limit.

The most straightforward constraint emerging from the AdS/CFT dictionary for a semi-classical bulk is that the CFT should have a large number of degrees of freedom, usually parameterized by N. Large N in the field theory implies a semi-classical bulk since its inverse scales as a positive power of the Planck length in AdS units: $N^{-1} \sim (\ell_P/\ell_{\text{AdS}})^{\#}$ for $\# > 0$. This is the bulk expansion parameter controlling AdS-scale quantum gravitational effects.[1]

[1] To have a theory that looks like Einstein gravity at low energies, we also need an expansion parameter that can suppress higher-spin fields. The 't Hooft coupling in gauge theory usually plays the role of this expansion parameter. Interestingly, like in the D1-D5 duality, certain features of Einstein gravity can be reproduced without explicitly invoking this assumption. We

Besides large N, a semi-classical theory of gravity in anti-de Sitter space has many universal features that must be encoded in any putative dual CFT. To explore the emergence of gravity from field-theoretic degrees of freedom, it is natural to try to reproduce these universal features by implementing some additional assumptions on a generic large-N CFT. There has been tremendous progress in this direction for the case of three-dimensional gravity [24,29–41], throughout which large central charge and a sparse low-energy spectrum play a prominent role. These powerful methods for the most part rely on the fact that all stress tensor interactions in the CFT are captured by the Virasoro block of the identity, which is assumed to dominate. The success of this particular approach is related to the topological nature of gravity in three dimensions, which precludes obvious generalizations to higher dimensions. Nevertheless, it is a compelling problem to reproduce features of higher-dimensional AdS gravity purely from the CFT. A small sample of work in this direction includes [28,42–52].

In this chapter, we will focus on a technical tool that has received little exposure in higher dimensions: modular invariance. For 2d CFTs, modular invariance can be used to precisely determine how sparse the spectrum should be to reproduce the thermal phase structure of 3d gravity [24] (see [53] for a similar consideration in supersymmetric theories). For theories obeying this sparseness constraint, the Cardy formula [26] – which is usually only valid asymptotically as $\Delta/c \to \infty$ – has an extended regime of validity down to energies $\Delta \sim c$. This precisely matches the bulk phase structure since the black holes begin dominating the ensemble at $\Delta \sim c$.

The relevance of modular invariance in higher-dimensional holographic CFTs has been much less explored. In [54,55], it was shown that modular invariance of the torus partition function implies the existence of an asymptotic formula that correctly reproduces the Bekenstein-Hawking entropy of the dual black brane. This formula is the higher-dimensional generalization of the Cardy formula and only holds in the limit of large energy for generic CFTs. Holographic CFTs, on the other hand, must have an extended range of validity of this formula as implied by the bulk phase structure. The goal of this chapter is to further exploit modular invariance and place constraints on CFTs such that they have this extended range of validity. We also want to match the precise phase structure of gravity, which is much richer than in two dimensions and exhibits both quantum and thermal phase transitions. One of the key challenges that we will face is that the functional form of the vacuum energy in higher dimensions is not uniquely fixed by conformal invariance, although we will discover several nontrivial constraints due to modular

will not explicitly implement any constraints on our field theories with the purpose of decoupling higher-spin fields.

invariance.

We can summarize our results as follows. A general CFT on $\mathbf{T}^d$ will have an extended Cardy formula and a universal phase structure if and only if the partition function is dominated by the vacuum contribution when quantizing along any cycle but the shortest one. Proving this will require using the modular constraints on the vacuum energy alluded to above. From here, we will consider large-N theories and exhibit distinct sets of necessary and sufficient sparseness conditions on the spectrum to achieve this vacuum domination.

In analyzing calculable theories that satisfy these necessary and sufficient conditions, and which therefore have a universal free energy, we are led to the construction of symmetric orbifold theories in higher dimensions. Symmetric orbifolds have been analyzed in great depth in two dimensions [56–62], and play an explicit role in the D1-D5 duality [63–65]. Still, they have not explicitly appeared in holographic dualities in higher dimensions nor, to the best of our knowledge, have they been constructed. For their construction, we use a similar procedure as in two dimensions to build a modular invariant partition function. This includes both untwisted and twisted sectors. For large-N symmetric product orbifolds, the density of states of the untwisted sector is shown to be slightly sub-Hagedorn, whereas for the twisted sector it is precisely Hagedorn. Saturation of the necessary and sufficient conditions for universality is then guaranteed by assuming that the subextensive parts of the vacuum energy vanish. This assumption constrains the choice of seed theory we can pick. This is somewhat of a loss of generality compared to two dimensions but can be expected by the increasing richness of CFTs in higher dimensions. Provided we pick the seed accordingly, the symmetric orbifolds reproduce the phase structure of higher-dimensional AdS gravity: they have an extended regime of validity of the Cardy formula and a Hagedorn transition at precisely the same temperature as the Hawking-Page transition in the bulk.

The chapter is organized as follows. We start in section 2.2 with a general discussion of CFTs on d-dimensional tori and modular invariance. In section 2.3 we summarize the phase structure of toroidally compactified gravity in anti-de Sitter spacetime. These two sections set the stage for the meat of the chapter. Section 2.4 is dedicated to a detailed discussion of the necessary and sufficient conditions that are required to have a universal free energy. The implementation of these conditions is then explored in section 2.5. We discuss the construction of orbifold theories on d-dimensional tori and show that symmetric product orbifolds have a universal free energy. We conclude with a discussion and outlook in section 2.6.

2.2 Generalities of CFT$_d$

We now introduce some of the basic technology of modular invariance that we will use to derive our general CFT results. For more details see [54,55]. In this chapter we will study conformal field theories defined on a Euclidean d-torus $\mathbf{T}^d$. We fix the metric on this torus to be

$$ds^2 = dx_0^2 + dx_1^2 + \cdots + dx_{d-1}^2 \tag{2.1}$$

with identifications

$$(x_0, x_1, .., x_{d-1}) \sim (x_0, x_1, .., x_{d-1}) + \sum_{i=0}^{d-1} n_i U_i \,. \tag{2.2}$$

where U_i are vectors defining the torus $\mathbf{T}^d$ and the n_i are integers. These vectors can be conveniently organized in a matrix as

$$U = (U_0 \quad \cdots \quad U_{d-1})^T = \begin{pmatrix} L_0 & \theta_{01} & \cdots & \theta_{0,(d-2)} & \theta_{0,(d-1)} \\ 0 & L_1 & \cdots & \theta_{1,(d-2)} & \theta_{1,(d-1)} \\ \vdots & \vdots & \ddots & \vdots & \vdots \\ 0 & 0 & \cdots & L_{d-2} & \theta_{(d-2),(d-1)} \\ 0 & 0 & \cdots & 0 & L_{d-1} \end{pmatrix} \tag{2.3}$$

and define a d-dimensional lattice of identifications. This matrix contains the lengths of the cycles along its diagonal and the θ_{ij} capture all possible twists of the torus $\mathbf{T}^d$. Modular invariance of the torus partition function for conformal field theories is a powerful constraint on the theory. The invariance can be stated as the action of large conformal transformations on the lattice spanned by the set $\{U_i\}$. These large conformal transformations form the group $SL(d, \mathbf{Z})$ and act on the matrix U in (2.3) by left multiplication. $SL(d, \mathbf{Z})$ is generated by two elements [66]

$$S = \begin{pmatrix} 0 & 1 & 0 & \dots & 0 & 0 \\ 0 & 0 & 1 & \dots & 0 & 0 \\ \vdots & \vdots & \vdots & \ddots & \vdots & \vdots \\ 0 & 0 & 0 & \dots & 0 & 1 \\ (-1)^{d+1} & 0 & 0 & \dots & 0 & 0 \end{pmatrix}, \quad T = \begin{pmatrix} 1 & 1 & 0 & \dots & 0 & 0 \\ 0 & 1 & 0 & \dots & 0 & 0 \\ \vdots & \vdots & \vdots & \ddots & \vdots & \vdots \\ 0 & 0 & 0 & \dots & 1 & 0 \\ 0 & 0 & 0 & \dots & 0 & 1 \end{pmatrix}. \tag{2.4}$$

They can be shown to generate any pairwise swap and a twist along any direction. For even d, we quotient by the center of the group $\{-1, 1\}$ to obtain $PSL(d, \mathbf{Z})$, but for simplicity we will universally refer to the group as $SL(d, \mathbf{Z})$. Using scale invariance to unit-normalize one of the cycle lengths shows that we have $(d-1)(d+2)/2$ real moduli captured by the matrix U.

In spacetime dimension greater than two, modular transformations generically change the spatial background of the theory (i.e. change the Hilbert space), making it difficult to relate the low-lying states to the high-lying states on a fixed background. However, as discussed in [54] there exist two choices of torus which allow for a high-temperature/low-temperature duality to be considered. The first is the background $S^1_\beta \times S^1_L \times \mathbf{T}^{d-2}_{L_\infty}$, where $L_\infty \gg \beta, L, \beta^2/L$. In this case by appealing to extensivity in the large directions we have the approximate invariance

$$\log Z(\beta) \approx (L/\beta)^{d-2} \log Z(L^2/\beta)\,. \tag{2.5}$$

This can be transformed into an exact high-temperature/low-temperature duality by passing to a density defined by dividing $\log Z(\beta)$ by the volume of the large torus as it decompactifies, but we will not pursue that here.

To produce an exact invariance on a compact manifold, we can also consider a special torus given by $S^1_\beta \times S^1_L \times S^1_{L^2/\beta} \times \cdots \times S^1_{L^{d-1}/\beta^{d-2}}$, for which

$$Z(\beta) = Z(L^d/\beta^{d-1})\,. \tag{2.6}$$

This invariance is obtained by an $SL(d, \mathbf{Z})$ transformation and a scale transformation. It will play an important role in our CFT analysis.

To deal with the case of a general torus where there is no high-temperature/low-temperature duality, we will find it useful to define some notation. For a d-dimensional torus of side lengths $L_0, L_1, \ldots, L_{d-1}$, where $\beta = L_0$, we will denote the partition function quantized in an arbitrary channel as:

$$Z[\mathcal{M}^d] = Z(L_i)_{\mathcal{M}_i} = \sum e^{-L_i E_{\mathcal{M}_i}}\,. \tag{2.7}$$

$Z[\mathcal{M}^d]$ denotes the Euclidean path-integral representation of our partition function, which treats space and time democratically. The next form of the partition function picks direction i as time and gives a Hilbert space interpretation of the path integral. Since the spatial manifold will change depending on which direction is chosen as time, we use the notation $\mathcal{M}_i$ to explicitly denote the spatial manifold. It is defined as $\mathcal{M}^d = \mathcal{M}_i \times S^1_{L_i}$. Brackets will always imply a Euclidean path-integral representation while parentheses will imply a Hilbert-space representation.

2.2.1 Review of higher-dimensional Cardy formulas

Now we will provide a derivation of the higher-dimensional Cardy formula on an arbitrary spatial manifold $S^1_\beta \times X$. We will only need the result for a spatial

torus, but we will keep the discussion general. The fact that modular transformations generically change the Hilbert space of the torus partition function will not provide an obstruction, although we will see in the resulting formulas that our high-temperature partition function and asymptotic density of states refer to the vacuum energy on a *different* spatial background in general.

We assume our theory to be local, modular invariant, and to have a spectrum of real energies on the torus that is bounded below by an energy that is discretely gapped from the rest of the spectrum. At asymptotically high temperature $\beta/V_X^{1/(d-1)} \to 0$, we can use extensivity of the free energy to replace our spatial manifold X with a torus $\mathbf{T}^{d-1}$ of cycle lengths $L_1 \leq L_2 \leq \cdots \leq L_{d-1}$ and no twists, with $V_X = L_1 \cdots L_{d-1} \equiv V_{\mathcal{M}_0}$. We therefore have

$$Z[S^1_\beta \times X] = Z(\beta)_X \approx Z(\beta)_{\mathcal{M}_0} = \sum e^{-\beta E_{\mathcal{M}_0}} \approx e^{\tilde{c} V_{\mathcal{M}_0}/\beta^{d-1}} \tag{2.8}$$

at asymptotically small β for some thermal coefficient $\tilde{c} > 0$. This thermal coefficient is not a priori related to any anomalies except in two dimensions. Considering a quantization along L_{d-1} gives us

$$Z(L_{d-1})_{\mathcal{M}_{d-1}} = \sum e^{-L_{d-1} E_{\mathcal{M}_{d-1}}} = e^{-L_{d-1} E_{\text{vac},\mathcal{M}_{d-1}}} \sum e^{-L_{d-1}(E - E_{\text{vac}})_{\mathcal{M}_{d-1}}} . \tag{2.9}$$

For $d = 2$ in a scale-invariant theory, β becoming asymptotically small is equivalent to L_{d-1} becoming asymptotically large, since only the ratio L_{d-1}/β is meaningful. However, for $d > 2$ we have the additional directions L_i which may prevent us from interpreting the quantization in the L_{d-1} channel as a low-temperature partition function which projects to the vacuum. To deal with this, consider the limit $L_{d-1} \to \infty$ where we indeed project efficiently to the vacuum:

$$\lim_{L_{d-1} \to \infty} \frac{\log Z(L_{d-1})_{\mathcal{M}_{d-1}}}{L_{d-1}} = -E_{\text{vac},\mathcal{M}_{d-1}} . \tag{2.10}$$

Using $Z(\beta)_{\mathcal{M}_0} = Z(L_{d-1})_{\mathcal{M}_{d-1}}$ gives us $E_{\text{vac},\mathcal{M}_{d-1}} = -\tilde{c} V_{\mathcal{M}_{d-1}}/\beta^d$. We are therefore able to extract the scaling of the vacuum energy as $E_{\text{vac},\mathcal{M}_{d-1}} \propto -V_{\mathcal{M}_{d-1}}/\beta^d$ as $\beta \to 0$. The proportionality coefficient, which we define as ε_{vac}, is $\varepsilon_{\text{vac}} = \tilde{c}$. Furthermore, notice that $E_{\text{vac},\mathcal{M}_{d-1}}$ is clearly independent of L_{d-1}, so this result is general even though we took the limit $L_{d-1} \to \infty$ to obtain it. In the general case of arbitrary L_{d-1} we can therefore write for $\beta \to 0$

$$Z(L_{d-1})_{\mathcal{M}_{d-1}} = e^{\tilde{c} V_{\mathcal{M}_0}/\beta^{d-1}} \sum e^{-L_{d-1}(E - E_{\text{vac}})_{\mathcal{M}_{d-1}}} . \tag{2.11}$$

Again equating with $Z(\beta)_{\mathcal{M}_0}$, we see that the excited states must contribute at subleading order, since the vacuum contribution is sufficient to obtain $Z(L_{d-1})_{\mathcal{M}_{d-1}} = Z(\beta)_{\mathcal{M}_0}$ at leading order in small β. The concern over the directions L_i and poor

projection to the vacuum alluded to earlier is therefore not a problem at leading order. We are finally left with

$$S(\beta) = (1 - \beta\partial_\beta) \log Z(\beta)_X \approx dV_X \varepsilon_{\text{vac}}/\beta^{d-1} \tag{2.12}$$

for the high-temperature entropy of a modular-invariant CFT on an arbitrary spatial background X.

Now we consider the implications for the density of states:

$$\rho(E_s) = \frac{1}{2\pi i}\int_{\alpha-i\infty}^{\alpha+i\infty} d\beta\, Z(\beta)_X e^{\beta E_s} \tag{2.13}$$

$$= \frac{1}{2\pi i}\int_{\alpha-i\infty}^{\alpha+i\infty} d\beta \left(e^{-\varepsilon_{\text{vac}} V_X/\beta^{d-1}} \sum e^{-\beta E}\right) e^{\varepsilon_{\text{vac}} V_X/\beta^{d-1} + \beta E_s}\,, \tag{2.14}$$

for some $\alpha > 0$. Performing a saddle-point on the part of the integrand outside of the parentheses and evaluating the integrand on this saddle $\beta_s \propto E_s^{-1/d}$ gives us the higher-dimensional Cardy formula:

$$\log \rho(E_s) = \frac{d}{(d-1)^{\frac{d-1}{d}}} (\varepsilon_{\text{vac}} V_X)^{\frac{1}{d}} E_s^{\frac{d-1}{d}}\,. \tag{2.15}$$

The saddle point implies $\beta_s \to 0$ as $E_s \to \infty$. To ensure that this saddle point is valid, we need to check that the part of the integrand in the parentheses, which we call $\tilde{Z}_X(\beta)$, does not give a big contribution on the saddle:

$$\tilde{Z}_X(\beta_s) = e^{-\varepsilon_{\text{vac}} V_X/\beta_s^{d-1}} \sum e^{-\beta_s E}\,. \tag{2.16}$$

From high-temperature ($\beta_s \to 0$) extensivity (2.8), we know that we can write this as

$$\tilde{Z}_X(\beta_s) \approx e^{-\varepsilon_{\text{vac}} V_X/\beta_s^{d-1}} e^{\tilde{c} V_X/\beta_s^{d-1}} = 1\,, \tag{2.17}$$

where we used $\tilde{c} = \varepsilon_{\text{vac}}$ (and one notices $\tilde{c}$ is independent of spatial background by replacing the high-temperature partition function on the given manifold with the high-temperature partition function on a torus of spatial lengths $L_1, \ldots L_{d-1}$ with $V_{\mathcal{M}_0} = V_X$). Our saddle-point approximation is therefore justified, and we have the higher-dimensional Cardy formula as advertised.

In particular, considering the spatial background to be $X = S^{d-1}$ gives the asymptotic density of local operators by the state-operator correspondence. In the rest of this chapter we will only be interested in the CFT on $\mathbf{T}^d$.

2.2.2 Review of vacuum energies in CFT

Normalization of vacuum energy

In a generic field theory, one is always free to shift the Hamiltonian by an arbitrary constant. This therefore shifts what we call the vacuum energy. Indeed, the well-known Casimir effect demonstrates that derivatives with respect to spatial directions dE_{vac}/dL_i are the physical observables, leaving an ambiguity in the normalization of E_{vac}. Additional structure, such as supersymmetry or modular invariance, disallows such an ambiguity. Even in a purely scale-invariant theory one can fix the normalization of the vacuum energy. Scale invariance requires that energies, and in particular the ground state energy, scale as inverse lengths under a rescaling of the spatial manifold: $E_{\text{vac}}(\lambda L_1, \lambda L_2, \ldots) = \lambda^{-1} E_{\text{vac}}(L_1, L_2, \ldots)$. This fixes the shift ambiguity in E_{vac}.

Subextensive corrections to the vacuum energy

The higher-dimensional Cardy formulas involves the vacuum energy density on $S^1 \times \mathbf{R}^{d-2}$, which by its relation to the extensive free energy density in a different channel is negative and has a fixed functional form. If we compactify more directions and make them comparable to the size of the original S^1, then we will in general get corrections to the asymptotic formula. For two-dimensional CFT there is only one spatial cycle so no such corrections can enter. To capture the essence of what happens, let us consider a three-dimensional CFT on $S^1_\beta \times S^1_{L_1} \times S^1_{L_2}$ with $L_1 < L_2$. The low-temperature partition function will project to the vacuum state on $S^1_{L_1} \times S^1_{L_2}$, which can be parameterized as

$$E_{\text{vac},L_1\times L_2} = -\frac{\varepsilon_{\text{vac}} L_2}{L_1^2}(1 + f(L_1/L_2))\,. \tag{2.18}$$

Let us define $y = L_1/L_2$. The function $f(y)$ is capturing all of the corrections beyond the asymptotic formula, so we have $f(0) = 0$ and $f(y \to \infty) = -1 + y^3$. In general, $f(y)$ is a nontrivial function of y. Later in the text we will derive some positivity and monotonicity constraints on $f(y)$ by using modular invariance, but for now let us exhibit its functional form for the free boson theory, shown in figure 2.1.

In higher dimensions, there are more independent ratios that can be varied, and in general the corrections beyond the asymptotic formula are given by some nontrivial function of $d-2$ dimensionless ratios $y_i = L_1/L_i$ which for simplicity we will often write as $f(\mathbf{y})$ with $\mathbf{y} = (y_2, y_3, \ldots, y_{d-1})$.

We will also find it useful to consider the parameterization of the vacuum energy

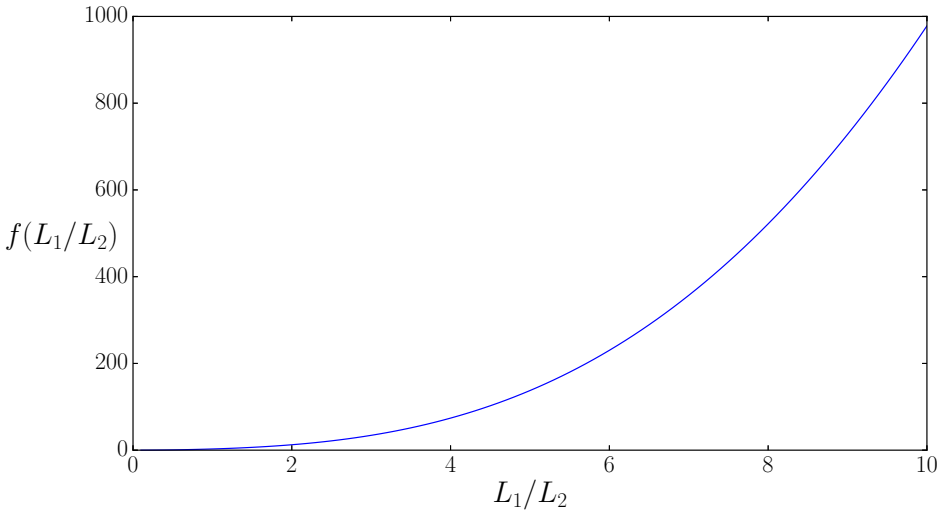

Figure 2.1: The functional form of $f(L_1/L_2)$ in the vacuum energy (defined in (2.18)) of a free boson in $2+1$ dimensions on a two-torus $\mathbf{T}^2$ with sides L_1 and L_2. As can be seen in the plot, $f(L_1/L_2)$ is positive and monotonically increasing.

in arbitrary dimension as

$$E_{\text{vac}} = -\frac{\varepsilon_{\text{vac}} V_{d-1}}{L_{\text{min}}^d} \left(1 + \tilde{f}(\psi)\right). \tag{2.19}$$

which always has the smallest cycle in the denominator. The key difference between $\tilde{f}(\psi)$ and $f(\psi)$ is that it is possible for $\tilde{f}(\psi)$ to be identically zero for all values of its arguments, whereas this is not the case for $f(\psi)$ as discussed in three dimensions above. We will find, for example, that gravity implies a vacuum energy structure with $\tilde{f}(\psi) = 0$ up to $1/N$ corrections. We will often just write $\tilde{f}(\psi) = 0$, by which we mean the equality up to $1/N$ corrections.

2.3 Phase structure of toroidally compactified AdS gravity

In this section we will recap what is known about the phase structure of gravity in AdS with a toroidally compactified boundary. This phase structure is easy to deduce for pure gravity without spontaneous breaking of translation invariance, which is the case we will restrict ourselves to. The most remarkable feature of this phase structure is the absence of any nontrivial finite-size corrections to the

vacuum energy and free energy, up to sharp phase transitions as circles become comparably sized. In other words, the function $\tilde{f}(\psi)$ defined in the previous section *vanishes* for all values of its arguments. As usual there will be nonzero contributions suppressed by $1/N$. Note that weakly coupled theories, including e.g. $\mathcal{N} = 4$ super Yang-Mills, do not realize this sort of structure [67]. We will not consider the possibility that the singular solutions used in [67] are relevant for the phase structure. An argument against them is as follows. Assume that such a singular solution provides the vacuum energy of the theory under multiple compactifications. By the higher-dimensional Cardy formula, there must therefore exist a black brane with higher entropy than AdS-Schwarzschild. Any such black brane should be modular S-related to the singular solution. But that means the "black brane" will be horizonless and singular, and if e.g. α' effects resolve the singularity and pop out a horizon, then the entropy should be proportional to some power of α'. But the ground state energy is a boundary term and is not proportional to α'. This is inconsistent, by the Cardy formula which relates the two.

We consider our theory at inverse temperature β on a spatial torus of side lengths L_i. The Euclidean solutions with the correct periodicity conditions are the toroidally compactified Poincaré patch, black brane, and $d-1$ AdS solitons

$$ds^2_{\text{pp}} = r^2 dx_0^2 + \frac{dr^2}{r^2} + r^2 d\phi_i d\phi^i \,, \tag{2.20}$$

$$ds^2_{\text{bb}} = r^2 \left(1 - (r_h/r)^d\right) dx_0^2 + \frac{dr^2}{r^2 \left(1 - (r_h/r)^d\right)} + r^2 d\phi_i d\phi^i \,, \tag{2.21}$$

$$ds^2_{\text{sol,k}} = r^2 dx_0^2 + \frac{dr^2}{r^2 \left(1 - (r_{0,k}/r)^d\right)} + r^2 \left(1 - (r_{0,k}/r)^d\right) d\phi_k^2 + r^2 d\phi_j d\phi^j \,, \tag{2.22}$$

all of which have the identification $x_0 \sim x_0 + \beta$. There are $d-1$ AdS solitons since there are $d-1$ circles that are allowed to pinch off in the interior. This means that we are picking supersymmetry-breaking boundary conditions around all cycles, which is motivated by maintaining S-invariance of our thermal partition function.

The parameter r_h ($r_{0,k}$) is fixed by demanding the x_0 (ϕ_k) circle caps off smoothly:

$$r_h = \frac{4\pi}{d\beta} \,, \qquad r_{0,k} = \frac{4\pi}{dL_k} \,. \tag{2.23}$$

Considering the ensemble at finite temperature and zero angular velocity, we need to compare the free energy of these solutions:

$$F_{\text{bb}} = -\frac{r_h^d V_{d-1}}{16\pi G} \,, \qquad F_{\text{sol,k}} = -\frac{r_{0,k}^d V_{d-1}}{16\pi G} \,, \qquad F_{\text{pp}} = 0 \,. \tag{2.24}$$

The Poincaré patch solution never dominates so we will not consider it in what

follows. We will also assume that the AdS soliton of minimal energy gives the vacuum energy of the theory under a toroidal compactification [68].

2.3.1 Thermal phase structure

We will first consider the thermal phase structure, which can be illustrated by fixing a spatial torus and varying the inverse temperature β. The AdS soliton with the cycle of smallest length $L_{\min}$ pinching off has minimal free energy and dominates all the other ones. We will denote this as the $k = \min$ soliton. Thus, the two relevant solutions are this $k = \min$ soliton and the black brane. These two exhibit a thermal phase transition at $\beta = L_{\min}$ with the black brane dominating the ensemble at high temperature $\beta < L_{\min}$. The energy at the phase transition is

$$E\big|_{r_h=\frac{4\pi}{dL_{\min}}} = -\partial_\beta \log Z = -(d-1)E_{\text{vac}}\,, \tag{2.25}$$

where $E_{\text{sol},k=\min} = F_{\text{sol},k=\min} = E_{\text{vac}}$ is the vacuum energy of the theory.

2.3.2 Quantum phase structure

A very important new feature in the phase structure of higher-dimensional toroidally compactified AdS spacetime is the existence of quantum phase transitions. These are phase transitions that can occur at zero temperature and are therefore driven by quantum fluctuations and not thermal fluctuations. They occur as we vary the spatial cycle sizes and reach a point where two spatial cycle sizes coincide and are minimal with respect to the rest. Let us call these cycle lengths L_1 and L_2 and pass from $L_1 < L_2$ to $L_1 > L_2$. In this case the vacuum energy exhibits a sharp transition from the $k = 1$ soliton to the $k = 2$ soliton. This is precisely the behavior that fixes $\tilde{f}(\psi) = 0$, as alluded to earlier. To exhibit a phase transition in the free energy instead of the vacuum energy, we need to restrict ourselves to the low-temperature phase $\beta > L_{\min}$ where the black brane does not dominate.

2.4 Necessary and sufficient conditions for universality

In this section we would like to highlight a few difficulties in generalizing a discussion from two dimensions to higher dimensions. Let us first consider a two-dimensional CFT with cycle lengths β and L. For such a theory, vacuum domination of the torus partition function in channel L, for arbitrary cycle size $L > \beta$, is

necessary and sufficient for universality of the partition function for all β. To see this, we write vacuum domination in the L channel as

$$Z(\beta)_L = Z(L)_\beta = \sum_{E_\beta} \exp\left(-LE_\beta\right) \approx \exp\left(-LE_{\text{vac},\beta}\right) = \exp\left(\frac{\pi c L}{6\beta}\right) . \tag{2.26}$$

Due to the fact that the vacuum energy for two-dimensional CFT is uniquely fixed by conformal invariance, we get a universal answer for the partition function. In the β channel, this form is that of an extensive free energy, and gives the Cardy formula in the canonical ensemble $S(\beta) = \pi c L/(3\beta)$.

In higher dimensions, vacuum domination of the torus partition function in one channel seems neither necessary nor sufficient for extensive Cardy growth in a different channel. This is because the vacuum energy on a generic torus is not uniquely fixed by conformal invariance. But it turns out we can use $SL(d, \mathbf{Z})$ invariance to show that a slightly modified version of the statement is valid. In particular, we will show that vacuum domination in all channels except that of the smallest cycle is necessary and sufficient for universality of the partition function for all β. Before we begin, we will prove some useful properties of the function $f(\psi)$ which characterizes the subextensive corrections to the vacuum energy and will play a starring role in our general CFT and symmetric orbifold analyses. Sections 2.4.1 and 2.4.2 will contain results about generic modular-invariant CFTs. Sections 2.4.3 and 2.4.4 will then specify to large-N theories.

2.4.1 Modular constraints on vacuum energy

We now utilize the connection between the vacuum energy and the excited states implied by modular invariance, as first pointed out in appendix A of [54]. We will find that, somewhat surprisingly, modular invariance constrains all subextensive corrections to the vacuum energy to have a fixed sign and monotonic behavior.

Consider a spatial torus with side lengths $L_1 \leq \cdots \leq L_{d-1}$ and take the quantization along β at low temperature, which efficiently projects to the vacuum:

$$\lim_{\beta\to\infty} \frac{\log Z(\beta)_{\mathcal{M}_0}}{\beta} = -E_{\text{vac},\mathcal{M}_0} = \frac{\varepsilon_{\text{vac}} V_{\mathcal{M}_0}}{L_1^d}(1 + f(\psi)) . \tag{2.27}$$

We also consider the $d-2$ quantizations $L_2, \ldots, L_{d-1}$, which give

$$\lim_{\beta\to\infty} \frac{\log Z(L_i)_{\mathcal{M}_i}}{\beta} = \frac{\varepsilon_{\text{vac}} V_{\mathcal{M}_0}}{L_1^d}(1+f(\psi\backslash y_i, 0)) + \lim_{\beta\to\infty} \frac{1}{\beta} \log\left(\sum_E e^{-L_i(E-E_{\text{vac}})_{\mathcal{M}_i}}\right) , \tag{2.28}$$

where $\psi \setminus y_i$ is the vector ψ without the y_i-th element. The reason for the different arguments of f is that in the L_i quantization, instead of the ratio L_1/L_i we have $L_1/\beta = 0$ as $\beta \to \infty$. The second term on the right-hand-side does not vanish since the logarithm of the shifted partition function becomes linear in β at large β due to extensivity.

We want to analyze the monotonicity properties of $f(\psi)$ with respect to its $d-2$ arguments. To analyze any given ratio y_i, we can equate the quantization along β with the quantization along L_i. This gives

$$\frac{\varepsilon_{\text{vac}} V_{\mathcal{M}_0}}{L_1^d} \left(f(\psi) - f(\psi \setminus y_i, 0)\right) = \lim_{\beta\to\infty} \frac{1}{\beta} \log\left(\sum_E \exp\left(-L_i (E - E_{\text{vac}})_{\mathcal{M}_i}\right)\right). \tag{2.29}$$

By unitarity, the right-hand-side is manifestly non-negative, so we conclude

$$f(\psi) - f(\psi \setminus y_i, 0) \geq 0\,. \tag{2.30}$$

Furthermore, the right-hand-side of (2.29) is a monotonically decreasing function of L_i. This means we can differentiate the left-hand-side with respect to L_i and obtain

$$f(\psi) - f(\psi \setminus y_i, 0) + L_i \partial_{L_i} f(\psi) \leq 0 \implies \partial_{L_i} f(\psi) \leq 0 \implies \partial_{y_i} f(\psi) \geq 0\,, \tag{2.31}$$

where the first implication follows from the previous positivity property. The second implication follows from the fact that increasing L_i is the same as keeping all ratios y_j fixed except for the ratio $y_i = L_1/L_i$, which is decreased. In particular, this means that the function increases under any possible variation. Furthermore, since $f(\mathbf{0}) = 0$ this means that $f(\psi) \geq 0$. These facts will be used heavily in what follows.

Modular invariance can also be used to constrain the behavior of the vacuum energy under spatial twists. By re-interpreting the spatial twist as an angular potential in a different channel, we can see that the vacuum energy cannot increase due to a spatial twist. The proof goes as follows. Consider the following partition function in the low-temperature limit with twist θ_{kj} between two spatial directions k and j:

$$\lim_{\beta\to\infty} \frac{\log Z(\beta; \theta_{kj})_{\mathcal{M}_0}}{\beta} = -E_{\text{vac}}(L_1, ..., L_{d-1}; \theta_{kj})\,. \tag{2.32}$$

Since the spatial directions are twisted, we may quantize along direction k, in which case the twist becomes an angular potential:

$$\lim_{\beta\to\infty} \frac{\log Z(L_k; \theta_{kj})_{\mathcal{M}_k}}{\beta} = \lim_{\beta\to\infty} \frac{1}{\beta} \log\left(\sum_E \exp\left(-L_k E_{\mathcal{M}_k} + i P_j \theta_{kj}\right)\right). \tag{2.33}$$

The introduction of θ_{kj} only adds phases to the partition function in this channel, which decreases its real part. The vacuum energy is always manifestly real, so when equating the two quantizations it will be the case that the partition function with angular potential will evaluate to a real number. This means that the vacuum energy, which is negative, will be strictly greater or equal to its value without twists. This will be used in section 2.5.

2.4.2 Necessary and sufficient conditions

With the properties of the vacuum energy in hand, we are now ready to show that vacuum domination in all but the smallest channel is necessary and sufficient to have a universal free energy.

First we show *sufficiency*. We consider an ordering $\beta < L_1 \leq \cdots \leq L_{d-1}$. Vacuum domination in the channels L_i means

$$Z(L_i)_{\mathcal{M}_i} = \exp\left(-L_i E_{\text{vac},\mathcal{M}_i}\right) . \tag{2.34}$$

As we saw in the previous section, the vacuum energy is not uniquely fixed for higher-dimensional CFTs. However, equating the $d-2$ quantizations lets us extract the vacuum energy:

$$Z(L_1)_{\mathcal{M}_1} = Z(L_2)_{\mathcal{M}_2} = \cdots = Z(L_{d-1})_{\mathcal{M}_{d-1}} \tag{2.35}$$

$$\implies -L_1 E_{\text{vac},\mathcal{M}_1} = -L_2 E_{\text{vac},\mathcal{M}_2} = \cdots = -L_{d-1} E_{\text{vac},\mathcal{M}_{d-1}} . \tag{2.36}$$

Since $E_{\text{vac},\mathcal{M}_i}$ is independent of L_i, we conclude that $E_{\text{vac},\mathcal{M}_i}$ is linear in the cycle lengths $L_{j\neq i}$. The β dependence is then fixed by dimensional analysis, and the coefficient is fixed by matching onto the asymptotic case of small β:

$$E_{\text{vac},\mathcal{M}_i} = -\varepsilon_{\text{vac}} V_{\mathcal{M}_i}/\beta^d . \tag{2.37}$$

Thus, we see that vacuum domination in all but the smallest channel determines the functional form of the vacuum energy. We can now use $Z(\beta)_{\mathcal{M}_0} = Z(L_i)_{\mathcal{M}_i}$ to get

$$Z(\beta)_{\mathcal{M}_0} = \exp\left(\varepsilon_{\text{vac}} L_i V_{\mathcal{M}_i}/\beta^d\right) = \exp\left(\varepsilon_{\text{vac}} V_{\mathcal{M}_0}/\beta^{d-1}\right) . \tag{2.38}$$

This is just the Cardy formula. In a regular CFT it holds only asymptotically in small β, but here we have shown that vacuum domination in the spatial channels L_i is sufficient to make it valid for all temperatures $\beta < L_i$. For $\beta > L_1$ we again have a universal expression for $Z(\beta)_{\mathcal{M}_0}$, which by assumption is given by the contribution of the vacuum only.

Showing that vacuum domination in all but the smallest cycle is *necessary* for universality requires the properties of $f(\psi)$ proven in the previous subsection.

Consider the quantization along an arbitrary channel of cycle size L_i

$$Z(L_i)_{\mathcal{M}_i} = \sum e^{-L_i E_{\mathcal{M}_i}} = e^{-L_i E_{\text{vac},\mathcal{M}_i}} \sum e^{-L_i (E-E_0)_{\mathcal{M}_i}} . \tag{2.39}$$

In two spacetime dimensions, it is the vacuum contribution in this channel that gives Cardy behavior in the β channel and therefore universality. The excited states contribute as positive numbers, and would ruin the Cardy behavior. Therefore it is necessary that they not contribute, i.e. necessary that we are vacuum dominated in this channel. In higher dimensions, one may worry that the excited state contributions cancel against the non-universal pieces of the vacuum energy, precluding the necessity of vacuum domination. However, by the positivity of $f(\psi)$ this can never happen. Thus, to get the correct Cardy behavior in the β channel it is necessary that the excited states do not contribute. This is true for arbitrary channel i. We conclude that it is necessary to be vacuum dominated in all but the smallest cycle.

It is interesting that for a universal free energy it is necessary and sufficient to have vacuum domination in all but the smallest channel. One could have suspected that explicit assumptions about the subextensive corrections to the vacuum energy would have to enter, but they do not.

We can state an equivalent set of necessary and sufficient conditions. To obtain a universal free energy for all β on an arbitrary rectangular torus, it is necessary and sufficient to have vacuum domination in the largest spatial cycle, with the vacuum energy taking the universal form with no subleading corrections. In fact, by using the non-negativity and monotonicity of the subextensive corrections, we can state the necessary and sufficient condition as vacuum domination in the largest spatial cycle, with the vacuum energy on a square torus of side length L equal to $\varepsilon_{\text{vac}}/L$.

In the rest of this section we will restrict attention to large-N theories.

2.4.3 Sparseness constraints without assuming $\tilde{f}(\psi) = 0$

It is difficult to make progress in the case where we make no explicit assumptions about the functional form of the vacuum energy. To achieve vacuum domination in all but the smallest channel of a large-N theory, we can bound the entire spectrum on an arbitrary spatial torus of side lengths $L_1 \leq L_2 \leq \cdots \leq L_{d-1}$ as

$$\rho(\Delta_{\mathcal{M}_0}) \lesssim \exp\left(L_1 \Delta_{\mathcal{M}_0}\right) , \qquad \Delta_{\mathcal{M}_0} \equiv (E - E_{\text{vac}})_{\mathcal{M}_0} . \tag{2.40}$$

This is a necessary and sufficient condition, although it is possible that it is implied by a more minimal set of necessary and sufficient conditions. To see how this

condition arises, one writes the partition function as

$$Z(\beta)_{\mathcal{M}_0} = \exp\left(-\beta E_{\text{vac}}\right) \sum \exp\left(-\beta \Delta_{\mathcal{M}_0}\right) \rho(\Delta_{\mathcal{M}_0}) \tag{2.41}$$

and bounds the density of states as (2.40) for the entire spectrum. At large N, with a vacuum contribution that scales exponentially in N, this suppresses all excited state contributions as soon as $\beta > L_1$. This means all cycles except the smallest will be vacuum-dominated, as required. We give another method of proof for vacuum domination in appendix A.1 which restricts the sparseness bound to only the light states, but requires an additional assumption on the field theory.

We can also show that it is necessary and sufficient to solve the problem on a spatial square torus, i.e. that the free energy is universal for all β on a spatial square torus of side length L. The necessary direction is obvious. To show sufficiency, consider the quantization along L:

$$Z(L)_{\mathcal{M}_{d-1}} = \exp\left(-L E_{\text{vac},\mathcal{M}_{d-1}}\right) \sum_{\Delta} \exp\left(-L \Delta_{\mathcal{M}_{d-1}}\right) \tag{2.42}$$

$$= Z(\beta)_{\mathcal{M}_0} \approx \exp\left(\varepsilon_{\text{vac}} L^{d-1}/\beta^{d-1}\right) . \tag{2.43}$$

where the final expression is by assumption of universality. The only way to satisfy this equality is for the contribution of the excited states and the subextensive corrections to the vacuum energy in the L channel to vanish. In particular we are vacuum dominated in the L channel. Taking arbitrary $L_{d-1} > L$ keeps us vacuum dominated since it is at even lower temperature:

$$Z(L_{d-1})_{\mathcal{M}_{d-1}} \approx \exp\left(\varepsilon_{\text{vac}} L_{d-1} L^{d-2}/\beta^{d-1}\right) . \tag{2.44}$$

In the β channel this gives us the ordinary Cardy formula with no subextensive corrections, and in another L channel we have

$$Z(L)_{\mathcal{M}_{d-2}} = \exp\left(-L E_{\text{vac},\mathcal{M}_{d-2}}\right) \sum_{\Delta} \exp\left(-L \Delta_{\mathcal{M}_{d-2}}\right) \tag{2.45}$$

$$= Z(L_{d-1})_{\mathcal{M}_{d-1}} \approx \exp\left(\varepsilon_{\text{vac}} L_{d-1} L^{d-2}/\beta^{d-1}\right) . \tag{2.46}$$

Again, this means that we are vacuum dominated in the L channel. Now we can consider arbitrary L_{d-2} satisfying $L < L_{d-2} < L_{d-1}$, for which we will remain vacuum dominated:

$$Z(L_{d-2})_{\mathcal{M}_{d-2}} \approx \exp\left(\varepsilon_{\text{vac}} L_{d-1} L_{d-2} L^{d-3}/\beta^{d-1}\right) . \tag{2.47}$$

By equating this expression with the partition function in the L_{d-1} channel, we see that we are still vacuum dominated in that channel. By continuing this procedure we are able to generalize to an arbitrary torus $\beta < L_1 < \cdots < L_{d-1}$, and we obtain

$$\log Z(\beta) = \begin{cases} \varepsilon_{\text{vac}} V_{\mathcal{M}_0}/\beta^{d-1}, & \beta < L_1 \\ \varepsilon_{\text{vac}} V_{\mathcal{M}_1}/L_1^{d-1}, & \beta > L_1 \end{cases} . \tag{2.48}$$

Altogether, we have that the free energy is universal at all temperatures on an arbitrary spatial torus. So solving the problem on a spatial square torus is both necessary and sufficient to solving the general problem, thanks to properties of the positivity of $f(\psi)$.

2.4.4 Sparseness constraints assuming $\tilde{f}(\psi) = 0$

In this section we will show that assuming $\tilde{f}(\psi) = 0$ (up to $1/N$ corrections) allows us to exhibit a constraint on the light spectrum that naturally generalizes the two-dimensional case. This is not too surprising, as $\tilde{f}(\psi) = 0$ is automatically true in two dimensions, although some more work will be required in higher dimensions.

We start by considering the special torus with ordering $\beta < L < L^2/\beta < \cdots < L^{d-1}/\beta^{d-2}$. As discussed in chapter 1, this special torus has an exact low-temperature/high-temperature duality $Z(\beta)_{\mathcal{M}_0} = Z(L^d/\beta^{d-1})_{\mathcal{M}_0}$. This will allow us to uplift the arguments of [24] to our case. In the upcoming manipulations, we will not keep explicitly the specification of the spatial manifold $\mathcal{M}_0$, since this duality allows us to keep our spatial manifold fixed once and for all.

By following the steps in [24], one can show that the partition function is dominated by the light states up to a theory-independent error. We will denote light states as those with energy $E < \epsilon$ for some arbitrary ϵ. We have

$$\log Z_{\text{light}}(L^d/\beta^{d-1}) \leq \log Z(\beta) \leq \log Z_{\text{light}}(L^d/\beta^{d-1}) - \log\left(1 - e^{\epsilon(\beta - L^d/\beta^{d-1})}\right). \tag{2.49}$$

This error grows arbitrarily large as $\beta \to L$ or $\epsilon \to 0$. For $\beta > L$ we can derive a similar upper and lower bound.

For a family of CFTs labeled by N, we assume that the vacuum energy also scales with N. This will be true in all examples we consider. When taking N large, we can scale $\epsilon \to 0$, in which case the partition function is squeezed by its bounds and given just by the light states up to $\mathcal{O}(1)$ corrections. In the context of assuming $\tilde{f}(\psi) = 0$, we then obtain universality

$$\log Z(\beta) = \begin{cases} \log Z_{\text{light}}(L^d/\beta^{d-1}) = -\frac{L^d}{\beta^{d-1}} E_{\text{vac}} & \beta < L \\ \log Z_{\text{light}}(\beta) = -\beta E_{\text{vac}} & \beta > L \end{cases}, \tag{2.50}$$

if and only if the density of light states is bounded as

$$\rho(\Delta) \lesssim \exp\left(\frac{L^d}{\beta^{d-1}}\Delta\right), \qquad \Delta \leq -E_{\text{vac}}\,, \tag{2.51}$$

where $\Delta = E - E_{\text{vac}}$. Notice that if we did not assume a universal form for

the vacuum energy with $\tilde{f}(\psi) = 0$, the free energy would still be very theory-dependent.

To generalize the argument above to an arbitrary d-torus, the idea will be to push the special torus very close to the square torus. From here, we can use the fact that whenever a partition function is dominated by the vacuum contribution at some inverse temperature β, then it will also be dominated by that contribution for larger β. Channel by channel, we will see that we will be able to generalize to an arbitrary torus. Assuming a universal form of the vacuum energy will be crucial for this argument.

It will be convenient to consider starting with a quantization along the L^{d-1}/β^{d-2} channel, because it is the largest cycle when $\beta < L$. We will now restore the explicit spatial manifold dependence since we will be considering quantizations along different channels. We have

$$Z(L^{d-1}/\beta^{d-2})_{\mathcal{M}_{d-1}} = Z(L^d/\beta^{d-1})_{\mathcal{M}_0} = Z(\beta)_{\mathcal{M}_0}\,. \tag{2.52}$$

By using (2.50) we can write this as

$$Z(L^{d-1}/\beta^{d-2})_{\mathcal{M}_{d-1}} = \exp\left(-\frac{L^d}{\beta^{d-1}}E_{\text{vac},\mathcal{M}_0}\right) = \exp\left(-\frac{L^{d-1}}{\beta^{d-2}}E_{\text{vac},\mathcal{M}_{d-1}}\right)\,. \tag{2.53}$$

This means that we are vacuum-dominated in the L^{d-1}/β^{d-2} channel.

Let us now take a larger cycle $L_{d-1} > L^{d-1}/\beta^{d-2}$, for which we will remain vacuum-dominated:

$$Z(L_{d-1})_{\mathcal{M}_{d-1}} = \exp\left(-L_{d-1}E_{\text{vac},\mathcal{M}_{d-1}}\right)\,. \tag{2.54}$$

Quantizing now along the the second largest cycle $L^{d-2}/\beta^{d-3} < L_{d-1}$ gives us

$$Z(L^{d-2}/\beta^{d-3}) = \exp\left(-L^{d-2}/\beta^{d-3}E_{\text{vac},\mathcal{M}_{d-2}}\right)\sum_{\Delta}\exp\left(-L^{d-2}\Delta_{\mathcal{M}_{d-2}}/\beta^{d-3}\right)\,. \tag{2.55}$$

But by our assumption $\tilde{f}(\psi) = 0$, we have

$$L_{d-1}E_{\text{vac},\mathcal{M}_{d-1}} = L^{d-2}E_{\text{vac},\mathcal{M}_{d-2}}/\beta^{d-3}\,, \tag{2.56}$$

which means that $Z(L^{d-2}/\beta^{d-3})$ is given by its vacuum contribution only. One can now consider $L_{d-2} > L^{d-2}/\beta^{d-3}$, for which we will remain vacuum-dominated in the L_{d-2} channel. By comparing to the L_{d-1} channel, we can verify that we remain vacuum-dominated there as well. We can now move to the L^{d-3}/β^{d-4} channel and continue this procedure up to and including the L channel. In a final step, we can compare to the β channel and see that it indeed has universal Cardy

behavior:

$$\log Z(\beta) = \frac{\varepsilon_{\text{vac}} V_{\mathcal{M}_0}}{\beta^d} \,. \tag{2.57}$$

There is no need now to consider smaller β since we have already considered general variations of the other $d-1$ cycles. Since the partition function is a function of $d-1$ independent dimensionless ratios, we have already captured all possible variations.

The generality of the torus that results from this procedure is restricted by the special torus with which we began. But notice that the special torus can be arbitrarily close to a d-dimensional square torus, which means this procedure results in a universal free energy on an arbitrary torus. From this argument it is clear that the only assumption made on the spectrum is the bound in (2.51). In fact, it is enough to impose this constraint for the square torus, since our procedure begins from that case (or arbitrarily close to it) and generalizes to an arbitrary torus. The sparseness constraint is therefore

$$\rho(\Delta) \lesssim \exp\left(L\Delta_{L\times L\times\cdots\times L}\right) \tag{2.58}$$

and is imposed only on the states with energies $E = \Delta + E_{\text{vac}} < 0$.

2.5 Symmetric Product Orbifolds in $d > 2$

In this section we construct orbifold conformal field theories in higher dimensions using a procedure analogous to the one in two dimensions. We will see that these theories contain both twisted and untwisted sector states and will give an estimate for the density of states within these sectors. Finally, we will show that under the assumption that $\tilde{f}(\psi) = 0$, the free energy has a universal behavior at large N which agrees with Einstein gravity.

2.5.1 A review of permutation orbifolds in two dimensions

In two dimensions, symmetric product orbifolds (or the more general permutation orbifolds) provide a vast landscape of two-dimensional CFTs with large central charge that have a potentially sparse spectrum and are thus of interest in the context of holography [69–72]. The goal of this section will be to extend these constructions to higher dimensions. We start by a review of permutation orbifolds in two dimensions which will set most of the notation that we will then carry over to higher dimensions. Permutation orbifolds are defined by the choice of two parameters: a "seed" CFT $\mathcal{C}$ and a permutation group $G_N \subset S_N$. A permutation

orbifold $\mathcal{C}_N$ is then defined to be

$$\mathcal{C}_N \equiv \frac{\mathcal{C}^{\otimes N}}{G_N} \,. \tag{2.59}$$

The procedure by which we take this quotient is called an orbifold. It projects out all states of the product theory that are not invariant under the action of the group. The Hilbert space thus gets restricted to

$$\mathcal{H}^{\otimes N} \longrightarrow \frac{\mathcal{H}^{\otimes N}}{G_N} \,, \tag{2.60}$$

where $\mathcal{H}$ is the Hilbert space of $\mathcal{C}$. This projection onto invariant states is crucial as it gets rid of most of the low-lying states and hence provides some hope of obtaining a sparse spectrum. When computing the torus partition function, this projection onto invariant states is implemented by a sum over all possible insertions of group elements in the Euclidean time direction. This is summarized by the following formula

$$Z_{\text{untw}} = \frac{1}{|G_N|} \sum_{g \in G_N} \; g \boxed{} \tag{2.61}$$

where the box represents the torus with the vertical direction being Euclidean time.

However, (2.62) is obviously not modular invariant as it singles out the time direction. Modular invariance is restored in the following way

$$Z_{\text{tot}} = \frac{1}{|G_N|} \sum_{g,h \in G_N | gh=hg} \; g \begin{array}{c} \boxed{} \\ h \end{array} \,. \tag{2.62}$$

The requirement that the two group elements must commute comes from demanding that the fields have well-defined boundary conditions [73]. The insertion of elements h in the spatial direction are interpreted as twisted sectors, where the boundary conditions of the fields are twisted by group elements. There is one twisted sector per conjugacy class of the group, which in the case of $G_N = S_N$ gives one twisted sector per Young diagram. In [69–71], the space of permutation orbifolds was explored and a criterion was given for these theories to have a well-defined large N limit (and thus a potential holographic dual). It was found that many properties of the spectrum depends solely on the group G_N and not on the choice of the seed theory. Groups that give a good large-N limit are called oligomorphic permutation groups [74–76]. Although a complete proof is still missing, it is believed permutation orbifolds by oligomorphic groups all have at least a Hagedorn density of light states, but the growth may be even faster [69,71]. For

the symmetric group, it was shown in [24,62] that the growth is exactly Hagedorn with the precise coefficient saturating the bound on the density of light states produced in [24].

Symmetric product orbifolds thus reproduce the phase structure of 3d gravity. Note that they are still far from local theories of gravity such as supergravity on $AdS_3 \times S^3$, as their low-lying spectrum is Hagedorn and so they look more like classical string theories. The D1-D5 CFT has a moduli space that is proposed to contain a point, known as the orbifold point, where the theory becomes a free symmetric product orbifold theory. According to this proposal, the orbifold point is connected to the point where the supergravity description is valid by an exactly marginal deformation. It is only the strongly coupled theory that is dual to supergravity, and from this point of view it is surprising that the free theory realizes the phase structure of gravity.

2.5.2 Symmetric product orbifolds in higher dimensions

In two dimensions, we saw that symmetric product orbifolds are examples of theories with a sparse enough spectrum to satisfy the bound from [24] and thus have a universal phase structure at large N. We would now like to construct weakly coupled examples of theories satisfying our new criteria in higher dimensions. In dimensions greater than two, it is in general much harder to construct large-N CFTs. One may of course take tensor products but these will never have a sparse enough spectrum. In fact, the spectrum below some fixed energy level will not even converge as $N \to \infty$. Imposing some form of Gauss' law to project out many of the low-lying states is usually done by introducing some coupling to a gauge field, which makes preserving conformal invariance highly non-trivial. A natural way to achieve this same projection is through the construction of orbifold conformal field theories familiar from two dimensions. To the best of our knowledge, there is no construction of orbifold conformal field theories in higher dimensions, which as explained in the previous subsection is perhaps the most natural way of obtaining theories that are conformal, have a large number of degrees of freedom, but also a sparse low-lying spectrum.

We will now describe the construction of symmetric product orbifolds in d dimensions.[2] We will construct the partition function, i.e. the Hilbert space and the spectrum of the Hamiltonian on $\mathbf{T}^{d-1}$. We comment on other properties of the theory such as correlation functions in the discussion section.

[2]Here we will assume that the group is S_N but the generalization to other permutation groups follows trivially from our construction.

The starting point is again to consider a seed CFT_d $\mathcal{C}$ and to define the orbifold theory $\mathcal{C}_N$ as

$$\mathcal{C}_N \equiv \frac{\mathcal{C}^{\otimes N}}{S_N} \tag{2.63}$$

The orbifolding procedure goes as follows. We start by projecting onto invariant states by inserting all elements of the group in the time direction. This gives

$$Z_{\text{untw}} = \frac{1}{N!} \sum_{g \in S_N} g \quad . \tag{2.64}$$

The box of the 2d case has now been lifted to a d-dimensional hypercube which again describes the torus. We will represent it by a $3d$ cube and leave the other dimensions implicit. Again, the mere projection is obviously not modular invariant. By applying elements of $SL(d, \mathbf{Z})$ (for instance the S element given in (2.4)), we quickly see that group elements must also be inserted in the space directions. Having well-defined boundary conditions for the fields constrains the d group elements to be commuting. The partition function of the orbifold theory is then defined as

$$Z_{\text{orb}} = \frac{1}{N!} \sum_{\substack{g_0,\ldots,g_{d-1} \in S_N \\ g_i g_j = g_j g_i \forall i,j}} g_0 \quad . \tag{2.65}$$

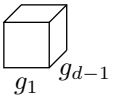

Twisted sector states will correspond to any states with non-trivial insertions in any of the space directions. The different twisted sectors are no longer labeled just by conjugacy classes, but by sets of $d-1$ commuting elements, up to overall conjugation. This orbifolding procedure describes a well-defined $SL(d, \mathbf{Z})$-invariant partition function.

2.5.3 Spectrum of the theory

The untwisted sector states

We now turn our attention to the spectrum of these orbifold theories. Other properties will depend strongly on the choice of seed. We start by considering the untwisted sector states. These are given by states of the product theory, up to symmetrization. From the point of view of the partition function, their contribution consists of all elements in the sum (2.65) where $g_1 = \ldots = g_{d-1} = 1$. Consider the contribution of a K-tuple to the density of states. A K-tuple is a state where K of the N CFTs are excited, while the other $N-K$ are in the vacuum.

The contributions of all possible K-tuples of distinct states are encapsulated by the following expression:

$$\rho(\Delta) = \int dK \int d\Delta_1 .... d\Delta_K \frac{1}{K!} \rho_0(\Delta_1) .... \rho_0(\Delta_K) \delta(\Delta - \sum_{j=1}^{K} \Delta_j) \,, \tag{2.66}$$

where $\Delta = E - NE_{\text{vac}}$, $\Delta_i = E_i - E_{\text{vac}}$ and ρ_0 is the density of states of the seed theory.[3] It can be shown that the contribution of K-tuples with subsets of identical states do not give a larger contribution than the one considered here, so it is sufficient to focus on this case. The combinatorial prefactor $1/K!$ was introduced to remove the equivalent permutations of the K states. One way to understand its inclusion is to consider how the orbifold projection is done. A given K-tuple in the product theory is made S_N invariant by summing over all of its possible permutations. For example, the 3-tuples $\{a, b, c\}, \{a, c, b\}, \{b, a, c\}, \{b, c, a\}, \{c, a, b\}, \{c, b, a\}$ of the pre-orbifolded theory lead to the same orbifolded 3-tuple and thus should only be counted once. The triple integral giving $\rho(\Delta)$, when left to its own devices without combinatorial prefactor, would count all six configurations.

Along with the states being distinct, let us first assume that each of the individual degeneracies can be approximated by the Cardy formula of the seed theory. The Cardy formula in higher dimensions was given in (2.15) and reads

$$\log \rho(E) = \frac{d}{(d-1)^{\frac{d-1}{d}}} (\varepsilon_{\text{vac}} V_{d-1})^{\frac{1}{d}} E^{\frac{d-1}{d}} \,. \tag{2.67}$$

Now let us proceed as in [69] to find the density of states. Performing the integrals over energies E_i by a saddle-point approximation where the large parameter is the total energy E, we find saddle-point values $E_i = E/K$ for all i. To assure that the state in each copy is distinct, we need the degeneracy to pick from to be much larger than K. Thus the validity of this assumption and the validity of the Cardy formula in each seed theory require, respectively,

$$\exp\left[\frac{d}{(d-1)^{\frac{d-1}{d}}} (\varepsilon_{\text{vac}} V_{d-1})^{\frac{1}{d}} (\Delta/K + E_{\text{vac}})^{\frac{d-1}{d}}\right] \gg K, \quad \Delta/K \gg |E_{\text{vac}}| \,. \tag{2.68}$$

We will check whether these conditions are satisfied at the end. Note that the second constraint implies that we can drop E_{vac} in the Cardy formula when expressed in terms of Δ. We thus have

$$\rho(\Delta) \sim \int dK \exp\left[d a K^{\frac{1}{d}} \Delta^{\frac{d-1}{d}} - K \log K + K\right] \tag{2.69}$$

[3] Here we use the notation that Δ is a shifted energy that satisfies $\Delta \geq 0$, but we wish to emphasize that it is *not* in any way related to the scaling dimension of a local operator.

with

$$a \equiv \frac{1}{(d-1)^{\frac{d-1}{d}}} (\varepsilon_{\text{vac}} V_{d-1})^{\frac{1}{d}} \,. \tag{2.70}$$

We can now do a second saddle-point approximation to evaluate the integral over K. The large parameter is again given by the total shifted energy Δ. The saddle point equation is

$$a\Delta^{\frac{d-1}{d}} K_s^{\frac{1-d}{d}} - \log K_s = 0 \,, \tag{2.71}$$

which gives

$$K_s \sim \frac{a^{\frac{d}{d-1}} \Delta}{\left(\log\left[a^{\frac{d}{d-1}} \Delta\right]\right)^{\frac{d}{d-1}}} \tag{2.72}$$

at large Δ. Plugging this back in the density of states we find

$$\rho(E) \sim \exp\left[(d-1) \frac{a^{\frac{d}{d-1}} \Delta}{\left(\log\left[a^{\frac{d}{d-1}} \Delta\right]\right)^{\frac{1}{d-1}}}\right] , \tag{2.73}$$

where we have used large Δ to drop subleading pieces which either have a larger power of the logarithm in the denominator or are terms proportional to $\log\log\Delta$. We find a growth of states that is slightly sub-Hagedorn and the growth increases with the dimension of the field theory. Inserting K_s in our necessary assumptions shows that they can be satisfied for large enough Δ. In particular, the second condition becomes

$$a^{\frac{d}{d-1}} \Delta \gg \exp\left[a \left|E_{\text{vac}}\right|^{\frac{d-1}{d}}\right] \tag{2.74}$$

which is then sufficient to satisfy the first condition. Here E_{vac} is the vacuum energy of the seed theory and does not scale with N. Notice also that K_s grows with Δ and must not violate the bound $K_s \leq N$. This implies a bound on our energies from the saddle:

$$a^{\frac{d}{d-1}} \Delta \lesssim N \left[\log(N)\right]^{\frac{d}{d-1}} \,. \tag{2.75}$$

So altogether our density of states formula is reliable in the range

$$\exp\left[a \left|E_{\text{vac}}\right|^{\frac{d-1}{d}}\right] \ll a^{\frac{d}{d-1}} \Delta \lesssim N \left[\log(N)\right]^{\frac{d}{d-1}} \,. \tag{2.76}$$

In particular we can consider energies that scale with N. However, as we will shortly see, the density of states quickly becomes dominated by the twisted sectors. Note that this growth of states is also a lower bound for any permutation orbifold as orbifolding by a subgroup of S_N always projects out fewer states.

The twisted sector states

We will now give a lower bound on the density of states coming from the twisted sectors. If the intuition from two dimensions carries over, it will be the twisted sectors that give the dominant contribution to the density of states. Indeed, this is the result we will find. We start by a more general discussion of twisted sector states and their contribution to the partition function.

A twisted sector is given by $d-1$ commuting elements $g_1, ..., g_{d-1}$ of S_N, up to overall conjugation. There is also a projection onto S_N-invariant states by summing over elements in the time direction but at this point we only focus on the identity contribution in that direction. We define $\mathbf{T}$ to be the original d-torus used to compute the partition function. We leave the dependence on the vectors $U_0, ..., U_{d-1}$ implicit. Let us consider the action of the subgroup $G_{g_1,...,g_{d-1}}$ of S_N (defined to be the group generated by $g_1, ..., g_{d-1}$) on the N copies of the CFT. The action of this group will be to glue certain copies of the CFT together. Concretely, let Φ^k denote a field on $\mathbf{T}$ of the k-th CFT, then in the twisted sector defined by $G_{g_1,...g_{d-1}}$ this field has boundary conditions

$$\Phi^k(x_0, x_1, ..., x_j + L_j, ..., x_{d-1}) = \Phi^{g_j(k)}(x_0, x_1, ..., x_j, ..., x_{d-1})\,. \tag{2.77}$$

Tracking the orbit of the k-th copy under $G_{g_1,...g_{d-1}}$ allows us to define a single field $\widetilde{\Phi}$ with modified boundary conditions. In particular it will have larger periods. A field $\widetilde{\Phi}^i$ can be defined for each orbit of the group $G_{g_1,...g_{d-1}}$ and we will denote the set of these orbits by

$$\{O_i\}\,, \quad i = 1, ...i_{\max}\,, \tag{2.78}$$

where $i_{\max}$ depends on the precise choice of $g_1, ..., g_{d-1}$. As the different orbits do not talk to each other, the path integral will split into a product of $i_{\max}$ independent path integrals, one over each field $\widetilde{\Phi}^i$. The new boundary conditions of the fields in a given O_i under the action of $G_{g_1,...,g_{d-1}}$ enable us to rewrite that particular contribution to the path integral as a torus partition function, but now with $\mathbf{T}$ replaced by a new torus $\widetilde{\mathbf{T}}_i$. The original identifications coming from (2.3) were

$$(x_0, x_1, .., x_{d-1}) \sim (x_0, x_1, .., x_{d-1}) + \sum_{i=0}^{d-1} n_i U_i\,. \tag{2.79}$$

for any integers n_i. Once the elements $g_1, ..., g_{d-1}$ are inserted the identifications are changed and they are encoded in a new torus. As these boundary conditions follow from the orbits, the identifications from the new torus are given by the elements in $G_{g_1,...,g_{d-1}}$ that leave the orbit invariant, i.e.

$$g_1^{m_1} ... g_{d-1}^{m_{d-1}} O_i = O_i\,. \tag{2.80}$$

This means that the identifications become

$$(x_0, x_1, .., x_{d-1}) \sim (x_0, x_1, .., x_{d-1}) + \sum_{i=0}^{d-1} m_i U_i \,. \tag{2.81}$$

with the m_i such that (2.80) is satisfied. Alternatively, one can define new vectors in the following way

$$\begin{aligned} \widetilde{U}_1 &= m_1^{\min} U_1 + m_{1,2} U_2 + ... + m_{1,d-1} U_{d-1} \,, \\ &\vdots \\ \widetilde{U}_{d-2} &= m_{d-2}^{\min} U_{d-2} + m_{d-2,d-1} U_{d-1} \,, \\ \widetilde{U}_{d-1} &= m_{d-1}^{\min} U_{d-1} \,, \end{aligned} \tag{2.82}$$

where $m_{d-1}^{\min}$ is the smallest integer m_{d-1} such that $g_{d-1}^{m_{d-1}} O_i = O_i$, $(m_{d-2,d-1}, m_{d-2}^{\min})$ are the pair with smallest non-zero m_{d-2} such that $g_{d-1}^{m_{d-2,d-1}} g_{d-2}^{m_{d-2}^{\min}} O_i = O_i$ and the $(m_1^{\min}, ..., m_{1,d-1})$ are the set of integers with minimal non-zero m_1 such that (2.80) is satisfied. These vectors define a new torus $\widetilde{\mathbf{T}}_i$ with volume

$$\mathrm{Vol}(\widetilde{\mathbf{T}}_i) = \left(\prod_j m_j^{\min} \right) \mathrm{Vol}(\mathbf{T}) \equiv |O_i| \mathrm{Vol}(\mathbf{T}) \,. \tag{2.83}$$

Since the g_i commute, $|O_i|$ is just the number of elements in the orbit O_i.

A twisted sector will thus give a set of new tori $\widetilde{\mathbf{T}}_i$ whose different volumes depend on the orbits of the action of $G_{g_1,...,g_{d-1}}$. For each orbit of that action, we will get a separate torus and schematically, this will give a contribution to the partition function of the form

$$Z_{\mathrm{tot}} \sim \prod_i Z(\widetilde{\mathbf{T}}_i) \,, \tag{2.84}$$

where the product over i is a product over the orbits. This is a generalization of Bantay's formula [58] to higher dimensions. For every orbit O_i we have

$$\mathrm{Vol}(\widetilde{\mathbf{T}}_i) = |O_i| \mathrm{Vol}(\mathbf{T}) \,, \tag{2.85}$$

where $|O_i|$ is the length of the orbit. We will now calculate the contribution to the partition function from a single non-trivial orbit of length $L = M^{d-1}$ giving a torus with equal rescaling M in all spatial directions. For simplicity, we also consider a case with $m_{i,j} = 0 \; \forall i \neq j$. The torus $\widetilde{\mathbf{T}}_i$ corresponding to this orbit is then

$$(\widetilde{U}_0, ..., \widetilde{U}_{d-1}) = (U_0, MU_1, ..., MU_{d-1}) \,. \tag{2.86}$$

We can always find elements $g_1, ..., g_{d-1}$ that produce the desired torus with equal scaling of the spatial cycles. To produce the new torus given in (2.86), we use for example the following elements:

$$\begin{aligned} g_1 &= (1 \ ... \ M)\,(M+1 \ ... \ 2M) ... \ (M^{d-1} - M + 1 \ ... \ M^{d-1})(M^{d-1}+1) \ ... \ (N) \\ g_2 &= (1 \quad M+1 \ ... \ M(M-1)+1) ... \\ &\quad (M^{d-1} - M(M-1) \quad M^{d-1} - M(M-2) \ ... \ M^{d-1})(M^{d-1}+1) \ ... \ (N) \\ &\vdots \\ g_{d-1} &= (1 \quad M^{d-2}+1 \ ... \ M^{d-2}(M-1)+1) ... (M^{d-2} \quad 2M^{d-2} \ ... \ M^{d-1}) \\ &\quad (M^{d-1}+1) \ ... \ (N) \end{aligned} \tag{2.87}$$

for $L = M^{d-1}$. For example in $d = 3$ and for $L = 9$, we get

$$\begin{aligned} g_1 &= (1\ 2\ 3)(4\ 5\ 6)(7\ 8\ 9)(10)...(N)\,, \\ g_2 &= (1\ 4\ 7)(2\ 5\ 8)(3\ 6\ 9)(10)...(N)\,. \end{aligned} \tag{2.88}$$

One can quickly check that all these elements commute and that they define an orbit of length L as well as $N - L$ singlets. One can also check that $m_1^{\min} = ... = m_{d-1}^{\min} = M$. We will call Z_{sq} this particular contribution to the partition function, and it reads

$$\begin{aligned} Z_{\text{sq}} &= Z(U_0, U_1, ..., U_{d-1})^{N-L} Z(U_0, MU_1, ..., MU_{d-1}) \\ &= Z(U_0, U_1, ..., U_{d-1})^{N-L} Z(U_0/L^{\frac{1}{d-1}}, U_1, ..., U_{d-1})\,, \end{aligned} \tag{2.89}$$

where we uniformly rescaled the torus and used $L = M^{d-1}$. From this, we can infer the behaviour of the density of states:

$$Z_{\text{sq}} = \sum_E \rho_{\text{sq}}(E) e^{-\beta E} = e^{-\beta E_{\text{vac}}(N-L)}\,(1 + \dots) \sum_E \rho_0(E) e^{-\beta E / L^{\frac{1}{d-1}}}\,. \tag{2.90}$$

We can ignore the excited states encapsulated in "..." as they will only increase $\rho_{\text{sq}}(E)$, which will increase our final answer. In this section, we are only after a lower bound for the density of states so we can ignore such terms. Shifting E to $L^{\frac{1}{d-1}}(E - E_{\text{vac}}(N-L))$ gives us

$$\rho_{\text{sq}}(E) = \rho_0(L^{\frac{1}{d-1}}(E - E_{\text{vac}}(N-L)))\,. \tag{2.91}$$

This will be the key formula to derive the final result.

In the full partition function we sum over all $L \leq N$ and for large L, we are in a regime where we may use the Cardy formula of the seed theory given in (2.15). To find the twisted sector that gives the maximal contribution at energy E, we

evaluate the sum over L using a saddle point approximation. The resulting saddle point equation for L is solved by

$$L_s = \frac{(E_{\text{vac}}N - E)}{dE_{\text{vac}}}\,, \tag{2.92}$$

which will be a good approximation provided $L_s \gg 1$. We now plug this back in (2.91) and use the Cardy formula (2.15) to obtain

$$\rho(E) \sim \exp\left[a\frac{(d-1)^{\frac{d-1}{d}}}{|E_{\text{vac}}|^{1/d}}(E - NE_{\text{vac}})\right]. \tag{2.93}$$

Note that this is a Hagedorn growth as in two dimensions but the coefficient of the Hagedorn growth depends on the vacuum energy of the seed theory. This is somewhat a loss of universality compared to two dimensions and it will be very important in what follows to understand precisely the properties of the vacuum energy of the orbifold theory. This will be the task of the next subsection. The regime in which this expression is reliable is for $1 \ll L_s \leq N$ which in terms of energies is

$$1 \ll \frac{E - NE_{\text{vac}}}{|E_{\text{vac}}|} \leq dN\,. \tag{2.94}$$

Finally, it is important to emphasize that this is merely a lower bound on the density of states[4]. We have only given the contribution from one type of twisted sectors and other sectors might dominate. We have also not taken into account the projection onto S_N invariant states by inserting commuting elements of the group in the time direction. In two dimensions, one can show that the estimate coming from this particular twisted sector (called long strings in $2d$) actually gives the dominant contribution. We will discuss this further when analyzing the free energy but we first turn our attention to the vacuum energy.

2.5.4 Vacuum energy of the orbifold theory

We want to understand precisely the properties of the vacuum energy of the orbifold theory. In two dimensions, it is clear that the central charge gets multiplied by N when going from the seed theory to the product (or orbifold) theory. Since the vacuum energy is fixed by the central charge, it also gets multiplied by N. Naively, one would expect a similar behavior in higher dimensions. The all-vacuum contribution in the untwisted sector indeed has energy NE_{vac}, but it may be possible

[4] In fact, the method used in this section only gives an estimate for the lower bound. We have only inserted one element - the identity - in the time direction and have not taken into account the projection to S_N invariant states. Following the method we will use in section 2.5.5 one can show that this estimate is actually precise.

that other twisted sectors give even more negative contributions. We will now address this possibility and show that it is impossible, so that the vacuum energy of the orbifold theory is in fact given as

$$E_{\text{vac}}^{\text{orbi}} = N E_{\text{vac}} \,. \tag{2.95}$$

To prove this, first recall that it is not necessary to consider twisted sectors inducing twists between any of the dimensions because they always increase the vacuum energy, as explained in section 2.4.1. The only thing we need to check is that rescalings of the torus do not give a contribution that is more negative than (2.95). A twisted sector in principle gives a product of partition functions if there is more than one orbit, but it will suffice to consider the case of a single orbit. This is because if there are different orbits, the vacuum energy is simply the sum of the vacuum energy for each orbit. In the case of a single orbit, the partition function looks like

$$Z = \sum_E e^{-\beta E} \,. \tag{2.96}$$

For a generic torus there can be angular potentials, but we have suppressed them since they will not influence the vacuum energy. Note that these values E are not directly the energy on the new spatial torus as there may have been a rescaling of the time direction. The vacuum energy of the orbifold theory $E_{\text{vac}}^{\text{orbi}}$ is simply the smallest such value of E. Now consider a twisted sector giving an arbitrary rescaling $U_i \to M_i U_i$ such that

$$\prod_{i=0}^{d-1} M_i = N \,. \tag{2.97}$$

This is needed as the scaling of the full torus must be equal to N if there is only one orbit. On such a torus, the vacuum contribution will be of the form

$$\begin{aligned} E_{\text{vac}}^{\text{orbi}}(M_i) &= -M_0 \frac{\varepsilon_{\text{vac}} V_{d-1} \prod_{i>0} M_i}{M_1^d L_1^d} \left(1 + f(\mathbf{y}_1)\right) \\ &= -\frac{N}{M_1^d} \frac{\varepsilon_{\text{vac}} V_{d-1}}{L_1^d} \left(1 + f(\mathbf{y}_1)\right) , \end{aligned} \tag{2.98}$$

where we used (2.97) and

$$\mathbf{y}_1 = \left(\frac{M_1 L_1}{M_2 L_2}, \ldots, \frac{M_1 L_1}{M_{d-1} L_{d-1}} \right) . \tag{2.99}$$

From (2.98) and using the monotonicity property of $f(\psi)$ under the increase of any of its arguments, it is clear that this expression is maximized for all $M_i = 1$ except for M_1. At first glance, it is not clear if increasing M_1 increases or decreases

the energy as it appears both in the denominator and in $f(\psi)$ which change in opposite directions. However, one can alternatively write the vacuum energy as

$$E_{\text{vac}}(M_i) = -\frac{N}{M_2^d}\frac{\varepsilon_{\text{vac}} V_{d-1}}{L_2^d}\left(1 + f(\mathbf{y}_2)\right), \tag{2.100}$$

with

$$\mathbf{y}_2 = \left(\frac{M_2 L_2}{M_1 L_1}, \ldots, \frac{M_2 L_2}{M_{d-1} L_{d-1}}\right). \tag{2.101}$$

In this form, it is clear that $M_1 > 1$ would only give a less negative value to the free energy. We have thus showed that to get the minimal contribution, we need

$$M_0 = N, \quad M_i = 1 \ \ \forall\, i\,, \tag{2.102}$$

which then gives precisely the vacuum energy (2.95).

Although this might appear as good news for the orbifold theory to be a "nice" theory, it is very bad news for any chance of universality at large N. We have shown in the previous section that having $\tilde{f}(\psi) = 0$ is a necessary condition for a universal free energy and an extended regime of the Cardy formula. Here, we see that the orbifold theory has $\tilde{f}(\psi) = 0$ only if the seed theory does. The choice of seed becomes crucial to reproduce the phase structure of gravity. In fact, this result is not so surprising. In two dimensions, we could consider ourselves lucky that the S_N orbifold theory, which is a free theory, reproduces the phase structure of Einstein gravity. It is only the strong coupling deformation of the orbifold theory that is dual to Einstein gravity so there is no a priori reason why one should have expected the orbifold theory to reproduce the phase structure of gravity. In higher dimensions, it appears that for a general seed, some form of coupling between the N CFTs must be introduced to force $\tilde{f}(\psi)$ to vanish. One might consider deforming the orbifold theory by some operator to achieve this effect. In particular, the existence of any exactly marginal deformations might allow reducing the Hagedorn density of light states to something compatible with Einstein gravity, as is proposed to occur in the D1-D5 duality. This could be directly connected to the vanishing of $\tilde{f}(\psi)$.

In the following subsection, we will show that choosing a seed theory with $\tilde{f}(\psi) = 0$ both gives a theory that saturates the sparseness bound and reproduces the phase structure of gravity.

2.5.5 Universality for $\tilde{f}(\psi) = 0$ and free energy at large N

If $\tilde{f}(\psi) = 0$, we have $E_{\text{vac}} = -\varepsilon_{\text{vac}} V_{d-1}/L_1^d$ where L_1 is the length of the smallest cycle. Inserting this expression in (2.93), we obtain

$$\rho(E) \sim \exp\left(L_1(E - NE_{\text{vac}})\right) \tag{2.103}$$

for the growth coming from the specific twisted sector we previously considered. Note that the coefficient of the Hagedorn growth precisely saturates the bound on the light states given in (2.58) if we put the theory on the square torus. At the upper end of the range of validity of (2.93) where $E = -(d-1)NE_{\text{vac}}$, we precisely recover the Cardy growth at the same energy. This indicates that the spectrum transitions sharply from Hagedorn to Cardy exactly where expected. However, we have only given a lower bound for the density of states as we only computed the contribution coming from a particular twisted sector. We will now show that for $\tilde{f}(\psi) = 0$ it is also an upper bound. We will do so by computing the free energy and see that it precisely reproduces the universal behavior discussed in section 2.4. This implies that the density of low-lying states is bounded above by (2.103), which becomes both a lower and upper bound. This means that no other twisted sector can give a bigger contribution and the density of states is well-approximated by (2.103).

To compute the free energy at large N, we will follow a similar procedure as that in two dimensions [62]. The starting point is a combinatorics formula first introduced by Bantay [59]. Let G be a finitely generated group and Z a function on the finite index subgroups of G that takes values in a commutative ring and is constant on conjugacy classes of subgroups. We have the following identity

$$\sum_{N=0}^{\infty} \frac{p^N}{N!} \sum_{\phi: G \to S_N} \prod_{\xi \in \mathcal{O}(\phi)} Z(G_\xi) = \exp\left(\sum_{H<G} p^{[G:H]} \frac{Z(H)}{[G:H]} \right), \tag{2.104}$$

where ϕ is an homomorphism from G to S_N and H are subgroups of G with finite index given by $[G : H]$. In our case, Z will be the partition function and $G = \pi_1(\mathbf{T}^d) = \mathbf{Z}^d$. This group is abelian and the sum over homomorphisms ϕ is equivalent to the sum over commuting elements introduced earlier. The image of ϕ acts on N letters (momentarily this will be the N copies of the CFT) by the usual S_N action and its orbit is denoted by $\mathcal{O}(\phi)$. The subgroup G_ξ consists of those elements of g such that $\phi(g)$ leaves ξ invariant. In fact, the left hand side is simply the generating function for the partition functions of the symmetric product orbifolds. It corresponds to

$$\mathcal{Z} = \sum_N p^N Z_N \,, \tag{2.105}$$

where Z_N is the partition function of $\mathcal{C}^{\otimes N}/S_N$ and thus the action of ϕ can be thought of as permuting the copies in $\mathcal{C}^{\otimes N}$. Just like in two dimensions, it is often more convenient to work with this generating function and to later find the coefficient of the term p^N to extract Z_N.

Bantay's formula equates the generating function to an exponential of a sum over new partition functions. This sum over partition functions really corresponds to a sum over new tori, and for a given index, the volume of the new tori will be the original volume times the index. Just as for $SL(2,\mathbf{Z})$, there is a very natural way to include all tori of a given index by using Hecke operators. Consider a torus to be described by the matrix U given in (2.3), which is upper triangular. Now consider the following set of matrices

$$\Omega_L = \left\{ \begin{bmatrix} a_0 & a_{01} & \cdots & a_{0,(d-2)} & a_{0,(d-1)} \\ 0 & a_1 & \cdots & a_{1,(d-2)} & a_{1,(d-1)} \\ \vdots & \vdots & \ddots & \vdots & \vdots \\ 0 & 0 & \cdots & a_{d-2} & a_{(d-2),(d-1)} \\ 0 & 0 & \cdots & 0 & a_{d-1} \end{bmatrix} \middle| \prod_i a_i = L, 0 \leq a_{j,i} < a_i \ \forall \ i,j \right\} \tag{2.106}$$

with L fixed. These matrices are elements of $GL(d,\mathbf{Z})$ and act on the lattice vectors U_i defining the torus according to $\widetilde{U} = HU$ with H an element of Ω_L. These new tori will have a volume L times larger than the original torus U. Consequently, the new lattice defined by the new torus is a sublattice H of $\mathbf{Z}^d$ and the index $[G:H]$ of H in $G = \mathbf{Z}^d$ is L. The purpose of these matrices is to parameterize the finite index subgroups of G so that we can write

$$\sum_{H<G} p^{[G:H]} \frac{Z(H)}{[G:H]} = \sum_{L>0} \frac{p^L}{L} \sum_{A\in\Omega_L} Z(AU)\,. \tag{2.107}$$

Fortunately, the right hand side can be rewritten in terms of Hecke operators for $SL(d,\mathbf{Z})$,

$$T_L Z(U) \equiv \sum_{A\in\Omega_L} Z(AU)\,, \tag{2.108}$$

which encapsulate the sum over different tori mentioned earlier. Note that the Hecke transform of Z is also an $SL(d,\mathbf{Z})$ modular invariant. Bantay's formula then becomes

$$\mathcal{Z}(U) = \exp\left(\sum_{L>0} \frac{p^L}{L} T_L Z(U) \right). \tag{2.109}$$

Because $T_L Z(U)$ is a function invariant under $SL(d,\mathbf{Z})$ [77], and it has a corresponding extensive free energy, its asymptotic growth is also given by the higher-dimensional Cardy formula. To see this directly, notice that $T_L Z(U)$ is a sum over

partition functions of different tori. Each of these obeys the higher-dimensional Cardy formula, although the explicit dependence on the volume of the torus in our higher-dimensional Cardy formula may seem confusing. Note however that at asymptotically large energies we have $E \propto V_{d-1}^{-1/(d-1)}$, so the volume of the torus cancels out and the formula can be written in terms of a dimensionless energy. Thus, there is no confusion as to "which volume" enters into the Cardy formula for $T_L Z(U)$. In fact, the situation is even better. The gap between the first excited state and the vacuum grows with L indicating that at large L, the Cardy formula will become a good estimate for the Hecke transformed partition function.

We are now ready to estimate the free energy. Let us take a rectangular d-torus with sides $\beta, L_1, ..., L_{d-1}$, i.e

$$U = \begin{pmatrix} \beta & 0 & \cdots & 0 & 0 \\ 0 & L_1 & \cdots & 0 & 0 \\ \vdots & \vdots & \ddots & \vdots & \vdots \\ 0 & 0 & \cdots & L_{d-2} & 0 \\ 0 & 0 & \cdots & 0 & L_{d-1} \end{pmatrix}, \tag{2.110}$$

and let us assume L_1 is the smallest spatial cycle. Writing $\tilde{p} = pe^{\beta E_{\text{vac}}}$,

$$\begin{aligned} \mathcal{Z} &= \exp\left(\sum_{L>0} \frac{\tilde{p}^L}{L} + \sum_{L>0} \frac{\tilde{p}^L}{L} \sum_{E>0} \widetilde{\rho}_{T_L}(E) e^{-\beta E}\right) \\ &= \left(\sum_{K=0}^{\infty} \tilde{p}^K\right) \exp\left(\sum_{L>0} \frac{\tilde{p}^L}{L} \sum_{E>0} \widetilde{\rho}_{T_L}(E) e^{-\beta E}\right), \end{aligned} \tag{2.111}$$

where we have defined $\tilde{\rho}_{T_L}(E)$ such that

$$e^{L\beta E_{\text{vac}}} T_L Z(U) = 1 + \sum_{E>0} \widetilde{\rho}_{T_L}(E) e^{-\beta E} \tag{2.112}$$

Using the Cardy formula, the sum over energies in (2.111) becomes

$$\sum_{E>0} e^{\left(daL^{\frac{1}{d}}(E+E_{\text{vac}}L)^{\frac{d-1}{d}}\right)} e^{-\beta E} \quad \sim \quad \exp\left(L|E_{\text{vac}}|\left(\frac{L_1^d}{\beta^{d-1}} - \beta\right)\right), \tag{2.113}$$

where we assumed L_1 to be the smallest cycle and used (2.70) as well as

$$E_{\text{vac}} = \frac{-\varepsilon_{\text{vac}} V_{d-1}}{L_1^d}. \tag{2.114}$$

The saddle point value for E is

$$E_s = |E_{\text{vac}}| L \left(1 + \frac{(d-1)L_1^d}{\beta^d}\right), \tag{2.115}$$

which will be large for large L. This justifies the use of the Cardy formula. The terms with low E will of course not be in the Cardy regime but these will only give a subleading contribution. Overall, the error on the each term in the sum over L will be of order $e^{-uL/\beta^{d-1}}$ for some positive order one number u that is theory dependent. Plugging (2.113) into (2.111) we get

$$\begin{aligned}\mathcal{Z} &= \left(\sum_{K=0}^{\infty}\tilde{p}^K\right)\exp\left(\sum_{L>0}\frac{1}{L}\left(\tilde{p}\exp\left(|E_{\rm vac}|\left(\frac{L_1^d}{\beta^{d-1}}-\beta\right)\right)\right)^L\right)\\ &= \left(\sum_{K=0}^{\infty}\tilde{p}^K\right)\exp\left(-\log\left(1-\tilde{p}e^{|E_{\rm vac}|\beta(L_1^d/\beta^d-1)}\right)\right)\\ &= \left(\sum_{K=0}^{\infty}\tilde{p}^K\right)\frac{1}{1-\tilde{p}e^{|E_{\rm vac}|\beta(L_1^d/\beta^d-1)}}\,. \end{aligned} \tag{2.116}$$

We can now extract the free energy. Note that because the vacuum energy is negative and proportional to N, the partition function diverges as $N\to\infty$ so we need to consider the shifted partition function and shifted free energy

$$\begin{aligned}\widetilde{Z} &\equiv e^{E_{\rm vac}\beta}Z\,,\\ \widetilde{F} &\equiv -\frac{\log\widetilde{Z}}{\beta}\,.\,. \end{aligned} \tag{2.117}$$

The shifted partition function will then simply be the term $\tilde{p}^N$ in (2.116), which is given by

$$\widetilde{Z}_N = \frac{\exp\left((N+1)|E_{\rm vac}|\beta\left(\frac{L_1^d}{\beta^d}-1\right)\right)-1}{\exp\left(|E_{\rm vac}|\beta\left(\frac{L_1^d}{\beta^d}-1\right)\right)-1}\,. \tag{2.118}$$

The free energy as $N\to\infty$ for $\beta < L_1$ is thus

$$\widetilde{F}_N(U) = -N|E_{\rm vac}|\left(\frac{L_1^d}{\beta^d}-1\right)\,. \tag{2.119}$$

For $\beta > L_1$, we get

$$\widetilde{F}_N(U) = \frac{1}{\beta}\log\left(1-\exp\left(|E_{\rm vac}|\beta\left(\frac{L_1^d}{\beta^d}-1\right)\right)\right)+F_{\rm cor}(\beta)\,, \tag{2.120}$$

where the $F_{\rm cor}(\beta)$ corresponds to another $\mathcal{O}(1)$ contribution coming from subleading corrections to the saddle point as well as the low energy contributions. The free energy thus has a phase transition at $\beta = L_1$ and goes from being $\mathcal{O}(1)$ to $\mathcal{O}(N)$. This precisely matches the phase structure of the bulk gravitational theory.

Modular invariance is not manifest in the shifted free energy above. In order to recover it, we consider the quantity

$$\mathscr{F}(U) = \lim_{N\to\infty}\frac{1}{N}F_N(U)\,, \tag{2.121}$$

where $F_N(U)$ is the unshifted free energy and $\mathscr{F}(U) = \mathscr{F}(\beta, L_1, ..., L_{d-1})$. Using the results obtained above,

$$\mathscr{F}(U) = \begin{cases} -\frac{\varepsilon_{\text{vac}} V_{d-1}}{\beta^d} & \beta < L_1 \\ -\frac{\varepsilon_{\text{vac}} V_{d-1}}{L_1^d} & \beta > L_1 \end{cases}, \tag{2.122}$$

where L_1 is the smallest cycle. The free energy is a modular covariant quantity which transforms under the S transform of $SL(d, \mathbf{Z})$ as

$$\mathscr{F}(\beta, L_1, ..., L_{d-1}) = \frac{L_1}{\beta} \mathscr{F}(L_1, ..., L_{d-1}, \beta). \tag{2.123}$$

Upon checking this transformation rule for (2.122), we see that in both regimes the free energy transforms as expected.

2.6 Discussion

In this chapter we have studied conformal field theories in dimensions $d > 2$ compactified on tori. The main goal was to explore the implications of the assumed invariance under the $SL(d, \mathbf{Z})$ modular group and see what additional constraints on the spectrum would reproduce the phase diagram of gravity in anti-de Sitter space. We have uncovered both similarities and differences with the two-dimensional case. We have presumably only scratched the surface of this interesting subject and many issues and open questions remain, some of which we list below.

2.6.1 Modular invariance

The modular group $SL(d, \mathbf{Z})$ consists of the large diffeomorphisms (i.e. not continuously connected to the identity element) which map a d-dimensional torus to itself. In two dimensions, there are well-known systems, such as the chiral fermion, whose partition function is not modular invariant. However, such theories have gravitational anomalies and can therefore a priori not be consistently defined on arbitrary manifolds. Moreover, when such theories appear in nature, as in the edge modes in the quantum Hall effect, the relevant anomalies are canceled due to an anomaly inflow mechanism which crucially relies on the existence of a higher-dimensional system to which the theory is coupled (for a higher-dimensional version of this statement see e.g. [78]). We are not aware of a local and unitary conformal field theory which is free of local gravitational anomalies and not modular invariant. But modular invariance is weaker than the absence of local gravitational anomalies. There are many modular invariant CFTs with $c_L - c_R \neq 0$ which have

gravitational anomalies, while modular invariance only implies that $c_L - c_R$ must be an integer multiple of 24. It would be interesting to explore the generalizations of these statements to higher dimensions.

Another approach to using modular invariance to learn about conformal field theories on tori is to consider bounds coming from the fixed points of $SL(d, \mathbf{Z})$. This would be a generalization of the "modular bootstrap" [79–86] to higher dimensions. This is valid for general conformal field theories, and taking a large-N limit may give insight into holographic theories.

2.6.2 State-operator correspondence

The usual arguments for the state-operator correspondence in conformal field theory rely on radial quantization and apply to the theory on the spatial sphere S^{d-1} times time. The local operators obtained in this way can be inserted on other manifolds as well but the one-to-one correspondence with states in the Hilbert space no longer applies. The main problem in applying radial quantization to the torus is that, as opposed to spheres, one can not smoothly shrink a torus of dimension larger than one to a point. Stated more precisely, the metric $ds^2 = dr^2 + r^2 d\Omega^2$ is not smooth at $r = 0$ unless Ω is the round unit sphere.

One cannot even apply the standard radial quantization argument to the conformal field theory on $S^1 \times \mathbf{R}^{d-2}$ times time. At $r = 0$, the metric $ds^2 = dr^2 + r^2 d\phi^2 + r^2 dx_i dx_i$ looks like a singular $\mathbf{R}^{d-2}$-dimensional plane, suggesting that some sort of surface operators might be relevant. That such operators are generically needed can for example be seen using the orbifold theories we studied in this chapter. Orbifold theories can be thought of as theories with a discrete gauge symmetry, and in case the theory lives on $S^1 \times \mathbf{R}^{d-2}$ we should include twisted sectors which involve twisted boundary conditions when going around the S^1. These twisted boundary conditions can be detected by a Wilson line operator for the discrete gauge field around the S^1. To create a non-trivial expectation value for the Wilson line operator, we need an operator which creates non-contractible loops, and for this we need an operator localized along a $(d-2)$-dimensional surface. One can think of such operators as a higher-dimensional generalization of the 't Hooft line operators. A local operator in $d > 2$ is unable to generate a non-trivial vev for the discrete Wilson line operator and can therefore not create twisted sector states. Surface operators of dimension $d-2$ which create twisted boundary conditions also feature prominently in the replica trick computations of entanglement entropy in dimensions $d > 2$; they are the generalized twist fields associated to the boundary of the entangling area.

If $(d-2)$-dimensional surface operators are the right operators for the theory on $S^1 \times \mathbf{R}^{d-2}$, it is plausible they are also relevant for CFT's on tori. One can for example consider the surface operators dual to periodic field configurations on $\mathbf{R}^{d-2}$, but it is not clear the resulting surface operator will have the right periodicity as well. Alternatively, one can study the Euclidean theory on an annulus times $\mathbf{T}^{d-2}$, with the annulus having inner radius R_1 and outer radius R_2. The Euclidean path integral in principle provides a map from states on the torus $S^1_{R_1} \times \mathbf{T}^{d-2}$ to $S^1_{R_2} \times \mathbf{T}^{d-2}$, and by taking the limit $R_1 \to 0$ one can imagine obtaining singular boundary conditions for a surface operator localized along a $(d-2)$-torus.

Clearly, more work is required to understand whether the above construction provides a useful version of the state-operator correspondence for field theories on tori, and if it does, what a useful basis for the space of surface operators could possibly be. There seems to be a significant overcounting, as one can construct a surface operator for any choice of state on the torus and for any choice of one-cycle on the torus. Currently, we do not even have a compelling compact Euclidean path integral representation of the ground state of the theory on the torus. See [6] for a more detailed discussion on these issues.

It might also be interesting to explore the state-operator correspondence from an AdS/CFT point of view. One would then need to glue Euclidean caps to the Lorentzian solutions discussed in section 2.3. Since the Lorentzian solutions require a choice of one-cycle which is smoothly being contracted in the interior, a similar choice will be needed for the Euclidean caps, leading apparently once more to the same overcounting as we observed above. It would still be interesting to construct the explicit form of the geometry where a Euclidean cap without the insertion of surface operators is smoothly glued to the Lorentzian AdS solutions. If such solutions could be found, its boundary geometry would provide a Euclidean path integral description of the ground state of the corresponding CFT, at least in the large N and strong coupling approximation.

2.6.3 Defining the orbifold theory

In section 2.5, we defined a prescription to compute the partition function of the orbifold theory. This prescription describes both the Hilbert space and the spectrum of the Hamiltonian on the torus. In two dimensions, the orbifolding prescription also fully describes the procedure to compute arbitrary correlation functions of (un)twisted sector local operators, at least in principle. In higher dimensions, because of the lack of a precise state-operator correspondence, it is not clear wether we have really fully specified a theory. For that, we need to determine the full set of correlation functions and hence know the set of operators

in the theory. It is clear that all untwisted sector correlation functions make sense in the orbifold theory so all local correlation functions are well-defined and calculable. Furthermore, the theory possesses a stress tensor as the stress tensor is always in the untwisted sector. Nevertheless, the questions touching the twisted sector states and/or line operators is much more obscure and it would be very interesting to understand the extent to which the orbifolding prescription fully determines these.

One way orbifold theories in higher dimensions can potentially appear (and therefore inherit a natural definition) are as discrete gauge theories that arise in the infrared limit of a gauge theory with spontaneously broken continuous gauge symmetry (e.g. $SU(N) \to S_N$). This would also explain how to couple the theory to other manifolds, an issue we turn to in the next section.

2.6.4 Orbifold theories on other manifolds

The orbifold theories we studied are most easily defined on tori. However, if we have fully defined a theory we should be able to put it on any manifold. Viewing them as theories with a discrete gauge group also provides a prescription for the sum over twisted sectors when computing the path integral for other manifolds. The sum over twisted sectors is the same as the sum over the space of flat connections modulo an overall conjugation, and for a manifold M this space is $\mathrm{Hom}(\pi_1(M), G)/G$. But even for flat space, where no sum over twisted sectors needs to be taken, there are still signs of the discrete gauge symmetry. In particular, one can consider surface operators which create twisted sector states even on the plane, and their correlation functions contain interesting new information. Such operators naturally arise in the context of Renyi entropy calculation in higher dimensions [87, 88].

2.6.5 Outlook

We have only begun to explore the properties of modular-invariant field theories on tori and their role in AdS/CFT. The interesting relations between the form of the ground state energy, universal free energy at high-temperature, sparseness conditions on the spectrum and vacuum dominance in the partition function beg for a deeper understanding. Is there a more precise relation between the low- and high-energy spectrum that can be rigorously established? Can subleading corrections be systematically analyzed? How much of the rich structure in $d = 2$ and the mathematics of $SL(2, \mathbf{Z})$ can be carried over to $d > 2$? Does all this shed any new light on which theories can have weakly coupled gravitational duals?

3 Holography at Finite Cutoff with a T^2 Deformation

This chapter is based on the following publication:

T. Hartman, J. Kruthoff, E. Shaghoulian and A. Tajdini,
"Holography at finite cutoff with a T^2 deformation",
JHEP **03** (2019), 004, `arXiv:1807.11401 [hep-th]`.

3.1 Introduction

Quantum gravity in finite volume is a difficult problem that is perhaps vital to fundamental cosmology. A natural question is how to apply holographic duality in this context. The avenue we will explore is to impose a hard radial cutoff in AdS and approach this problem as a deformation of AdS/CFT.

The precise relation between a radial cutoff in the bulk geometry and a cutoff in the boundary field theory is a longstanding puzzle in AdS/CFT, discussed since the advent of the duality itself. The UV/IR relation [27] of the duality provides a clue but is far from a precise relationship. In addition to being an important entry in the AdS/CFT dictionary, finding such a relationship may prove fruitful in decoding local physics in the bulk and in constructing a framework for holography in more general spacetimes.

Most of the work on this topic has focused on understanding the long distance physics of the original CFT, in the spirit of the renormalization group [89–94]. Recently, a different perspective was emphasized in [17], in the context of pure 3d gravity. Here the goal is not to understand the original CFT, but to explicitly

deform the CFT so that it reproduces the bulk physics with Dirichlet boundary conditions at finite cutoff. This is a deformed theory in the bulk, dual to a deformed theory on the boundary. The proposal in [17] is that 3d gravity at finite radial cutoff is dual to a 2d CFT deformed by the irrelevant operator $T\bar{T}$, a deformation previously studied in the field theory context by Zamolodchikov and Smirnov [95, 96]. The analytic tractability of CFT deformations by this operator, which follows primarily from the Zamolodchikov factorization equation, allows nontrivial checks of the proposal. This deformation and its holographic interpretation were explored further in [97–106].

In this chapter, we propose an effective field theory (EFT) dual to a general bulk theory at finite cutoff, generalizing the $T\bar{T}$ deformation to higher dimensions and allowing for matter couplings. In the field theory, the tool that will replace the factorization property of $T\bar{T}$ is large-N factorization.

We will first provide a recipe to derive the necessary CFT deformation for arbitrary bulk theories in AdS_{d+1}. Using this recipe, we will find the deformation in several examples. For example, for pure Einstein gravity in $d = 3, 4$, the deformation of the CFT is

$$\frac{\partial S}{\partial \lambda} = \int d^d x \sqrt{\gamma} \left((T_{ij} + b_d G_{ij})(T^{ij} + b_d G^{ij}) - \frac{1}{d-1} (T^i_i + b_d G^i_i)^2 \right) , \qquad (3.1)$$

where λ is a dimensionful coupling, $b_d \propto \lambda^{2/d-1}$ with a coefficient given below, and G_{ij} is the Einstein tensor for the boundary metric. (The expression for arbitrary d is below.)

This flow equation, in which the stress tensor T_{ij} also depends on λ, determines the classical action of the boundary EFT. The background terms in (3.1) induce a redefinition of the operator T_{ij} along the flow, and are necessary to match correlation functions, even on flat backgrounds. We also derive the explicit flow equation for CFTs with scalar operators or at finite $U(1)$ charge density. The scalar case leads to an effective field theory deformed by $\mathcal{O}^2 - (\partial J)^2$, which provides a simple toy model for (3.1). The $U(1)$ case allows us to compare to charged black holes in Einstein-Maxwell theory.

With the CFT deformations in hand we compute various quantities in the deformed CFT and compare to bulk AdS quantities at finite cutoff, finding perfect agreement for $\lambda > 0$. In particular, we will match the two-point correlation functions in vacuum, as well as the energy spectrum and thermodynamics.

A finite Dirichlet cutoff in the bulk is a dramatic, and perhaps violent, deformation of the gravitational theory. Intuitively, this is because gravity with reflecting boundary conditions induces negative image masses on the other side of the wall,

which screen the gravitational force. This raises the possibility that the theory violates causality, as discussed in [17,107,108], or that the dual EFT cannot be UV-completed as an ordinary quantum field theory for positive λ (see e.g. [109]). We will sidestep these issues by restricting the discussion to physics below the cutoff, where both sides of the duality appear to make sense, at least perturbatively. Some speculations on the the UV are mentioned in the discussion section.

It is also possible to consider the deformation with $\lambda < 0$. In this case, the asymptotic density of states is super-Hagedorn in the UV, giving a scaling $\log \rho \propto E^{\frac{2(d-1)}{d}}$. Intriguingly, this scaling agrees with the density of states of p-branes (with $p = d-1$) in the semiclassical approximation [110–113]. The matching with Hagedorn scaling in $d = 2$ is an important aspect of relating (a single-trace version of) this deformation to little string theory [114–118].

The derivation starts with the Hamilton-Jacobi equation in the bulk, and uses the techniques of holographic renormalization developed in [89,90,119,120]. However, instead of trying to relate (3.1) to an RG equation, we view it as the definition of a boundary EFT that can be studied on its own terms. This is the perspective taken in [17], in contrast to the earlier work cited above. This approach leaves open the mysterious question emphasized in [91,121] of what coarse-graining or cutoff procedure in the QFT actually produces the flow (3.1). If this procedure were known, then (3.1) would need to emerge from it automatically, whereas in our approach the bulk Hamiltonian must be input by hand.

Although the operator (3.1) has been derived from a bulk calculation, it is an EFT operator, giving a purely field-theoretic definition of the deformation, as in the 2d case. Like in 2d, the deformation is defined order by order in conformal perturbation theory in λ, but unlike in 2d, it is only unambiguously defined in perturbation theory in $1/N$. For $d = 2$ a nonperturbative definition for the theory on Minkowski spacetime is provided by the S-matrix [98], or at $c = 24$ with certain sign of the coupling by critical string theory [122].

As this work was being completed, [123] appeared, which also derives the source-free versions of equation (3.1) and the corresponding equation (3.53) with $U(1)$ charge.

3.1.1 The dictionary at finite cutoff

In the rest of this introduction, we will present our proposed dictionary for the EFT dual to a sharp radial cutoff in AdS. Begin by choosing coordinates

$$ds^2 = g_{\mu\nu}dx^\mu dx^\nu = N(r)^2 dr^2 + r^2 \gamma_{ij} dx^i dx^j \ , \tag{3.2}$$

with $N(r) \to 1/r$ near the boundary and where we have set the AdS radius $\ell_{AdS} = 1$. The usual AdS/CFT dictionary states

$$Z_{CFT}[\gamma_{ij}, J] = \lim_{r_c \to \infty} Z_{grav}[g^0_{ij} = r_c^2 \gamma_{ij}, \phi_0 = r_c^{\Delta - d} J] \ . \tag{3.3}$$

On the left is the CFT generating function, in the metric γ_{ij}, with source J for a scalar operator $\mathcal{O}$ of dimension Δ. (Later we will generalize to spinning sources.) On the right is the gravitational path integral with the Dirichlet boundary conditions

$$g_{ij}(r_c, x) = g^0_{ij}(x), \quad \phi(r_c, x) = \phi_0(x) \ . \tag{3.4}$$

In (3.3), we have inserted the explicit factors of the radial cutoff r_c to ensure that CFT correlators, computed by $\left(\frac{1}{\sqrt{\gamma}} \frac{\delta}{\delta J}\right) \left(\frac{1}{\sqrt{\gamma}} \frac{\delta}{\delta \gamma_{ij}}\right) \cdots \log Z$, are normalized to be independent of r_c.

There is considerable arbitrariness in how the dictionary (3.3) should be extended to finite r_c. We choose the simplest prescription, which is to assume that the same dictionary defines an effective boundary theory at finite r_c:

$$Z_{EFT}[r_c; \gamma_{ij}, J] = Z_{grav}[g^0_{ij} = r_c^2 \gamma_{ij}, \phi_0 = r_c^{\Delta - d} J] \ . \tag{3.5}$$

It is not clear that the right-hand side always makes sense, even classically, since Dirichlet boundary conditions for gravity are problematic (e.g. [124]). Nor is it guaranteed that the QFT on the left really exists. We will simply take the assumption (3.5) as our starting point, and explore whether it leads to a reasonable prescription. We will see in several examples that it does make sense, at least perturbatively about a background, and that the QFT can be constructed as a deformation of the original CFT.

The deformation involves operators inserted at coincident points. In general, this would be problematic and require a careful definition of the composite operator. However, at large N, we can simply define this operator by normal ordering, in the sense of discarding self-contractions. This is the procedure that will reproduce semiclassical physics in the bulk and is what we adopt here. Equivalently, $\mathcal{O}(x)^2$ is defined to be the leading non-identity operator in the $\mathcal{O}(x)\mathcal{O}(y)$ OPE that is not suppressed in the $1/N$ expansion.

The rescaling of the sources in (3.5) is natural in the CFT limit, but may not be the most natural choice far from the boundary. Since we will keep track of the full nonlinear source dependence, this is just a change of variables that does not affect the physics. The choice of counterterms at finite cutoff is ambiguous; in particular, to connect to the usual CFT answers as the coupling goes to zero, any counterterms – not necessarily even local or Lorentz-invariant – can be added as long as they vanish in the zero coupling limit. As we will see in sections 3.2-3.3,

the choice of counterterms affects the flow that is derived in the dual field theory. Different choices will lead to different flows in the dual EFT, which by design will have been constructed to match bulk physics at finite cutoff. We will always make the simplest choice of only including the usual holographic counterterms.

The boundary theory on the left of (3.5) is labeled an effective field theory because it has irrelevant operators, and therefore will not make sense at high enough energy. It is defined in conformal perturbation theory as a CFT plus irrelevant operators. We do not provide a nonperturbative definition of the theory, although we will see that certain quantities – like the energy spectrum at finite volume and correlation functions – can be formally calculated at finite r_c.

In the next two sections, the goal is to systematically derive the EFT as a deformation of the original CFT.

Throughout the chapter, we work classically in the bulk, and to leading order in $1/N$ in the boundary. Our notation is as follows:

Bulk coordinates:	(r, x)
Bulk spacetime metric:	$g_{\mu\nu}$
Induced metric at $r = r_c$:	$g^0_{ij}(x) = g_{ij}(r_c, x)$
CFT metric:	$\gamma_{ij} = r_c^{-2} g^0_{ij}$
Bulk scalar field:	ϕ
Boundary value:	$\phi_0(x) = \phi(r_c, x)$
CFT source:	$J = r_c^{d-\Delta}\phi_0$
Bulk on-shell action:	$W[g^0, \phi_0]$
Bulk Brown-York tensor:	$\widetilde{T}_{ij}$
Boundary stress tensor:	$T_{ij} = r_c^{d-2}\widetilde{T}_{ij}$

Various sign conventions are in appendix A.2.

3.2 Scalar example

We first consider the case where gravity is decoupled, and the bulk theory consists of just a scalar field ϕ. This section serves to illustrate the methods, including differences from the standard holographic RG, but otherwise stands alone from the rest of the chapter and can be skipped. The final answer is equivalent to results found in e.g. [91, 92, 100, 125], but our approach is to add nonlinear source dependence to the classical action of the EFT. This gives a local prescription in the

boundary theory, in contrast to the scalar discussion in [100], which was phrased in terms of the non-local effective action.

3.2.1 Flow equation of the dual EFT

Classically, the bulk path integral is computed by the on-shell action, $W[r_c;\phi_0(x)]$. The flow of this functional is governed by the Hamilton-Jacobi equation,

$$\frac{\partial}{\partial r_c}W[r_c;\phi_0] = -H[\phi_0, \frac{\delta W}{\delta\phi_0}]\,, \tag{3.6}$$

where $H[\phi,\pi]$ is the scalar Hamiltonian for evolution in the r direction. To derive the EFT at finite cutoff, we write $Z_{grav} = e^{-W}$, apply the flow equation to the dictionary (3.5), then translate back to the field theory:

$$\begin{aligned}\frac{d}{dr_c}Z_{EFT}[r_c;J = r_c^{d-\Delta}\phi_0] &= H[\phi_0, -\frac{\delta}{\delta\phi_0}]e^{-W[r_c;\phi_0]} \\ &= H[\phi_0, -\frac{\delta}{\delta\phi_0}]Z_{EFT}[r_c;J = r_c^{d-\Delta}\phi_0]\end{aligned} \tag{3.7}$$

This is now written as a total derivative, because ϕ_0 is fixed but J is not. (Second variations $\frac{\delta^2 W}{\delta\phi_0^2}$ drop out in the classical limit, reproducing (3.6).) Next, bring the Hamiltonian inside the EFT path integral to obtain

$$\begin{aligned}&\frac{d}{dr_c}Z_{EFT}[r_c;J = r_c^{d-\Delta}\phi_0] \\ &\quad= \int D\varphi H[\phi_0, -r_c^{d-\Delta}\sqrt{\gamma}\mathcal{O}]\exp\left(-S_{EFT}(r_c,J;\varphi) + \int d^dx\sqrt{\gamma}\mathcal{O}\phi_0 r_c^{d-\Delta}\right)\,.\end{aligned} \tag{3.8}$$

φ denotes the fields in the boundary theory. Equating this with $\frac{d}{dr_c}Z_{EFT} = \int D\varphi\frac{d}{dr_c}e^{-S_{EFT}+\int\sqrt{\gamma}OJ}$ gives the flow equation for the EFT:

$$\frac{d}{dr_c}S_{EFT} = -H[r_c^{\Delta-d}J, -r_c^{d-\Delta}\sqrt{\gamma}\mathcal{O}] + \frac{d-\Delta}{r_c}\int d^dx\sqrt{\gamma}J\mathcal{O}\,. \tag{3.9}$$

It is convenient to absorb the source term into the action (and not write the φ dependence explicitly),

$$\hat{S}_{EFT}(r_c,J) = S_{EFT}(r_c,J) - \int d^dx\sqrt{\gamma}J\mathcal{O}\,. \tag{3.10}$$

Then the flow equation takes the form $\frac{d}{dr_c}\hat{S}(r_c,J(r_c)) = -H$. This derivative is taken at fixed value of the bulk boundary condition ϕ_0, so with $J'(r_c) = \frac{d-\Delta}{r_c}J(r_c)$.

For EFT calculations, it is more natural to define the flow in terms of the partial derivative at fixed J,

$$\frac{\partial}{\partial r_c}\hat{S}_{EFT}(r_c, J) = -H[r_c^{\Delta-d}J, -r_c^{d-\Delta}\sqrt{\gamma}\mathcal{O}] + \frac{d-\Delta}{r_c}\int d^dx\sqrt{\gamma}J\mathcal{O}\,. \tag{3.11}$$

This is the final result for the scalar. At each step along the flow, the operator $\mathcal{O}$ must be redefined according to

$$\mathcal{O} = -\frac{1}{\sqrt{\gamma}}\frac{\delta}{\delta J}\hat{S}_{EFT}\ . \tag{3.12}$$

Therefore (3.11), with the latter relation plugged in, should be viewed as a functional PDE for $\hat{S}$, similar to the Hamilton-Jacobi equation. The difference is that (3.11) defines the flow of a local action on the boundary, whereas the Hamilton-Jacobi equation (3.6) defines the flow of the non-local, on-shell action in the bulk.

3.2.2 Free massive scalar

To make this formalism explicit, consider a free, massive scalar field in the bulk,

$$S_{bulk} = \frac{1}{2}\int d^{d+1}x\sqrt{g}\left((\partial\phi)^2 + m^2\phi^2\right) + \frac{d-\Delta}{2}\int_{\partial M} d^dx\sqrt{g^0}\phi_0^2\ , \tag{3.13}$$

with $m^2 = \Delta(\Delta-d)$, in vacuum AdS, $ds^2 = \frac{dr^2}{r^2} + r^2dx^2$. The boundary counterterm is added to cancel the leading divergence in the action. The radial Hamiltonian is

$$H[\phi_0, \pi] = \frac{1}{2}\int d^dx N(r_c)\left(\frac{\pi^2}{\sqrt{g^0}} - 2(d-\Delta)\pi\phi_0 - \sqrt{g^0}(\partial\phi_0)^2\right)\ . \tag{3.14}$$

The counterterm has been included by integrating by parts to write it as a bulk term in the action. The EFT dual to this theory at finite cutoff is defined by the flow equation (3.11), which together with our dictionary gives

$$\frac{\partial}{\partial r_c}\hat{S}_{EFT}(r_c, J) = \frac{1}{2}\int d^dx\left(-r_c^{d-2\Delta-1}\mathcal{O}^2 + r_c^{2\Delta-d-3}(\partial J)^2\right). \tag{3.15}$$

This defines the corresponding deformation of the CFT, where r_c is now viewed as a dimensionful coupling constant of the EFT.[1]

[1] Note that the linear term in (3.9) canceled, due to the counterterm. In principle we should include additional counterterms to cancel all of the divergences, which would produce additional terms in the deformation; however this is unnecessary to compute the two-point function. We will include the full set of counterterms in the gravitational case.

3.2.3 Scalar correlators

Now we will demonstrate how to obtain bulk correlation functions at finite cutoff, using the boundary theory defined by (3.15). The background terms play a crucial role. Of course this check is guaranteed to succeed, because by design, the bulk and boundary correlators obey the same flow equation.

In the bulk, the on-shell action is quadratic, so for any value of r_c it takes the form

$$W[r_c, \phi_0(k)] = \frac{1}{2}\int \frac{d^d k}{(2\pi)^d}\phi_0(k)\phi_0(-k)F(r_c;k)\ . \tag{3.16}$$

F is calculated by solving the wave equation with Dirichlet boundary conditions and plugging into the action. This is a standard exercise that leads to

$$F(r_c;k) = r_c^d(d-\Delta) + r_c^{d+1}\left.\frac{\partial_r(r^{-d/2}K_\nu(k/r))}{r_c^{-d/2}K_\nu(k/r)}\right|_{r=r_c} \tag{3.17}$$

where $\nu = \sqrt{d^2/4+m^2}$. According to our dictionary (3.5), this gives the boundary two-point function $G(r_c;k) = -r_c^{2(\Delta-d)}F(r_c;k)$. The function G is defined through the correlator in momentum space:

$$\langle \mathcal{O}(\mathbf{k})\mathcal{O}(\mathbf{k}')\rangle = (2\pi)^d\delta(\mathbf{k}+\mathbf{k}')G(r_c;k). \tag{3.18}$$

Now we will reproduce this from a boundary calculation. The flow equation (3.11) implies for the two-point function

$$\begin{aligned}\frac{\partial}{\partial r_c}\left(\frac{1}{\sqrt{\gamma}}\frac{\delta}{\delta J}\right)\left(\frac{1}{\sqrt{\gamma}}\frac{\delta}{\delta J}\right)\log Z_{EFT}\Big|_{J=0} &= -\frac{\delta}{\delta J}\frac{\delta}{\delta J}\left\langle\frac{\partial}{\partial r_c}\hat{S}_{EFT}\right\rangle\Big|_{J=0} \\ &= -\int d^dx\frac{\delta}{\delta J}\frac{\delta}{\delta J}\left\langle \tfrac{1}{2}r_c^{2\Delta-d-3}(\partial J)^2 - \tfrac{1}{2}r_c^{d-2\Delta-1}O^2\right\rangle\Big|_{J=0}\end{aligned} \tag{3.19}$$

Therefore

$$\frac{d}{dr_c}G = -k^2r_c^{2\Delta-d-3} + r_c^{d-2\Delta-1}G^2\ . \tag{3.20}$$

In the last term, we have invoked the large-N normal-ordering procedure discussed below (3.5) to write

$$\frac{\delta}{\delta J(x_1)}\frac{\delta}{\delta J(x_2)}\langle\mathcal{O}(x)^2\rangle\Big|_{J=0} = 2\frac{\delta\langle\mathcal{O}(x)\rangle}{\delta J(x_1)}\frac{\delta\langle\mathcal{O}(x)\rangle}{\delta J(x_2)}\Big|_{J=0} = 2G(x-x_1)G(x-x_2)\,, \tag{3.21}$$

where $G(x-x_1) = \langle\mathcal{O}(x)\mathcal{O}(x_1)\rangle$. The solution of (3.20), if we impose the CFT form at $r_c\to\infty$, is $G(r_c;k) = -r_c^{2(\Delta-d)}F(r_c;k)$, with $F(r_c;k)$ given by (3.17).

Notice that the correlator does not flow for $\Delta = (d+1)/2$, which has a natural explanation in the bulk. This value of the scaling dimension corresponds to a conformally coupled scalar. Weyl invariance then allows us to rescale r_c (or more accurately ℓ_{AdS}, but this has the same effect since we have set $\ell_{AdS} = 1$). Notice that Weyl invariance is crucial; the argument does not work for massless fields in the bulk (unless $d = 1$), and it is easily checked that the correlator for such fields has a nontrivial flow. We will see this feature again in section 3.7.1 when we compute the flow of the two-point function of a Maxwell gauge field, where we will find that the correlator does not flow when $d = 3$.

3.3 Deriving the deformation with gravity

Now we turn to the general case of gravity coupled to matter. The deformation can be derived in two different ways. The first is to find an equation for the trace of the renormalized Brown-York stress tensor, just as was done in two dimensions by [100]. The second derivation is more directly analogous to the scalar example in section 3.2, and follows from the observation that the partition function of the EFT on a radial slice has to be a solution to the radial Wheeler-DeWitt equation in order to describe gravitational physics.

The two derivations are essentially equivalent, but offer different perspectives. We will describe both.

3.3.1 Trace equation

Consider a Euclidean radial slicing of the form

$$ds^2 = \frac{dr^2}{r^2} + g_{ij}(r,x)dx^i dx^j, \tag{3.22}$$

where $g^0_{ij}(x) \equiv g_{ij}(r_c, x)$ is the metric on the cutoff surface. The renormalized Brown-York stress tensor is [126]

$$\widetilde{T}_{ij} = \frac{1}{8\pi G}\left(K_{ij} - K g^0_{ij} + (d-1)g^0_{ij}\right) - a_d \widetilde{C}_{ij}\ , \tag{3.23}$$

where a_d is a constant. See the appendix for conventions. We have separated the counterterms into two pieces: The counterterm $\int_{\partial M}\sqrt{g^0}$ gives the g^0_{ij} contribution above, and the curvature-dependent counterterms define the quantity $\widetilde{C}_{ij}[g^0_{ij}]$. Tildes are reserved for bulk quantities which will appear in our final deformation; they need to be appropriately rescaled to translate into EFT variables. This stress

tensor satisfies

$$\widetilde{T}^i_i + a_d \widetilde{C}^i_i = -4\pi G \left[(\widetilde{T}_{ij} + a_d \widetilde{C}_{ij})^2 - \frac{1}{d-1} (\widetilde{T}^i_i + a_d \widetilde{C}^i_i)^2 \right] - \frac{\widetilde{R}}{16\pi G} + \widetilde{t}^r_r \,, \quad (3.24)$$

where $\tilde{t}_{ij}$ is the matter stress tensor. This equation can be derived by plugging in the expression for $\widetilde{T}_{ij}$ in the right-hand side and using the Hamiltonian constraint (for the radial slicing) in the bulk:

$$K^2 - K_{ij}K^{ij} - d(d-1) - \widetilde{R} + 16\pi G \widetilde{t}^r_r = 0 \,. \quad (3.25)$$

From this equation for the stress tensor, we can infer the deformation in the field theory, in the sense of a flow equation. We will temporarily drop the matter term $\widetilde{t}_{ij}$ to derive the flow for pure Einstein gravity. We write the deformation of the classical action in terms of a local operator X as

$$\frac{\partial S_{EFT}}{\partial \lambda} = \int d^d x \sqrt{\gamma} X \,, \quad (3.26)$$

with λ a dimensionful parameter that governs the size of the deformation.

In a theory with only one dimensionful scale λ, invariance under a change of units implies for the effective action

$$\lambda \frac{\partial W}{\partial \lambda} = \frac{1}{\Delta_\lambda} \int d^d x \sqrt{\gamma} \langle T^i_i \rangle \,, \quad (3.27)$$

with Δ_λ the mass dimension of λ. Combining (3.27) and (3.26) with the *bulk* trace relation (3.24) suggests the deformation

$$X = (T_{ij} + a_d r_c^{d-2} \widetilde{C}_{ij})^2 - \frac{1}{d-1} (T^i_i + a_d r_c^{d-2} \widetilde{C}^i_i)^2 - \frac{r_c^d}{d\lambda} \left(\widetilde{t}^r_r - \frac{\widetilde{R}}{16\pi G} - a_d \widetilde{C}^i_i \right) . \quad (3.28)$$

This is a field theory equation, so T_{ij} is the field theory stress tensor, and indices are raised with γ^{ij}. It was obtained from (3.24) by replacing bulk with boundary quantities, $g^0_{ij} = r_c^2 \gamma_{ij}$, and $\widetilde{T}_{ij} = r_c^{2-d} T_{ij}$. Other tilded quantities must also be rescaled, which we will do when considering explicit examples.

With this choice of deformation operator, we have $\Delta_\lambda = -d$ and the relation between the boundary coupling λ and bulk radial cutoff r_c is

$$\lambda = \frac{4\pi G}{d\, r_c^d} \,. \quad (3.29)$$

For a four or five dimensional bulk

$$\widetilde{C}_{ij} = \widetilde{G}_{ij} = G_{ij}, \qquad a_d = \frac{1}{8\pi G(d-2)} \,, \quad (3.30)$$

with $\widetilde{G}_{ij}$ the Einstein tensor for g^0_{ij} and G_{ij} the Einstein tensor for γ_{ij}. In general dimensions for a flat metric γ_{ij} we have $\widetilde{C}_{ij} = 0$.

There are some subtleties in this argument. The first is the issue of anomalies. The expression (3.28) includes terms built entirely from background fields. The $O(r_c^0)$ background-only terms in $r_c\partial_{r_c} W$, which occur only in even d, give precisely the conformal anomaly (since they correspond to $\log r_c$ terms in W). The interpretation is that we are implicitly measuring the UV cutoff in units of λ, so the UV cutoff changes along the flow, and this contributes to (3.26) via the Weyl anomaly. In other words, S_{EFT} must be regulated, and the effect of the regulator has been included in (3.28). This will be clear in the even-dimensional examples below.

Also, in (3.28), we have assumed that there are no additional contributions, beyond the trace anomaly, from renormalization. This is not obvious, and will only be justified *a posteriori* by comparison to the bulk. Finally, the composite operators in (3.28) must be regulated somehow. In the 2d case, it turned out that the regulator was unnecessary, due to the factorization property [95]; in higher dimensions, we use the large-N normal ordering procedure discussed in section 3.1.1.

Let us now give the explicit form of the deformation X in two, three, and four boundary dimensions without bulk matter. In two and four dimensions we will make the contribution of the trace anomaly manifest.

Deformation in $d = 2$

In two boundary dimensions, the deformation was already derived in the references cited above, but we will give it for completeness. The trace anomaly is

$$\mathcal{A} \equiv \langle T^i_i \rangle_{CFT} = -\frac{c}{24\pi} R = -\frac{r_c^2}{16\pi G}\widetilde{R}\,, \tag{3.31}$$

where we used $c = 3/2G$ and $R = r_c^2\widetilde{R}$. In $d = 2$ we have $\widetilde{C}_{ij} = 0$ since all curvature counterterms are absent. Combining this with (3.31) we deduce that the deformation is

$$X = T_{ij}T^{ij} - (T^i_i)^2 - \frac{1}{2\lambda}\mathcal{A}\,. \tag{3.32}$$

The first two terms are often denoted in terms of $T\bar{T} \equiv 1/8\left(T_{ij}T^{ij} - (T^i_i)^2\right)$. As discussed above, the total deformation X includes both the explicit deformation of the EFT Lagrangian by the operator $\delta\mathcal{L} = T\bar{T}\delta\lambda$, and the contribution from the Weyl anomaly as we rescale the UV cutoff.

Deformation in $d = 3$

For a three dimensional boundary, there is no trace anomaly, so the deformation is

$$X = (T_{ij} + a_3 r_c G_{ij})^2 - \frac{1}{2}(T^i_i + a_3 r_c G^i_i)^2 \ . \tag{3.33}$$

In this equation, $a_3 r_c$ has to be expressed in terms of boundary data:

$$a_3 r_c = \frac{1}{6^{1/3}} \left(\frac{1}{8\pi G}\right)^{2/3} \lambda^{-1/3} = \alpha_3 \lambda^{-1/3} \ . \tag{3.34}$$

Here α_3 is a function of N on the boundary, but is independent of λ. The deformation of the boundary theory is thus

$$X = \left(T_{ij} + \frac{\alpha_3}{\lambda^{1/3}} G_{ij}\right)^2 - \frac{1}{2}\left(T^i_i + \frac{\alpha_3}{\lambda^{1/3}} G^i_i\right)^2 \tag{3.35}$$

Note that despite the inverse powers of λ, the CFT limit $\lambda \to 0$ is regular, since the first order deformation is $\delta\mathcal{L} = \lambda X$.

Deformation in $d = 4$

In a four dimensional boundary theory, the trace anomaly for a theory dual to Einstein gravity is

$$\mathcal{A} = -\frac{C_T}{8\pi}\left(G_{ij}G^{ij} - \frac{1}{3}(G^i_i)^2\right) \ , \tag{3.36}$$

with $C_T = \frac{1}{8G}$ [127]. Therefore the deformation (3.28) may be written

$$X = T_{ij}T^{ij} - \frac{1}{3}(T^i_i)^2 + 2a_4 r_c^2 \left(G^{ij}T_{ij} - \frac{1}{3}G^i_i T^j_j\right) - \frac{1}{4\lambda}\mathcal{A} \tag{3.37}$$

with $a_4 r_c^2 = \alpha_4 \lambda^{-1/2}$. As before, α_4 is fixed in terms of $1/G$.

Comments on the flow equation

Note that in going infinitesimally from $r_c \to r_c + \delta r_c$, the *deformed* T_{ij}, at the value r_c, must be used on the right-hand side of the flow equation. This means that, like the Hamilton-Jacobi equation, it must be viewed as a functional equation for S, with $T_{ij} = -\frac{2}{\sqrt{\gamma}}\frac{\delta S}{\delta \gamma^{ij}}$. The difference, however, is that this defines the flow of a local functional – the EFT action – whereas the Hamilton-Jacobi equation governs the flow of the bulk on-shell action.

There is one last subtlety to address in the meaning of the flow equation (3.27). This is written as a partial derivative $\frac{\partial}{\partial\lambda}$ because the EFT metric, and other sources if present, are held fixed. Ultimately, however, the dictionary (3.5) equates

the bulk theory to a boundary theory where the boundary metric $\gamma_{ij} = r_c^{-2} g^0_{ij}$ may itself be a function of r_c. The only time this will occur in our examples is when we consider bulk black hole geometries to compute the deformed energy spectrum. In this case, γ_{00} is r_c-dependent but the metric is diffeomorphic to the original, undeformed metric. Thus we can compare quantities computed in the deformed and undeformed metrics simply by a coordinate rescaling at the end of the calculation. But if the intrinsic geometry of the boundary changes along the flow, then the bulk is dual to $S_{EFT}[\lambda, \gamma_{ij}(\lambda)]$, which includes an additional term $\frac{1}{2} T^{ij} \partial_{r_c} \gamma_{ij}$ in the total flow equation for $\frac{d}{d\lambda} S_{EFT}$.

Sources for irrelevant operators can induce a large backreaction, destroying the AdS boundary. This is not a problem here because of the finite radial cutoff — the backreaction is assumed to be small where the flow starts, at some large but finite r_c, and any problems with the AdS asymptotics occur only for $r > r_c$. This is similar to the situation in the boundary EFT, where the CFT deformed by an irrelevant operator is sensible below the cutoff set by the mass scale of the deformation.

3.3.2 Wheeler-DeWitt method

Another perspective on this derivation is provided by the Wheeler-DeWitt equation. This is closer to the scalar derivation in section 3.2, where we translated the bulk Hamilton-Jacobi equation into a deformation of the dual EFT. We will also include matter sources in this discussion.

Without gravity, the Hamilton-Jacobi equation governs the flow of the on-shell action $\frac{\partial}{\partial r_c} W[r_c; \phi_0]$, with boundary sources held fixed. But once gravity is included, this equation is trivial, because the on-shell action is no longer an explicit function of the cutoff r_c — explicit dependence on r_c is a pure diffeomorphism, so does not affect the value of the action. Instead, the action depends on the cutoff only via the induced metric, $W = W[g^0_{ij}, \phi_0]$. To keep track of this, we define the flow with boundary values of non-metric fields $\phi_0(x)$ held fixed, but make the induced metric a function of the cutoff, $g^0_{ij} = g^0_{ij}(r_c, x)$.

Assume the bulk metric takes the form (3.2). The renormalized on-shell action (i.e. including holographic counterterms) obeys

$$\frac{d}{dr_c} W[g^0_{ij}(r_c, x), \phi_0] = \frac{1}{2} \int d^d x \sqrt{g^0}\ \widetilde{T}^{ij} \partial_{r_c} g^0_{ij} \tag{3.38}$$

where $\widetilde{T}^{ij}$ is the renormalized Brown-York stress tensor, since it is obtained by

varying the renormalized on-shell action. Writing $g^0_{ij} = r_c^2 \gamma_{ij}$, this becomes

$$r_c \frac{d}{dr_c} W[g^0_{ij}(r_c, x), \phi_0] = \int d^d x \sqrt{g^0} \widetilde{T}^i{}_i + \frac{r_c^3}{2} \int d^d x \sqrt{g^0} \widetilde{T}^{ij} \partial_{r_c} \gamma_{ij} \ . \tag{3.39}$$

At this point, this separation of the trace is somewhat arbitrary, but useful, as we will see. This is turned into a flow equation by substituting the Hamiltonian constraint into the first term. In general, this constraint can be written

$$\widetilde{T}^i{}_i = \Theta \ , \tag{3.40}$$

where Θ is built from both $\widetilde{T}_{ij}$ and the matter fields. Although (3.39) has no dynamics as written, once we replace $\widetilde{T}^i{}_i \to \Theta$, it becomes the classical Wheeler-DeWitt equation, which encodes the dynamical equations of the classical bulk theory, and is the gravitational analogue of the Hamilton-Jacobi equation.

Now we repeat the argument used in the scalar case to derive the flow equation in the dual EFT. First, write Θ in terms of the canonical data:

$$\Theta = \Theta[g^0_{ij}, p_{ij}, \phi_0, \pi] \ , \tag{3.41}$$

where $p_{ij} \equiv \sqrt{g^0} \widetilde{T}_{ij}$ and π is the momentum conjugate to ϕ. Translating (3.38) into the language of the boundary field theory, we have

$$r_c \frac{d}{dr_c} Z_{EFT}[r_c; \gamma_{ij} = r_c^{-2} g^0_{ij}, J = r_c^{d-\Delta} \phi_0] \tag{3.42}$$

$$= - \left(\int d^d x \sqrt{g^0}\, \Theta[g^0_{ij}, -\frac{2\delta}{\delta g^{0ij}}, \phi_0, -\frac{\delta}{\delta \phi_0}] + r_c \int d^d x\, \partial_{r_c} \gamma_{ij} \frac{\delta}{\delta \gamma_{ij}} \right) Z_{EFT} \ . \tag{3.43}$$

Pulling this inside the EFT path integral, as we did for the scalar around (3.8), gives (up to the anomaly)

$$r_c \frac{d}{dr_c} \hat{S}_{EFT} = r_c^d \int d^d x \sqrt{\gamma}\, \Theta[r_c^2 \gamma_{ij}, r_c^2 \sqrt{\gamma} T_{ij}, r_c^{\Delta - d} J, -r_c^{d-\Delta} \mathcal{O}] + \frac{r_c}{2} \int d^d x \sqrt{\gamma}\, T^{ij} \partial_{r_c} \gamma_{ij} \ . \tag{3.44}$$

We have included the full source dependence in $\hat{S}_{EFT}$, defined e.g. as in (3.10) for a scalar source with corresponding generalizations for other fields. As discussed above, counterterms are also included, so the flow includes the contribution of the trace anomaly.

3.3.3 The final prescription

To recap, the general answer is as follows. The deformation of the boundary effective field theory is given by the flow equation

$$r_c \frac{\partial}{\partial r_c} S_{EFT} = r_c^d \int d^d x \sqrt{\gamma}\, \Theta \,. \tag{3.45}$$

Θ is the right-hand side of the constraint equation (3.40), with the rescalings appropriate to translate from bulk to boundary variables,

$$g^0_{ij} \to r_c^2 \gamma_{ij}, \quad \widetilde{T}_{ij} \to r_c^{2-d} T_{ij}, \quad \phi_0 \to r_c^{\Delta - d} J, \quad \pi \to \sqrt{\gamma} r_c^{d-\Delta} \mathcal{O} \,. \tag{3.46}$$

The partial derivative in (3.45) is taken with γ_{ij}, J held fixed – but to match the bulk, the sources and background metric must also be modified along the flow according to (3.44). The rescalings of $J, \mathcal{O}$ for spin-L fields have additional factors of r_c^L. For bulk p-forms, which we will consider for $p = 1$ in the next subsection, we have

$$\phi^0_{\mu_1 \cdots \mu_p} \to r_c^{\Delta - d + p} J_{\mu_1 \cdots \mu_p} \,, \qquad \pi^{\mu_1 \cdots \mu_p} \to \sqrt{\gamma} r_c^{d - \Delta - p} \mathcal{O}^{\mu_1 \cdots \mu_p} \,. \tag{3.47}$$

3.3.4 Matter contributions and the $U(1)$ case

Matter is automatically included in the prescription (3.45), simply by including the matter Hamiltonian $\tilde{t}^r_r$ on the right-hand side of the constraint equation (3.40). This reproduces, for example, the scalar results in section 3.2, upon sending $G \to 0$ with the matter action held fixed.

Another interesting case is a $U(1)$ gauge field A_μ in the bulk, dual to a conserved $U(1)$ current in the boundary field theory. The Dirichlet boundary condition in AdS/CFT fixes the non-normalizable mode of A_μ, which means fixing the chemical potential μ of the boundary field theory.

For a Maxwell field in the bulk the Euclidean Lagrangian is given by

$$\mathcal{L}_m = \frac{1}{4e^2} F_{\mu\nu} F^{\mu\nu}. \tag{3.48}$$

Its stress tensor follows from the usual prescription and the rr component reads

$$\tilde{t}^r_r = \frac{1}{4e^2} F_{ij} F^{ij} - \frac{1}{2e^2} F^{ri} F_{ri} \tag{3.49}$$

To apply our dictionary, we can write this in terms of the canonical momentum π_i of the gauge field in the bulk,

$$\tilde{t}^r_r = \frac{1}{4e^2} F_{ij} F^{ij} - \frac{e^2}{2} \frac{\pi_i \pi^i}{\left(\sqrt{g^0}\right)^2}. \tag{3.50}$$

The canonical momentum π_i and bulk non-normalizable mode $A_{(0)i}$ are related to the boundary operator and source as

$$\pi_i \to \sqrt{\gamma} r_c^2 J_i, \quad A_{(0)i} \to A_i. \tag{3.51}$$

In combination with (3.46), we find

$$\tilde{t}_r^r = -\frac{e^2}{2} r_c^{2-2d} J_i J^i + \frac{1}{4e^2} r_c^{-4} F_{ij} F^{ij}, \tag{3.52}$$

where all contractions are done with γ_{ij}. The flow of the effective action is thus

$$r_c \frac{\partial}{\partial r_c} S_{EFT} = r_c^d \int d^d x \sqrt{\gamma} \left(\Theta_{\text{grav}} - \frac{e^2}{2} r_c^{2-2d} J_i J^i + \frac{1}{4e^2} r_c^{-4} F_{ij} F^{ij} \right). \tag{3.53}$$

For a complete identification of bulk data with boundary data, we have to convert constants such as e^2 to boundary data. This quantity has dimension $3-d$ and is related to the coefficient C_J of the two-point function of conserved currents. Specifically, in the field theory on $\mathbb{R}^d$ this two-point function is

$$\langle J_i(x) J_j(y) \rangle = \frac{C_J}{(2\pi)^d} \left(\partial^2 \delta_{ij} - \partial_i \partial_j \right) \frac{1}{|x-y|^{2(d-2)}}, \tag{3.54}$$

and the relation between C_J and e^2 is given by

$$e^2 = \frac{1}{C_J \alpha_J}, \quad \alpha_J = \frac{(d-1)\Gamma(d/2)}{2^{d-2} \pi^{d/2} \Gamma(d)}. \tag{3.55}$$

This allows us to translate any coefficient in (3.53) to functions of λ and dimensionless numbers that are, as we will see, powers of N. For example, rewriting the r_c dependence in terms of λ, we find:

$$\frac{\partial S_{EFT}}{\partial \lambda} \supset \int d^d x \sqrt{\gamma} \left(\frac{\sigma_1}{\lambda^{2/d}} J_i J^i - \frac{\sigma_2}{\lambda^{2(d-2)/d}} F_{ij} F^{ij} \right) \tag{3.56}$$

with

$$\sigma_1 = \frac{1}{8\pi \alpha_J C_J} \left(\frac{4\pi}{d} \right)^{2/d} G^{(2-d)/d}, \quad \sigma_2 = \frac{\alpha_J C_J}{16\pi} \left(\frac{4\pi}{d} \right)^{2(d-2)/d} G^{(d-4)/d}. \tag{3.57}$$

The Newton constant G is proportional to some power of N, so σ_1 and σ_2 are fully expressed in terms of boundary data. Said another way, the coefficients can be expressed in terms of the central charges C_J and C_T of the two-point functions of a conserved $U(1)$ current J_i and a conserved spin-two current T_{ij}.

3.4 Random metrics via Hubbard-Stratonovich

The deformation can also be understood as coupling to a random background metric. This was explored in $d = 2$ in [17, 109]. Here we will show that in general d, the radial flow equation for the induced metric — that is, the bulk Einstein equation for γ_{ij} — is precisely the flow induced by coupling to a random background metric. In this section we assume γ_{ij} is flat.

Let us introduce a symmetric two-tensor h_{ij} as our Hubbard-Stratonovich field and rewrite the deformation as

$$\exp\left(-\delta\lambda\int d^dx\sqrt{\gamma}\left(T_{ij}T^{ij}-\frac{1}{d-1}(T^i_i)^2\right)\right)\sim \\ \int\mathcal{D}h\exp\left(-\frac{1}{16\delta\lambda}\int d^dx\sqrt{\gamma}(h^2-h_{ij}h^{ij})+\frac{1}{2}\int d^dx\sqrt{\gamma}h_{ij}T^{ij}\right), \quad (3.58)$$

where $h = h^i_i$. From this rewriting we see that the deformation corresponds to coupling to a metric perturbation h_{ij}, and averaging over h_{ij}. The saddle point equations are

$$h\delta_{ij}-h_{ij}-4\delta\lambda T_{ij}=0\,. \quad (3.59)$$

Taking the trace of this equation tells us that $(d-1)h = 4\delta\lambda T^i_i$, so

$$h_{ij}=-4\delta\lambda\left(T_{ij}-\frac{T^k_k}{d-1}\gamma_{ij}\right). \quad (3.60)$$

Assuming a large, classical background stress tensor, this can be interpreted as a change $\delta\gamma_{ij}$ in the effective metric seen by the field theory.

Now let's compare to the bulk. The radial evolution equation for the induced metric on a fixed-r slice is Hamilton's equation,

$$\partial_{r_c}g_{ij}=16\pi GN\left(\pi_{ij}-\frac{\pi^k_k}{d-1}g_{ij}\right), \quad (3.61)$$

where the lapse and canonical momentum are

$$N=\frac{1}{r_c},\qquad \pi_{ij}=\frac{1}{8\pi G}(K_{ij}-Kg_{ij})\,. \quad (3.62)$$

Setting $g_{ij} = r_c^2\gamma_{ij}$, this becomes

$$r_c^3\frac{\partial\gamma_{ij}}{\partial r_c}=16\pi G\left(\widetilde{T}_{ij}-\frac{\widetilde{T}^k_k}{d-1}\gamma_{ij}\right)\,. \quad (3.63)$$

Upon rescaling $\widetilde{T}_{ij} = r_c^{2-d}T_{ij}$ and using (3.29), this agrees with the flow of the effective metric (3.60).

At first order in the deformation, the effective metric is

$$ds^2 = ds_0^2 - 4\lambda\langle T_{ij}\rangle dx^i dx^j \ . \tag{3.64}$$

Viewed as a bulk equation for the induced metric, this is the usual dictionary for the boundary stress tensor in terms of subleading terms in the bulk metric.

Let us compute the propagation speed when T_{ij} is diagonal with components $T_{tt} = \epsilon$, $T_{ii} = \frac{\epsilon}{d-1}$. With this choice, we can focus on a two dimensional plane, say the (t, x) plane, to perform this calculation. In Lorentzian signature, the null geodesics in this plane are

$$-dt^2 - 4\lambda \langle T_{tt}\rangle \, dt^2 + dx^2 - 4\lambda \langle T_{xx}\rangle \, dx^2 = 0 \, . \tag{3.65}$$

In the small λ limit the propagation speed v is thus

$$v = 1 + 2\lambda\epsilon \frac{d}{d-1} + \mathcal{O}(\lambda^2) \, . \tag{3.66}$$

For the theory on $\mathbb{R}^{d-1}$, $\epsilon \geq 0$ and this speed is superluminal for $\lambda > 0$. However for the theory on e.g. $\mathbb{T}^{d-1}$ with thermal periodicity conditions along the spatial cycles, the vacuum necessarily has $\epsilon < 0$ [1], in which case we can have $v > 1$ for $\lambda < 0$ as well.

3.5 Spectrum

In this section we will consider the deformed energy spectrum of a large-N CFT under the T^2 deformation. Thanks to factorization, we will have a single differential equation that governs all energy levels. We will solve this equation and match the answer to a bulk computation of the energy at finite cutoff of black holes in anti-de Sitter space. We will consider the general case of finite sources for curvature and $U(1)$ charge, which will require considering charged AdS-Reissner-Nordström black holes with curved horizons.

3.5.1 Field theory analysis

We study field theories on a manifold $\mathbb{R} \times \mathcal{M}^{d-1}$ with metric

$$ds^2 = d\tau^2 + h_{ab} dx^a dx^b \, . \tag{3.67}$$

The flow defined by $\partial S/\partial\lambda = \int d^d x \sqrt{\gamma} X$ implies the same flow for the Hamiltonian and therefore for the energy levels, $\partial E/\partial\lambda = \int d^{d-1} x \sqrt{\gamma} X$. Considering states

that preserve the symmetries of h_{ab} and in which large-N factorization holds, and after passing to densities by dropping the spatial volume integrals, we have

$$\frac{\partial \epsilon}{\partial \lambda} = \left\langle T_{ij} + \frac{\alpha_d}{\lambda^{\frac{d-2}{d}}} G_{ij} \right\rangle^2 - \frac{1}{d-1} \left\langle T_i^i + \frac{\alpha_d}{\lambda^{\frac{d-2}{d}}} G_i^i \right\rangle^2 . \tag{3.68}$$

Equation (3.68) is valid for any d if $\mathcal{M}^{d-1}$ is flat, and for $d = 3, 4$ when $\mathcal{M}^{d-1}$ is arbitrary. This is the main object to study in the field theory as it will determine the deformed spectrum of our states of interest as a function of the deformation parameter λ. We will now solve this differential equation for various backgrounds.

Before discussing the deformation in full generality, let us focus on the simplest case in which the CFT is living on a square torus $\mathbb{T}^{d-1}$. For this background the Einstein tensor G_{ij} vanishes and moreover there are no trace anomalies. Let us assume that the states do not carry any momentum so that the stress tensor is diagonal in these states. The diagonal components of the stress tensor are given in terms of the energy density as

$$\langle T_{\tau\tau} \rangle = \epsilon, \quad \langle T_{aa} \rangle = \frac{1}{\prod_{b \neq a} L_j} \frac{d(\epsilon \prod_b L_b)}{dL_a} . \tag{3.69}$$

For a square torus the stress tensor is diagonal with equal spatial components, and the differential equation becomes

$$\frac{\partial \epsilon}{\partial \lambda} = \frac{d-2}{d-1} \epsilon^2 - \frac{2\epsilon}{(d-1) L^{d-2}} \partial_L (L^{d-1} \epsilon). \tag{3.70}$$

Solutions to this differential equation in terms of the energy $E = \epsilon L^{d-1}$ are given by

$$E = \frac{(d-1) L^{d-1}}{2d\lambda} \left(1 - \sqrt{1 - \frac{4d\lambda}{d-1} \frac{M}{L^d}} \right) , \tag{3.71}$$

where the undetermined constant was fixed by requiring that as $\lambda \to 0$ we obtain the energy in the undeformed theory $E^0 = M/L$.

At $E^0_{\text{max}} := (d-1) L^{d-1}/(4d\lambda)$ the energy levels exhibit a "square-root singularity" and become complex. For the theory with $\lambda > 0$, which we will argue is dual to the finite cutoff theory in AdS, this affects an infinite number of positive energy states. This suggests a maximum energy and hence a sharp UV cutoff. In the bulk description, it affects all states with energies for which a black hole of the given energy would not fit inside the cutoff, i.e. its horizon radius is bigger than r_c. For the theory with $\lambda < 0$, this can only affect negative energy states in the spectrum, which will necessarily exist if e.g. we pick thermal periodicity conditions along the spatial cycles [1]. While the theory with $\lambda > 0$ has complex energy states for any λ

and L, the theory with $\lambda < 0$ can only have complex energy states for sufficiently large $-\lambda/L^d$.

We now consider the general case, where we will solve the differential equation for the energy levels with finite $U(1)$ charge density on S^{d-1} ($k = 1$) or $\mathcal{H}^{d-1}$ ($k = -1$). The metric is given by

$$ds^2 = d\tau^2 + R^2 d\Sigma_{d-1}^2, \tag{3.72}$$

with $R^2 d\Sigma_{d-1}^2$ the metric on an S^{d-1} or $\mathcal{H}^{d-1}$ with radius R and volume $R^{d-1}V_{d-1}$. (The flat slicing case treated above is captured by taking the flat metric on Σ_{d-1}, which in the below equations will mean setting $k = 0$, $V_{d-1} = 1$ and $R = L$.) For simplicity, let us restrict to states that preserve the spatial symmetries. This means that the stress tensor is given by

$$T_{\tau\tau} = \epsilon, \quad T_{aa} = h_{aa} \frac{1}{(d-1)R^d} \partial_R \left(R^{d-1} \epsilon \right) \ . \tag{3.73}$$

In the presence of finite $U(1)$ charge density the deformation was shown in section 3.3.4 to be given by

$$X = \left(T_{ij} + \frac{\alpha_d}{\lambda^{\frac{d-2}{d}}} G_{ij} \right)^2 - \frac{1}{d-1} \left(T_i^i + \frac{\alpha_d}{\lambda^{\frac{d-2}{d}}} G_i^i \right)^2 + \frac{\sigma_1}{\lambda^{2/d}} J^i J_i - \frac{\sigma_2}{\lambda^{\frac{2(d-2)}{d}}} F_{ij} F^{ij} \ , \tag{3.74}$$

where σ_i are dimensionless constants given in (3.57). For simplicity, let us study the deforming operator when A_i is independent of field theory coordinates. Following the same logic as above, the flow of the energy levels in the deformed theory are given by

$$\frac{\partial \epsilon}{\partial \lambda} = \left\langle T_{ij} + \frac{\alpha_d}{\lambda^{\frac{d-2}{d}}} G_{ij} \right\rangle^2 - \frac{1}{d-1} \left\langle T_i^i + \frac{\alpha_d}{\lambda^{\frac{d-2}{d}}} G_i^i \right\rangle^2 + \frac{\sigma_1}{\lambda^{2/d}} \left\langle J^i J_i \right\rangle \ . \tag{3.75}$$

Again, by using large-N factorization, we can write all terms as products of one-point functions. We will consider the current one-point functions to vanish when $i \neq 0$, so these states only have a non-zero charge density, which enters into the final term in the flow equation as

$$\langle J^i J_i \rangle = \langle J^i \rangle \langle J_i \rangle = - \left(\frac{Q}{V_{d-1} R^{d-1}} \right)^2 , \tag{3.76}$$

with Q the dimensionless charge. The differential equation for the energy levels is

then given by

$$\frac{\partial\epsilon}{\partial\lambda} = \frac{d-2}{d-1}\left(\epsilon - \frac{(d-1)k\alpha_d}{2R^2\lambda^{1-2/d}}\right)^2 - \frac{2}{(d-1)R^{d-2}}\frac{\partial\left(R^{d-1}\epsilon\right)}{\partial R}\left(\epsilon - \frac{(d-1)(d-2)k\alpha_d}{2R^2\lambda^{1-2/d}}\right)$$
$$- \frac{(d-3)^2\left(d^2-3d+2\right)\alpha_d^2}{4R^4\lambda^{2(1-2/d)}} - \frac{\sigma_1 Q^2}{\lambda^{2/d}R^{2d-2}V_{d-1}^2}\,. \tag{3.77}$$

The equation can be simplified by defining an energy variable $x = R^{d-1}\epsilon - (d-1)(d-2)R^{d-3}k\alpha_d/(2\lambda^{1-2/d})$. It is solved by energy density $\epsilon = E/(R^{d-1}V_{d-1})$, with

$$E = \frac{(d-1)R^{d-1}V_{d-1}}{2d\lambda}\left(\frac{(d-2)dk\lambda^{2/d}\alpha_d}{R^2} + 1 - \right.$$
$$\left.\sqrt{1 - \frac{4dM\lambda}{(d-1)V_{d-1}R^d} + \frac{2(d-2)dk\lambda^{2/d}\alpha_d}{R^2} + \frac{4\sigma_1 d^2Q^2\lambda^{2-2/d}}{(d-2)(d-1)R^{2d-2}V_{d-1}^2}}\right). \tag{3.78}$$

For $d = 2, 3$ we see that this reduces to the CFT energy M/R as $\lambda \to 0$. (For $d = 2$ we only consider the chargeless case $Q = 0$.) For $d = 4$ the CFT limit picks up a Casimir term and becomes $M/R + 12|k|V_3\alpha_4^2/R$. For $d > 4$ the limit is singular, reflecting the fact that there are more counterterms we have neglected to include in deriving our deformation. Our bulk calculations will be done with the same set of counterterms, which will result in us matching the $d > 4$ cases between bulk and boundary as well.

3.5.2 Bulk analysis

Having obtained the energy levels in the deformed theory, we now turn to a comparison with the bulk. In the bulk, we want to do a quasi-local energy calculation at a finite radial cutoff for the AdS-Reissner-Nordström black hole metric with boundary geometry S^{d-1} ($k = 1$), $\mathbb{R}^{d-1}$ ($k = 0$), or $\mathcal{H}^{d-1}$ ($k = -1$). The topology can be arbitrary and will only enter into the volume V_{d-1}. The action for the theory is

$$S = -\int d^{d+1}x\sqrt{g}\left(\frac{R}{2\kappa^2} - \frac{1}{4e^2}F^2 + \frac{d(d-1)}{2\kappa^2}\right) \tag{3.79}$$

where $\kappa^2 = 8\pi G$ and the gauge coupling is e. This has as solution the charged black hole:

$$ds^2 = \left(\frac{k}{R^2} - \frac{r_0}{r^{d-2}} + r^2 + \frac{q^2}{r^{2d-4}}\right) d\tau^2 + \frac{dr^2}{\frac{k}{R^2} - \frac{r_0}{r^{d-2}} + r^2 + \frac{q^2}{r^{2d-4}}} + r^2 R^2 d\Sigma_{d-1}^2, \tag{3.80}$$

$$A = \frac{ieq}{c\kappa}\left(-\frac{1}{r^{d-2}} + \frac{1}{r_+^{d-2}}\right) d\tau, \qquad c = \sqrt{\frac{d-2}{d-1}}\,, \tag{3.81}$$

where r_+ is the horizon location and Σ_{d-1} has volume V_{d-1} and is a unit sphere, plane, or hyperboloid depending on k. The conserved mass and dimensionless $U(1)$ charge of the CFT are

$$M = \frac{(d-1)R^{d-1}V_{d-1}}{16\pi G}\, r_0\,, \qquad Q = \frac{\sqrt{(d-1)(d-2)}R^{d-1}V_{d-1}}{e\kappa}\, q\,. \tag{3.82}$$

Using $E = \int \sqrt{\det \tilde{\tilde{h}}}\, \widetilde{T}_{\mu\nu} u^\mu u^\nu = \int \sqrt{\det \tilde{\tilde{h}}}\, \widetilde{T}_{\tau\tau} g^{\tau\tau}$ for $\tilde{h}_{ab} dx^a dx^b = r^2 R^2 d\Sigma_{d-1}^2$ the non-radial spatial metric, we find the energy at finite radial cutoff r_c to be

$$E = \frac{(d-1)V_{d-1}R^{d-1}r_c^{d-1}}{8\pi G}\left(\frac{k}{2R^2r_c^2} + 1 - \sqrt{1 - \frac{r_0}{r_c^d} + \frac{k}{R^2r_c^2} + \frac{q^2}{r_c^{2d-2}}}\right). \tag{3.83}$$

This expression is correct for $d > 2$ if $k = 0$ and for $d = 3, 4$ if $k \neq 0$. The general dimensional answer for $k \neq 0$ can also be obtained but would (further) clutter the equation.

To translate to field theory we need to apply our dictionary to the quantity $E_{\text{bulk}} = \int \sqrt{\det \tilde{\tilde{h}}}\, \widetilde{T}_{\tau\tau} g^{\tau\tau} \to \int (r_c^{d-1}\sqrt{\det h})(r_c^{2-d} T_{\tau\tau})(r_c^{-2}\gamma^{\tau\tau}) = r_c^{-1} E_{\text{bdry}}$. Using the expressions for α_i and σ_i in the previous section and identifying

$$\lambda = \frac{4\pi G}{dr_c^d}\,, \tag{3.84}$$

we find perfect agreement between E_{bdry} calculated in this way and E_{bdry} calculated in the field theory analysis of the previous subsection.

Note that we calculated the bulk energy by integrating $\tilde{T}_{\mu\nu}u^\mu u^\nu$. Often, the quasilocal energy is defined by integrating $\tilde{T}_{\mu\nu}u^\mu t^\nu$, which differs by a function of r_c. Both choices are acceptable, as long as we compare to the correct quantity in the boundary theory. The energy computed from $\tilde{T}_{\mu\nu}u^\mu u^\nu$ is the conserved charge associated to translations by a unit vector, and is therefore equal to the field theory energy in the metric $-dt^2 + \cdots$. The energy defined by integrating $\tilde{T}_{\mu\nu}u^\mu t^\nu$ is equal to the energy of the boundary theory in the metric induced at the cutoff surface, $-\gamma_{tt}dt^2 + \cdots$. Since we are comparing to the EFT energy in Minkowski spacetime with the usual (unit normalized) time coordinate, the correct comparison is to $\tilde{T}_{\mu\nu}u^\mu u^\nu$.

3.6 Thermodynamics

So far, we have only considered the flow of the spectrum of the deformed theory, but there are other quantities that also exhibit a non-trivial flow under the deformation. Two important quantities that reveal some of the intricate features of the T^2 deformation are the entropy and speed of sound. We will consider both quantities for the case of the effective theory on a flat background.

3.6.1 Entropy density

The interpretation of our deformation in terms of a finite cutoff in an AdS bulk requires a particular sign for the deformation, in our conventions $\lambda > 0$. The case $\lambda < 0$ is also interesting to consider. (If matter or sources are present there will be fractional powers of λ, so the theory needs to be defined more carefully, but here we will only consider the sourceless case without matter.) In this case the deformed energy levels for $E > 0$ always remain real, so we can analyze what happens in the deep UV of our system. In the local CFT we begin with, the high energy density of states scales as

$$S \sim E^{\frac{d-1}{d}} \ . \tag{3.85}$$

The deformation shifts the energies, and changes the entropy accordingly. Denote by $E_0(\lambda, E)$ the initial energy of a state that has energy E after the flow, which is easily calculated by inverting (3.71). Inputting into (3.85) gives the entropy of the flowed theory,

$$S(\lambda, E) \sim E_0(\lambda, E)^{\frac{d-1}{d}} \sim \left(E + E^2 L b\right)^{\frac{d-1}{d}} \tag{3.86}$$

with L the system size and $b = -\frac{d}{d-1}\frac{\lambda}{L^d} > 0$ a dimensionless parameter. For $ELb \ll 1$ the entropy reduces to the extensive scaling indicative of a local QFT, while for $ELb \gg 1$ the entropy becomes

$$S \sim E^{\frac{2(d-1)}{d}}. \tag{3.87}$$

Notice that this scaling is Hagedorn for $d = 2$, as discussed in [114–116], and super-Hagedorn for $d > 2$. Interestingly, this super-Hagedorn scaling matches the density of states of $(d-1)$-branes in the semiclassical approximation [110–113]. The black holes in such a theory would have negative specific heat, like those in flat space. In fact, for $d = 4$ the entropy scaling matches that of five-dimensional Schwarzschild black holes in flat space. It would be fascinating if the quantum theory defined by the irrelevant T^2 deformation considered here gave a new route to quantization of a theory of membranes.

The $\lambda > 0$ theory

Equation (3.86) does not apply to generic theories with $\lambda > 0$. This is because the CFT formula (3.85) is generically an asymptotic formula, while the $\lambda > 0$ deformation makes energies above an $E_{\max}$ complex, as in (3.71). However, for holographic theories, or alternatively for modular invariant theories with a particular pattern of center symmetry breaking [128], this formula has an extended range of validity [55], holding down to energies $-(d-1)E_{\rm vac}$. (For $d = 2$ this extended range is equivalent to a sparse light spectrum [24]; for the connection to a sparse light spectrum in $d > 2$ see [1, 128].) This means that the ensuing formulas can be applied to the $\lambda > 0$ theory for states in the window $-(d-1)E_{\rm vac} < E < E_{\max} = (d-1)L^{d-1}/(4d\lambda)$.

An intriguing aspect of the deformation considered is that it preserves center symmetry for theories where it is present. It was argued in [128] that the presence and pattern of spontaneous breaking of this symmetry is a robust way of reproducing aspects of semiclassical bulk physics when the boundary theory is placed on nontrivial topology. For example, the fact that the symmetry is unbroken means we can write correlation functions on quotient spacetimes (at leading order in N) in terms of a sum over images of the correlation function in the original spacetime; this important property is manifest from the bulk description, and in our dual EFT is kept intact by the preservation of center symmetry along the T^2 flow.

3.6.2 Speed of sound

The speed of sound in these theories also shows interesting behavior. Fixing to flat space and using the pressure $p = \frac{1}{(d-1)L^{d-2}}\frac{dE}{dL}$ and the energy levels (3.71), we find

$$c_s = \sqrt{\frac{\partial p}{\partial \rho}} = \left(\frac{1}{d-1}\right)^{1/2}\left(\frac{1+(d-2)M\tilde{\lambda}}{1-2M\tilde{\lambda}}\right)^{1/2}, \tag{3.88}$$

where $\tilde{\lambda} = \frac{2d\lambda}{(d-1)L^d}$. In the $\tilde{\lambda} \to 0$ limit this reduces to the usual result, $c_s = 1/\sqrt{d-1}$. Moreover, the function is monotonic and diverges precisely at $M_{\max}$ set by the square-root singularity in the energies. Hence for any positive λ there exist finite-temperature states set by M for which the speed of sound becomes arbitrarily large. This behaviour is identical to the two dimensional case [17]. The speed of sound in a theory with $\tilde{\lambda} < 0$ needs to be interpreted with care, since the above formula is a thermodynamic formula. As seen in the previous subsection, the $\tilde{\lambda} < 0$ theory has a super-Hagedorn density of states, so the canonical ensemble is ill-defined at any temperature.

In the bulk, the computation of the speed of sound in AdS with a Dirichlet wall

at $r = r_c$ was done in [129]. They find

$$c_s^2 = \frac{1}{d-1}\left(1 + \frac{d}{2\left(r_c^d/r_0^{d/(d-2)} - 1\right)}\right). \tag{3.89}$$

Using (3.82) and (3.84) to trade r_0 and r_c for M and λ, we see that this matches exactly with the field theory speed of sound found in (3.88).

3.7 Two-point functions

So far, we have computed the spectrum and certain thermodynamic quantities of the deformed theory and found that they match with the dual bulk computation. To understand the role of the background terms, and demonstrate how the dictionary works more generally, we will also compute and compare 2-point correlation functions. In section 3.2.3 this was already done for scalar correlators. Here we will compute the flow of two-point functions of conserved $U(1)$ currents and stress tensors. The results will agree with the bulk calculation at finite cutoff. We will limit the discussion to vacuum two-point functions on flat space.

3.7.1 $U(1)$ current correlators

Conserved $U(1)$ currents arise from gauge fields in the bulk. We have seen in section 3.3.4 that such gauge fields give rise to two terms in the deformation, which are the analogues of ∂J and $\mathcal{O}$ seen in (3.11) for the scalar case. In particular, the flow of the effective action is

$$\frac{\partial W[A]}{\partial \lambda} = \int d^d x \left(X_0 + \frac{\sigma_1}{\lambda^{2/d}} J^i J_i - \frac{\sigma_2}{\lambda^{\frac{2(d-2)}{d}}} F_{ij} F^{ij}\right), \tag{3.90}$$

where $F_{ij} = \partial_i A_j - \partial_j A_i$ and σ_i the dimensionless constants found in (3.57). The operator X_0 is the deformation for gravity only. We now wish to compute the flow of the current two-point function by taking functional derivatives with respect to A,

$$\partial_\lambda \langle J^l(x) J^m(y)\rangle = \frac{\delta}{\delta A_l(x)} \frac{\delta}{\delta A_m(y)} \left\langle \int d^d y' \left(-\frac{\sigma_1}{\lambda^{2/d}} J^i J_i + \frac{\sigma_2}{\lambda^{2(d-2)/d}} F_{ij} F^{ij}\right) \right\rangle. \tag{3.91}$$

Using

$$\langle J^l(x) J^m(y)\rangle = \frac{\delta \langle J^m(y)\rangle}{\delta A_l(x)} \tag{3.92}$$

and taking the large N limit, the flow equation for the current correlator can be written as

$$\partial_\lambda \langle J^l(x) J^m(y)\rangle = 2\int d^d y' \left(-\frac{\sigma_1}{\lambda^{2/d}} \langle J^l(x) J_i(y')\rangle \langle J^i(y') J^m(y)\rangle + \frac{\sigma_2}{\lambda^{2(d-2)/d}} \left\langle \frac{\delta F_{ij}(y')}{\delta A_l(x)} \frac{\delta F^{ij}(y')}{\delta A_m(y)} \right\rangle \right). \tag{3.93}$$

This flow equation simplifes in momentum space, where Lorentz invariance forces the two point function of J^i to be of the form [130]

$$\langle J^l(\mathbf{k}) J^m(-\mathbf{k})\rangle = C(\lambda, k)\pi^{lm}, \quad \pi^{lm} = \delta^{lm} - \frac{k^l k^m}{k^2}, \tag{3.94}$$

with C a function of λ and k that completely fixes the two-point function. We have also stripped the delta function enforcing momentum conservation, just as in the scalar case. Plugging this in (3.93), we find

$$\partial_\lambda C(\lambda, k) = -\frac{2\sigma_1}{\lambda^{2/d}} C(\lambda, k)^2 + \frac{4k^2\sigma_2}{\lambda^{2(d-2)/d}}. \tag{3.95}$$

Notice that this flow was also found in [91]. This differential equation is supplemented with the CFT initial condition as $\lambda \to 0$, which, in position space, is just (3.54). The solution is then

$$C(\lambda, k) = -\sqrt{\frac{2\sigma_2}{\sigma_1}} k\lambda^{\frac{3-d}{d}} \frac{K_{d/2-2}(2\sqrt{2\sigma_1\sigma_2} k\lambda^{1/d} d)}{K_{d/2-1}(2\sqrt{2\sigma_1\sigma_2} k\lambda^{1/d} d)}, \tag{3.96}$$

with K the modified Bessel function of the second kind. When we insert the expressions for σ_i to write this in terms of r_c, we find an exact match with the bulk computations done in [131]. Let us study the $d = 3$ case in a bit more detail. Using the values of σ_i given in (3.57), we find that the correlator is given by

$$\langle J^l(\mathbf{k}) J^m(-\mathbf{k})\rangle = -\frac{C_J}{4\pi} k\pi^{lm}, \tag{3.97}$$

which is precisely the (Fourier transform of) the initial CFT value (3.54). Thus for $d = 3$ the correlator does not flow. As explained at the end of section 3.2.3, this is due to the fact that the bulk theory is conformal in this case.

In even dimensions (3.96) contains logarithms and to implement the initial condition as $\lambda \to 0$ it is convenient to analytically continue in d and do the Fourier trachapterto position space, just as is done in [131]. The $\lambda \to 0$ limit is singular for $d > 4$, but this simply reflects the fact that there are additional counterterms that we have neglected to include. Including them via our procedure will result in a finite answer.

3.7.2 Stress-tensor correlators

Let us now consider correlators of the stress tensor at finite λ which we will show are dual to the propagator of gravitational perturbations at some constant $r = r_c$ surface in the bulk. We will start with the field theory computation and compare that with the bulk calculation afterwards.

Stress tensor correlators are computed by taking functional derivatives of the effective action $W = -\log Z$,

$$\langle T_{i_1 j_1}(x_1) \cdots T_{i_n j_n}(x_n) \rangle = \frac{2}{\sqrt{\gamma}} \frac{\delta}{\delta \gamma^{i_1 j_1}(x_1)} \cdots \frac{2}{\sqrt{\gamma}} \frac{\delta}{\delta \gamma^{i_n j_n}(x_n)} (-W[\gamma, \lambda]) \,. \tag{3.98}$$

Again, we will focus on the two-point function of T_{ij} on $\mathbb{R}^d$ in the vacuum. Moreover, as we need the deformation for a general curved background to compute the correlators, we will only consider two, three and four boundary dimensions. As explained in section 3.3 our derivation works generally, but becomes more tedious in $d > 4$. Our deformation is

$$\frac{\partial W}{\partial \lambda} = \int d^d x \sqrt{\gamma} \left[\left(T_{ij} + \frac{\alpha_d}{\lambda^{\frac{d-2}{d}}} G_{ij} \right)^2 - \frac{1}{d-1} \left(T_i^i + \frac{\alpha_d}{\lambda^{\frac{d-2}{d}}} G_i^i \right)^2 \right], \tag{3.99}$$

where $\alpha_d = (d^{1-2/d}(d-2)(\pi G)^{2/d} 2^{1+4/d})^{-1}$. To compute the flow of the stress-tensor two-point function, we proceed analogously as for the gauge field. We go to momentum space, where stress tensor two-point functions in the vacuum can be written in terms of following two tensor structures (again omitting the overall delta function which enforces momentum conservation)

$$\langle T_{ij}(\mathbf{k}) T_{lm}(-\mathbf{k}) \rangle_\lambda = A(k, \lambda) \Pi_{ijlm} + B(k, \lambda) \pi_{ij} \pi_{lm}, \tag{3.100}$$

$$\pi_{ij} = \delta_{ij} - \frac{k_i k_j}{k^2}, \quad \Pi_{ijlm} = \frac{1}{2}(\pi_{il}\pi_{jm} + \pi_{im}\pi_{jl}) - \frac{1}{d-1} \pi_{ij}\pi_{lm}. \tag{3.101}$$

Note that in $d = 2$ the first structure Π_{ijlm} vanishes identically. Taking derivatives with respect to the metric and decomposing the expression in terms of Π_{ijlm} and $\pi_{ij}\pi_{lm}$ we find

$$\partial_\lambda A(k, \lambda) = -2 \left(A(k, \lambda) - \alpha_d k^2 \lambda^{-(d-2)/d} \right)^2, \qquad \partial_\lambda B(k, \lambda) = 0 \,, \tag{3.102}$$

where in deriving the above equations we kept leading terms in $1/N$ and used $\langle T_{ij} \rangle = 0$. The identity

$$\frac{\delta G_{ij}}{\delta g^{lm}} = \frac{1}{4} \left(k^2 \delta_{lm} \pi_{ij} - k^2 \delta_{jm} \pi_{il} + \delta_{im} k_l k_j - \delta_{ij} k_l k_m \right) + l \leftrightarrow m \,, \tag{3.103}$$

$$= \frac{d-2}{2(d-1)} k^2 \pi_{ij} \pi_{lm} - \frac{1}{2} k^2 \Pi_{ijlm} \tag{3.104}$$

which leads to

$$\frac{\delta G_{pq}}{\delta g^{ij}}\frac{\delta G^{pq}}{\delta g^{lm}} - \frac{1}{d-1}\frac{\delta G^{p}_{p}}{\delta g^{ij}}\frac{\delta G^{q}_{q}}{\delta g^{lm}} = \frac{k^4}{4}\Pi_{ijlm}\,, \tag{3.105}$$

is useful in deriving the above. The Ricci scalar term present in the trace relation for $d = 2$ is topological once integrated and does not contribute to the correlation functions.

The constancy of B under the flow of the deformation has the following consequence. Upon taking the trace of (3.100) we find that

$$\langle T^i_i(\mathbf{k})T^m_m(-\mathbf{k})\rangle_\lambda = B(k,\lambda)(d-1)^2. \tag{3.106}$$

In $d = 2$, this is proportional to central charge, therefore in a $T\bar{T}$ deformation of holographic CFTs, (3.102) immediately implies that the central charge does not flow. This is consistent with both the field theory result [102] and the bulk gravity computation [100]. Also, in any odd dimensional CFT, there is no anomaly and hence $B(k,\lambda) = 0$. In even dimensions, there is a trace anomaly, but by expanding the trace anomalies around the Minkowski spacetime we find $B(k,\lambda) = 0$ in $d \geq 4$.

The solution for $A(k,\lambda)$ is given by

$$A(k,\lambda) = -\frac{\tilde{k}\lambda^{1/d-1}}{2d}\frac{K_{1-d/2}(\tilde{k}\lambda^{1/d})}{K_{d/2}(\tilde{k}\lambda^{1/d})} + \alpha_d k^2 \lambda^{-(d-2)/d}\,, \tag{3.107}$$

where K is the modified Bessel function of the second kind and $\tilde{k} = d\sqrt{\frac{2(d-2)\alpha_d}{d}}k = \left(\frac{d}{4\pi G}\right)^{1/d}k$. Note that due to the second term above, this solution has a smooth limit as $\lambda \to 0$ and matches exactly onto the CFT answer for $d \leq 4$. In $d = 3$ the form of the two point function is simple and given by

$$A(k,\lambda)|_{d=3} = \frac{\sqrt{6}\alpha_3^{3/2}k^3}{1 + k\sqrt{6\alpha_3}\lambda^{1/3}}\,. \tag{3.108}$$

As in the case of gauge fields, even dimensions have logarithms in the small λ limit. For $d > 4$ one needs to add more counterterms to find a smooth limit as $\lambda \to 0$. Our result is in agreement with the known bulk result for the two-point function of the stress tensor [132]. However, note that in [132] the Einstein tensor counterterm is absent and computing the on-shell action gives only the first term in (3.107). In that approach, the correct correlator is found by dropping local terms arising from the Bessel functions, whereas in our approach local terms cancel with counterterms and the correlator has the correct power law behaviour when $\lambda \to 0$.

3.8 Discussion

We have studied effective field theories defined by the flow (3.1). The calculability of quantities like the deformed energy spectrum and correlation functions came from our assumption of large-N factorization. The operator defining the flow was extracted by considering bulk AdS physics; in this context we provided evidence that the dimensionful parameter λ is related to a sharp radial cutoff in the bulk.

An important challenge facing development of this approach is $1/N$ corrections. These are essential to gain a better handle on quantum gravity in finite patches of spacetime. Our deforming operator was selected by a bulk classical analysis, which can be modified by quantum effects.

Another interesting direction to pursue is the case of $d = 1$. The techniques we use are general and can be applied to e.g. Jackiw-Teitelboim gravity in two dimensions. In the limit where the cutoff is taken to be close to the boundary, the deformed theory should correspond to the Schwarzian theory [133–135].

As mentioned in the introduction, the gravity theory with a Dirichlet cutoff is rather strange, and the dual EFT is correspondingly strange. One possibility is that the theory makes sense only as an 'intermediate step' in a bigger calculation. For example, the full AdS/CFT duality can, in principle, be cut at some arbitrary surface $r = r_c$, then recovered by integrating over all fields at the cutoff, including the metric. (See for example in [91].) In this calculation, the bulk partition function with finite cutoff appears in the first step, but the dual EFT is then coupled to gravity and to another theory in the UV. This is similar to the role of the wavefunction in the dS/CFT correspondence as formulated in [136] — there, the wavefunction of the universe is calculated with a Dirichlet boundary condition at fixed time, but physical observables are obtained only after integrating over boundary conditions. In the AdS case, this suggests that although our EFT may not make sense in the UV as a quantum field theory, it should be possible to UV-complete the theory when coupled to gravity. (This suggests the existence of an anti-swampland: a class of effective field theories that cannot be UV-completed *unless* coupled to gravity!)

Part II:
Classification of Topological Insulators

Vake be'j te bange

4 Topological Insulators

Ever since Lev Landau introduced his theory of second order phase transitions in 1937 [137], a tremendous progress on the study of phases of matter has been made. In this paradigm, a phase is described by a local order parameter and its vacuum expectation value (vev). For example, the Landau theory can be used to describe the ferro- to paramagnetic phase transition, which can arise when the temperature of, say, a magnet is increased above a certain critical temperature. The order parameter is then used to measure an order in the system, which in this case is the ordering of spins measured by the magnetic moment M. The ferromagnetic phase is ordered and so M acquires a non-zero vev, while in the paramagnetic phase the spins are not ordered and the vev of M vanishes. Moreover, due to the fact that the spins in the paramagnetic phase are not ordered, the system (in that phase) possesses a spin-flip symmetry that is not present in the ferromagnetic phase. Thus, in the ferro- to paramagnetic phase transition, this symmetry is (spontaneously) broken.

The beauty of this description of the ferro- to paramagnetic phase transition is that it applies more generally to any symmetry-based phase transition. Using order parameters and symmetry breaking these transitions can be discussed in a unified way, but as always, there are exceptions. One of those exceptions are topological phases and their transitions. Their description follows a rather different trajectory than the one proposed by Landau. Instead of focussing on the symmetries and their breaking, one focusses on an entirely different aspect: topology.

Topology is a branch is mathematics that studies (smooth) deformations of objects and can be used to distinguish objects that cannot be smoothly deformed in one another. For instance, with topology one can distinguish a donut from an apple. Of course, this is true from just looking at them; the apple has no holes, whereas

the donut has one. However, for more abstract objects that appear in mathematics all the time, one cannot just look at the objects and determine how many *holes* it has. This requires a more abstract notion of distinguishability and is precisely where topology (among other reasons) was developed for.

In physics, topology appears in numerous places, such as string theory, quantum field theory and condensed matter physics. Although these branches of physics are very different from each other and the topology might appear in different ways, they all have in common that certain observables such as conductivities are very robust and do not change when perturbing the system slightly. Moreover, only certain values for such observables are allowed, whereas others are forbidden. One therefore says that those values are *topologically* protected and result in a *quantisation* of the value of the observable. In the apple and donut example, something similar happens for the observable that measures the number of holes: a donut has one hole, not a half or a quarter. In fact, the analogy goes further. When the donut or apple is squeezed slightly, the number of holes does not change, only when one squeezes hard or tears the donut or apple apart, the number of holes can change.

From a physics point of view, these properties of observables sound very counterintuitive and they are, because most of the observables we know are not like that at all. They change slightly when external parameters, such as temperature, magnetic field or an applied voltage are varied a little bit. It is thus remarkable that there are, in fact, physical systems that do behave rather robustly and have observables that cannot be changed so easily. These systems possess a hidden form of topology analogous to the number of holes in the donut and apple example. In this dissertation we will embark on a journey to learn more about these fascinating systems and study a special class of them called topological insulators. These systems distinguish themselves by having a topology present in reciprocal space that is ultimately responsible for the quantisation of certain observables.

To understand what types of observables we will be talking about and what a topological insulator is, let us study an example in more detail. This will allow us to appreciate these new phases of matter and understand their revolutionary properties. The simplest example to study is in fact also one of the first examples of a topological insulator: the integer quantum Hall phase [138–140].

4.1 The quantum Hall state

The quantum Hall phase can occur in a two dimensional electron gas subject to a perpendicularly applied, strong magnetic field. As the temperature of such a

system is lowered, the Hall conductance σ_{xy} displays a rather striking property as a function of the magnetic field: it follows a staircase-like function with well-defined plateaus at integer multiples of e^2/h. From a physics point of view, this quantisation of the Hall conductivity is rather surprising, since it implies some sort of mechanism that prevents other values of σ_{xy}. Normally, one would say that this might be due to (crystal) symmetries, but since the quantum Hall effect persists in the presence of disorder, this cannot be the case. Moreover, the external magnetic field breaks time-reversal symmetry, so there is also no protection of the plateau values is coming from that. What else could protect the quantisation of σ_{xy}? Indeed, the topology we discussed!

In a seminal work by Thouless, Kohmoto, Nightingale and den Nijs [141], it was shown that there is a connection between topology or more specifically between topology of the band structure in momentum space and σ_{xy}. To understand their result and see what topology we are dealing with, let us study a simplified Hamiltonian that displays these topologically non-trivial features already. It will have, in momentum space, two bands separated by a band gap, so that it corresponds to an insulator. The most general Hamiltonian with these properties is,

$$H = a_i(\mathbf{k})\sigma^i, \tag{4.1}$$

where $i = x, y, z$, σ^i the Pauli matrices and $a_i(\mathbf{k})$ generic functions of the momenta k_x and k_y that take values on the first Brillouin zone, so $-\pi \leq k_{x,y} < \pi$. The functions a^i are thus periodic with period 2π. The bands of this model are given by the two eigenvalues of H,

$$E_\pm = \pm E, \quad E = \sqrt{a_i(\mathbf{k})a^i(\mathbf{k})}. \tag{4.2}$$

The band gap conditions is thus the statement that $E > 0$ throughout the first Brillouin zone. The corresponding eigenfunctions are

$$\alpha_\pm = \begin{pmatrix} a_z \pm E \\ a_x - ia_y \end{pmatrix}. \tag{4.3}$$

This is the spectrum of the Hamiltonian (4.1) and is all there is to know about it, so where is the topology hiding? One natural way to look for is how the states $\alpha_\pm$ change as we change the momentum. For small changes of the momentum, the changes in the states will be small as well and hence violating the robustness condition we seek for. But what about large excursion through the Brillouin zone, for instance if we go around the first Brillouin zone? To study that question, we parametrise the eigenvectors $\alpha_\pm$ by a sphere of radius E. In particular, writing $a_x = E\sin(\theta)\cos(\phi)$, $a_y = E\sin(\theta)\sin(\phi)$, $a_z = E\cos(\theta)$, we see that

$$\alpha_\pm = E\begin{pmatrix} \cos(\theta) \pm 1 \\ \sin(\theta)e^{-i\phi} \end{pmatrix} \tag{4.4}$$

The angles θ and ϕ parametrise the sphere S^2 and are functions of k_x and k_y. The key observation is now that there is no restriction on the range of θ and ϕ. In fact, their range can be smaller than we are used to for a sphere and hence they cover only part of the sphere, but they can also be larger. Consequently, the sphere can be covered multiple times or fractions of that. Partial coverings of the sphere can be changed to integer coverings by changing the functions a_i slightly without closing the gap. For integer coverings of the sphere this cannot be done without closing the gap. In fact, this *covering* number or more generally, winding number is the topology we were looking for. The topology comes from how many times the Brillouin zone is wrapped around the sphere S^2. To compute the winding number, we can actually compute the value of a good old friend, the integrated Berry curvature! For the Hamiltonians in question, (4.1), the Berry curvature takes the form [142],

$$\mathcal{F}_{k_x k_y} = -\frac{i}{2}\epsilon^{ijk}\hat{a}_i \partial_{k_x}\hat{a}_j \partial_{k_y}\hat{a}_k, \tag{4.5}$$

which is then integrated over the Brillouin zone to get the winding number ν:

$$\nu = \frac{i}{2\pi}\int_{\mathrm{BZ}} d^2k\ \mathcal{F}_{k_x k_y}. \tag{4.6}$$

The hat in (4.5) signifies that these are normal vectors in the direction of $\mathbf{a} = (a_x, a_y, a_z)$. After integration we obtain the winding number ν associated to one state, namely the state in the valance band. The conduction band is usually disregarded as there is always a gap and does not contribute to the physics at low energies. In more general cases when more bands are present, we need to sum over all occupied states to get the total winding.

The non-trivial result of TKNN is that there is a relation between this topology, i.e. the winding, and the Hall conductivity σ_{xy}. They showed, using the Kubo-formula that

$$\sigma_{xy} = \frac{e^2}{h}\nu_{\mathrm{tot}} = \frac{e^2}{h}\sum_{\alpha\in\mathrm{occ.}}\frac{i}{2\pi}\int_{\mathrm{BZ}} d^2k\ \mathcal{F}^{(\alpha)}_{k_x k_y}, \tag{4.7}$$

where α is a label indicating the occupied energy eigenstates over which we sum. To get some feeling for the winding number ν, consider,

$$a_x = \sin(k_x), \quad a_y = \sin(k_y), \quad a_z = m + \cos(k_x) + \cos(k_y). \tag{4.8}$$

The corresponding Hamiltonian is indeed gapped for any mass $|m| \neq 0, 2$. Computing ν, we find that it is a function of m in a special way [143]:

$$\nu = \begin{cases} 1, & 0 < m < 2 \\ -1, & -2 < m < 0 \\ 0, & \text{otherwise} \end{cases}. \tag{4.9}$$

Thus, depending on the mass, the winding number is either zero, 1 or -1. Using the TKNN result, we can therefore conclude that there is only a non-trivial Hall conductance for $|m| < 2$.

This form for the winding number also displays another crucial behaviour of topological insulators. When we vary the mass m, there is a jump in ν whenever the gap closes somewhere in the Brillouin zone. In other words, gap closing and reopening (so crossing the critical values $m = 0$ and $m = \pm 2$) changes ν discontinuously and thus induces a topological phase transition. This is a general feature, not only of topological insulators, but also of topological phases in general. In fact, this can be used to define what a topological phase is: it is a phase of matter robust under deformation of the Hamiltonian that do not close the gap. This makes a topological phase much different from ordinary (symmetry-based) phases and transitions, since in that case symmetries are broken upon going from one to another phase. For topological phases that is not the case, they retain their symmetry on either side of the transition.

Another intriguing general property of topological insulators is the existence of boundary modes. For the class of Hamiltonians H we consider here, this can be easily demonstrated by going to position space and solving the Dirac equation in the presence of a boundary. To do so, we first have to take the continuum limit of the explicit Hamiltonian we have considered before:

$$H = \sin(k_x)\sigma_x + \sin(k_y)\sigma_y + (m + \cos(k_x) + \cos(k_y))\sigma_z. \tag{4.10}$$

To take the continuum limit, we simply take the size of the first Brillouin zone to infinity, so that it looks like a two-dimensional plane and we only need to take the leading order in the momenta pieces. The result is,

$$H = k_x\sigma_x + k_y\sigma_y + m\sigma_z, \tag{4.11}$$

where we absorbed a factor of 2 in m. Going to position space then results in a Dirac operator,

$$D = -i\sigma_x\partial_x + -i\sigma_y\partial_y + m\sigma_z. \tag{4.12}$$

This operator acts on a two-component fermion Ψ. Let us introduce a boundary by making m depend on y so that $m(y)$ is positive for $y \to \infty$, but negative at large negative values of y This appears to be a rather blurry boundary, but one can also imagine making the region where $m(y)$ changes sign very small, making the boundary sharper. Interestingly, this Dirac operator has a zero mode. Let us set the momentum of the fermion in the x direction to zero, so that we end up with the differential equation,

$$\partial_y\Psi(y) = -\sigma_x m(y)\Psi(y). \tag{4.13}$$

The normalisable solution is given by

$$\Psi(y) = \exp\left(-\int_{y_0}^{y} m(y')dy'\right)\begin{pmatrix}1\\1\end{pmatrix}, \tag{4.14}$$

This zero mode only depends on the sign change of m, since for large values of y, Ψ is exponentially suppressed, and sharply peaks near $y = y_0$. Crucially, it also does not depend on the details of the mass profile. This zero mode was first found by Jackiw and Rebbi in [144]. Due to the zero-mode's ignorance about the details of the mass profile, they are robust agains small changes in $m(y)$; only changing the asymptotics of $m(y)$ will alter the localised nature of the zero-mode. Said differently, the zero-mode is topologically protected edge mode located at $y = y_0$ and is yet another hallmark of topological insulators.

Staring a bit longer at these results, we also see another intriguing property. The boundary mode is a localised excitation as long as the mass changes sign as a function of y. But from (4.9), where we did not have any boundary present, a change in sign of m changes the winding and hence the topological phase as well. Of course, we have taken a continuum limit here, so these results for the winding cannot be copied directly, but this will not affect the physics. We thus see that on the phase boundaries between topologically trivial and non-trivial insulators there are edge states and that their presence is determined by topology of the system without boundary. Even more important, since the vacuum is always considered topologically trivial, a topologically non-trivial insulator on a finite slab of material has boundary modes. This is a manifestation of the *bulk-boundary correspondence*. Due to this intimate relationship, the topology of the band structure can be probed experimentally by studying the edges using angle-resolved photoemission spectroscopy.

Thus far, our discussion has revealed two very important features of topological insulators, even though we focused on a particular class of Hamiltonians. First, we have seen that topological insulators have a band structure that can be topologically non-trivial, i.e can have non-zero value for ν. Second, this topology manifests itself as boundary modes whenever the material has boundaries.

Note also that we have not taken into account any interactions. In fact, this will be assumed throughout this part of the dissertation. This simplifies the analysis a lot, but still leaves a wealth of interesting topological phases at our disposal as we will discover in chapters 5 and 6. Including interactions is a challenging endeavour, which we will discuss briefly in the summary and outlook.

Before moving on to discuss what we want to do with these topological insulators and what role they play in this dissertation, let us present the same system from a high-energy theory perspective. This was also mentioned briefly in chapter 1.

A high-energy perspective

To understand the quantum Hall state from a more high-energy perspective, one can think of it in the following way. Start with a massive Dirac fermion Ψ in 2+1 dimensions coupled to a background $U(1)$ gauge field A_μ, which signifies the electron in $2+1$ dimensions coupled to an external magnetic and electric field. The Euclidean action for this system is

$$S = \int d^3x \, \overline{\Psi} \left(i\gamma^\mu D_\mu + m \right) \Psi \tag{4.15}$$

with γ^μ the gamma matrices satisfying the Clifford algebra $\{\gamma^\mu, \gamma^\nu\} = -2\delta^{\mu\nu}$, m the mass of the fermion and

$$D_\mu = \partial_\mu - iA_\mu. \tag{4.16}$$

Since the Dirac fermion is massive we can integrate it out and consider the low energy effective theory for energies E below the mass m. At these energies, we cannot excite any of the modes of the fermion so that it is acting as an insulator or in more high-energy terminology, there are no propagating degrees of freedom at energies below m. Since the theory is quadratic in Ψ the path integral over Ψ can be done exactly and gives the partition function,

$$Z[A, m] = \det \left(i\gamma^\mu D_\mu + m \right) = \exp \left(\mathrm{Tr} \log \left(i\gamma^\mu D_\mu + m \right) \right). \tag{4.17}$$

Expanding the term in the exponent in the last equality to lowest order in E/m, we get

$$S_{\text{eff}} = -i \frac{k}{4\pi} \int d^3x \, \epsilon^{\mu\nu\rho} A_\mu \partial_\nu A_\rho + S_{\text{div}}. \tag{4.18}$$

It is not too difficult to derive this result, see [145, 146] for more details. We note two things about this effective action S_{eff}. The first part is known as (Abelian) Chern-Simons theory. This theory does not have propagating degrees of freedom in accord with what we said before and is what one would expect from an insulating system. The second piece, S_{div}, also arises after expanding the log in (4.17) to second in A_μ, but is not finite. It is linearly divergent and will be dealt with momentarily.

Besides just S_{eff}, there are more terms, which are small as E/m becomes small and so for energies E well below the gap, the physics is completely captured by the Chern-Simons action. To make contact with the quantum Hall effect, let us see what the conductivity is. Conductivities appear as the coefficients relating external electric fields to currents. In particular for the J_i component of the current, we have

$$J_i = \sigma_{ij} E_j \tag{4.19}$$

so

$$\sigma_{ij} = \frac{\delta J_i}{\delta E_j}. \tag{4.20}$$

Moreover, the current J_i is the functional derivative of S_{eff} with respect to A_i and upon writing $E_j = \partial_\tau A_j$, we can get the Hall conductivity from S_{eff} as

$$\sigma_{ij} = \frac{\delta^2 S_{\text{eff}}}{\delta A_i \delta \partial_\tau A_j}. \tag{4.21}$$

Performing the functional derivatives, yields:

$$\sigma_{xy} = -i\frac{k}{2\pi}, \tag{4.22}$$

which is a result in Euclidean signature. To go back to Lorentzian signature, we simply strip off the $-i$. To relate to the quantum Hall physics, it is thus clear that we need to know whether k is quantised or not, since that will make σ_{xy} quantised as well. Luckily, as is explained beautifully in [147], k is indeed required to be quantised as a result of gauge invariance of the action (4.18). In fact, by restoring units, one finds that $\hbar k/e^2 = \nu$ needs to be an integer, so that

$$\sigma_{xy} = \frac{k}{2\pi} = \frac{e^2}{h}\nu, \tag{4.23}$$

as it should. Notice also that this is exactly the same as we found before. The value of k can also be computed once the fermion Ψ has been integrated out. Naively, this will give the wrong result, but a more careful analysis, which also regularizes the divergent piece S_{div}, gives either $\nu = 0$ or 1, depending on the sign of the mass m. It is no coincidence that this feature is exactly the same as we encountered before as well. Other values of ν can also be obtained by considering multiple fermion flavours in (4.15). The important point is that the effective action will still take the form of a Abelian Chern-Simons theory and so one can also take that action as a starting point, with any integer ν and use it for an effective description of a quantum Hall state with $\sigma_{xy} \sim \nu$.

This perspective also reveals another interesting feature of the quantum Hall state. Namely, as alluded to before, when the systems is put on a manifold $\mathcal{M}$ with boundary, there is a non-zero conductance that is purely localised on the boundary. In the Chern-Simons perspective, this is nothing but the statement that the Chern-Simons action on manifolds with boundaries is not gauge invariant under $A_\mu \to A_\mu + \partial_\mu \alpha$, since then

$$S \to S - i\frac{k}{4\pi}\int_{\partial\mathcal{M}} d^2x \epsilon^{\mu\nu} A_\mu \partial_\nu \alpha. \tag{4.24}$$

Moreover, in the case of non-empty boundary, the variational problem of the action also has to be supplemented with boundary conditions. Without going in too

much detail here, these boundary conditions have the effect of inducing degrees of freedom on the boundary that are also not gauge invariant, but cancel the non-gauge invariance of the bulk action so that the full system (bulk plus boundary) is gauge invariant again. A process known as anomaly inflow. The boundary degrees of freedom are rather simple and form a theory of ν free chiral scalar fields in 1+1 dimensions. These modes are gapless and are responsible for the Hall conductivity in the quantum Hall state. Each chiral scalar is responsible for e^2/h worth of conductivity and so the quantisation of the Hall conductivity is coming from the number of degrees of freedom that live on the boundary.

4.2 Anybody out there?

We have now briefly seen some of the properties of quantum Hall states and argued that many of them are also present in other topological phases. One of the objectives of this part in the dissertation is to understand the landscape of topological phases or more specifically of topological insulators. This question is similar to the universality classes studied in the context of the Landau paradigm. This resulted in a list of possible (symmetry-based) phase transitions and we would like to understand here whether we can make such a list for topological insulators as well. Due to the topological nature of these phases there are discrete labels assigned to each phase and so one might be able to indeed enumerate them and in fact find *all* of them.

But what is the point in classifying topological insulators? What do we learn from enumerating all topological phases? First of all, since this is a theoretical physics dissertation, there is a wealth of interesting physics going on that has been measured in some way or another, but in some cases still lacks theoretical understanding. By enumerating all topological phases, one can understand them more systematically and see what the common features are in much the same way as we saw for topological insulators in the above. Second, knowing how many topological phases there are, might also reveal phases that on the basis of a simple analysis appear to exist but have not been measured experimentally yet. It can therefore predict new phase, new topological invariants and thus new physics in both the bulk as well as along the boundary.

How then, do we classify the quantum Hall phases that we saw in the previous section? Each quantum Hall phase is specified by an integer, which we denoted by ν. Since any two quantum Hall phases with different integers are separated by gap-closing, the quantum Hall phases are classified by an integer. In particular, the value of the topological invariant classifies the quantum Hall phases. In the next

two chapters, 5 and 6, we embark on a quest to find more topological invariants that distinguish one topological insulator from another. The novelty of this work as compared to others is the rather simple set of rules that we derive to find *all* topological invariants in a given material with a particular set of symmetries.

The symmetries that we will be mostly be concerned with are symmetries of the lattice and time-reversal symmetry. Symmetries of the lattice are operations on the lattice points that map it to other lattice points or itself. For example, this could be a (discrete) translation symmetry along the lattice directions or a reflection in some line or plane. These symmetries have the effect of constraining not only the wavefunction in real space, but also in reciprocal space. In reciprocal space, it means that the full band can be constructed from knowledge of the band in a smaller part of the Brillouin zone, called the fundamental domain. Moreover, for instance when a reflection symmetry is present, the bands can be even or odd under the reflection and hence assigns additional labels to the bands. These additional labels are the eigenvalues of the symmetry operation and is one of the key concepts we will use in the classification in chapter 5. A few details about crystal symmetries has been gathered in appendix A.3.

The other symmetry we will be interested in is time-reversal symmetry (TRS). This symmetry, denoted by T, flips the arrow of time and therefore also flips the sign of the momentum in reciprocal space. At momenta in the (first) Brillouin zone that are invariant under time-reversal, time-reversal will commute with the (Bloch) Hamiltonian and can thus cause the spectrum to become degenerate there. Generically, this is indeed what happens and is referred to as Kramers' degeneracy. In the classification this has the effect of changing not only the eigenvalues we talked about in the above, but also the topological invariants. The topological invariants will not be valued in the integers anymore as we saw for the quantum Hall phases, but will now only take the values 0 and 1. Understanding how this invariant can be understood intuitively in the presence of other crystal symmetries will be a major part of both chapters 5.

On the free level, there are two types of time-reversal symmetry, depending on square of T. As we discuss in appendix A.3, the square can either be $+1$ for spinless particles or -1 when the spin of the electron is take into account. These form two big symmetry classes that are denoted by class AI and AII. There is also a class for systems that are not invariant under time-reversal, which is denoted as class A. Together they form Dyson's three-fold way, [148]. In this dissertation we will be mostly concerned with classes A and AII, but occasionally mention class AI as well. Besides class A, AI and AII, there are in fact seven more classes found by Altland and Zirnbauer [149] that are concerned with systems possessing a chiral symmetry or particle-hole symmetry.

After having found a set of topological insulators in chapter 5 in each class, it is crucial to check our results, not only to determine whether the invariants we found are actual *topological* invariants, but also to be able to claim a completeness of our set of topological insulators. One way this could be done is by setting up an experiment and trying to see whether the new topological phases actually exist. Unfortunately, this is extremely difficult, since it is hard to find an explicit representative Hamiltonian within each phase that is realised in Nature as well. Moreover, showing completeness experimentally is virtually impossible. Instead, let us return to our theoretical laboratory. Here we are much more fortunate, since in mathematics the classification of topological insulators can be put on a very rigorous footing. Within the framework known as K-theory, we can indeed verify whether the claims made in 5 are correct. In chapter 6 we will embark on this verification by explicitly computing the mathematical objects responsible for the classification of topological insulators. For the simple cases that we checked, we can indeed show that our simple set of rules give the correct classification of topological insulators.

This concludes the introduction to the second part of this dissertation. We have discussed the basics of topological insulators through a simple topological insulator, the integer quantum Hall phase. This provides enough background to understand the following chapter, but for some technical tools that we use and an introduction in K-theory, see appendices A.3 through A.5.

5 Combinatorial Classification of Crystalline Topological Insulators

This chapter is based on the following publications:

J. Kruthoff, J. de Boer, J. van Wezel, C. L. Kane and R-J. Slager,
"Topological Classification of Crystalline Insulators through Band Structure Combinatorics",
Phys. Rev. X **7** (2017) 4, 041069, `arXiv:1612.02007 [cond-mat.mes-hall]`.

J. Kruthoff, J. de Boer and J. van Wezel,
"Topology in time-reversal symmetric crystals",
Submitted to Scipost, `arXiv:1711.04769 [cond-mat.str-el]`.

5.1 Introduction

The tenfold periodic table has been a cornerstone in the description of the connection between topology and symmetry [150, 151]. It specifies the number of topologically distinct ground states that are possible in free fermion systems in any number of dimensions, if their behaviour under time-reversal symmetry, particle-hole symmetry, and chiral symmetry is given [152]. The combinations of discrete symmetries on which the ten classes in the table are based, do not include any spatial symmetries. Materials in nature however, are made up out of atoms which are often positioned in a periodic crystal structure containing crystal symmetries. Indeed, the very existence of periodic band structures for electrons is a consequence of the breaking of translation symmetry by an atomic lattice. It is well-known that within time-reversal symmetric topological insulators, the discrete transla-

tional symmetries surviving within the atomic lattice lead to the definition of weak invariants in three dimensions, which need to be used in addition to the tenfold periodic table to get a full classification of the topological state [153, 154]. This procedure can be generalized to include any space group symmetry in two and three spatial dimensions [155] and is expected to become experimentally accessible and relevant in the presence of lattice defects [156–161]. More generally, the interplay of the rich structure of space group symmetries and topology entails an active field of research, providing for new phases and according quasiparticles [162–172].

In addition to their role in characterizing topological insulators, lattice symmetries are also vital in describing the phases that emerge on the boundary between topologically distinct phases. A notable example is found in gapless Weyl semimetals [173], one of which has been recently identified experimentally in TaAs [174–176]. The topological origin of these Weyl phases ensures the presence of specific surface states, called Fermi-Arcs, which connect the band crossings in the bulk. The presence of either three-fold rotations or nonsymmorphic space group symmetries in these materials guarantees that the bulk band crossings cannot be gapped, and it therefore also protects the corresponding Fermi-arcs [177–179].

In this chapter, we use space group symmetries to provide a simple, but universal, algorithm for identifying and labelling distinct crystalline topological phases. We address crystals with or without time-reversal, but broken particle-hole, chiral symmetries or any other anti-commuting or anti-unitary symmetry, in all physically relevant spatial dimensions. The method specifies all possible phases of spinless particles in class A, in one or two dimensions, and in three dimensions up to a subtle open K-theoretical question addressed later on. For class AII, we will find interesting new $\mathbf{Z}_2$ invariants but do not prove completeness. In chapter 6, we will do various non-trivial checks in K-theory that confirm our results.

The algorithm essentially uses elementary representation theory to characterise topologically distinct band structures. In two dimensions this results in the complete list of allowed topological phases shown in Table 5.1. The equivalent table in three dimensions can be constructed using the same procedure. Our arguments agree with the mathematical computations in terms of twisted equivariant K-theory, as proposed by Freed and Moore [181]. This connection elucidates not only on putting involved mathematical notions in a straightforward physical setting but most importantly provides a formal mathematical underpinning of our classification.

The algorithm will be worked out in detail below, but can be presented here on a heuristic level. The occupied bands in a crystal are described by Bloch functions on the Brillouin zone (BZ). These functions transform under the crystal symmetry

	A		AII	
$\mathcal{G}$	Representation	Chern number	Representation	Torsion invariants
$p1$	$\mathbf{Z}$	$\mathbf{Z}$	$\mathbf{Z}$	$\mathbf{Z}_2$
$p2$	$\mathbf{Z}^5$	$\mathbf{Z}$	$\mathbf{Z}$	$\mathbf{Z}_2^4$
pm	$\mathbf{Z}^3$	0	$\mathbf{Z}$	$\mathbf{Z}_2^2$
pg	$\mathbf{Z}$	0	$\mathbf{Z}$	$\mathbf{Z}_2$
cm	$\mathbf{Z}^2$	0	$\mathbf{Z}$	$\mathbf{Z}_2$
$p2mm$	$\mathbf{Z}^9$	0	$\mathbf{Z}$	$\mathbf{Z}_2^4$
$p2mg$	$\mathbf{Z}^4$	0	$\mathbf{Z}$	$\mathbf{Z}_2^2$
$p2gg$	$\mathbf{Z}^3$	0	$\mathbf{Z}$	$\mathbf{Z}_2^2$
$c2mm$	$\mathbf{Z}^6$	0	$\mathbf{Z}$	$\mathbf{Z}_2^3$
$p4$	$\mathbf{Z}^8$	$\mathbf{Z}$	$\mathbf{Z}^3$	$\mathbf{Z}_2^3$
$p4mm$	$\mathbf{Z}^9$	0	$\mathbf{Z}^3$	$\mathbf{Z}_2^3$
$p4gm$	$\mathbf{Z}^6$	0	$\mathbf{Z}^2$	$\mathbf{Z}_2^2$
$p3$	$\mathbf{Z}^7$	$\mathbf{Z}$	$\mathbf{Z}^4$	$\mathbf{Z}_2^3$
$p3m1$	$\mathbf{Z}^5$	0	$\mathbf{Z}^4$	$\mathbf{Z}_2^3$
$p31m$	$\mathbf{Z}^5$	0	$\mathbf{Z}^3$	$\mathbf{Z}_2^3$
$p6$	$\mathbf{Z}^9$	$\mathbf{Z}$	$\mathbf{Z}^4$	$\mathbf{Z}_2^3$
$p6mm$	$\mathbf{Z}^8$	0	$\mathbf{Z}^4$	$\mathbf{Z}_2^3$

Table 5.1: The complete classification of topological phases of spinless particles in class A and spin$-\frac{1}{2}$ particles in class AII, both within two-dimensional crystals. The wallpaper groups $\mathcal{G}$ in the first row are denoted in the Hermann-Mauguin notation [180]. The second and fourth column denotes the number of integers that need to be specified in order to completely characterise the representation of the valance bands of a topological phase in the corresponding wallpaper group, whereas the third and fifth column signifies whether or not a Chern number/torsion invariant is present. The total classification is the (direct) sum of the representation and Chern number/torsion invariants within each class.

in a particular way which changes as one goes from a generic point in the BZ to a high symmetry point as outlined in more detail in appendix A.3. As there are different ways of reaching such high symmetry points, the transformation rules of Bloch functions need to satisfy gluing conditions which ensure their mutual compatibly [182]. The possible valence band structures in a crystal are thus limited to ones that are consistent with the gluing conditions implied by its crystal symmetry. The way a valence band transforms under crystal symmetries can only be altered by exchanging it with a conduction band, which necessarily involves a closing of the band gap. Since topological phases of matter are defined to be robust to changes that keep the gap open, an alteration in the transformation properties

of the valence band can be interpreted as a topological phase transition. This is analogous to the way changes in more familiar topological invariants, such as the Chern number or TKNN invariant [141, 183], are necessarily accompanied by a closing of the gap, which we also saw in section 4.1. We therefore find that the transformation properties of the valance band characterise its topological phase, and need to be included in the topological classification. We describe the transformation properties of the valence band by a set of integers, which, together with the Chern number and $\mathbf{Z}_2$ invariants, completely specifies the topological phase of any crystal within class A or AII (modulo topologically trivial bands). Taking robustness of a topological phase under smooth deformations of the Hamiltonian and counting modulo topologically trivial bands (which we discuss below in more detail) as the starting point of our method, we can rigorously show for class A that the invariants identified are indeed topological, and that we find the complete set of distinct invariants. This should be contrasted with the alternative approach of generalising known topological invariants, such as for example in [184], where completeness and topological invariance cannot be guaranteed. For class AII, such a proof is more difficult, since the K-theory computations have not been done in the literature, except for some simple space groups in two dimensions, see [5] for a more thorough exposition.

This chapter is organized as follows. We first present the example of a specific two-dimensional crystal structure to illustrate the classification scheme on a conceptual level, and to introduce some notation. In section 5.4 we then discuss the general case in two dimensions. We show in Section 5.5 that three dimensional topological insulators in class A and AII can be classified using the same scheme after taking into account some additional subtleties. Generalizations to other classes will also be considered in this section.

5.2 Some examples

To give a conceptual description of the proposed classification scheme, we first focus on two particular examples of a two-dimensional crystal whose crystal structures fall within the symmorphic wallpaper groups $p4mm$ and $p4$. For $p4mm$, we assume no time-reversal symmetry, hence we will be in class A, but for $p4$ we will consider the system to be in class AII.

5.2.1 $p4mm$ in class A as an example

Consider a square array of atoms with lattice spacing a, which is set to unity ($a = 1$) in the remainder of this chapter. The lattice is spanned by the lattice vectors $\mathbf{t}_1 = (1, 0)$ and $\mathbf{t}_2 = (0, 1)$. Besides the lattice translations, the crystal is symmetric under all operations that leave a square invariant. These symmetries form the point group $G = D_4$, which is generated by a reflection t about the x-axis and an in-plane 90°-rotation r. A general element g of the space group $p4mm$ consists of the combination elements R of the point group D_4 and a translation along a vector $\mathbf{X} = n_1\mathbf{t}_1 + n_2\mathbf{t}_2$. In momentum space, we have two reciprocal lattice vectors $\mathbf{g}_1 = 2\pi(1, 0)$ and $\mathbf{g}_2 = 2\pi(0, 1)$. We parametrise the Brillouin torus as a square with $-\pi \leq k_{x,y} \leq \pi$. Using this parametrisation, the point group elements act as

$$r \cdot (k_x, k_y) = (-k_y, k_x), \quad t \cdot (k_x, k_y) = (k_x, -k_y). \tag{5.1}$$

The fundamental domain Ω thus consists of the region with momentum values $0 \leq k_x \leq \pi,\ 0 \leq k_y \leq k_x$, as shown in Figure 5.1.

Within the fundamental domain, there are fixed points of (part) of the symmetry operators in D_4. As we explain in detail in appendix A.3, the electronic states with momenta corresponding to such a fixed point sit in unitary irreducible representations of the corresponding stabilizer group. In the condensed matter literature, these special momenta are also called high-symmetry points and for the case at hand are shown in figure 5.1. The corresponding stabilizer groups are given in table 5.2.

As an example, consider the origin $\Gamma = (0, 0)$. The momentum of Bloch states at this point in the first Brillouin zone is held fixed under both r, and t, and any combination of reflections and rotations. The same is true for $M = (\pi, \pi)$, because under r and t this point is mapped onto itself modulo a reciprocal lattice vector. The presence of reflections in the group D_4, also allows entire lines in the first Brillouin zone to be left invariant under some of the point group operations. One readily verifies that $l_1 = (k_x, 0)$ is left invariant by t, while $l_2 = (\pi, k_y)$ and $l_3 = (k_x, k_x)$ are invariant under the action of r^2t and rt, respectively. At the intersection of l_1 and l_2 we find the point $X = (\pi, 0)$, which must be left invariant under both the symmetries that leave l_1 unaffected, and the symmetries that keep l_2 fixed.

The stabilizer groups at high symmetry points may necessitate bands at those points to become degenerate. This can be seen directly from the way a space group element acts on the Bloch function $\Psi_{\mathbf{k},i}(\mathbf{r})$ with band index i, position $\mathbf{r}$,

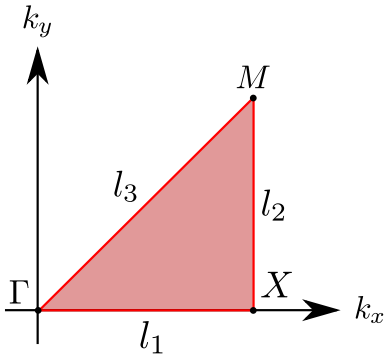

Figure 5.1: The fundamental domain (shaded red) Ω of the first Brillouin zone. It contains only points that are not related to each other by transformations in the point group D_4, as described by equation (5.1). high symmetry lines are indicated in red, and high symmetry points in black.

and wave vector $\mathbf{k}$:

$$\{R|\mathbf{x}\} \cdot \Psi_{\mathbf{k},i}(\mathbf{r}) = \sum_j \Gamma^{\mathbf{k}}_{ij}(\{R|\mathbf{x}\})\Psi_{R\cdot\mathbf{k},j}(\mathbf{r}-\mathbf{x}). \tag{5.2}$$

The point group element R transforms a Bloch function with momentum $\mathbf{k}$ to a Bloch function with momentum $R\cdot\mathbf{k}$. Bloch functions with different band indices j, but equal momentum $\mathbf{k}$, may be mixed by the matrix $\Gamma^{\mathbf{k}}_{ij}(\{R|\mathbf{x}\})$. The Bloch functions can always be arranged so that this matrix is a unitary irreducible representation of the space group element $\{R|\mathbf{v}\}$. For generic points in the fundamental domain away from high symmetry locations, is usually just a phase factor (i.e. a one-dimensional representation). The elements of the space group for which $\mathbf{x}$ is a pure lattice translation, combine Bloch functions $\Psi_{R\cdot\mathbf{k},j}(\mathbf{r}-\mathbf{x})$ that differ from the functions $\Psi_{R\cdot\mathbf{k},j}(\mathbf{r})$ by pure phase factors. Space groups consisting only of these types of elements, such as $p4mm$, are called symmorphic, and in dealing with these space groups we only need to consider ordinary representations of the point groups when determining the $\Gamma^{\mathbf{k}}_{ij}(\{R|\mathbf{v}\})$. For nonsymmorphic space groups, which contain screw axes or glide planes, and have elements with $\mathbf{v}$ a fraction of a lattice translation, projective representations of the point groups need to be taken into account. See appendix A.3 for an example.

Since the Hamiltonian is symmetric with respect to the space group of the lattice, eigenstates of space group elements must also be eigenstates of energy. Equation (5.2) shows the eigenstates of $\{R|\mathbf{v}\}$ to be linear combinations of $\Psi_{R\cdot\mathbf{k},j}(\mathbf{r})$, so these states must all have equal energy. For states at high symmetry points, such that $R\cdot\mathbf{k}=\mathbf{k}$, all bands at $\mathbf{k}$ connected by $\Gamma^{\mathbf{k}}_{ij}(\{R|\mathbf{v}\})$ are then necessarily

	$\mathbf{k}$	stabilizer group $G_{\mathbf{k}}$
Γ	$(0,0)$	D_4
M	(π,π)	D_4
X	$(\pi,0)$	$\mathbf{Z}_2 \times \mathbf{Z}_2 = \{e, r^2, t, r^2t\}$
l_1	$(k_x,0)$	$\mathbf{Z}_2 = \{e, t\}$
l_2	(π,k_x)	$\mathbf{Z}_2 = \{e, r^2t\}$
l_3	(k_x,k_x)	$\mathbf{Z}_2 = \{e, rt\}$
$\mathrm{int}(\Omega)$	(k_x,k_y)	$\{et\}$

Table 5.2: The stabilizer groups contained within the space group $p4mm$. These stabilizer groups consist of all symmetry operations which keep the momentum of a particular high symmetry point or line fixed. The fundamental domain Ω in this case contains momentum points with $0 < k_x < \pi$ and $0 < k_y < k_x$, and its interior is denoted $\mathrm{int}(\Omega)$.

degenerate. This conclusion can also be expressed on the level of the Hamiltonian itself. If the full Hamiltonian is written as a sum of Bloch Hamiltonians $H(\mathbf{k})$, the action of the crystal symmetries can be described by:

$$\Gamma_{\mathbf{k}}(R)H(\mathbf{k})\Gamma_{\mathbf{k}}(R)^{-1} = H(R\cdot\mathbf{k}) \Rightarrow [\Gamma_{\mathbf{k}}(R), H(\mathbf{k})] = 0 \quad \text{if } R\cdot\mathbf{k} = \mathbf{k}. \tag{5.3}$$

Here $\Gamma_{\mathbf{k}}(R)$ is a unitary (matrix) representation of the point group element R, or equivalently, an operator enacting its symmetry transformation. The Bloch Hamiltonian commutes with the elements of the stabilizer groups at the associated high symmetry points and lines. At these locations, the eigenfunctions of the Bloch Hamiltonian are thus also eigenfunctions of the elements of the stabilizer group. Conversely, the collection of states in the valence band with momentum $\mathbf{k}$, forms a representation of the stabilizer group $G_{\mathbf{k}}$. This representation consists of unitary irreducible representations of $G_{\mathbf{k}}$, which represent either individual bands (one-dimensional irreducible representations) or sets of necessarily degenerate bands (higher-dimensional irreducible representations). Determining the irreducible representations of $G_{\mathbf{k}}$ can thus be interpreted as a recipe for constructing the entire set of valence bands at high symmetry locations. As we will see in the following, however, it is necessary to impose additional constraints when considering the structure of the valence bands throughout the first Brillouin zone.

These constraints come from the fact that representations along high symmetry lines need to connect properly, i.e continuously, to representations at their endpoints, the high symmetry points. That is, if a Bloch state has a certain eigenvalue for a symmetry transformation on a high symmetry line, that eigenvalue cannot suddenly change at the endpoint of the line. Let us be a bit more concrete for $p4mm$. In this case, the bands at Γ and M form a representation of D_4, and at

	$\{1\}$	$\{t\}$
$l_{i,+}$	1	1
$l_{i,-}$	1	-1

Table 5.3: The character table of $\mathbf{Z}_2$. The irreducible representations along the line l_i are denoted by $l_{i,\pm}$. The columns are labelled by the conjugacy classes of $\mathbf{Z}_2$, containing all symmetry operations that share the same character for each representation. Here $\pm$ signifies whether states are respectively even or odd under the symmetry transformation.

	$\{1\}$	$\{r^2\}$	$\{r, r^3\}$	$\{t, r^2t\}$	$\{rt, r^3t\}$
Γ_0	1	1	1	1	1
Γ_1	1	1	1	-1	-1
Γ_2	1	1	-1	1	-1
Γ_3	1	1	-1	-1	1
Γ_4	2	-2	0	0	0

Table 5.4: The character table of D_4 at Γ. The irreducible representations are denoted by Γ_i. The columns are labelled by the conjugacy classes of D_4. The stabilizer group at M is also D_4 and has the same character table, but the irreducible representations are denoted by M_i.

X of $\mathbf{Z}_2 \times \mathbf{Z}_2$. Along the lines l_i connecting these three points, the bands need to form a representation of $\mathbf{Z}_2$. Symmetry transformations making up a $\mathbf{Z}_2$ group structure always have eigenvalues ± 1, so that the eigenstates along l_i can be either even $(+)$ or odd $(-)$ under the transformation:

$$R_i \left|u_{\mathbf{k}}, \pm\right\rangle \quad = \quad l_{i,\pm}(R_i) \left|u_{\mathbf{k}}, \pm\right\rangle \tag{5.4}$$

Here R_i is an element of the stabilizer group $\mathbf{Z}_2$ along l_i, and $|u_{\mathbf{k}}, j\rangle$ represents a state at momentum $\mathbf{k}$ with reflection eigenvalue ± 1. The eigenvalues $l_{i,\pm}(R_i) = \pm 1$ in general are representations of the stabilizer group $\mathbf{Z}_2$ along l_i. Since the representations are one-dimensional (i.e. they apply to a non-degenerate band), they can be replaced by their characters, which equal the eigenvalues ± 1. In the general case of higher dimensional representations, or having a degenerate set of Bloch functions, the representations become matrices.

If we now follow a particular band along a high symmetry line l_i towards its endpoint, the eigenvalues of the symmetry transformation are preserved along the line. On the high symmetry point at the end of the line, the state is symmetric under more symmetries, and gains some additional quantum numbers describing those, but it retains the eigenvalue that it carried along the line. We are thus restricted in the choice of representation on the high symmetry points by the

	$\{1\}$	$\{r^2\}$	$\{t\}$	$\{r^2t\}$
X_0	1	1	1	1
X_1	1	1	-1	-1
X_2	1	-1	1	-1
X_3	1	-1	-1	1

Table 5.5: The character table of $\mathbf{Z}_2 \times \mathbf{Z}_2$ at X. Irreducible representations in this case are denoted by X_i and the columns are labelled by the conjugacy classes of $\mathbf{Z}_2 \times \mathbf{Z}_2$.

representations along the high symmetry lines. In other words, when we follow any band towards an endpoint of l_i, its representation induces either a representation of D_4 or of $\mathbf{Z}_2 \times \mathbf{Z}_2$, depending on the endpoint. In terms of character tables, this means that the characters in the character table corresponding to the common elements at l_i and the high symmetry points need to agree. For example, suppose a band transforms as $l_{1,-}$, i.e. it is odd under t along l_1. As the entire line l_1 is held fixed by t, the action of t at the endpoint X must be the same as its action along l_1. Consulting the character table 5.5, we see that at X, the band must thus transform as either X_1 or X_3.

At Γ, the other endpoint of l_1, the band should similarly remain odd under t. According to the character table 5.4, we then see that at Γ, the band must transform as either Γ_1 or Γ_3. In fact, the two-dimensional representation Γ_4 is also a possibility, as long as there is an additional even band along l_1. In that case, the even and odd bands becoming degenerate at Γ would be consistent with t being represented in Γ_4 by a two-dimensional matrix with eigenvalues 1 and -1 (the character for Γ_4 in table 5.4 is the sum of eigenvalues). At Γ the two band then form a doublet of D_4.

Repeating this analysis for even bands along l_1, the entries in tables 5.5 and 5.4 for the conjugacy classes $\{t\}$ and $\{t, r^2t\}$ respectively, need to be 1. Hence, even bands along l_1 end in X_0 or X_2 at X and go to Γ_0, Γ_2 or Γ_4 at Γ. Applying similar constraints to all high symmetry locations ensures a consistent representation of the entire set of valence bands throughout the fundamental domain.

Completing the list of which representations along lines l_i enhance to which representations at the endpoints Γ, X, and M results in Table 5.6. It shows for example that starting from a given representation at Γ, only certain representations at the other high symmetry locations are allowed. Below we will use this information to define a set of integers that specifies the representation of the complete set of valance bands. These integers then characterize the topological phase in space group $p4mm$, modulo Chern numbers (in class A).

	group enhancement	rep. enhancement
l_1	$D_4 \leftarrow \mathbf{Z}_2$	$\Gamma_0, \Gamma_2, \Gamma_4 \leftarrow l_{1,+}$
	$D_4 \leftarrow \mathbf{Z}_2$	$\Gamma_1, \Gamma_3, \Gamma_4 \leftarrow l_{1,-}$
	$\mathbf{Z}_2 \times \mathbf{Z}_2 \leftarrow \mathbf{Z}_2$	$X_0, X_2 \leftarrow l_{1,+}$
	$\mathbf{Z}_2 \times \mathbf{Z}_2 \leftarrow \mathbf{Z}_2$	$X_1, X_3 \leftarrow l_{1,-}$
l_2	$D_4 \leftarrow \mathbf{Z}_2$	$M_0, M_2, M_4 \leftarrow l_{2,+}$
	$D_4 \leftarrow \mathbf{Z}_2$	$M_1, M_3, M_4 \leftarrow l_{2,-}$
	$\mathbf{Z}_2 \times \mathbf{Z}_2 \leftarrow \mathbf{Z}_2$	$X_0, X_3 \leftarrow l_{2,+}$
	$\mathbf{Z}_2 \times \mathbf{Z}_2 \leftarrow \mathbf{Z}_2$	$X_1, X_2 \leftarrow l_{2,-}$
l_3	$D_4 \leftarrow \mathbf{Z}_2$	$\Gamma_0, \Gamma_3, \Gamma_4 \leftarrow l_{3,+}$
	$D_4 \leftarrow \mathbf{Z}_2$	$\Gamma_1, \Gamma_2, \Gamma_4 \leftarrow l_{3,-}$
	$D_4 \leftarrow \mathbf{Z}_2$	$M_0, M_3, M_4 \leftarrow l_{3,+}$
	$D_4 \leftarrow \mathbf{Z}_2$	$M_1, M_2, M_4 \leftarrow l_{3,-}$

Table 5.6: The list of consistency relations between representation along high symmetry lines l_i and possible representations at their endpoints Γ, X, and M.

Counting the topological phases protected by *p4mm*

The topological phases we would like to characterize, are defined to be phases of matter which are stable under any deformations that do not close the gap between valence and conductions bands, and that do not change the crystal symmetry. Deformations that do close the gap, necessarily cause either the representation of the set of valance bands or the Chern numbers to change. This means that a topological phase can be uniquely specified by the representation of its set of valance bands and its Chern numbers. For the specific case of the space group *p4mm*, there are no Chern-numbers [163] due to the reflection symmetry in D_4, and so its topological phases within class A are completely specified once the representation of the set of valance bands is known. In table 5.6 we already identified constraints on the allowed representations, which we will now employ to classify the possible topological phases of *p4mm*.

The representation of the set of valance bands, denoted by $\mathcal{V}$, is built out of a number of irreducible representations at each high symmetry point. To specify $\mathcal{V}$, we therefore simply count the number of bands in each irreducible representation at the high symmetry points, subject to the constraints in Table 5.6. Formally, these numbers are allowed to be negative as well as positive, because in the underlying K-theory the counting of bands is always relative. For real materials one can restrict attention to just positive integers. As can be seen from the character tables 5.4, 5.5 there are five irreducible representations at both Γ and M, and four at X. This results in 14 integers, $n_i^{\mathbf{k}}$, signifying how many bands there are at $\mathbf{k}$

transforming under the representation labeled i at that point. For example, the integer n_2^X indicates the number of bands at X transforming as X_2.

We can then consult Table 5.6 to see that only certain representations at Γ, X and M are possible depending on whether the bands are odd or even along the connecting lines l_i. This relates the integers $n_i^{\mathbf{k}}$ at different high symmetry points to each other. For instance, the number of even bands along l_1, $n_0^{l_1}$ must be equal to the combined number of bands in Γ_0, Γ_2 and Γ_4 at Γ,

$$n_0^{l_1} = n_0^\Gamma + n_2^\Gamma + n_4^\Gamma. \tag{5.5}$$

Moreover, going to the other endpoint, X, the number of even bands must equal the sum of those in X_0 and X_2. The combination of the two relations between the number of even representations along the high symmetry lines and the combined numbers of representations at its endpoints then implies a direct relation between the high symmetry points:

$$n_0^\Gamma + n_2^\Gamma + n_4^\Gamma = n_0^X + n_2^X. \tag{5.6}$$

Repeating these steps for the odd bands along l_1, we find a similar relation,

$$n_1^\Gamma + n_3^\Gamma + n_4^\Gamma = n_1^X + n_3^X. \tag{5.7}$$

The integer n_4^Γ specifying the number of bands in the two-dimensional representation Γ_4 appears in both sets of relations, because a doublet at Γ must split into both an even and odd band along l_1. The analysis for the remaining high symmetry lines l_2 and l_3 is similar and yields the relations:

$$\begin{aligned}
n_0^\Gamma + n_3^\Gamma + n_4^\Gamma &= n_0^M + n_3^M + n_4^M && (5.8)\\
n_1^\Gamma + n_2^\Gamma + n_4^\Gamma &= n_1^M + n_2^M + n_4^M && (5.9)\\
n_0^M + n_2^M + n_4^M &= n_0^X + n_3^X && (5.10)\\
n_1^M + n_3^M + n_4^M &= n_1^X + n_2^X. && (5.11)
\end{aligned}$$

The six relations between integers $n_i^{\mathbf{k}}$ show that they cannot be chosen independently, and they thus reduce the number of integers required to specify the complete representation of the set of valance bands. In fact, only five of the six relations are independent from each other. That is, the rank of the system of equations relating different integers $n_i^{\mathbf{k}}$ has rank $m = 5$. This implies that $14 - m = 9$ integers need to be specified to characterize the set of valance bands. These nine integers completely fix how many valence bands there are and under which representations they transform on all high symmetry points in the fundamental domain. We thus conclude that the topological phases of spinless particles in class A protected by *p4mm* space group symmetry can be classified by a set of nine integers, i.e. by elements of $\mathbf{Z}^9$. We will refer to these topological invariants as *representation invariants*.

5.2.2 $p4$ with $T^2 = -1$

In class AII the representation theory is similar and is discussed at length in appendix A.3. Here we will see this machinery at work for the space group $p4$ and not $p4mm$, since the non-abelian nature of the point group makes the analysis technically more involved and might obscure the physics involved.

The space group $p4$ is the same as $p4mm$, but without the reflection generator t. As a result, Γ and M are invariant under the full four-fold rotation r, whereas at X there is only a two-fold rotational symmetry, r^2. As discussed in appendix A.3, to find the representations D with time-reversal symmetry included in class AII, we first find the representations with TRS absent, but of the double cover of the point group. The double cover is constructed by adding an additional element that $\bar{e}$ to the original point group that squares to the identity. It implements the fact that upon rotating a spin$-\frac{1}{2}$ over 2π, its wavefunction will be multiplied by -1, rather than 1. Insisting on having a system in class AII, meaning that all states are fermionic, implies that the representation of $\bar{e}$ must be proportional to $-\infty$. We will call these representations fermionic. For $p4$, the double group at Γ and M is $\mathbf{Z}_8$, but at X it is $\mathbf{Z}_4$. The fermionic representaions at Γ and M are then those that have eigenvalues $e^{\pi i k/4}$ for $k = 1, 3, 5, 7$, whereas at X the eigenvalues are $\pm i$.

Consider next the addition of time reversal symmetry (in this case with $T^2 = -1$). Each electronic state at momentum k must now have a partner state with the same energy, but opposite spin, at $-k$. These two partner states necessarily come together into a single two-fold degenerate state at high symmetry points. This is the celebrated Kramers degeneracy, and it is shown schematically in figure 5.2. Since one state in a Kramers pair is always related to a partner state by TRS, the transformations of a Kramers pair under symmetry operations now produce pairs of related eigenvalues. With only four-fold rotational symmetry, all relavent (i.e. fermionic) representations are complex, hence, as can be seen from (A.41), $I = 0$ for all them. Thus there is a single possible pair of eigenvalues at X, but two different allowed pairs at Γ and M. Listing the number of occupied Kramers pairs in each representation thus gives five integers, which are connected by two relations, since the number of bands at each high-symmetry point must be equal. In this case then, there are three independent representation invariants.

The representation labels are topological invariants, but by themselves they do not yet completely specify the band structure. Just like crystals with broken TRS may possess Chern numbers in addition to band labels, the representation invariants in crystals with unbroken TRS need to be supplemented with *torsion invariants*. These include the well-known Fu-Kane-Mele [185,186], or $\mathbf{Z}_2$, invariants in two and

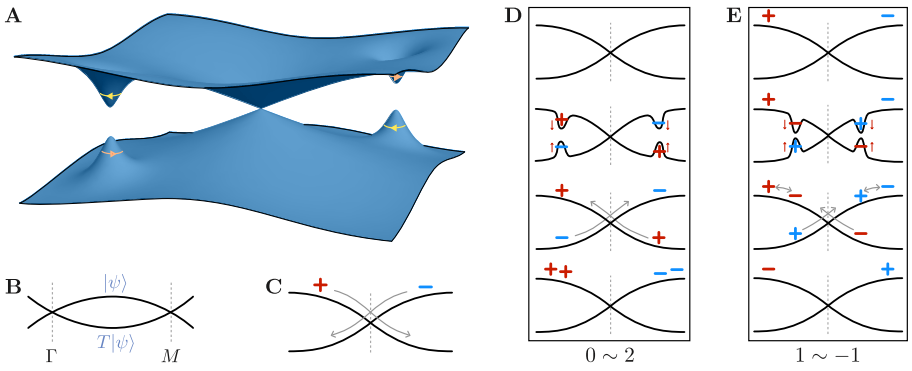

Figure 5.2: **a** The typical band structure of a Kramers' pair close to a high-symmetry point. Two bands related by the time-reversal operation necessarily come together into a degenerate Kramers pair at the time-reversal invariant momentum in the centre. Also shown schematically, is a band inversion which brings together states at points away from the high-symmetry momentum. This results in the formation of vortices in the Berry connection, indicated here by yellow and orange arrows. **b** A more schematic representation of two bands containing states $|\psi\rangle$ and $T|\psi\rangle$, which form Kramers pairs at two time-reversal invariant momenta, chosen here to be Γ and M. **c** Vortices in the Berry connection, depicted by + and −, can be moved throughout the Brillouin zone without annihilating. The color indicates the band to which the vortices belong. **d** An even number of vortices can be created by a band inversion within a set of states related by TRS. **e** Vortices can hop between partner bands using a band inversion to create two vortex anti-vortex pairs.

three dimensions ($\mathrm{FKM}_{2,3}$), as well as a generalisation of line invariants [187]. That crystal symmetries can be central in determining whether of not invariants other than the representation labels may arise in any given material is already known from the case with broken time-reversal symmetry. There, the famous Thouless-Kohmoto-Nightingale-den Nijs (TKNN) invariant, or total Chern number, is zero when reflection symmetries are present [163].

5.3 Torsion invariants in class AII

All torsion invariants are related to the presence of Berry curvature in some of the occupied electronic bands. To define a systematic procedure for identifying which torsion invariants are allowed to be non-zero in any time-reversal symmetric

crystal, we interpret Chern numbers for individual bands as counting the number of vortices in its Berry connection. The generic procedure for creating such vortices is a continuous change in the Hamiltonian which closes the gap between two bands, takes them through each other, and again gaps any points of intersection. After this band inversion a vortex of one handedness resides in one of the bands, and one of the opposite handedness (an anti-vortex) in the other. Once formed, vortices can be moved throughout the Brillouin zone without closing any gaps, or breaking any symmetry, using non-topological changes in the Hamiltonian.

If the Hamiltonian is always time-reversal symmetric, then any change to an electronic state at momentum $\mathbf{k}$ is accompanied by an opposing change in the partner state at $-\mathbf{k}$. Vortices in TRS materials thus necessarily come in vortex anti-vortex pairs, as shown schematically in figure 5.2. The pairs can be moved through the Brillouin zone, and even brought together at time-reversal invariant momenta, but they cannot annihilate there, due to the orthogonality of the electronic states within a Kramers pair.

Since vortices are created in pairs, the total vorticity, or total Chern number, within any pair of TRS-related bands is always zero. It is known however that vortices do not annihilate at high-symmetry points, because the (Berry) connection of the individual bands to the Kramers degenerate pair at the high-symmetry points does not mix the bulk time-reversed states [188]. This makes it possible to consider the Chern number of just one band within each pair, as proven rigorously in [188]. We have to keep in mind however, that a band inversion *within* the pair of TRS-related bands does not constitute a topological phase transition, as it does not close the gap at the Fermi level. As shown in figure 5.2, two vortices or anti-vortices can be created in each band this way, without changing the topological classification of the system. What cannot be done without going through a topological phase transition, is turning an even Chern number into an odd one. There is thus a $\mathbf{Z}_2$ invariant which can be expressed in terms of the Chern number C of a single band as

$$\begin{aligned} \mathrm{FKM}_2 &= N \mod 2 \\ &= C \mod 2, \end{aligned} \tag{5.12}$$

with $N = N_+ - N_-$ the total vorticity, given by the difference in the numbers of vortices and anti-vortices. This is the Fu-Kane-Mele invariant for two-dimensional materials in class AII [189]. If multiple Kramers pairs are occupied, the corresponding FKM_2 invariants are summed.

A major advantage of the vortex picture of FKM invariants, is that the effects of crystal symmetry on its allowed values become much more transparent. In the lattice with only four-fold rotational symmetry for example, a vortex at some

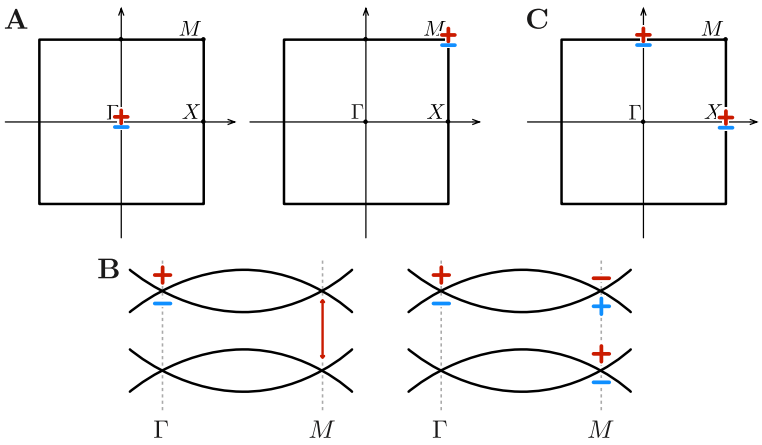

Figure 5.3: **a** Topologically non-trivial vortex configurations with $p4$ symmetry in class AII. **b** A band inversion involving a second, trivial, Kramers pair connects the configurations with a single vortex at Γ to one with an FKM_2-trivial band with vortices at both Γ and M, and one FKM_2-non-trivial band with only a vortex at M. Notice, however, that the final situation cannot be deformed into a band with a single vortex at M and no vortices in the second band. That would require a change in the value of the new torsion invariant described in section 5.3.2. **c** Vortex configuration with $p4$ symmetry in class AII in which the FKM_2 invariant is trivial, but the new invariant of section 5.3.2 is not.

generic momentum $\mathbf{k}$ must always be accompanied by three other vortices at symmetry-related momenta. Such states have a topologically trivial FKM invariant ($\mathrm{FKM}_2 = 0$) because N is even. Topologically non-trivial states can be constructed by having a single vortex either at Γ or M, whereas a vortex at X again implies two vortices in the full Brillouin zone, and thus a trivial FKM invariant. All these configurations are shown schematically in figure 5.3.

In fact, a configuration with a single vortex at Γ can be turned into a configuration with a single vortex at M plus a band with trivial FKM invariant, if we allow for a second, trivial, Kramers pair to be present in the set of valence bands [170]. The two configurations are then connected by a band inversion, as shown in figure 5.3. As in the case without symmetries, the FKM invariant can thus take two possible values, signifying an even or odd number of vortices, without regard to where in the Brillouin zone the vortices occur.

To make the vortex picture of the FMK_2 invariant more precise, one can resort to studying transition function, as was done for the case without crystal symmetries in [190, 191]. For a detailed analysis with crystal symmetry, see the appendices

of [4], but also section 6.5.

5.3.1 Line invariants

The identification of FKM invariants with vorticity, and the methodology of seeing how they are affected by lattice symmetries, works for all possible crystal structures in two and three dimensions, and is suited for class AI as well as AII. Additional features, however, may be identified if there are lines in the Brillouin zone that are mapped onto themselves by both TRS and a crystal symmetry, such as reflection, inversion, or two-fold rotation. On such lines, a one-dimensional topological invariant ν_1, known as the line invariant or Lau-Brink-Ortix (LBO) invariant, can be defined [187].

The one-dimensional line invariants are in fact closely related to the vortices appearing in two dimensions. For example, in a crystal characterised only by a single reflection symmetry in the x axis, the lines at $k_x = 0$ and $k_x = \pi$ are each mapped onto themselves by the reflection symmetry, and also by time-reversal. A line invariant can be defined on each of these lines, but they are related by the expression

$$\mathrm{FKM}_2 = \nu_1^0 + \nu_1^\pi \mod 2. \tag{5.13}$$

The vortices in the Berry connection again provide an intuitive way to understand this. If $\mathrm{FKM}_2 = 1$, there is one vortex at some momentum $\mathbf{k}$, and an anti-vortex in the time-reversed state with the same energy at $-\mathbf{k}$. Both of these must lie on the k_x axis because of the reflection symmetry. Keeping in mind that reciprocal space is periodic owing to the translational symmetry of the atomic lattice, there are then two distinct ways the Berry connection between the vortices could behave. Examples of both are sketched in figure 5.4, which depicts a projection of the matrix-valued Berry connection onto the highest energy state. The connection either makes an odd number of complete windings along the line $k_x = 0$ and an even number along $k_x = \pi$, or the other way around. The field of Berry connections can be altered by gauge transformations and non-topological changes in the Hamiltonian. Since these do not affect the parities ν_1^0 and ν_1^π of the number of windings along the two lines, however, the line invariants cannot be changed without going through a topological transition.

In the crystal with only a reflection symmetry, there are thus two ways for the FKM invariant to be non-trivial, depending on which of the two line invariants is non-trivial. Likewise, there are two ways for the FKM invariant to be trivial, having the line invariants either both zero, or both one. The latter case arises for example from a connection that winds the same way along all lines of constant k_x but does not contain a vortex. The two independent torsion invariants in the

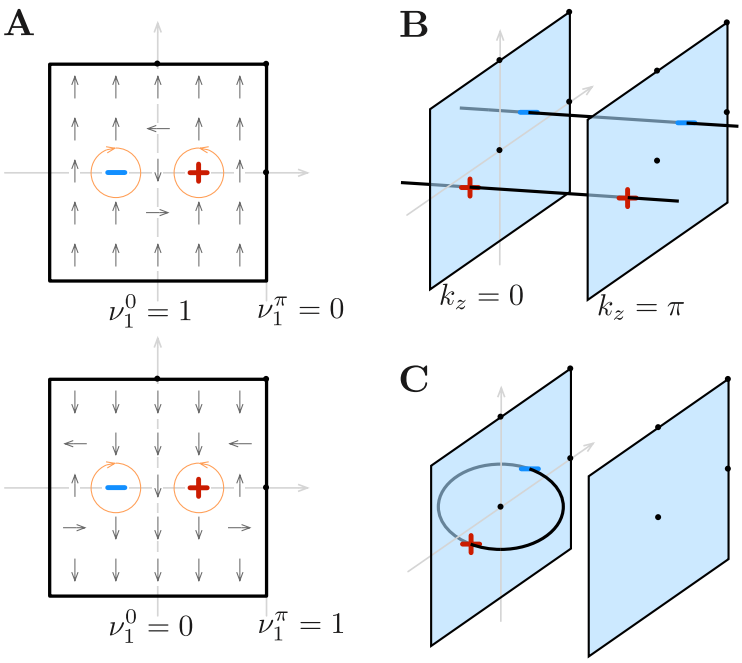

Figure 5.4: **a** Sketch of the Berry connection projected onto the highest energy state within a Kramers pair. A vortex and anti-vortex pair can arise in two topologically distinct ways within a Berry connection vector field that is continuous on the Brillouin zone torus. **b** Sketch of vortex lines extending across the bulk of a three-dimensional Brillouin zone with trivial FKM_3 invariant. **c** Sketch of a vortex line extending into the bulk of a three-dimensional Brillouin zone, and closing onto itself. This situation is described by a non-trivial FKM_3 invariant.

crystal with only a reflection symmetry thus add a factor $\mathbf{Z}_2^2$ to its topological classification.

The heuristic arguments presented here in terms of vortices, are given a formal foundation in the appendix of [4], where it is shown that the link between line invariants and the FKM_2 invariant, arising from vortices in the Berry connection, holds in general. To fully classify topological insulators both of the torsion invariants, as well as the relations between them, need to be consistently taken into account.

5.3.2 A new invariant

The combination of line and FKM invariants constitutes all known torsion invariants in time-reversal symmetric crystals. This, however, cannot be the full picture. Consider, for example, the crystal with only two-fold rotational symmetry. There are many lines in the Brillouin zone that can be mapped onto themselves by both TRS and the two-fold rotation. Most of these lines can be smoothly deformed into one another, and it suffices to define line invariants on the $k_x = 0, \pi$ and $k_y = 0, \pi$ lines. These are again related to each other by the FKM_2 invariant, giving a total of three independent torsion invariants.

A possible configuration with all invariants equal to zero would be to have no vortices present in the band structure at all. Another possible configuration with the same values for all invariants would be to have vortices present at all high-symmetry points. Because of the rotational symmetry, however, vortices cannot be spread out away from the high-symmetry points by any deformation of the Hamiltonian. That is, all Berry curvature is always concentrated in delta-peaks at the high-symmetry points. To see this, simply consider the generic form of a Hamiltonian for two valence bands near a time-reversal symmetric point,

$$H(\mathbf{k}) = (a_x^i k_i)\sigma_x + (a_y^i k_i)\sigma_y + (a_z^i k_i + m)\sigma_z, \tag{5.14}$$

where $i = x, y$ and we introduced a small mass m that we take to zero. The Berry curvature of one of the valence bands is

$$\mathcal{F}_{k_x k_y} = -\frac{im}{2} \frac{a_x^x a_y^y - a_y^x a_x^y}{((a_x^i k_i)^2 + (a_y^i k_i)^2 + (a_z^i k_i + m))^{3/2}}, \tag{5.15}$$

which in the $m \to 0$ limit is proportional to $\delta^{(2)}(\mathbf{k})$, unless $a_x^x a_y^y - a_y^x a_x^y = 0$, in which case the curvature is zero. In the non-trivial curvature case, one can try to smear [1] this vorticity, but due to the fact that $\mathcal{F}$ is odd outside $\mathbf{k} = 0$, smearing will never remove the delta function. Due to the local analysis at $\mathbf{k} = 0$, this does not exclude vortices outside of $\mathbf{k} = 0$. Indeed, since in the presence of TRS only there is just the relation between the band at $\mathbf{k}$ and its partner band at $-\mathbf{k}$), there could be non-trivial vortex-anti-vortex pairs in the full band structure in such a way that the curvature of a single band is non-trivial. Only an odd number of such pairs would then result in a topologically non-trivial phase as discussed around equation (5.12).

In the presence of even rotation symmetries, this changes, since $\delta^{(2)}(\mathbf{k})$ is the only possible form of $\mathcal{F}$ that is odd around $\mathbf{k} = 0$, rotationally invariant and does not

[1] Here we mean changing the distribution of curvature in a small neighbourhood U without changing the integral of $\mathcal{F}$ over U.

vanish once integrated over $\mathbf{R}^2$, i.e the full BZ. More so, the number of vortex-anti-vortex pairs that could be present outside $\mathbf{k} = 0$ is always even and hence give rise to trivial topology. For odd rotations, this is not true, since there can be three vortex-anti-vortex pairs around $\mathbf{k} = 0$.

If one insists on smearing, then time-reversal or crystal symmetry would have to be broken. For example, in the former case, smearing is easily achieved by keeping m finite in the Hamiltonian (5.14). As we do not allow deformations that break the symmetry, the delta function curvature singularity is frozen at $\mathbf{k} = 0$. A slight subtlety is then for three-fold rotations, where the curvature can be smeared without breaking any symmetry and without altering the topological invariant. We will discuss this in a bit more detail below.

Consequently, the situation with four vortices in $p2$ can only be deformed into the situation without vortices if either the gap is closed or the symmetry broken, since those vortices are frozen at high-symmetry (and time-reversal invariant) points. These two phases must thus be considered topologically distinct, and there must exist an additional $\mathbf{Z}_2$ or torsion invariant distinguishing them.

In fact, it is easily seen that every combination of values of the two line invariants and one FKM invariant can be realised with precisely two distinct configurations of vortices on the high-symmetry points. Again, these can never be smoothly deformed into each other, and should be distinguished by the new torsion invariant. Additional evidence for the existence of the new invariant can be found in two places. First of all, it is known that in certain cases a band structure with an odd total number of vortices in all valence bands at the Γ point has distinct physical properties from a band structure with an odd number of vortices at M, even if all line and FKM invariants are the same [155, 192]. This difference is manifested when a topological defect is introduced into the crystal, which will be either charged or not, depending on the configuration of vortices [192]. The topological defect in such cases may thus be seen as indicator for the new invariant.

Furthermore, in the specific case of a crystal with only two-fold rotational symmetry, the K-theory in the presence of time reversal symmetry may be explicitly computed, as discussed in the next chapter. This shows that in this specific case, the Brillouin zone hosts two invariants at its edges, and two invariants in its bulk. These correspond directly to the two line invariants, the one FKM invariant, and the one new invariant found by counting vortices. Notice that although K-theory calculations in the presence of TRS are very challenging in all but this simplest case, counting vortices in topologically distinct situations as suggested in the current approach is always straightforward.

In each of the situations with equal line and FKM invariants but different vortex

configurations, the topologically distinct phases can be distinguished by finding out whether or not a vortex is present at Γ. The new invariant can thus be determined by calculating the Berry curvature of a single Kramers pair partner in a small region encircling the Γ point. This procedure is guaranteed to be well-defined, because the rotational symmetry forbids the spreading of Berry curvature away from high-symmetry points.

An especially interesting situation to consider in the light of this new invariant, is that of a crystal with three-fold symmetry. In that case, there is a TRS point at Γ with rotational symmetry, a TRS point at M without any point group symmetry, and a point at K that is invariant under rotations, but not under TRS. Looking at the allowed representations at Γ, there is one real representation that allows for three vortices (or equivalently, a single charge-three vortex) to be formed there. These vortices can be moved to M or K by transformations of the Hamiltonian that do not close the gap or break the lattice symmetry. However, there is also a complex representation at Γ, which allows for a single (charge-one) vortex to be formed there. This single vortex cannot be moved away from Γ, because of the rotational symmetry. It can also not be transformed into a situation with three vortices without going through a topological phase transition. A similar charge-one vortex may also exist at K, accompanied by an anti-vortex at $-K$, and again such a vortex cannot be moved away from the high-symmetry point. The parity of the numbers of charge-three vortices anywhere in the Brillouin zone, and charge-one vortices at Γ and at K, are therefore three independent torsion invariants. Notice that in this case, the representations of the bands at Γ in fact determine which $\mathbf{Z}_2$ invariants are allowed. This is reminiscent of the way that rotational symmetries of the lattice may be used to determined the Chern number of class A materials modulo the order of the rotation [193].

Concluding, the recipe for finding all torsion invariants is thus a matter of finding all non-trivial vortex configurations with two simple rules: First, vortices are stuck at high-symmetry points and lines, meaning that vortices are frozen at high-symmetry points, but can move along high-symmetry lines. Second, relations such as (5.13) have to be enforced. For $p4$ this thus means that the total number of $\mathbf{Z}_2$ invariants is 3 and the total classification for $p4$ symmetric topological insulators in class AII is $\mathbf{Z}^3 \oplus \mathbf{Z}_2^3$. Similarly, for $p2$ and $p3$ we get $\mathbf{Z} \oplus \mathbf{Z}_2^4$ and $\mathbf{Z}^4 \oplus \mathbf{Z}_2^3$, respectively.

Combining the list of allowed torsion invariants with that of representation invariants, table 5.1 presents the full classification of spin-full electrons in two-dimensional crystals with time-reversal symmetry. The total classification is the direct sum of the representation and torsion invariants. This does not exclude the possible existence of relations amongst them. In fact, we already encountered such

relations between representation invariants and Chern numbers in class A, as well as for example for materials with $p3$ symmetry in class AII. As far as the counting of topological invariants is concerned, however, the total classification is given by the sum of invariants. The same algorithm can be used to straightforwardly compute the analogous table for three-dimensional crystals and layer groups, keeping in mind there may be additional torsion invariants in higher dimensions.

5.4 General wallpaper group

The method exemplified by our analysis of the two examples in class A and AII can be applied in the same way to all wallpaper groups. The first step is always to determine the fundamental domain Ω. After that, the point group operations are used to identify high symmetry points and lines as well as their corresponding stabilizer groups. The correspondence between representations of the stabilizer groups along high symmetry lines, and those at the high symmetry endpoints, then yield the allowed combinations of their irreducible representations, akin to the example of Table 5.6. For class AII, this procedure is slightly more involved as one has to use the fermionic representations of the double cover of the point group G instead of the bosonic representations of G. Furthermore, one has to use the theory of time-reversal symmetric representations as outlined in appendix A.3 to construct the relevant irreducible representations.

To specify a representation of the full set of valance bands, an integer $n_i^{\mathbf{k}}$ should be assigned to each irreducible representation i at high symmetry point $\mathbf{k}$, which specifies the number of valence bands for those values of i and $\mathbf{k}$. The previously listed relations between irreducible representations along high symmetry lines and their endpoints, can then be converted into a set of m independent relations between the integers $n_i^{\mathbf{k}}$. A representation of the complete set of valance bands is specified by $n-m$ integers, where n is the total number of integers $n_i^{\mathbf{k}}$ one started with. Finally, we need to consider Chern numbers and torsion invariants. The Chern numbers can only be present in wallpaper groups that do not contain reflections, because the Berry curvature is odd under reflection. For groups that do allow a Chern number, this one additional integer should be added to the set of $n_i^{\mathbf{k}}$ in order to have a complete specification of the set of valence bands. It should be noted that the Chern numbers modulo the order of the point group can also be obtained from the symmetry eigenvalues of the point group on the high-symmetry points [163]. Here, our goal is to go beyond this subset and enumerate all topologically distinct phases. This covers class A. In class AII, we instead need to determine all possible torsion invariants. How this is done was discussed in detail in the previous section.

Four of the 17 wallpaper groups, pg, $p2gg$, $p2mg$ and $p4gm$, i.e. the nonsymmorphic ones, need special attention. In these cases, the representations of the stabilizer group become projective representations. This is a consequence of the fact that we cannot separate their point group actions R from the translations $\mathbf{v}$, and as a result an additional phase factor needs to be accounted for in the analysis [165, 177, 179, 194]. As long as this subtlety is properly taken into consideration however, the procedure outlined above can still be applied in precisely the same way. This again enables us to identify the set of integers and torsion invariants needed to completely specify the topological phase given the space group symmetry.

Table 5.1 collects our results, and classifies all topological phases in class A and AII for any of the 17 wallpaper groups. In class A, it exactly agrees with the mathematical computation in terms of K-theory as proposed by Freed and Moore in [181]. This mathematical theory has been formally proven to classify all topological phases of gapped free fermions. The connection between our method and K-theory therefore constitutes a mathematical proof that we classified *all* crystalline topological phases of spinless electrons within class A. This for example guarantees that the crystalline topological phases protected by $p4mm$ symmetry identified in the previous section exhaust all possibilities for such phases. The agreement between K-theory calculations and the full list of wallpaper groups in table 5.1 based on our combinatorial arguments, can be made explicit using the results of [195–197]. In class AII, we are much less fortunate, since there are almost no K-theory computations available. In chapter 6, we will embark on such computations ourselves for a few simple space groups and show that they match with the heuristic arguments presented for class AII in the preceding sections.

A comment on topologically trivial bands

Before moving on to higher dimensions, let us comment briefly on an important issue in the classification, namely that our counting is done modulo topologically trivial bands. As mentioned in passing in the above, we consider two bands to be distinct under smooth deformations up to the addition of trivial bands. More explicitly, this implies that two band structures are topologically equivalent when they can be made to be equal upon adding topologically trivial sets of bands. In the present context, and in accord with K-theory, trivial band structures are defined to be particle-hole symmetric pairs of bands. To be precise then, we really consider the combined topological invariant of all bands below a gap in the spectrum at any energy (not necessarily at the Fermi level), and consider the trivial set of bands to be a pair with equal topological indices in which one is occupied and one unoccupied. This definition reflects the fact that negative integers may appear

in the K-theory, and in our classification, corresponding to bands of holes, rather than electrons. This necessity of including the concept of negative integers in the definition of equivalence is a direct consequence of the fact that the elements in K-theory are difference classes, which necessitates the existence of a trivial element.

5.5 Three dimensions

Class A

Our method can also be straightforwardly applied to crystal structures in three dimensions. For a general space group G and its associated first Brillouin zone with high symmetry points $\mathcal{M}^i$, the first step is to determine the representations of the stabilizer groups $G_{\mathcal{M}^i}$ for all $\mathcal{M}^i$. A set of integers $n_j^{\mathcal{M}^i}$ can then be introduced to indicate the number of valence bands in representation j at high symmetry point $\mathcal{M}^i$. These integers are not independent, because they are constrained by the compatibility relations imposed by high symmetry lines connecting various $\mathcal{M}_i$, as shown pictorially in Figure 5.5. Giving a list of values for a complete set of independent integers $n_j^{\mathcal{M}^i}$ amounts to a characterisation of the set of valence bands, so that finding the number of independent integers in a given space group is equivalent to classifying its possible topological phases. In three dimensions, it is possible to have high symmetry planes, but these do not add any compatibility relations beyond those already imposed by the high symmetry lines.

As in the two-dimensional case, the combinatorial argument does not indicate the possible values of Chern-numbers, which need to be included in a full classification of topologically distinct phases. Fortunately, they can be obtained in a straightforward manner. Chern numbers are always given by two-dimensional integrals. For example, the TKNN invariant is an integral over the full Brillouin zone in two dimensions. For crystals in three dimensions, the Chern number will likewise be given by an integral over a two-dimensional plane within the first Brillouin zone. In the absence of band crossings, the Chern number can be evaluated as a sum of contributions from the integration of individual valance bands. The Chern numbers evaluated on two parallel two-dimensional planes must be equal by continuity.

If a three-dimensional crystal contains high symmetry planes, these may be used as convenient locations for defining a set of Chern numbers. Firstly, such a plane can host a nonzero Chern number if and only if there is no reflection symmetry within the plane, mimicking two dimensional case. Moreover, a high symmetry plane in three dimensions is always left invariant by a reflection acting perpendicular to

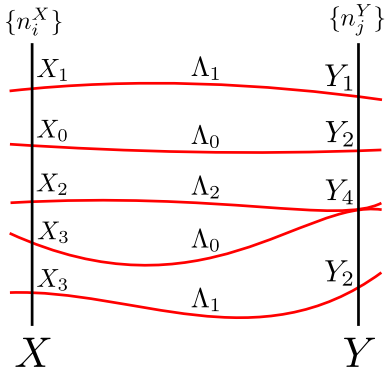

Figure 5.5: Sketch of the relations between high symmetry points imposed by high symmetry lines. A set of valance bands is shown between two generic high symmetry points X and Y, which are left invariant under the symmetry transformations contained in the stabilizer groups G_X and G_Y. The irreducible representations of G_X and G_Y may be labelled as X_i and X_j. Each of the bands needs to fall within one of these representations at the corresponding high symmetry points. The representations on X and Y, however, need to be compatible with the representations Λ_j of the high symmetry line connecting X and Y. The remaining set of independent integers indicating how many bands are in which representations at the high symmetry points, finally determines the number of possible topologically distinct configurations of the set valence bands, matching the abstract K-theory classification.

the plane, under which the bands can be even or odd. Separate Chern numbers $c_\pm$ can then be assigned to the full set of even or odd bands, and are obtained by summing the contributions from individual even or odd bands. For a full characterisation of the topological phase, both numbers c_+ and c_- need thus to be specified for all high symmetry planes in the first Brillouin zone. However, these Chern numbers are not independent in the same sprit as the constraints found above. Namely, a general plane in the Brillouin zone, on a small distance away from the high symmetry plane, may have its (single) Chern number c equal to zero. In that case, c_+ must equal $-c_-$ on the high symmetry plane, to ensure continuity. Therefore only a nontrivial *mirror* Chern number $c_m = (c_+ - c_-)/2$ can be defined in this scenario [198].

The other possibility is that the general plane has a non-zero Chern number c, so that $c_+ + c_-$ must equal c by continuity. This situation results in relations between the Chern numbers on distinct but parallel high symmetry planes. For example, suppose there are mirror planes at $k_z = 0$ and $k_z = \pi$ that have Chern numbers

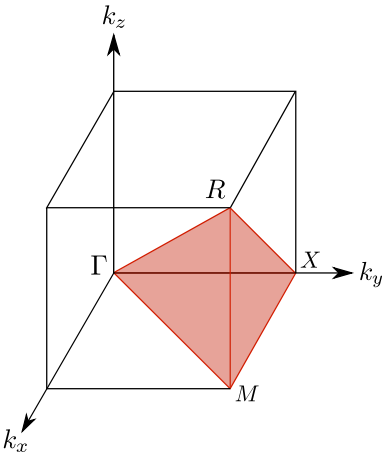

Figure 5.6: Fundamental domain of the octahedral group O_h (shaded red). The red high symmetry lines connect the high symmetry points Γ, M, X and R.

$c^0_\pm$ and $c^\pi_\pm$, respectively. If a general plane between $k_z = 0$ and $k_z = \pi$ has its total Chern number equal to c, then this implies

$$\begin{aligned} c &= c^0_+ + c^0_- \\ c &= c^\pi_+ + c^\pi_-. \end{aligned} \tag{5.16}$$

Combining these two equations then yields the relation

$$c^0_+ + c^0_- = c^\pi_+ + c^\pi_-. \tag{5.17}$$

Out of the four Chern numbers characterising the two high symmetry planes, only three are independent. Notice that these are exactly the same type of relations as the constraints between high symmetry points that we introduced in Section 5.4. The combination of all independent Chern numbers and the set of independent integers obtained from the representations of the valance bands, constitute our classification of topological phases in class A.

As a concrete working example of the classification scheme in three dimensions, consider the symmorphic space group $Pm\bar{3}m$ (no. 221), for which we compute the K-theory (modulo torsion) in appendix A.3. This space group has an octahedral point group, O_h, which contains the symmetries of a cube and has 48 elements. O_h is generated by the following elements

$$\begin{aligned} r \cdot \mathbf{k} &= (-k_z, k_y, k_x), \\ t \cdot \mathbf{k} &= (k_y, k_x, -k_z), \\ I \cdot \mathbf{k} &= -\mathbf{k}. \end{aligned} \tag{5.18}$$

The fundamental domain is shown in Figure 5.6. It contains six high symmetry lines coming from the two, three and fourfold rotation axes. The endpoints of these lines are the high symmetry points Γ, R, X and M, which have stabilizer groups O_h, O_h, $D_4 \times \mathbf{Z}_2$ and $D_4 \times \mathbf{Z}_2$, respectively. The high symmetry points all have 10 different irreducible representations, so that 40 integers can be introduced to specify the set of valence bands. The high symmetry lines yield 25 relations between these integers, which in this particular case were in fact already found by Wigner [182]. Taking into account the dependencies between the relations, 22 integers remain to be specified in order to fully characterise the set of valence bands. The relations coming from mirror planes do not add any additional constraints on these 22 integers, since they are already implicitly satisfied by taking into account the constraints coming from the high symmetry lines.

The octahedral point group has no Chern numbers, because within each high symmetry plane there is a perpendicular reflection plane. Hence, we find that a topological phase in class A protected by O_h symmetry is classified by $\mathbf{Z}^{22}$, i.e by 22 integers. Once again this result can be corroborated by calculations from a more formal, mathematical perspective. As shown in appendix A.3, the result from such a K-theory calculation is exactly the same, modulo torsion, as that obtained in our combinatorial approach.

This also brings us to a slight subtlety mentioned already in the beginning of this chapter, namely that in two dimensions our approach and the K-theory agree perfectly, but in three dimensions, there could still be torsion invariants that we are missing. These torsion invariants would, for example arise from two dimensional slices in the Brillouin zone having the topology of $\mathbf{RP}^2$, since the second cohomology group of this space is $\mathbf{Z}_2$.

Class AII

In three dimensions, the analysis of symmetry eigenvalues and the corresponding representation invariants is completely analogous to that in two dimensions. The torsion invariants on the other hand, feature an additional entry special to three dimensions, the FKM_3 invariant. To understand this invariant in terms of the vortices in the Berry connection, consider the planes $k_z = 0$ and $k_z = \pi$, which are mapped onto themselves by the time-reversal operation. On these planes, two-dimensional FKM_2 invariants may be defined. Much like line invariants are related to FKM_2, the invariants of the two planes are related to FKM_3 by the expression

$$\mathrm{FKM}_3 = \mathrm{FKM}_2^0 + \mathrm{FKM}_2^\pi \mod 2. \tag{5.19}$$

An intuitive understanding can again be found using vortices in the Berry connection. A single vortex and anti-vortex on for example the plane $k_z = 0$ can

be extended into the third direction as a vortex line, or flux tube. If the vortex line extends all the way to the plane $k_z = \pi$, both planes have non-trivial FKM_2 invariants. On the other hand, if the line closes onto itself and forms a vortex loop, the FKM_2 invariant at $k_z = \pi$ will be trivial, and there will be a non-trivial FKM_3 invariant in the bulk of the Brillouin zone. This situation is shown schematically in figure 5.4. Notice that a single FKM_3 invariant may connect multiple parallel planes on which FKM_2 invariants can be defined. Incorporating the effect of crystal symmetry on whether or not FKM_3 invariants are allowed is a matter of understanding the effects it has on vortex lines. When inversion symmetry is present, it is known that FKM_3 can be computed using the inversion eigenvalues [199], and is therefore in our classification absorbed in the representation invariants. A more detailed derivation of these heuristic arguments is given in the appendices of [4].

An interesting example of a three-dimensional crystal, is one with space group $P2/m$ (nr. 10). Such a crystal has inversion symmetry, and a two-fold rotation symmetry around the k_z-axis. The representation invariants can be straightforwardly identified. Concerning the torsion invariants, we see that they cannot be non-trivial on $k_z = 0, \pi$ planes, because the inversion symmetry forbids single vortices even at high-symmetry points. Since the values of both the line invariants and new invariants are related to the presence of vortices at high-symmetry points, these too must be trivial. Moreover, due to (5.19), FKM_3 is also zero. We thus find no torsion invariants in this crystal. Notice that this implies the $\mathbf{Z}_2$ invariant in for example [199], is in our description absorbed into the representation invariants.

5.6 Conclusions

In this chapter, we presented a straightforward combinatorial procedure that can be used to give a classification of distinct topological phases of spinless particles within class A and spin$-\frac{1}{2}$ particles in class AII, by taking into account the space group symmetries of a material. The classification is shown to be *complete* in one and two spatial dimensions for class A. In three dimension, the completeness of the classification relies on a subtle point regarding the possible presence of torsion in K-theory. In class AII, we have no proof that our classification is complete in two and three dimensions. Nevertheless, we will show that the classification does not contradict with the K-theory computations. In particular, we show that in certain simple cases, there is an exact agreement between our heuristic arguments and the K-theory computations.

6 K-theory Classification of Crystalline Topological Insulators

This chapter is based on the following publication:

L. Stehouwer, J. de Boer, J. Kruthoff and H. Posthuma,
"Classification of crystalline topological insulators through K-theory",
Submitted to Advances in Theoretical and Mathematical Physics,
`arXiv:1811.02592 [cond-mat.mes-hall]`.

6.1 Introduction

In the previous chapter, we proposed an algorithm to count the number of topological phases given a crystal and symmetry class (A or AII). In this chapter we want to verify these statements by connecting our analysis to a well-defined mathematical question. This connection was first noticed by Hořava and Kitaev. They found that there is an intricate relation between the classification of gapped free fermions and the classification of vector bundles, [150,200], using the mathematical framework of K-theory. It was not until the work of Freed and Moore [181] that a complete proposal was formulated to classify topological phases of free fermions by including not only time-reversal or particle-hole symmetry, but also the crystal symmetries that these fermions experience.

The proposal of Freed and Moore involves the computation of a certain objects in K-theory. K-theory is a branch of mathematics that can be used to classify vector bundles and captures all topological invariants present for a given symmetry class and crystal. These invariants describe both global and local information of valence bands. Although we can treat these invariants in a unifying way, from a physics point of view, global and local invariants describe different aspects of the

valence bands. The local invariants describe the bands locally, meaning that they are topological invariants associated with the representation theory of the space group. In chapter 5, we discussed how these invariants can be determined and why they are part of the classification of topological insulators. Global invariants like the Chern number, discussed in section 4.1, and the FKM invariants from the previous chapter are described by an integral over the Brillouin zone. Even in the vortex picture, where the Berry curvature is localised at points, the topological invariant is still non-local since an integral over a small neighbourhood around that point is required to compute it. We introduced this picture in chapter 5 to accommodate for non-trivial crystal symmetries in a systematic and simple way. The purpose of this chapter is to check whether the counting we proposed in chapter 5 indeed matches with the K-theory computations. For class A in two and three dimensions, we know that this is the case, but for class AII, no comparison could be made due to the sparseness literature on explicit computations of the relevant K-theories.

Outline, summary of results and comparison

This chapter is organised as follows. In section 6.2 we will introduce some basic terminology in algebraic topology and K-theory by discussing an example of a crystal with only time-reversal symmetry. The next section, section 6.3 contains the meat of the chapter. We discuss in more detail what K-theory we want to compute to classify topological insulators with time-reversal and crystal symmetry. To compute these K-theories we describe the construction of an Atiyah-Hirzebruch spectral sequence and compute two examples in detail. Section 6.4 is devoted to various other examples we computed, for example, we compute, for the first time, the full classification of a two dimensional crystal with time-reversal in class AII and a four fold rotation symmetry. Furthermore, we also determine the twisted representation rings, which are needed in the spectral sequence, in an algorithmic way. In section 6.5 we mention various subtleties and future directions. Finally, in appendices A.4 and A.5 we have gathered various mathematical details on K-theory, the spectral sequence construction, twists and twisted group algebras.

Computing twisted equivariant K-theory groups using an Atiyah-Hirzebruch spectral sequence is not new. In previous works, [201, 202], an Atiyah-Hirzebruch spectral sequence was also proposed and used to compute the classification for certain symmetry groups and classes. In this work, we fill in certain gaps left open in these works and put the computation of the K-theory groups with an Atiyah-Hirzebruch spectral sequence on a firm mathematical footing. We have gathered most of these details in the appendix A.5.

The K-theory groups we have computed match with known results in the literature,

but also agree with a set of heuristic arguments presented in chapter 5 in the cases where we have explicit results. In particular, for the Altland and Zirnbauer classes AI and AII with an order two symmetry in two dimensions, our results match with those in [169, 170, 203]. These works extended the analysis by Kitaev in [150] to include additional order two symmetries such as a reflection or two fold rotation symmetry. The basis of this analysis is Clifford algebras, which allow for a straightforward implementation of order two symmetries, but for more complicated symmetries, such a procedure is more difficult. In those cases one has to resort to more sophisticated computational methodes of which we outline one in this chapter.

6.2 Time-reversal only

In this section we shall focus on topological insulators with only unbroken time-reversal symmetry on a two-dimensional lattice without any additional rotation or reflection symmetries. Such topological phases belong to either symmetry class AI or AII [151]. In the former case the time-reversal operator T squares to the identity, whereas in the latter case it squares to minus the identity. To classify such topological insulators, we need to know how many topologically distinct insulators there are with this symmetry. As was explained in the introduction, with distinct we mean that upon going from one to the other phase, either the gap closes or the symmetry is broken. For a more formal definition, see [181].

The classification is most easily understood by translating the problem to momentum space, where discrete translations cause the momenta to only take values in a two-dimensional Brillouin torus $\mathbf{T}^2$. We visualize this torus as the square $[-\pi, \pi] \times [-\pi, \pi]$ with opposite sides identified. Due to time-reversal symmetry, a non-trivial group acts on this two-torus which sends k to $-k$, which is intuitively clear as reversing time should reverse the sign of momenta. Time-reversal symmetry can also easily be shown to be an anti-unitary symmetry. Another example of a possible anti-unitary symmetry (which we will not consider in this chapter) is particle-hole symmetry, which acts trivially on the torus. Since we will ignore interactions the momenta k are conserved quantities that can be used to label the states in our Hilbert space. The states with label k are exactly the momentum k Bloch waves. The collection of all these Hilbert spaces form a vector bundle. This vector bundle is the collection of all valence and conduction bands and since we are dealing with insulators here, there is a gap between them. In a (topological) insulator, only the valence bands are physically relevant. For the classification, we hence focus on this finite-dimensional sub-bundle.

The classification of topological insulators has now been translated into a mathematical question about the classification of vector bundles over the torus. In the absence of time-reversal symmetry, such a classification can be performed using standard (complex) K-theory. With time-reversal symmetry, things get a little more exotic, since time-reversal is an antiunitary operator which in particular anticommutes with the imaginary unit i. Nevertheless, Atiyah [204] generalized K-theory to incorporate this symmetry and dubbed it Real K-theory. Specifically, for class AI and AII, we need to compute $KR^{-q}(\mathbf{T}^2)$. Here the $\mathbf{T}^2$ is the two-dimensional Brillouin zone and the index q labels the various Altland-Zirnbauer classes [149]. In this situation we need $q = 0, 4$ as they indicate class AI and AII respectively. It is actually not too hard to compute these K-theory groups [150,181]. The result is

$$KR^0(\mathbf{T}^2) = \mathbf{Z}, \quad KR^{-4}(\mathbf{T}^2) = \mathbf{Z} \oplus \mathbf{Z}_2. \tag{6.1}$$

The conventional computation of these groups uses various basic properties of KR-theory, which cannot be generalized to include point group symmetries. Moreover, this computation is rather unsatisfactory as it gives no insight into what these invariants mean and where they come from. Part of the motivation of this work and of [3,4] is to understand what the physical origin is of these invariants and what computational tool makes this physical origin manifest. In particular, we would like to see how the gluing of representations reveals itself in the computation. Looking ahead, we can interpret the result (6.1) as follows. The invariants $\mathbf{Z}$ are local in nature and just give the rank of the bundle, i.e. they represent the number of valence bands present. The more interesting invariant $\mathbf{Z}_2$ is a global two-dimensional strong topological invariant called the Fu-Kane-Mele invariant and is related to topologically protected edge states [186,189].

In order to better understand the physical origin, we decompose the Brillouin zone into various parts that are easy for K-theory to handle. Within K-theory we have the freedom to consider a so-called stable equivalent space instead of the torus. Fortunately, there exists a nice space that is stably equivalent to the torus. This space is a certain wedge sum of one and two-dimensional spheres[1]. Moreover, K-theory is additive under taking such wedge sums and hence we only have to compute the K-theories of spheres, see the end of Section 6.3.1 for a more precise statement. Physically, this means that we are looking at properties of the band structure insensitive to (part of) the discrete translation symmetry. The two-dimensional sphere just represents the (compactified) momentum space of a topological insulator without translation symmetry and the K-theory then gives the topological invariants associated with this Brillouin zone. For instance, the Chern number in the IQHE is just the complex K-theory of the 2-sphere and is

[1] The wedge sum of two spaces is the union of the two spaces but where one point of the first space is identified with one point of the second.

known not to rely on translational symmetry. After computing the K-theories of all such pieces, one simply assembles all these pieces together by taking direct sums.

In two dimensions, going from the torus to the sphere can be accomplished by identifying the boundary of the square $[-\pi, \pi] \times [-\pi, \pi]$ with a single point. Let us focus on this sphere for the moment. After this operation, the time-reversal action of $\mathbf{Z}_2$ on the Brillouin zone torus reduces to an action on the sphere that is still given by the formula $k \mapsto -k$ if we view the sphere as $\mathbf{R}^2 \cup \infty$. Now suppose we have a Hilbert bundle $\mathcal{H}$ over the sphere with time-reversing operator T, i.e. a bundle map $T : \mathcal{H}_k \to \mathcal{H}_{-k}$, where $\mathcal{H}_k$ denote the fibers of the bundle $\mathcal{H}$. There are two special points at $k = 0$ and $k = \infty$ under the action of time-reversal at which the Bloch states with momentum k are mapped to themselves. This gives vector space automorphisms on the corresponding fibers $\mathcal{H}_k$. In class AI (so $T^2 = 1$), the operator T acts as an effective complex conjugation on the Bloch states of momenta $k = 0$ and $k = \infty$. In more mathematical jargon, there are canonical real structures on the vector spaces $\mathcal{H}_0$ and $\mathcal{H}_\infty$. In class AII, when T squares to -1, we instead have canonical quaternionic structures at $k = 0$ and $k = \infty$. In particular, we deduce that the space of Bloch waves at these special points is even dimensional, which is a manifestation of Kramer's theorem. However, at a generic point on the sphere, the momenta are not preserved by T, so that the state spaces at these points do not admit any extra structure.

We have now discussed how time-reversal acts on the Brillouin zone once the torus is reduced to a sphere. To include more complicated symmetries later on, it is convenient to view the sphere as being build up out of points, intervals and disks. We have chosen these particular building blocks because they are topologically trivial, i.e. contractible. Such a collection of building blocks is called a CW-complex. The building blocks themselves are called d-cells where d is the dimension of the block. When additional symmetries are present, such a CW-complex has to respect the symmetry. By this is meant that for each cell the symmetry must either fix it completely or map it to a different cell in the decomposition. In the case of time-reversal symmetry for instance, such a CW-complex is given in Figure 6.1. In this figure, we also gave the cells an orientation that is preserved by the symmetry, which is visualized by the direction of the arrows on the 1-cells. Note that the north and south pole are fixed by the $\mathbf{Z}_2$ action and hence constitute the 0-cells. The 1-cells are a line from p_0 to p_∞ and its symmetry-related partner. The same is true for the 2-cells, which are the two hemispheres. This yields a practical setting to do the classification using K-theory, because we can simply classify the bundles over these d-cells and then glue them together consistently. Let us see how this works in more detail.

To start, we consider the complex and Real K-theory of spheres. It is a known fact that the K-theory of a point in degree $-p$ is equal to the (reduced) K-theory of a p-dimensional sphere. The results are given in Table 6.1. Bundles on the 0-cells, i.e the north and south pole in Figure 6.1, are classified by $KR^0(\mathrm{pt})$. In class AI, we have $KR^0(\mathrm{pt}) = \mathbf{Z}$ for each of the two fixed points. The $\mathbf{Z}$ now assigned to the north and south pole are simply given by the dimension of the fiber at those points. In class AII we get for each fixed point $KR^{-4}(\mathrm{pt}) = \mathbf{Z}$, which is given by the quaternionic dimension of the fiber. On the two intervals there is no real or quaternionic structure. Hence we should assign the (reduced) complex K-theory of the interval, where the boundary points of the interval are identified with each other. This K-theory is equal to the (reduced) complex K-theory of the circle, which is zero. The precise reason for this assignment is addressed in detail in the appendix. Finally to the two hemispheres, we assign the (reduced) complex K-theory of a sphere, which is $\mathbf{Z}$. As before, the sphere appears here because we are identifying the boundary of the disc to a point. If our Hilbert space of states is to be preserved by the time-reversal symmetry, the bundle over the two 2-cells should come in pairs that are mapped into each other by the action of time-reversal symmetry. It is thus enough to know the bundle on one such 2-cell and hence under T, the two copies of $\mathbf{Z}$ are identified. We thus have $\mathbf{Z}^2$ in zero dimensions (0-cells), a 0 in one dimension (1-cells) and $\mathbf{Z}$ in two dimensions (2-cells).

To get to a complete classification of topological insulators, we have to make sure that our assignment of bundles to cells is consistent. This can be done by imposing constraints in successive dimensions. For dimension zero, this means that when the fibers above the 0-cells are all extended to the 1-cells, the result should be consistent. In our case this means that the state spaces at the points $k = 0$ and $k = \infty$ should have the same dimension, thereby reducing the $\mathbf{Z}^2$ we found before to $\mathbf{Z}$.

This approach is intuitively clear and can easily be generalized to include point group symmetries. However, as advocated in the beginning, the approach of assigning representations to points is only part of the full classification. To get the other part, the global part, we should check consistency of assignments of bundles (not just representations) to higher-dimensional cells. This becomes a lot more difficult and it is hard to understand for generic crystal symmetries. In the case without time-reversal symmetry, these invariants are most of the time first Chern numbers, but there are exceptions [201]. The invariants that can take any integer value can be understood by using the equivariant Chern character [205] or Segal's formula [206], which also has an extension to the twisted case [207]. However, for crystals invariant under time-reversal symmetry, the invariants are often torsion

invariants and take only particular integer values. There is no systematic way of understanding them in the sense that there is no explicit formula for this piece. Instead, when assigning bundles to higher-dimensional cells, we have to check which bundles can be realized as a certain cohomological boundary and quotient out by these. The result will indeed give the $\mathbf{Z}_2$-invariant of equation (6.1), but it requires some abstract mathematical theory to see this. Physically, however, there is a heuristic way of understanding these invariants as vortex-anti-vortex pairs in the connection on the bundle, which was presented in the beginning of this section.

Below we will formalize the heuristic arguments given above and put them on a firm mathematical footing. The example we have seen in this section will be computed again using machinery that allows for a generalization to more complicated crystal symmetries. To illustrate this, we compute the full classification for topological insulators in class AII on a two dimensional lattice with a twofold rotation symmetry.

6.3 The spectral sequence and applications

Now we come to the core of the chapter. In the above we gave a heuristic classification of topological insulators with time-reversal symmetry. We will now make this classification precise and generalize to cases with non-trivial crystal symmetry. The strategy of this section will be to introduce all necessary tools. We will then reconsider the example without any crystal symmetry but with time-reversal symmetry. Whenever appropriate, we will mention the physical motivation and interpretation for these tools along the way.

Let us consider topological insulators in d dimensions in class A, AI or AII, possibly with a point group symmetry. We denote the full classical symmetry group of the Brillouin zone by G. If present, G therefore contains time-reversal symmetries and point group symmetries but no translational symmetries. These are taken into account by the topology of our Brillouin zone torus. Let us denote by $\mathcal{G}$ the space group and G its (magnetic) point group that does not contain time-reversal symmetry, then the space group $\mathcal{G}$ is a group extension

$$1 \to \mathbf{Z}^d \to \mathcal{G} \to G \to 1, \tag{6.2}$$

where $\mathbf{Z}^d$ represents the discrete lattice translations in d spatial dimensions. When this extension is split, the space group is called symmorphic and non-symmorphic otherwise. We will focus on the former from now on and comment on the non-symmorphic case in the discussion. We will assume that there are no other symmetries, such as gauge symmetries with which the time-reversal operator could

mix.

In order to classify topological phases in the sense of Freed and Moore [181], we have to compute a joint generalization of Real and equivariant K-theory. In particular, we want to take two additional things into account. First of all, we want to keep track of which elements in G act antiunitarily or not. For this we will use a map ϕ which sends an element of G to $+1$ if it is unitary and to -1 if it is antiunitary. Moreover, we want to know how elements of G acting on the Brillouin zone lift to elements acting on the fiber. This is most easily accounted for by a twist τ, a suitable group two-cocycle. This twist encodes the action of the symmetries on the quantum Hilbert space. For example, it prescribes whether $T^2 = \pm 1$. But it also provides the signs coming from taking the spin of particle into account. For example, an n-fold rotation operator R for spin$-\frac{1}{2}$ particles satisfies $R^n = -1$. This minus sign is also encoded in τ.

Let us for a moment describe the situation in more precise abstract mathematical terms. Assume we have the following data:

(i) a finite group G acting on a space X (in our case $X = \mathbf{T}^d$, the Brillouin zone);

(ii) a homomorphism $\phi : G \to \mathbf{Z}_2$;

(iii) a group 2-cocycle $\tau \in Z^2(G, U(1)_\phi)$ with values in the circle group $U(1)$ with G-action $g \cdot e^{i\theta} = e^{i\phi(g)\theta}$.

Such a cocycle τ is a special case of the more general twists defined by Freed and Moore [181], called ϕ-twisted central extensions. Using such data, Freed and Moore [181] defined a version of twisted equivariant K-theory denoted by

$$ {}^{\phi}K_G^{\tau}(X), \tag{6.3}$$

which was further studied in [208]. It was also argued that this K-theory group classifies free fermion topological insulators protected by the quantum symmetry defined by G, ϕ and τ.

To connect with more common language used in the physics literature, we describe the G, ϕ and τ that occur in the classification of crystalline topological insulators. Firstly, a class A topological insulator with point group G_0 simply has $G = G_0$ and ϕ and τ are both trivial. For class AI, G will instead be the magnetic point group, i.e. it will contain both point symmetries and time-reversal symmetry. We will only consider magnetic point groups of the form $G = G_0 \times \mathbf{Z}_2^T$, with $\mathbf{Z}_2^T$ the action of time-reversal symmetry on the Brillouin zone, even though the mathematical machinery developed here can handle more general point groups as well. For instance, one could also consider cases in which the time-reversal operator

is a combination of the usual time-reversal operator with a lattice translation or point group symmetry in G_0. For $G = G_0 \times \mathbf{Z}_2^T$ in class AI, $\phi : G \to \mathbf{Z}_2$ will simply be projection onto the second factor and τ will be trivial. Finally, for class AII, we again take $G = G_0 \times \mathbf{Z}_2^T$ to be the magnetic point group and ϕ the same projection, but now we pick τ in such a way that the twisted group action represents the desired action on the quantum Hilbert space. In particular, we pick τ so that time-reversal squares to -1, reflections square to -1 and rotation by 2π equals -1. To assure a consistent choice, a precise construction of τ for a given point group G_0 is given at the end of appendix A.5.

It is shown in [208, Thm 3.11] that the groups ${}^{\phi}K_G^{\tau}(X)$ satisfy certain equivariant versions of the homotopy, excision, additivity and exactness axioms of Eilenberg and Steenrod. The fact that our twisting class is defined by a group cocycle implies that these axioms are exactly the axioms for an equivariant cohomology theory on the category of G-spaces as defined in Bredon [209, §I.2]. This is what makes the following computations mathematically sound; as explained in [209, §IV.4] the axioms guarantee the existence of the Atiyah–Hirzebruch spectral sequence. Moreover, the orbifold point of view advocated in [208] allows us to change the group G and the space X as long as the quotient space remains the same and we keep the same stabilizer. This is useful in some computations, see the end of Section 6.3.3. For more details on how the K-theory we use is defined, see appendix A.5.

We are therefore left with the task to compute the K-theory ${}^{\phi}K_G^{\tau}(\mathbf{T}^d)$ of the Brillouin zone dressed with ϕ and τ. The technique to compute these groups goes along the lines that we have discussed in the previous section. We first decompose the Brillouin zone into cells and view them as a CW-complex. Non-trivial symmetries have to leave these complexes invariant. Such complexes are equivariant G-CW complexes, which is nothing more than an upgraded version of the unit cell in momentum space. After having found this G-CW complex, we use an Atiyah-Hirzebruch spectral sequence to compute ${}^{\phi}K_G^{\tau}(S^i)$, which are assembled to give ${}^{\phi}K_G^{\tau}(\mathbf{T}^d)$. Let us now formalize this computational method.

6.3.1 A general method: the Atiyah-Hirzebruch spectral sequence

The spectral sequence for the computation of the twisted equivariant K-theory of a space X is constructed by using a decomposition as a G-CW complex $X^0 \subseteq \cdots \subseteq X^d = X$, where the superscript on the cells indicates the dimension of the subspace. For the applications considered in this chapter, X is either a torus $\mathbf{T}^d$ or a sphere S^d (we will remark on how to reduce the computation of the K-theory

of the torus to the K-theory of a sphere at the end of this section). A spectral sequence is a successive approximation method converging to the desired answer in a number of steps. For us these steps will always be finite and in fact, most of the time only two steps are necessary. These steps are usually referred to as pages. The first page of the spectral sequence, just as in the last example, is given by equivariant assignments f of the K-theory of spheres to the cells of X. For the 0-cells X^0, this means that we assign to each $k \in X^0$ a twisted representation of the stabilizer group H_k of that point. These representations, which are twisted using τ and the map ϕ, are conveniently packaged in the twisted representation ring ${}^{\phi}R^{\tau}(H_k)$. These objects are actually not rings, but since they are equal to the usual representation ring of H_k in case ϕ and τ are trivial, we will keep on referring to them as twisted representation rings. Details about twists and twisted representations can be found in appendix A.5. So f maps k to an element of the twisted representation ring ${}^{\phi}R^{\tau}(H_k)$ of the corresponding stabilizer group H_k. By equivariance is meant that f preserves the symmetry in the following sense: f is required to map gk to the resulting conjugate representation in ${}^{\phi}R^{\tau}(gH_kg^{-1}) = {}^{\phi}R^{\tau}(H_{gk})$. More generally, we equivariantly assign higher representation rings ${}^{\phi}R^{\tau-q}(H_\sigma)$ (i.e. the higher degree twisted equivariant K-theory of a point, see appendix A.5.1 for details) to p-cells σ. These classify twisted H_σ-equivariant bundles over q-spheres, instead of over just a point. The grid of such assignments of representation rings for each p and q form the first page of the spectral sequence and is denoted by $E_1^{p,-q}$. Those assignments can be shown to be equivalent to Bredon p-cochains with values in the coefficient functor ${}^{\phi}\mathcal{R}_G^{\tau-q}$. In appendix A.5.2 we define these coefficient functors and present a derivation of this result. Intuitively, the functor ${}^{\phi}\mathcal{R}_G^{\tau-q}$ keeps track of both the (higher) representations at fixed loci and how they restrict to each other. For Bredon p-cochains, this functor will pick out the stabilizer group of the p-cells and assign degree $-q$ twisted representation rings to the p-cells. It should be noted here that the action of group elements on the higher representation rings can be tedious to determine explicitly in certain examples, so that the equivariance of f can result in nontrivial results. One example of this is given in Section 6.3.2.

To go to the next page of the spectral sequence, we have to take the cohomology of the first page with respect with the first differential, which in our case is known as the Bredon differential. In fact, the first differential maps $E_1^{p,-q}$ to $E_1^{p+1,-q}$ and is given by the differential of Bredon cohomology, which is

$$(df)(\sigma) = \sum_{\mu \in C^p(X)} [\mu : \sigma] f(\mu)|_{G_\sigma}, \tag{6.4}$$

with $C^p(X)$ denoting the set of p-cells of X and f a Bredon p-cochain. Here $f(\mu)|_{G_\sigma}$ means that we take the higher twisted representation of G_μ that f assigns

to μ and restrict it to a representation of G_σ. The notation $[\mu : \sigma]$ stands for an integer factor that tells us in which way μ intersects the boundary of the $p+1$-cell σ. In general the behavior and computation of this number can be quite complicated, but if our CW-complex is sufficiently nice, this number is usually just a sign depending on a fixed orientation. For example, if we have a line (1-cell) ℓ oriented from the endpoint p_0 to the other endpoint p_1, i.e. $\partial\ell = p_1 - p_0$, then we simply have

$$[\ell : p_1] = 1, \quad [\ell : p_0] = -1 \tag{6.5}$$

and of course $[\ell : \mathrm{pt}] = 0$ if pt is not an endpoint of ℓ. If instead $\sigma = A$ is a 2-cell that lies in a disk surrounded by a couple of intervals $\ell_1, \ldots, \ell_k$, then $[A : \ell_i] = \pm 1$ depending on whether the orientations of the line ℓ_i coincide with the orientation of A. In more general situations, where there is nontrivial gluing present, it can be computed as the degree of a certain map between spheres. This map is exactly the same as for the cellular boundary map in ordinary cellular homology, which can be found for example in Hatcher's book [210].

The second page is the cohomology of the first page with respect to the differential $d : E_1^{p,-q} \to E_1^{p+1,-q}$ given in (6.4). Mathematically speaking the second page entry $(p, -q)$ therefore equals the degree p Bredon equivariant cohomology of X with coefficient functor ${}^\phi\mathcal{R}_G^{\tau-q}$. For the third and higher order pages, we need to know the higher differentials, which are much more abstractly defined and no explicit form is known. Therefore, until more is known about this it is not possible to fully classify topological phases for general point groups using this method. It is however often the case in practice that we can arrive at a definite answer without knowing explicit expressions for the higher differentials. At least it is known that the rth differential is of bidegree $(r, 1-r)$, so $d_r : E_r^{p,-q} \to E_r^{p+r,-q+1-r}$. Therefore, for d-dimensional spaces, the rth differential d_r is zero for all $r > d$. For more details on the construction of the spectral sequence and explicit definitions, see appendix A.5.2.

But how do we construct the twisted equivariant K-theory of X from the data of the spectral sequence? After taking the cohomology with respect to the dth differential, we arrive at the final page, $E_\infty^{p,-q}$. We can construct the K-theory by extensions out of $E_\infty^{p,-p}$, so by equating p and q. In two dimensions, this means that there exist exact sequences

$$0 \to E_\infty^{2,-2} \to F \to E_\infty^{1,-1} \to 0, \tag{6.6}$$

$$0 \to F \to {}^\phi K_G^\tau(X) \to E_\infty^{0,0} \to 0, \tag{6.7}$$

see the final paragraph of appendix A.5.2 for the details. Unfortunately, these sequences do not split in general. Therefore the K-theory is not always fully determined by the spectral sequence (unless of course we would explicitly determine

the maps in these sequences, which is a tedious exercise). We will call this the problem of non-unique extensions, which unfortunately is intrinsic to our approach. An example of this phenomenon will be addressed in Section 6.3.3.

Now that the spectral sequence is contained in our toolbox, we will explain how to reduce the computation of equivariant K-theory of the Brillouin torus $\mathbf{T}^d$ to the computation of the K-theory of spheres. For this we use an equivariant stable homotopy equivalence that generalizes [181, Thm 11.8]. This equivalence adresses the decomposition of the Brillouin torus in terms of spheres. Indeed, if the action of G on $\mathbf{T}^d = S^1 \times \cdots \times S^1$ can be realized as the restriction of an action of $H^d \rtimes S_d$, where H acts on S^1 and S_d permutes the copies of S^1, then $\mathbf{T}^d$ is equivariantly stably homotopy equivalent to a wedge of spheres. More explicitly, this means in two dimensions that there is an isomorphism

$$ {}^{\phi}K_G^{\tau}(\mathbf{T}^2) \cong {}^{\phi}K_G^{\tau}(S^2) \oplus {}^{\phi}\widetilde{K}_G^{\tau}(S^1 \vee S^1). \tag{6.8} $$

Here the tilde indicates the reduced K-theory and $S^1 \vee S^1$ is a space that looks like the figure 8, which is nothing but the boundary of the Brillouin zone torus $\mathbf{T}^2$ seen as a square $[-\pi, \pi] \times [-\pi, \pi]$ with opposite sides identified. Note that the symmetry G could potentially interchange the two S^1's of the figure eight, for example in case there is a fourfold rotation symmetry. If there is no group element permuting the two copies of the circle, the K-theory decomposes further as

$$ {}^{\phi}K_G^{\tau}(\mathbf{T}^2) \cong {}^{\phi}K_G^{\tau}(S^2) \oplus {}^{\phi}\widetilde{K}_G^{\tau}(S^1) \oplus {}^{\phi}\widetilde{K}_G^{\tau}(S^1), \tag{6.9} $$

where we used that

$$ {}^{\phi}\widetilde{K}_G^{\tau}(S^1 \vee S^1) = {}^{\phi}\widetilde{K}_G^{\tau}(S^1) \oplus {}^{\phi}\widetilde{K}_G^{\tau}(S^1). \tag{6.10} $$

A similar isomorphism as in (6.9) exists in three dimensions under the given assumptions. The relation between reduced and unreduced K-theory ${}^{\phi}K_G^{\tau}(X)$ is

$$ {}^{\phi}K_G^{\tau}(X) = {}^{\phi}K_G^{\tau}(\mathrm{pt}) \oplus {}^{\phi}\widetilde{K}_G^{\tau}(X). \tag{6.11} $$

When using the equivariant splittings (6.8) and (6.9), we can thus compute the unreduced K-theory and then strip of the ${}^{\phi}K_G^{\tau}(\mathrm{pt})$-part to obtain the reduced K-theory. Note that the assumption that the action of G comes from some action of $H^d \rtimes S_d$ does not always hold, so that we cannot always use (6.8). If for example three-fold rotations are present, we seem to be bound to applying the Atiyah-Hirzebruch spectral sequence to the Brillouin zone torus directly.

Since the K-theory of a one-dimensional space X is easy to compute, the isomorphism (6.9) effectively reduces computations of the K-theory of a two-dimensional torus to a two-dimensional sphere. Indeed, for one-dimensional spaces all higher

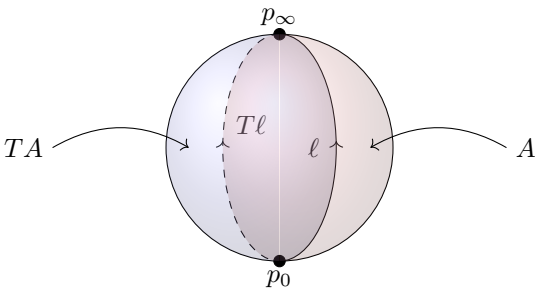

Figure 6.1: A $\mathbf{Z}_2$-CW structure of the $\mathbf{Z}_2$-space S^2 that is the one-point compactification of the two-dimensional representation of $\mathbf{Z}_2$ given by $k \mapsto -k$. We have denoted this action by T.

differentials vanish and $E_\infty^{2,-2} = 0$, so that the exact sequences (6.6) and (6.7) reduce to a single exact sequence. Because the twisted representation ring ${}^\phi R^\tau(G)$ is torsion free (for $q = 0$), so is $H^0(X, {}^\phi\mathcal{R}_G^\tau)$. Hence the resulting sequence splits, giving us

$$ {}^\phi K_G^\tau(X) \cong H^0(X, {}^\phi\mathcal{R}_G^\tau) \oplus H^1(X, {}^\phi\mathcal{R}_G^{\tau-1}). \tag{6.12}$$

Despite the absence of torsion in the first term, the second term can give rise to torsion of which we will see examples below. The torsion in H^1 was anticipated before in [211] for systems in class AII with a reflection symmetry in one dimension.

6.3.2 Time-reversal only: revisited

Let us now illustrate how the Atiyah-Hirzebruch spectral sequence formalizes the intuitive approach of the last section. So again we will take $X = S^2$ with the $\mathbf{Z}_2$-action $k \mapsto -k$ with the $\mathbf{Z}_2$-CW-structure as given in Figure 6.1. We will consider the classes AI ($T^2 = 1$) and AII ($T^2 = -1$) simultaneously and note the distinctions along the way. Mathematically, we distinguish between the two classes by picking the twist $\tau = \tau_0$ to be trivial in class AI and $\tau = \tau_1$ nontrivial in class AII. The higher twisted representation rings of $\mathbf{Z}_2$ and the trivial subgroup $1 \subseteq \mathbf{Z}_2$ are given in Table 6.1. Note that the stabilizers of the 0-cells are both $\mathbf{Z}_2$, while for the other cells the stabilizer is trivial.

We will start by computing all Bredon cohomology groups that are necessary for obtaining the K-theory group from the spectral sequence. These cohomology groups are the ones that correspond to second page entries of the spectral sequence which could possibly influence the three desired entries $E_\infty^{0,0}$, $E_\infty^{1,-1}$ and $E_\infty^{2,-2}$ of the final page occurring in the exact sequences of equation (6.6) and (6.7). Because the

	${}^{\phi}R^{\tau_0-q}(\mathbf{Z}_2)$ = $KR^{-q}(\mathrm{pt})$	${}^{\phi}R^{\tau_1-q}(\mathbf{Z}_2)$ = $KR^{-q-4}(\mathrm{pt})$	${}^{\phi}R^{\tau_0-q}(1)$ = $K^{-q}(\mathrm{pt})$	${}^{\phi}R^{\tau_1-q}(1)$ = $K^{-q}(\mathrm{pt})$
$q=0$	$\mathbf{Z}$	$\mathbf{Z}$	$\mathbf{Z}$	$\mathbf{Z}$
$q=1$	$\mathbf{Z}_2$	0	0	0
$q=2$	$\mathbf{Z}_2$	0	$\mathbf{Z}$	$\mathbf{Z}$
$q=3$	0	0	0	0
$q=4$	$\mathbf{Z}$	$\mathbf{Z}$	$\mathbf{Z}$	$\mathbf{Z}$
$q=5$	0	$\mathbf{Z}_2$	0	0
$q=6$	0	$\mathbf{Z}_2$	$\mathbf{Z}$	$\mathbf{Z}$
$q=7$	0	0	0	0
$q=8$	$\mathbf{Z}$	$\mathbf{Z}$	$\mathbf{Z}$	$\mathbf{Z}$
$\vdots$				

Table 6.1: The twisted representation rings in the case of $G_\sigma = \mathbf{Z}_2$ and $G_\sigma = 1$. They are 8-periodic in the degree.

second differential (which is of bidegree $(2,1)$) is the only possibly nonzero higher differential, we have $E_3 = E_\infty$. Therefore we have to compute $H^p_G(S^2, {}^{\phi}\mathcal{R}_G^{\tau-q})$ for (p,q) equal to $(0,0),(0,1),(1,1),(2,1)$ and $(2,2)$.

First we have to find all necessary Bredon equivariant cochains, as they constitute the first page $E_1^{p,-q}$. We start with $p = q = 0$. So we consider the equivariant 0-cochains with values in ${}^{\phi}\mathcal{R}_G^{\tau}$, which here are the equivariant maps from the set $\{p_0, p_\infty\}$ to ${}^{\phi}R^{\tau}(\mathbf{Z}_2) = \mathbf{Z}$ for both twists. Because the 0-cells are completely fixed by the group, all 0-cochains are equivariant. Therefore the equivariant 0-cochains are spanned by two basis elements π_0 and π_∞ over $\mathbf{Z}$:

$$C^0_{\mathbf{Z}_2}(S^2, {}^{\phi}\mathcal{R}_G^{\tau}) = \langle \pi_0, \pi_\infty \rangle_{\mathbf{Z}} = \mathbf{Z}^2. \tag{6.13}$$

Here π_0 maps p_0 to $1 \in {}^{\phi}R^{\tau}(\mathbf{Z}_2)$ and p_∞ to $0 \in {}^{\phi}R^{\tau}(\mathbf{Z}_2)$. For π_∞ the roles of p_0 and p_∞ are interchanged. In more basic terms: π_0 assigns a state space of dimension one to p_0 and a zero space to p_∞, while π_∞ assigns a zero space to p_0 and a one-dimensional space to p_∞.

Going up to $p = 1, q = 0$, there is only one equivariant 1-cochain, so that

$$C^1_{\mathbf{Z}_2}(S^2, {}^{\phi}\mathcal{R}_G^{\tau}) = \langle \lambda \rangle_{\mathbf{Z}} = \mathbf{Z}. \tag{6.14}$$

Indeed, from Table 6.1 it is clear the this cochain is an equivariant map from $\{\ell, T\ell\}$ to $\mathbf{Z}$. By equivariance, it is uniquely specified by specifying its value on ℓ, which we take to be 1 for λ. In case the reader is interested in the actual value of

$\lambda(T\ell)$, simply note that the action of T on the representation ring is just complex conjugation. In case T acts on the representation ring of a nontrivial group this will result in the complex conjugation of nontrivial representations, which are in general not isomorphic to the original representation. However, a complex vector space is noncanonically isomorphic to its complex conjugation since it has the same dimension. Hence the automorphism that T induces on ${}^{\phi}R^{\tau}(1)$ is simply the identity, thus $\lambda(T\ell) = \lambda(\ell) = 1$. Along the way we will see that this automorphism is not always trivial and acts with minus the identity on the higher representation ring of degree -2. This is the heart of the matter, since it is the aspect that creates torsion in this example.

For $q = 1$, the situation simplifies, since the degree -1 representation ring of the trivial group equals zero. Hence there are no equivariant 1-cochains or 2-cochains with values in ${}^{\phi}\mathcal{R}_G^{\tau-1}$. The degree -1 representation ring of $\mathbf{Z}_2$ depends on whether the twist τ is taken trivial (class AI) or nontrivial (class AII). For τ trivial it equals $\mathbf{Z}_2$ and for τ nontrivial it equals 0. In class AII, we therefore also have no equivariant 0-cochains with values in ${}^{\phi}\mathcal{R}_G^{\tau-1}$. In class AI instead, the equivariant 0-cochains are spanned by π_0 and π_∞, just as for $q = 0$. However, this time they are a basis over $\mathbf{Z}_2$:

$$C^0_{\mathbf{Z}_2}(S^2, {}^{\phi}\mathcal{R}_G^{\tau-1}) = \langle \pi_0, \pi_\infty \rangle_{\mathbf{Z}_2} = \mathbf{Z}_2^2. \tag{6.15}$$

Here π_0 maps p_0 to the nontrivial element of $\mathbf{Z}_2$ and p_∞ to the trivial element, while for π_∞ it is the other way around.

Finally, for $q = 2$ there are some subtleties. The degree -2 representation ring of the trivial group is equal to $\mathbf{Z}$. Analogously to $q = 0$, we get that the 1-cochains are spanned over $\mathbf{Z}$ by a single element λ with $\lambda(\ell) = 1$. Similarly, the 2-cochains are spanned by a single element α with $\alpha(A) = 1$. However, unlike for $q = 0$, we have that

$$\alpha(TA) = T\alpha(A) = -\alpha(A) = -1. \tag{6.16}$$

This is because the action of T on the degree -2 representation ring is -1, as can be shown by an explicit analysis using Clifford algebras, using the explicit definitions in appendix A.2. We can conclude that the relevant part of the first page of the spectral sequence for class AI and class AII respectively is given in the following table:

	$p = 0$	$p = 1$	$p = 2$
$q = 0$	$C^0_G(S^2, {}^{\phi}\mathcal{R}_G^{\tau_0}) = \mathbf{Z}^2$	$C^1_G(S^2, {}^{\phi}\mathcal{R}_G^{\tau_0}) = \mathbf{Z}$	
$q = 1$	$C^0_G(S^2, {}^{\phi}\mathcal{R}_G^{\tau_0-1}) = \mathbf{Z}_2^2$	$C^1_G(S^2, {}^{\phi}\mathcal{R}_G^{\tau_0-1}) = 0$	$C^2_G(S^2, {}^{\phi}\mathcal{R}_G^{\tau_0-1}) = 0$
$q = 2$		$C^1_G(S^2, {}^{\phi}\mathcal{R}_G^{\tau_0-2}) = \mathbf{Z}$	$C^2_G(S^2, {}^{\phi}\mathcal{R}_G^{\tau_0-2}) = \mathbf{Z}$

	$p=0$	$p=1$	$p=2$
$q=0$	$C_G^0(S^2, {}^\phi\mathcal{R}_G^{\tau_1}) = \mathbf{Z}^2$	$C_G^1(S^2, {}^\phi\mathcal{R}_G^{\tau_1}) = \mathbf{Z}$	
$q=1$	$C_G^0(S^2, {}^\phi\mathcal{R}_G^{\tau_1 -1}) = 0$	$C_G^1(S^2, {}^\phi\mathcal{R}_G^{\tau_1 -1}) = 0$	$C_G^2(S^2, {}^\phi\mathcal{R}_G^{\tau_1 -1}) = 0$
$q=2$		$C_G^1(S^2, {}^\phi\mathcal{R}_G^{\tau_1 -2}) = \mathbf{Z}$	$C_G^2(S^2, {}^\phi\mathcal{R}_G^{\tau_1 -2}) = \mathbf{Z}$

With the information we have gathered now, we can construct the second page, consisting of Bredon cohomologies. Let us start off by computing $H_G^0(S^2, {}^\phi\mathcal{R}_G^\tau)$. For this we need to compute the kernel of the Bredon differential

$$d : \mathbf{Z}^2 = C_G^0(S^2, {}^\phi\mathcal{R}_G^\tau) \to C_G^1(S^2, {}^\phi\mathcal{R}_G^\tau) = \mathbf{Z}. \tag{6.17}$$

On the 0-cochain π_∞ it acts as

$$d\pi_\infty(\ell) = \pi_\infty(\partial\ell)|_1 = \pi_\infty(p_\infty - p_0)|_1 = \pi_\infty(p_\infty)|_1 - \pi_\infty(p_0)|_1 = \pi_\infty(p_\infty)|_1, \tag{6.18}$$

where the symbol $|_1$ denotes the restriction of the representation to the trivial group. In class AI, this restriction maps complex vector spaces with a real structure T to their underlying complex vector space. Since all complex vector spaces admit a real structure, this implies that the restriction map ${}^\phi R^\tau(\mathbf{Z}_2) \to {}^\phi R^\tau(1)$ is the identity. In class AII, where $T^2 = -1$, the restriction is multiplication by two, because only complex vector spaces of even dimension admit a quaternionic structure. Hence we get

$$d\pi_\infty = \begin{cases} \lambda & \text{if } \tau = \tau_0, \\ 2\lambda & \text{if } \tau = \tau_1. \end{cases} \tag{6.19}$$

Using the orientation we analogously get that $d\pi_0 = -d\pi_\infty$. In both class AI and AII, we see that the degree zero cohomology equals

$$\ker d = H_G^0(S^2, {}^\phi\mathcal{R}_G^\tau) \cong \mathbf{Z}. \tag{6.20}$$

In general, this cohomology group contains all local topological invariants. More precisely, the zeroth degree cohomology group is actually a mathematical formalization of the heuristic method of consistently assigning representations to point sketched in Section 6.2 and used extensively in [3] and [4].

The next row of the second page is easily deduced from the first page. In class AII, all cochains vanish and therefore so do the cohomology groups. In class AI nontrivial 0-cochains exist, but not in higher degrees. Therefore the differential is necessarily zero and the second page equals the first page.

The final relevant cohomology group is $H_G^2(S^2, {}^\phi\mathcal{R}_G^{\tau-2})$. In this case, T induced a non-trivial automorphism on ${}^\phi R^{\tau-2}(1)$ given by -1, so that

$$d\lambda(A) = \lambda(\partial A) = \lambda(\ell) - T\lambda(\ell) = 2\lambda(\ell) = 2, \tag{6.21}$$

hence $d\lambda = 2\alpha$ for both $\tau = \tau_0$ and τ_1, so that $\operatorname{im} d = 2\mathbf{Z}$. The kernel of d acting on 2-cochains is $\mathbf{Z}$, since we are in top degree. Thus $H^2_G(S^2, {}^{\phi}\mathcal{R}_G^{\tau-2}) = \mathbf{Z}_2$.

Summarizing the results by filling in the second page of the spectral sequence, we get the following tables for $T^2 = 1$ and $T^2 = -1$ respectively:

	$p=0$	$p=1$	$p=2$
$q=0$	$H^0_G(S^2, {}^{\phi}\mathcal{R}_G^{\tau_0}) = \mathbf{Z}$		
$q=1$	$H^0_G(S^2, {}^{\phi}\mathcal{R}_G^{\tau_0-1}) = \mathbf{Z}_2^2$	$H^1_G(S^2, {}^{\phi}\mathcal{R}_G^{\tau_0-1}) = 0$	$H^2_G(S^2, {}^{\phi}\mathcal{R}_G^{\tau_0-1}) = 0$
$q=2$			$H^2_G(S^2, {}^{\phi}\mathcal{R}_G^{\tau_0-2}) = \mathbf{Z}_2$

	$p=0$	$p=1$	$p=2$
$q=0$	$H^0_G(S^2, {}^{\phi}\mathcal{R}_G^{\tau_1}) = \mathbf{Z}$		
$q=1$	$H^0_G(S^2, {}^{\phi}\mathcal{R}_G^{\tau_1-1}) = 0$	$H^1_G(S^2, {}^{\phi}\mathcal{R}_G^{\tau_1-1}) = 0$	$H^2_G(S^2, {}^{\phi}\mathcal{R}_G^{\tau_1-1}) = 0$
$q=2$			$H^2_G(S^2, {}^{\phi}\mathcal{R}_G^{\tau_1-2}) = \mathbf{Z}_2$

When $T^2 = -1$, we immediately see that all higher differentials vanish. The spectral sequence thus collapses at E_2 and the exact sequences (6.6) and (6.7) reduce to the single exact sequence

$$0 \to \mathbf{Z}_2 \to KR^{-4}(S^2) \to \mathbf{Z} \to 0. \tag{6.22}$$

Since $\mathbf{Z}$ is a free group, the sequence splits. This gives us $KR^{-4}(S^2) = \mathbf{Z} \oplus \mathbf{Z}_2$. Moreover, using the spectral sequence it can easily be shown that $\widetilde{KR}^{-4}(S^1) = 0$ (for an example of a computation of the K-theory of a one-dimensional space using the spectral sequence, see the next section). By the equivariant splitting (6.9), the K-theory of the torus is thus

$$KR^{-4}(\mathbf{T}^2) = \mathbf{Z} \oplus \mathbf{Z}_2, \tag{6.23}$$

which confirms the result using a different approach, see equation (6.1). It is worth noting that the torsion invariant $\mathbf{Z}_2$ managed to appear because of the nontrivial action of T induced by complex conjugation and not by the torsion in the KR-theory of a point as it does when computing $KR^{-4}(S^2)$ using the methods of for example Freed and Moore [181].

For $T^2 = 1$ another lesson is to be learned from this example. Namely, note that as long as we do not know any expression for the second differential $d_2 : \mathbf{Z}_2^2 \to \mathbf{Z}_2$, we cannot uniquely determine the K-theory group by the spectral sequence method. However, we know from other methods that $KR^0(S^2) = \mathbf{Z}$ so that this differential must be surjective. If in future research an explicit expression for the second differential is found, it would be interesting to compute it in this example.

6.3.3 Time-reversal and a twofold rotation symmetry

For a more exciting example, we now also include a rotation R by π. So we take the symmetry group $G = \mathbf{Z}_2 \times \mathbf{Z}_2 = \{1, R\} \times \{1, T\}$. We twist the group so that the twisted group algebra satisfies the desirable physical situation on the quantum level, namely $R^2 = T^2 = -1$ and $TR = RT$. This thus represents spinful fermions on a two-dimensional square lattice with twofold rotation symmetry and hence the wallpaper group is $p2$. On the Brillouin torus $\mathbf{T}^2 = [-\pi, \pi]^2/\sim$ these symmetries act as $Tk = -k$ and $Rk = -k$.

Before the topological computations, we first have to compute the twisted Bredon coefficients, i.e. the representation rings and the relevant maps between them. Note that the only stabilizers that occur are G and $H := \{1, TR\}$, so we only have to compute twisted representations for these groups. Because of this exceptional role played by TR it is useful to set $S := TR$ and forget about T for the moment. Note that in the twisted group algebra, $Si = -iS$, $S^2 = 1$ and $SR = RS$. The twisted group algebras are abstractly isomorphic to matrix algebras:

$$ {}^{\phi}\mathbf{C}^{\tau}H = \frac{\mathbf{R}[i,S]}{(i^2 = -S^2 = 1, iS = -Si)} \cong |Cl_{1,1}| \cong M_2(\mathbf{R}) \tag{6.24} $$

$$ {}^{\phi}\mathbf{C}^{\tau}G = \frac{\mathbf{R}[i,S,R]}{(i^2 = R^2 = -S^2 = 1, iS = -Si, RS = SR, iR = Ri)} \cong M_2(\mathbf{C}), \tag{6.25} $$

where the last isomorphism follows because the twisted group algebra is ${}^{\phi}\mathbf{C}^{\tau}H \otimes_{\mathbf{R}} \mathbf{C}$. Therefore the twisted group algebra of H is Morita equivalent to the algebra $\mathbf{R}$, while the twisted group algebra of G is Morita equivalent to the algebra $\mathbf{C}$. The representation rings are therefore

$$ {}^{\phi}R^{\tau-q}(H) \cong KR^{-q}(\mathrm{pt}) \tag{6.26} $$

$$ {}^{\phi}R^{\tau-q}(G) \cong K^{-q}(\mathrm{pt}), \tag{6.27} $$

see appendix A.5.1 for details on higher degree representation rings. The restriction map in degree zero

$$ \mathbf{Z} \cong {}^{\phi}R^{\tau}(G) \to {}^{\phi}R^{\tau}(H) \cong \mathbf{Z} \tag{6.28} $$

is just given by mapping a complex vector space to its underlying real space and hence it is given by multiplication by two. For $q = 1$, the restriction map can only be zero, since $K^{-1}(\mathrm{pt}) = 0$. For $q = 2$ restriction is a map

$$ \mathbf{Z} \cong {}^{\phi}R^{\tau-2}(G) \to {}^{\phi}R^{\tau-2}(H) \cong \mathbf{Z}_2, \tag{6.29} $$

so it can either be zero or reduction mod 2. It is possible to explicitly check which it is by using explicit Clifford modules, but it turns out that we do not need to

know which one it is in order to compute the K-theory. The only remaining map between representation rings is the action of R on the representation ring. This action is given by conjugating modules over ${}^{\phi}\mathbf{C}^{\tau}H$ with R. Since R is in the center of ${}^{\phi}\mathbf{C}^{\tau}G$, the automorphism on ${}^{\phi}R^{\tau}(H)$ resulting from this is trivial. On the two relevant higher degree representation rings

$$ {}^{\phi}R^{\tau-1}(H) = {}^{\phi}R^{\tau-2}(H) = \mathbf{Z}_2 \tag{6.30}$$

the action of R is trivial as well because $\mathbf{Z}_2$ has no nontrivial automorphisms.

In order to compute the full twisted equivariant K-theory of the Brillioun zone torus, we first use the equivariant splitting method, giving the isomorphism 6.9. Secondly we apply the spectral sequence on the components. Note that the circles occuring in the isomorphism, i.e. $k_x = 0$ and $k_y = 0$ in the Brillouin zone, have identical group actions. Hence they give isomorphic K-theory groups and we only have to compute one. Next we have to decide on G-CW decompositions of our new spaces S^2 and S^1. Since the action of R is the same as the action of T, we can reuse the G-CW structure of the last example for S^2 as given in Figure 6.1. For the circle we use the one-dimensional sub-G-CW complex of the G-CW structure on S^2.

Let us start by computing the twisted equivariant K-theory of the circle. We compute the K-theory by using 6.12 for one-dimensional spaces. The zeroth-cohomology $H^0_G(S^1, {}^{\phi}\mathcal{R}^{\tau}_G)$ is analogous to the example in the previous subsection. We can define $\mathbf{Z}$-bases of equivariant 0-cochains π_0, π_∞ and 1-cochains λ. In contrast with the last example, we now have complex vector spaces on the fixed points and real vector spaces on the k-cells for $k > 0$. Recall that the restriction map sends a complex vector space to its underlying real space and therefore this map is given by multiplication by two. The Bredon differential is thus given by

$$ d\pi_\infty(\ell) = \pi_\infty(\partial\ell)|_H = 2 \implies d\pi_\infty = 2\lambda. \tag{6.31}$$

Similarly $d\pi_0 = -2\lambda$. Hence $H^0_G(S^1, {}^{\phi}\mathcal{R}^{\tau}_G) \cong \mathbf{Z}$. Notice that for the first cohomology group $H^1_G(S^1, {}^{\phi}\mathcal{R}^{\tau-1}_G)$ the twisted representation ring of G vanishes in te corresponding degree, so that the differential equals zero. Hence this cohomology group is equal to the group of equivariant 1-cochains $\langle\lambda\rangle_{\mathbf{Z}_2}$, which equals the twisted representation ring of H in degree -1. We conclude that $H^1_G(S^1, {}^{\phi}\mathcal{R}^{\tau-1}_G) \cong \mathbf{Z}_2$. Via equation (6.12), we arrive at

$$ {}^{\phi}K^{\tau}_G(S^1) = \mathbf{Z} \oplus \mathbf{Z}_2. \tag{6.32}$$

Since ${}^{\phi}K^{\tau}_G(\mathrm{pt}) = {}^{\phi}R^{\tau}(G) = \mathbf{Z}$, we see that ${}^{\phi}\widetilde{K}^{\tau}_G(S^1) = \mathbf{Z}_2$ for both circles in the splitting of the torus. These are precisely the invariants proposed by Lau et al. in [211] and when non-trivial represent a Möbius twist in the Hilbert space of

states along the invariant circles at $k_x = 0$ and $k_y = 0$. Our K-theory computation thus provides a mathematical proof of the existence of this invariant.

Now we turn to the computation of the twisted equivariant K-theory of the 2-sphere. We use the same bases of equivariant cochains $\{\pi_0, \pi_\infty\}, \{\lambda\}$ and $\{\alpha\}$ as in the last example. For the zeroth cohomology, $H^0_G(S^2, {}^\phi\mathcal{R}^\tau_G)$, the computation is equivalent to the one in the previous subsection, hence $H^0_G(S^2, {}^\phi\mathcal{R}^\tau_G) = \mathbf{Z}$. Going to $q = 1$, we see that there are no 0-cochains, since ${}^\phi R^{\tau-1}(G) = 0$. The differential on 1-cochains gives

$$\begin{aligned} d\lambda(A) &= \lambda(\partial A)|_H = \lambda(\ell) - \lambda(R\ell)|_H && (6.33)\\ &= \lambda(l)|_H - R\lambda(\ell)|_H && (6.34)\\ &= 0, && (6.35)\end{aligned}$$

since R necessarily acts trivially on ${}^\phi R^{\tau-1}(H) = \mathbf{Z}_2$. Hence the cohomology groups are equal to the cochain groups:

$$H^0_G(S^2, {}^\phi\mathcal{R}^{\tau-1}_G) = 0, \quad H^1_G(S^2, {}^\phi\mathcal{R}^{\tau-1}_G) = \mathbf{Z}_2, \quad H^2_G(S^2, {}^\phi\mathcal{R}^{\tau-1}_G) = \mathbf{Z}_2. \tag{6.36}$$

Since for $q = 2$ the 1-cochains and 2-cochains are exactly the same, the above computation also applies to the computation of the cohomology in degree 2. Therefore it follows that $H^2_G(S^2, {}^\phi\mathcal{R}^{\tau-2}_G)$ equals $\mathbf{Z}_2$ as well. The relevant part of the second page is thus conveniently summarized in the following table.

	$p = 0$	$p = 1$	$p = 2$
$q = 0$	$H^0_G(S^2, {}^\phi\mathcal{R}^\tau_G) = \mathbf{Z}$		
$q = 1$	$H^0_G(S^2, {}^\phi\mathcal{R}^{\tau-1}_G) = 0$	$H^1_G(S^2, {}^\phi\mathcal{R}^{\tau-1}_G) = \mathbf{Z}_2$	$H^2_G(S^2, {}^\phi\mathcal{R}^{\tau-1}_G) = \mathbf{Z}_2$
$q = 2$			$H^2_G(S^2, {}^\phi\mathcal{R}^{\tau-2}_G) = \mathbf{Z}_2$

The second differential $d_2 : H^0_G(S^2, {}^\phi\mathcal{R}^\tau_G) \to H^2_G(S^2, {}^\phi\mathcal{R}^{\tau-1}_G)$ is either zero or reduction modulo 2. Independent of this distinction, the kernel of d_2 is abstractly isomorphic to $\mathbf{Z}$. Hence the relevant part of the final page of the spectral sequence agrees with the diagonal $p = q$ in the table above. The exact sequences (6.6) and (6.7) that follow from the spectral sequence now reduce to

$$0 \to \mathbf{Z}_2 \to F \to \mathbf{Z}_2 \to 0, \tag{6.37}$$

$$0 \to F \to {}^\phi K^\tau_G(S^2) \to \mathbf{Z} \to 0. \tag{6.38}$$

Note that the second sequence splits. Unfortunately, the first exact sequence implies only that $F = \mathbf{Z}_2^2$ or $F = \mathbf{Z}_4$. Hence the Atiyah-Hirzebruch spectral sequence gives that ${}^\phi K^\tau_G(S^2)$ is either $\mathbf{Z} \oplus \mathbf{Z}_2^2$ or $\mathbf{Z} \oplus \mathbf{Z}_4$, depending on whether the first exact sequence splits or not. We can conclude from equation 6.9 that

$${}^\phi K^\tau_G(\mathbf{T}^2) \cong \mathbf{Z} \oplus \mathbf{Z}_2^4 \quad \text{or} \quad {}^\phi K^\tau_G(\mathbf{T}^2) \cong \mathbf{Z} \oplus \mathbf{Z}_2^2 \oplus \mathbf{Z}_4. \tag{6.39}$$

To determine which of these two is the correct one, we employ the equivariant Mayer-Vietoris exact sequence. We can focus on the sphere since two possibilities for the K-theory originated there. Take open G-neighbourhoods of the north and south pole as $U_1 = S^2 \setminus \{p_\infty\}$ and $U_2 = S^2 \setminus \{p_0\}$. Now consider the following part of the equivariant Mayer-Vietoris exact sequence with respect to U_1 and U_2:

$$\cdots \to {}^{\phi}K_G^{\tau-1}(U_1 \cap U_2) \to {}^{\phi}K_G^{\tau}(S^2) \to {}^{\phi}K_G^{\tau}(U_1) \oplus {}^{\phi}K_G^{\tau}(U_2) \to \dots \tag{6.40}$$

Note that both U_1 and U_2 are G-contractible to a point. Hence

$${}^{\phi}K_G^{\tau}(U_1) \oplus {}^{\phi}K_G^{\tau}(U_2) \cong {}^{\phi}K_G^{\tau}(\mathrm{pt}) \oplus {}^{\phi}K_G^{\tau}(\mathrm{pt}) \cong \mathbf{Z}^2.$$

Moreover, $U_1 \cap U_2$ is G-homotopy equivalent to the equator S^1. To compute the twisted equivariant K-theory of this S^1, note that the action of the subgroup H' generated by R is free. This implies that we can quotient this subgroup without having to worry about orbifold-type singularities. Since there is a homeomorphism $S^1/H' \cong S^1$, we arrive at a circle with a trivial H-action. Because twisted K-theory of orbifolds is invariant under equivalence [208], we see that

$${}^{\phi}K_G^{\tau-1}(U_1 \cap U_2) \cong {}^{\phi}K_G^{\tau-1}(S^1) \cong {}^{\phi}K_H^{\tau-1}(S^1). \tag{6.41}$$

The new twist is simply the restriction of the old twist to H and since $(TR)^2 = 1$, the twist results in nonequivariant KO-theory. Using suspensions and reduced KO-theory, we then arrive at

$$\begin{aligned} {}^{\phi}K_G^{\tau-1}(U_1 \cap U_2) &\cong KO^{-1}(S^1) \cong KO^{-1}(\mathrm{pt}) \oplus \widetilde{KO}^{-1}(S^1) && (6.42)\\ &\cong KO^{-1}(\mathrm{pt}) \oplus KO^{-2}(\mathrm{pt}) \cong \mathbf{Z}_2^2. && (6.43) \end{aligned}$$

Hence the equivariant Mayer-Vietoris sequence takes on the form

$$\cdots \longrightarrow \mathbf{Z}_2^2 \xrightarrow{f_1} {}^{\phi}K_G^{\tau}(S^2) \xrightarrow{f_2} \mathbf{Z}^2 \longrightarrow \dots \tag{6.44}$$

A simple diagram chasing argument now shows that ${}^{\phi}K_G^{\tau}(S^2)$ does not contain any 4-torsion. Indeed, suppose that $a \in {}^{\phi}K_G^{\tau}(S^2)$ satisfies $4a = 0$. We will show that this implies $2a = 0$. First note that $4f_2(a) = f_2(4a) = 0$. However, the image of f_2 is torsion-free so we necessarily have that $f_2(a) = 0$. We can conclude that a is in the kernel of f_2. By exactness, this implies that there is some $b \in \mathbf{Z}_2^2$ such that $f_1(b) = a$. Now it follows by the group structure of $\mathbf{Z}_2^2$ that $2a = 2f_1(b) = f_1(2b) = f_1(0) = 0$ as desired.

The twisted equivariant K-theory for $p2$ symmetry in class AII is thus,

$${}^{\phi}K_G^{\tau}(\mathbf{T}^2) \cong \mathbf{Z} \oplus \mathbf{Z}_2^4, \tag{6.45}$$

which exactly agrees with the heuristic arguments proposed in [4]. In particular, there it is argued that each $\mathbf{Z}_2$ invariant comes from a vortex anti-vortex pair in the Berry connection stuck at the high-symmetry points. In this case, there are four of such point and hence four $\mathbf{Z}_2$ invariants. The part of this K-theory coming from the sphere was also computed in [170]. Our method now provides a rigorous mathematical proof of this computation.

Notice that the spectral sequence also gives insight on the origin of the invariants. First of all, the $\mathbf{Z}$ factor is simply the rank of the bundle. Next we have two $\mathbf{Z}_2$'s that are Möbius-type line invariants along the two cycles of the torus and are simply the invariants already found in [211]. On the Brillouin zone sphere remaining after the equivariant splitting, we have again one such $\mathbf{Z}_2$-line invariant. Finally, we have the fourth $\mathbf{Z}_2$-invariant, which is a Fu-Kane-Mele-type surface invariant on the Brillouin sphere. We discuss a possible connection between these invariants and the vortex picture in the Section 6.5. Also note that from the equivariant Mayer-Vietoris exact sequence we could only determine the type of torsion and not the full K-theory group. It is the combination with the Atiyah-Hirzebruch spectral sequence that resulted in the final answer.

6.4 Generalizations

We will now discuss various generalizations of the simple examples we studied in the previous section. Furthermore, we will give an algorithmic method to compute the twisted representations rings.

6.4.1 Other crystal symmetries

In the above we performed computations involving either no spatial symmetries or a twofold rotation. The computation of the last section can be generalized straightforwardly to a fourfold rotation. The only thing that requires extra attention is that even though the splitting (6.8) holds true, the K-theory does not split further according to equation (6.9). This is because the fourfold rotation interchanges the two circles of the figure eight. So one really has to compute the K-theory of the figure eight. The final result for a fourfold rotation in class AII is

$$ {}^{\phi}K^{\tau}_{\mathbf{Z}_4\times\mathbf{Z}_2^T}(\mathbf{T}^2) = \mathbf{Z}_2^3 \oplus \mathbf{Z}^3. \tag{6.46}$$

Just as for a twofold rotation, there are two torsion invariants coming from the spherical Brillouin zone: one is a line invariant and one a surface invariant. However, there is only one $\mathbf{Z}_2$-invariant corresponding to the boundary figure eight,

since the two line invariants of the last section are identified by the fourfold rotation. It is amusing to see that this computation exactly agrees with the more heuristic arguments presented in [4]. There are three high-symmetry points (not related by any symmetry operation) at which vortex anti-vortex pairs can be stuck, giving rise to three $\mathbf{Z}_2$ invariants. The free part of the K-theory is simply the consistent assignment of representations as discussed in previous subsections.

It is interesting to do the same computation for wallpaper groups with reflections. For instance, let us consider a two-dimensional crystal with a single reflection symmetry. On the Brillouin torus this symmetry acts as $t \cdot k = (k_x, -k_y)$ for $k \in \mathbf{T}^2$. Just as for the twofold rotation symmetry, we have that on the fibers $t^2 = -1$. Going through the spectral sequence analysis, we find that the spectral sequence method gives a unique answer by itself. The K-theory is given by

$$ {}^{\phi}K^{\tau}_{\mathbf{Z}_2 \times \mathbf{Z}_2^T}(\mathbf{T}^2) = \mathbf{Z}_2^2 \oplus \mathbf{Z}, \tag{6.47} $$

in class AII. This result also agrees with [4]. The $\mathbf{Z}_2$ invariants come from the circles fixed under the reflection symmetry. Note that one of these circles is part of the figure eight boundary, whereas the other comes from the circle of reflection on the sphere after the equivariant splitting (6.8). The part of the K-theory coming from the sphere (in particular exactly one of the two $\mathbf{Z}_2$ invariants) was also obtained in [169, 170, 203].

For more complicated symmetries, the method becomes rather involved. For example, symmetries with elements of odd order can in two spatial dimensions only occur on a hexagonal lattice, so one has to take the non-trivial identifications of the Brillouin zone into account. The Brillouin zone will still be a torus, but the equivariant splitting we used in the previous section becomes more difficult. Also we cannot make use of the real structure TR in the same way we did above; in case of an odd order rotation the stabilizer of a generic point will be trivial instead. Moreover, TR will anticommute with reflections in class AII, see the example at the end of this section. The basic difficulty as the symmetry group gets larger is computing the twisted group algebras and their representation rings; determining them using abstract algebra as we did in equations (6.24) and (6.25) quickly becomes tedious. One way forward is to give an alternative way of describing and constructing the twisted representation rings. Essentially, the only requirement for the construction of these twisted representation rings is knowing how many representations exist and which are real, complex and quaternionic. More precisely, if the number of real, complex and quaternionic irreducible (ϕ, τ)-twisted representations of G is denoted by n_k with $k = \mathbf{R}, \mathbf{C}, \mathbf{H}$, we have

$$ {}^{\phi}R^{\tau}(G) = K^0(\mathrm{pt})^{n_{\mathbf{C}}} \oplus KR^0(\mathrm{pt})^{n_{\mathbf{R}}} \oplus KR^{-4}(\mathrm{pt})^{n_{\mathbf{H}}}. \tag{6.48} $$

Once this data has been computed, the higher order rings follow from the Bott

clock, see appendix A.5.1. Remember that although we refer to ${}^{\phi}R^{\tau}(G)$ as rings, they are actually not rings. The task we are thus left with is to determine the integers n_k. In other words, we need an adequate representation theory for twisted groups. From a physics point of view, such a theory was outlined in [194] and we will now showcase this to make contact with the approaches to such problems by the crystallography community. It would also be interesting to see this point of view compared with the Wigner test, which is the appropriate generalization of the Frobenius-Schur indicator as given in [194]. Although we will not give a rigorous proof of the connection between the representation theory of space groups and twisted representation rings, we will give evidence for such a connection below and in appendix A.5.1.

In the rest of this section, we will mention the procedure of [194] and illustrate it using a simple example. For this we will need to briefly change gears. We formulate twisted groups in terms of double covers and twisted representations as double-valued representations. To see how this formulation is related to the twists τ in the main text, the reader may wish to consult the final paragraph of appendix A.5. Although this procedure works for both class AI and AII, let us focus on the latter. For simplicity we assume that $G = G_0 \times \mathbf{Z}_2^T$, where $\mathbf{Z}_2^T$ represents the time-reversal action on the Brillouin zone and G_0 consists of the other symmetries. We have written G in this way, because G_0 will be lifted to a linear action on the Hilbert space, whereas time-reversal lifts to an anti-linear action. Let us focus first on G_0. In class AII, we are dealing with fermions (class AI assumes the system is bosonic) and we have to consider a certain double cover of G_0, which we denote by $\widehat{G}_0$. The representations of the double cover take the usual signs into account that come for example from rotations over 2π acting with a minus sign on the Hilbert space. In this sense they form the structure analogous to the twist τ in the rest of this chapter. It is usually intuitively clear which double cover is desirable, but for a general point group G_0 of a d-dimensional lattice it can be described by the following abstract mathematical construction. The double cover should be the pullback of the negative Pin group $\mathrm{Pin}_-(d)$ covering the orthogonal group:

$$\begin{array}{ccccccccc} 1 & \longrightarrow & \mathbf{Z}_2 & \longrightarrow & \widehat{G}_0 & \longrightarrow & G_0 & \longrightarrow & 1 \\ & & \| & & \downarrow & & \downarrow & & \\ 1 & \longrightarrow & \mathbf{Z}_2 & \longrightarrow & \mathrm{Pin}_-(d) & \longrightarrow & O(d) & \longrightarrow & 1. \end{array}$$

The reason that it is not the spin group is that this group would only account for rotations, not for reflections. In other words, $\mathrm{Spin}(d)$ is only a double cover of $SO(d)$. The reason that we pick the negative Pin group $\mathrm{Pin}_-(d)$ instead of the other central extension $\mathrm{Pin}_+(d)$ of $O(d)$, is that in $\mathrm{Pin}_+(d)$ reflections square to the

identity instead of to the desired -1[2]. It is useful to note that if $G_0 = D_n$ is the symmetry group of an n-gon, then $\widehat{G}_0$ is known as the dicyclic group of order $4n$. Twisted representations of the group G_0 can now be described as certain ordinary representations of the double cover group $\widehat{G}_0$. Let us call representations fermionic when the newly introduced subgroup $\mathbf{Z}_2 \subseteq \widehat{G}_0$ acts nontrivially. Representations where the $\mathbf{Z}_2$ acts trivially are called bosonic. This exactly means that 2π rotations (or double reflections) act by -1 on fermionic representations and trivially on bosonic representations. In general, the double cover will admit both fermionic and bosonic representations, but for systems in class AII the Hilbert space is organized in terms of fermionic representations only. Given these fermionic representations, we are now ready to add in time-reversal symmetry. This enlarges the group with another generator T that squares to minus one. Set-theoretically, we can write the full group acting on the Hilbert space as [3]

$$\widehat{G} = \widehat{G}_0 \sqcup A\widehat{G}_0, \tag{6.49}$$

where A is an antiunitary symmetry operator, i.e. $\phi(Ag) = -1$ for any $g \in \widehat{G}_0$. Notice that starting with any group $\widehat{G}$ and any nontrivial homomorphism $\phi : \widehat{G} \to \mathbf{Z}_2$, we could have created such a decomposition by taking $\widehat{G}_0 = \ker \phi$ and picking some $A \notin \ker \phi$. Usually one takes $A = T$, but other forms of A are also possible. For example, in the example in the previous subsection, for $H := \{1, TR\}$ we would have $A = TR$ and $\widehat{G}_0 = \{1, -1\}$, with -1 the non-trivial element in the double cover of the trivial group. Notice also that the choice of A in (6.49) is a bit arbitrairy as $A' = Ag$ for $g \in \widehat{G}_0$ instead of A will give rise to unitarily equivalent representations.

To construct time-reversal symmetric representations, we simply follow the logic as outlined in section A.3. Before discussing some examples, let us mention that an important subtlety is when the unbroken symmetry group of the fixed point does not contain any antiunitary symmetries. In that case the representations remain complex, i.e. case c), just as we saw in Table 6.1 in the case of a trivial stabilizer group.

For a rotation symmetry $\mathbf{Z}_n$, the double cover is $\mathbf{Z}_{2n}$ which has n complex fermionic representations for n even. For n odd, there are $n-1$ complex fermionic representations and one quaternionic representation. Due to time-reversal symmetry the

[2] When other symmetries such as gauge or flavour symmetries are present or when there are interactions, the double cover could also be $\mathrm{Pin}_-(d)$. Although it would be interesting to map out all possible choices, it is beyond to scope of the present work.

[3] Note that in the previous section, we used G to denote the group acting on the Brillouin zone. The group $\widehat{G}$ is the lift of that group to a group acting on the Hilbert space in which time-reversal, 2π rotation and double reflections square to minus one. Hence fermionic representations of $\widehat{G}$ are equivalent to twisted representations of G.

complex fermionic representations will pair up and hence the twisted representation ring of degree $-q$ of $G = \mathbf{Z}_n \times \mathbf{Z}_2^T$ is

$$ {}^{\phi}R^{\tau-q}(G) = \begin{cases} K^{-q}(\mathrm{pt})^{n/2} & \text{if } n = \text{even} \\ K^{-q}(\mathrm{pt})^{(n-1)/2} \oplus KR^{-q-4}(\mathrm{pt}) & \text{if } n = \text{odd} \end{cases} . \tag{6.50} $$

This is exactly the same result as one would get by constructing the representation ring of the twisted group algebra, which is a more formal way of computing the twisted equivariant K-theory of a point. More details on that construction can be found in the appendix. A more non-trivial example is $G_0 = \mathbf{Z}_2 \times \mathbf{Z}_2$. This group is generated by t_1 and t_2, which represent reflections in the k_x and k_y axis respectively. The double cover of this group is Q_8, the quaternion group. The action of G_0 on the Brillouin zone torus $\mathbf{T}^2$ has four fixed points $(0,0)$, $(0,\pi)$, $(\pi,0)$ and (π,π) and four fixed circles $(0,k_y)$, (π,k_y), $(k_x,0)$ and (k_x,π). The fixed points have stabilizer group G_0. We will analyze the representations of the cover of this group first. The group Q_8 has five representations of which only one is fermionic, since for all other representations $-1 \in Q_8$ acts trivially. This fermionic representation is just its regular action on the quaternions $\mathbf{H}$, which is a two-dimensional representation over the complex numbers. We denote the generators of Q_8 by $\hat{t}_1$ and $\hat{t}_2$. The representation is concretely given by

$$ \rho(\hat{t}_1) = i\sigma_1, \quad \rho(\hat{t}_2) = i\sigma_2 \tag{6.51} $$

where σ_i are the Pauli matrices. Note that since we are at fixed points whose stabilizer group is the full point group, we have $A = T$. To determine what time-reversal does with these representations, we have to find out whether ρ and $\bar{\rho}$ are unitarily equivalent. Clearly this is the case, since $N = i\sigma_2$ is an explicit unitary matrix that intertwines ρ with $\bar{\rho}$. To see this, note that it anticommutes with all purely imaginary matrices in this representation. Given this N, we have

$$ N\bar{N} = -\sigma_2^2 = -1 = +T^2. \tag{6.52} $$

Thus we are in case a) and we have ${}^{\phi}R^{\tau-q}(G) = KR^{-q}(\mathrm{pt})$.

For the fixed circles the twisted representation theory of the stabilizer is unexpectedly interesting. Consider for example the circle $k_y = 0$. This circle is fixed by $H = \{1, t_2\}$, which lifts to the double cover $\widehat{H} = \{1, \hat{t}_2, \hat{t}_2^2, \hat{t}_2^3\}$. The full set of elements in the double cover (including time-reversal) that leave $k_y = 0$ fixed is $\{1, \hat{t}_2, \hat{t}_2^2, \hat{t}_2^3\} \sqcup TR\{1, \hat{t}_2, \hat{t}_2^2, \hat{t}_2^3\}$, hence we pick $A = TR$, where $R = \hat{t}_1\hat{t}_2$ is the lift of the twofold rotation in the double group. Note that $A^2 = 1$, but since A contains the rotation R it anticommutes with the reflections. Even though the fermionic representations $\rho_\pm$ of $\widehat{H}$ have complex eigenvalues $\pm i$ for the reflection, these two irreps nevertheless belong to case a). To see this, first note that since these representations are one-dimensional over the complex numbers, N drops out. Hence

two such representations are unitarily equivalent if and only if they are equal. Now note that there is an extra minus sign that cancels the minus sign coming from complex conjugation. Indeed we have $\bar{\rho}_\pm = \rho_\mp$ and hence

$$\bar{\rho}_\pm(A^{-1}\hat{t}_2 A) = \rho_\mp(-\hat{t}_2) = \rho_\pm(\hat{t}_2). \tag{6.53}$$

For the other fixed circles the exact same argument holds. At the fixed circles we therefore have two real representations and hence the representation ring is

$${}^{\phi}R^{\tau-q}(H \times \mathbf{Z}_2^T) = KR^{-q}(\mathrm{pt}) \oplus KR^{-q}(\mathrm{pt}). \tag{6.54}$$

From this computation, one immediately sees that a lot of torsion will appear in the spectral sequence. We will not compute the full K-theory for this crystal group here, but we expect the exact sequences that result from the spectral sequence to split.

The approach given in this section has a natural extension to non-symmorphic symmetries, but the computations become more tedious. We will discuss these symmetries further in the discussion section.

6.4.2 Class AI

Topological insulators in class AI satisfy $T^2 = 1$. The bundle therefore has a real structure given by T. In the absence of a point-group symmetry, the K-theory classifying topological insulators is Real K-theory KR, which we computed in (6.1). When the topological insulator has a non-trivial crystal symmetry, the twist τ is trivial. Therefore we have to compute equivariant Real K-theory, which for a group G is denoted by KR_G. We can again use the spectral sequence method to compute the relevant K-theory groups. For a single reflection symmetry in class AI we find that

$$KR_{\mathbf{Z}_2}(\mathbf{T}^2) = \mathbf{Z}^3, \tag{6.55}$$

which is again in agreement with [169, 170, 203]. The invariants are purely coming from the representations at the fixed points together with a non-trivial glueing condition.

It turns out that for other symmetries, the K-theory for class AI is much harder to compute. In the examples we considered, the computations are plagued by the higher differentials of the spectral sequence. This problem appears especially in class AI because in two dimensions, the second differential can only make a nontrivial contribution in case the (twisted) stabilizer H_k of some zero-cell k admits a real representation. In contrast to class A (where all representations are complex) and in class AII (where real representations do appear sometimes), real

representations are the norm in class AI. This is because time-reversal is a real structure. In particular whenever H_k contains T, the trivial representation of H_k is always real. Therefore the second differential can often make contributions to the K-theory, but we have not been able to show what these contributions are for a general crystal symmetry. What we do know however is that for the analogous computation of the one done in 6.3.3 (i.e. time-reversal and a twofold rotation symmetry) the K-theory is one of the two groups

$$KR_{\mathbf{Z}_2}(\mathbf{T}^2) = \mathbf{Z}^5 \text{ or } KR_{\mathbf{Z}_2}(\mathbf{T}^2) = \mathbf{Z}^5 \oplus \mathbf{Z}_2. \tag{6.56}$$

We were not able to show which of these two is the actual answer, but the analysis in [212] suggests that there cannot be any torsion in this case. In this work a four-fold rotation symmetry is considered and it is shown that a $\mathbf{Z}_2$ invariant appears because the two complex representations form a two dimensional representation at the fixed points $(0,0)$ and (π,π) once time-reversal symmetry is taken into account. An effective time-reversal operator TR can be defined that squares to minus one and hence at these points the vector bundle has the same quaternionic structure that is found in class AII. This observation was crucial to show that there is a single $\mathbf{Z}_2$ for $p4$ in class AI. For a twofold rotation symmetry a similar construction does not work, which is why we believe $KR_{\mathbf{Z}_2}(\mathbf{T}^2) = \mathbf{Z}^5$. From the point of view of the spectral sequence, this would be the case if the second differential d_2 (of which no convenient explicit expression is known) is surjective. In [201], it is indeed argued that in this case d_2 is surjective, just like we found in case when no point symmetries were present.

We have also computed the KR-theory associated to $p4$ rotation symmetry in class AI, but we ran into the same problems as for $p2$. However, from the above discussion, we know that there should be a single $\mathbf{Z}_2$ invariant. If a closed expression for the second differential is derived, it would therefore be interesting to show rigorously that d_2 is surjective for $p2$, but not surjective for $p4$.

In case of more non-trivial crystal symmetries, the representation theory and hence its twisted rings can be computed using the technique outlined above. The difference is that now we are interested in the bosonic representations of $\hat{G}$. In other words, we do not have to consider the double cover group, but instead we can work with the point group itself, thus (6.49) changes to $G = G_0 \sqcup AG_0$. If A happens to commute with all $g \in G_0$, this means we just have to determine the real representation theory of G_0. So, for example let us consider a point group D_4. This group has five representations and all are realizable over the real numbers. These representations are thus in case a). The twisted representation ring is then

$${}^{\phi}R^{\tau-q}(D_4 \times \mathbf{Z}_2^T) = KR^{-q}(\mathrm{pt})^5 \tag{6.57}$$

Again for a generic point on the torus, there is an unbroken symmetry group

$H = \{1, TR^2\}$, hence a smart choice would be to pick $A = TR^2$. Notice that again $(TR^2)^2 = 1$ and TR^2 commutes with all elements of G. For the subgroup H we have $H_0 = \{1\}$, whose representation obviously belongs to case a), hence ${}^{\phi}R^{\tau-q}(H) = KR^{-q}(\mathrm{pt})$. The geometric action of D_4 on the torus has three other non-trivial stabilizer groups, two isomorphic to $\mathbf{Z}_2$ and one isomorphic to $\mathbf{Z}_2 \times \mathbf{Z}_2$. The representation rings for these two groups also only consist of copies of $KR^{-q}(\mathrm{pt})$, since all representations are real. In fact, we have

$$ {}^{\phi}R^{\tau-q}(\mathbf{Z}_2 \times \mathbf{Z}_2^T) = KR^{-q}(\mathrm{pt}), \tag{6.58} $$

$$ {}^{\phi}R^{\tau-q}(\mathbf{Z}_2 \times \mathbf{Z}_2 \times \mathbf{Z}_2^T) = KR^{-q}(\mathrm{pt}). \tag{6.59} $$

6.4.3 Class A

In class A the spectral sequence is well-known [213, 214] and the computations are a lot more tractable. There are no antiunitary operators and the K-theory is just Atiyah & Segal's complex equivariant K-theory [215], but possibly twisted. The twist now comes purely from non-symmorphic symmetries. Let us focus on symmorphic symmetries so that there is no twist. In this case, the relevant exact sequences in the spectral sequence constructed here will always split and so unlike in class AI and AII, we get a unique answer. One might wonder whether the higher differentials could give non-trivial contributions. Firstly, since $\mathcal{R}_G^{-q} = 0$ for odd q, every other row on the second page of the spectral sequence is trivial so that the second differential always vanishes. Moreover, in two dimensions the third and higher differentials always vanish. Thus we can easily determine the equivariant K-theory exactly.

Indeed, since in the complex case $\mathcal{R}_G^{-2} = \mathcal{R}_G$, one quickly sees that the exact sequences (6.6) and (6.7) imply that

$$ K_G(X) \cong H^0_G(X, \mathcal{R}_G) \oplus H^2_G(X, \mathcal{R}_G). \tag{6.60} $$

This isomorphism also holds in three dimensions, since in that case the third differential gives no additional contribution. We will illustrate this fact by a short argument. If X is three-dimensional, the arguments above give us the isomorphism

$$ K_G(X) \cong \ker\left(d_3 : H^0_G(X, \mathcal{R}_G) \to H^3_G(X, \mathcal{R}_G)\right) \oplus H^2_G(X, \mathcal{R}_G). \tag{6.61} $$

Now note that in class A, the Bredon cochains map into ordinary representation rings of subgroups $H \subseteq G$. Since these representation rings are always torsion-free, so are all groups of Bredon cochains. Since $H^0_G(X, \mathcal{R}_G)$ is a kernel of a $\mathbf{Z}$-linear map between Bredon cochains, it must therefore also be torsion-free and hence so is $\ker d_3$. But by the equivariant Chern character isomorphism [205]

$$ K_G(X) \otimes \mathbf{C} \cong H^0_G(X, \mathcal{R}_G \otimes \mathbf{C}) \oplus H^2_G(X, \mathcal{R}_G \otimes \mathbf{C}), \tag{6.62} $$

we already know that the formula (6.60) holds modulo torsion. Therefore, there must be an isomorphism $\ker d_3 \cong H^0_G(X, \mathcal{R}_G)$. Note that even though this argument does not imply that d_3 vanishes, it still implies that it can be ignored in abstract computation.

Let us reflect on the results we have just established in class A. First of all, in light of [3], we see that there is indeed a clear distinction between the representations at fixed points and how they are glued to the representations at lines on the one hand, which are captured by $H^0_G(X, \mathcal{R}_G)$, and higher-dimensional invariants, such as Chern numbers on the other hand, which are in $H^2_G(X, \mathcal{R}_G)$. In two dimensions, one can check by explicit computation that H^2_G is torsion-free, but in three dimensions it is known that it contains torsion in certain examples [201]. Nevertheless, the torsion-free part is still captured by the proposed algorithm in [3]. The torsion is hard to understand systematically, but intuitively one expects it to arise from either non-symmorphic space groups or non-trivial identifications due to the crystal structure. Since the Bredon cohomology of a complex is something purely combinatorial, equation 6.60 provides an algorithmic approach to computing the K-theory for class A in full generality. It would be interesting to develop such an algorithm and compare it to the results of [201]. In fact, comparing with existing literature on the equivariant K-theory associated with the space group $F222$, we see that [201] obtains an $\mathbf{Z}_2$ invariant in class A, whereas in [216] this K-theory is found to be torsion-less. We leave a detailed analysis of this discrepancy to future work.

We also briefly mention a useful alternative method to determine the K-theory groups in class A in some cases. Namely, in the cases in which the equivariant splitting method applies, the classification is determined by the equivariant K-theory of representation spheres. The nontwisted complex K-theory of representation spheres is easily determined in terms of purely representation-theoric data as was described by Karoubi, see the survey paper [217]. It would be interesting to research whether pure representation-theoretic data could describe the K-theory of representation spheres in case time-reversal is included.

6.5 Discussion

We have outlined a way to compute the K-theory that classifies topological insulators with or without time-reversal symmetry and with non-trivial crystal symmetry. Using an Atiyah-Hirzebruch spectral sequence, we computed these groups in a couple of examples and saw that often more work is needed to compute the exact answer. Nevertheless, it is noteworthy that the classification with K-theory

matches with the rather heuristic arguments presented in [3, 4], at least for the examples that we computed. Moreover, with the techniques of crystallography, we were able to give an algorithmic way of computing the twisted representation rings in any degree.

In our K-theory computations, we have also stumbled upon some difficulties that in general seem hard to overcome. Firstly, there is the fact that as of yet no explicit expression for the higher differentials of the spectral sequence is known, even in the simplest cases. For nonequivariant complex K-theory, it is known that the second differential vanishes and the third differential is the extended third Steenrod square Sq^3, which is the composition

$$H^p(X, \mathbf{Z}) \to H^p(X, \mathbf{Z}_2) \xrightarrow{Sq^2} H^{p+2}(X, \mathbf{Z}_2) \xrightarrow{\beta} H^{p+3}(X, \mathbf{Z}), \tag{6.63}$$

where Sq^2 is the second Steenrod square and β is the Bockstein homomorphism associated to the exact sequence

$$0 \to \mathbf{Z} \xrightarrow{\times 2} \mathbf{Z} \to \mathbf{Z}_2 \to 0. \tag{6.64}$$

This result has been generalized to twisted complex K-theory in [218], but even in nontwisted equivariant K-theory the situation is much more involved as is illustrated in [214]. Real K-theory on the other hand even introduces a second differential and is less studied in the literature. For KO-theory (the K-theory that classifies real vector bundles instead of complex ones, i.e. KR-theory with trivial involution) it has long been known that the second differential is the (appropriately extended) second Steenrod square [219]. Keeping the applications in mind, it would be interesting to work out explicit expressions of the higher differentials for small groups and CW-complexes from their abstract definition. Intuitively, a non-trivial rth differential represents obstructions of extending the vector bundle on a d dimensional subspace to an $d + r$ dimensional subspace. This intuitive understanding was used in [201] to argue that a non-trivial rth differentials is an obstruction of smoothly extending (i.e. without gap closing) a topological insulator on a d-cell to an $(d+r)$-cell. Surprisingly, this allowed the authors to construct explicit expressions for the higher differentials in specific examples. It would be would be interesting to rigorously show that this construction works in general.

The second and more fundamental difficulty in using the spectral sequence method is the problem of non-unique extensions. Indeed, since the exact sequences (6.6) and (6.7) are not always split, we cannot determine the K-theory uniquely unless we explicitly know the maps involved. In Section 6.3.3 we had to face this problem, since torsion groups appeared both in degree 1 and degree 2 simply because $KR^{-1}(\mathrm{pt}) = KR^{-2}(\mathrm{pt}) = \mathbf{Z}_2$. With just the Atiyah-Hirzebruch spectral sequence in our toolbox, this problem could only be solved by explicitly determining all

maps involved in our exact sequences, which is tedious even in simple examples. In order to fully determine the (especially 2-)torsion invariants for general point groups, we will need a supplement to the spectral sequence. The supplement we used in Section 6.3.3 was the equivariant Mayer-Vietoris exact sequence. There are several other possibilities for such a supplement. One would be an Adams-type spectral sequence. Such spectral sequences are made precisely to measure the torsion part of groups of stable homotopy classes of maps between spaces. Another supplement, which was recently discussed in [220], relates a K-theory with a non-unique extension problem to one which does have a unique extension through a notion of T-duality.

Setting aside these difficulties, it would also be interesting to apply our method to topological superconductors and insulators with a chiral symmetry. These cases cover the remaining 7 Altland-Zirnbauer classes [149] and might also give many new invariants that can be studied experimentally. A simple example would be to study a topological superconductor with only particle hole symmetry C which can square to $+1$ or -1. Such systems are in class D and C, respectively. In two dimension the classification without any symmetry is just $\mathbf{Z}$ and it would be interesting to see how crystal symmetry changes this. However, even though chiral symmetries are incorporated in the framework of Freed & Moore's K-theory, it does not seem to be well-suited for this purpose. For example, for class AIII a short argument shows that the Freed-Moore K-theory group of S^1 vanishes in case no other symmetries are present. This contradicts the ten-fold way, which says that in one dimension class AII topological insulators on a spherical Brillouin zone are classified by $\mathbf{Z}$. As argued in [208, §3.5], this discrepancy results from the fact that the types of K-theory that include chiral symmetries are no longer realizable by finite-dimensional bundles as Freed and Moore assume. However, this seems to contradict the physical principle that our topological insulators only admit a finite number of bands. Assuming that the K-theory defined in [208] is the physically relevant type of K-theory, we know from this work that it satisfies the desired axioms for cohomology. In that case, the higher representation rings admit an obvious generalization to particle-hole reversing symmetries and a version of the spectral sequence similar to the one developed here therefore probably holds.

Another very interesting class of symmetries, which we have not touched upon yet, are non-symmorphic symmetries. In two dimensions most symmetries are symmorphic, but in three dimensions there is a large class of crystals that exhibit some form of non-symmorphicity. The implementation of such symmetries in our recipe is mathematically challenging, because non-symmorphic crystals give twists that can vary throughout the Brillouin zone. The known representation theory of non-symmorphic space groups seems to reveal that these non-trivial

twists can result in a change in the type of representation at fixed loci and hence in different K-theory at different points. We leave a full understanding of these twisted representation rings and a rigorous construction of the spectral sequence for non-symmporphic space groups to future work.

In the introduction we explained an intuitive picture of the $\mathbf{Z}_2$ invariants in class AII that was put forward in [4]. In particular, when crystal symmetries are present it was argued in [4] that in two dimensions the vortex anti-vortex pair is stuck on fixed points whenever there is a rotation symmetry and stuck on fixed circles whenever there is a reflection symmetry. In string theory there is a analogous interpretation. Witten showed in [221] that there is a direct relation between the charges of D-branes on orbifolds and equivariant K-theory. Depending on what string theory is considered and whether there are involutions present, various versions of K-theory classify the corresponding D-brane charges. Moreover, at the orbifold singularity, say $\mathbf{C}^2/\mathbf{Z}_n$, only charge-$n$ D-branes can be peeled off, other charges are stuck on the singularity, branes with these charges are called fractional branes. In K-theory this means that only certain vector bundles see the singularity. This is similar to the fact that only 2 vortex anti-vortex pairs can be moved away from a fixed point with n-fold rotation symmetry for topological insulators in class AII. Thus a single vortex anti-vortex pair is frozen on the fixed point.

Although this frozen vortex picture gives the correct number of $\mathbf{Z}_2$ invariants for the example we computed, this interpretation is not immediately clear from our K-theory computations. One way to clarify this, is by using a localisation technique by Segal and Atiyah-Segal [215, 222][4]. Originally, this is a result that applies to (untwisted) equivariant complex K-theory, $K_G(X)$, and uses the fact that $K_G(X)$ is an $R(G)$-module, with $R(G)$ the representation ring of G. Generalisations to other K-theories have also been mentioned in the literature, [223, 224]. For instance, in the latter reference, this technique has been applied to the three-dimensional diamond structure in class A, which has a non-trivial twist. For our purposes we would have to be generalise the localisation technique to cases in which a time-reversing operator is present as well, which we hope to pursue in future work.

[4] We thank Gregory Moore for this suggestion.

A Appendices

A.1 Alternate proof without assuming $\tilde{f}(\psi) = 0$

In this appendix we will try to generalize the proof in section 2.4.3 to the case where we make no assumptions on the form of the vacuum energy. To illustrate the point, we will work in three spacetime dimensions and make the spatial manifold explicit. We will again be using a proof like that of [24], but this time we will take $N \to \infty$ from the start.

Consider a rectangular three-torus with side lengths β, L_1, and L_2 with $\beta < L_1 < L_2$. We have the relations

$$Z(\beta)_{L_1\times L_2} - Z(L_1)_{\beta\times L_2} = Z(\beta)_{L_1\times L_2} - Z(L_2)_{\beta\times L_1} = 0 \implies \tag{A.1}$$

$$\left(\sum_L e^{-\beta E_{L_1\times L_2}} - \sum_L e^{-L_1 E_{\beta\times L_2}}\right) + \left(\sum_H e^{-\beta E_{L_1\times L_2}} - \sum_H e^{-L_1 E_{\beta\times L_2}}\right) = 0\,, \tag{A.2}$$

$$\left(\sum_L e^{-\beta E_{L_1\times L_2}} - \sum_L e^{-L_2 E_{\beta\times L_1}}\right) + \left(\sum_H e^{-\beta E_{L_1\times L_2}} - \sum_H e^{-L_2 E_{\beta\times L_1}}\right) = 0\,. \tag{A.3}$$

Notice that light states L and heavy states H are playing triple duty, since the spatial background changes in the different quantizations. In any given quantization, the states L refer to negative energy states that scale with a positive power of N while H refers to positive energy states that scale with a positive power of N. We eliminate the consideration of states with $\mathcal{O}(1)$ energies by bounding their density of states so that their contribution is $\mathcal{O}(1)$ and therefore subleading.

We now assume that for $\beta < L_1$ and $\beta < L_2$, we have

$$\sum_L e^{-L_1 E_{\beta\times L_2}} \gg \sum_L e^{-\beta E_{L_1\times L_2}}, \qquad \sum_H e^{-L_1 E_{\beta\times L_2}} \ll \sum_H e^{-\beta E_{L_1\times L_2}}, \tag{A.4}$$

$$\sum_L e^{-L_2 E_{\beta\times L_1}} \gg \sum_L e^{-\beta E_{L_1\times L_2}}, \qquad \sum_H e^{-L_2 E_{\beta\times L_1}} \ll \sum_H e^{-\beta E_{L_1\times L_2}}. \tag{A.5}$$

These inequalities can be proven to be true in two spacetime dimensions and for the special torus in a general number of dimensions. In fact, it is what makes a proof like that of [24] work.

Using these inequalities, we can approximate the above equalities as

$$\sum_L e^{-L_1 E_{\beta\times L_2}} \approx \sum_H e^{-\beta E_{L_1\times L_2}}, \qquad \sum_L e^{-L_2 E_{\beta\times L_1}} \approx \sum_H e^{-\beta E_{L_1\times L_2}}. \tag{A.6}$$

Then we can use $Z_H(L_1)_{\beta\times L_2} \ll Z_H(\beta)_{L_1\times L_2} \approx Z_L(L_1)_{\beta\times L_2}$ and $Z_H(L_2)_{\beta\times L_1} \ll Z_H(\beta)_{L_1\times L_2} \approx Z_L(L_2)_{\beta\times L_1}$ to approximate the partition function in the L_1 and L_2 channels as

$$Z(L_1)_{\beta\times L_2} = Z_L(L_1)_{\beta\times L_2} + Z_H(L_1)_{\beta\times L_2} \approx Z_L(L_1)_{\beta\times L_2}\,, \tag{A.7}$$

$$Z(L_2)_{\beta\times L_1} = Z_L(L_2)_{\beta\times L_1} + Z_H(L_2)_{\beta\times L_1} \approx Z_L(L_2)_{\beta\times L_1}\,. \tag{A.8}$$

We see that under the assumptions (A.4) and (A.5), the partition function is vacuum dominated in the L_1 and L_2 channels if and only if

$$\rho(E_{L_1\times L_2} < 0) \lesssim e^{L_1(E-E_{\text{vac}})_{L_1\times L_2}}. \tag{A.9}$$

As explained in section 2.4 this is necessary and sufficient for a universal free energy at all temperatures on an arbitrary spatial torus.

In general dimension, the sufficient conditions for a universal free energy are the $d-1$ inequalities that generalize (A.5) and a sparse light spectrum:

$$\rho(\Delta) \lesssim \exp\left(L_{\min}\Delta\right), \tag{A.10}$$

where $L_{\min}$ is the minimum cycle size of the spatial torus.

A.2 Conventions

In this appendix we outline the conventions, in Euclidean signature, that were used in chapter 3. The path integral is over e^{-S}. The bulk action is

$$S = -\frac{1}{16\pi G}\int_M \sqrt{g}(R-2\Lambda) - \frac{1}{8\pi G}\int_{\partial M}\sqrt{g^0}K + S_{ct} + S_{matter}\,. \tag{A.11}$$

The gravitational counterterm is

$$S_{ct} = \frac{1}{8\pi G}\int_{\partial M}\sqrt{g^0}(d-1+\mathcal{L}_{curv}), \tag{A.12}$$

where in $d = 3, 4$ the curvature counterterm is $\mathcal{L}_{curv} = \frac{1}{2(d-2)}R[g^0]$ [126], and higher dimensional curvature counterterms can be found in [225]. The extrinsic curvature is $K_{\mu\nu} = \nabla_{(\mu}n_{\nu)}$ with n the outward-pointing normal. The Brown-York stress tensor is defined by

$$\delta S = \frac{1}{2}\int_{\partial M}\sqrt{g^0}\,\widetilde{T}^{\mu\nu}\delta g^0_{\mu\nu}\ , \tag{A.13}$$

and the convention for the stress tensor in the boundary theory is similar.

Our sign conventions for the Euclidean generating functional in the EFT are summarized by

$$Z[J, h_{ij}, A_i] = \left\langle e^{\int d^dx\sqrt{\gamma}(J\mathcal{O}+A_iJ^i-\frac{1}{2}h_{ij}T^{ij})}\right\rangle\ . \tag{A.14}$$

This choice, together with our sign choices in the bulk action, produces positive boundary two-point functions in position space, for example $\langle\mathcal{O}(x)\mathcal{O}(y)\rangle = \left(\frac{1}{\sqrt{\gamma}}\frac{\delta}{\delta J}\right)^2\log Z = |x-y|^{-2\Delta}$. This is subtle due to divergences in the Fourier transform from momentum to position space; for $\Delta > d/2$, the calculation is done in momentum space, and the Fourier transform to position space is done by analytic continuation in Δ, or by putting a hard cutoff $|k| < \Lambda$ and adding local counterterms to eliminate divergences.

A.3 Time-reversal and crystal symmetries

This appendix is devoted to some background material in crystal symmetries and time-reversal symmetry. We will first discuss the former and later on see how the inclusion of the latter adds some spice to that. This section mostly reviews group theoretic aspects and we refer to [194, 226] for a more thorough analysis. Our focus will be on an algorithm that determines all representations of lattice symmetries. To determine the band structure and characterise it completely, we have to know these representations, because they dictate how the energy eigenstates states transform under the symmetry. Throughout the discussion and also in the coming two chapters, we will ignore all interactions and focus therefore on the realisation of the symmetries on the one-particle level.

Crystal symmetry

Parts of this subsection were taken from the appendices of [3, 4]

A crystal is a periodic alignment of atoms in one, two or three dimensions, spanned by lattice vectors $\mathbf{t}_i$. Under the action of certain symmetries the crystal is unchanged, for example lattice translation or a four-fold rotation symmetry. Together, these symmetries form the space group $\mathcal{G}$ and consist of a translational part $\Pi = \mathbf{Z}^d$ and a point group G. The translational symmetry captures the periodic structure, whereas the point group consists of rotations, reflections and possibly inversion in three dimensions that leave the crystal unchanged. The two parts of the space group can be intertwined in two ways; they can either be symmorphic or non-symmorphic. Symmorphic crystals are the simplest type of crystals, since

$$\mathcal{G} = G \times \mathbf{Z}^d \tag{A.15}$$

and so there is no mixing between the translational piece and point group piece. In two dimensions 13 out of the 17 crystal structures are like that, but in three dimensions these symmetries form a minority; 73 out of 230. In that case, the majority are space groups that are non-symmorphic and contain elements that are not pure rotations or reflections. The space group is then a semi-direct product of Π and G:

$$\mathcal{G} = G \ltimes \mathbf{Z}^d. \tag{A.16}$$

An example of a symmetry that mixes between G and Π would be a *glide symmetry* t_g. If (x, y) is a lattice point, then a glide reflection could act for instance as

$$t_g \cdot (x, y) = (x, -y) + (1/2, 0) \tag{A.17}$$

which has the distinghuised property that $t_g^2 = (1, 0)$, i.e. a pure translation. Such elements only exist for non-symmorphic space groups.

Space group elements can be represented using the Seitz notation. Given an element g of a space group we write

$$g = \{R|\mathbf{v}\} \tag{A.18}$$

where R is an element of the point group and is thus a rotation or reflection. The vector $\mathbf{v}$ represents a translation. In the symmorphic case, $\mathbf{v}$ needs to be a integer multiple of the lattice vectors $\mathbf{t}_i$, but for the non-symmorphic symmetries fractions are allowed, as we saw in A.17. If $\mathbf{x}$ is a lattice vector in the crystal, then g acts on $\mathbf{x}$ according to

$$g \cdot \mathbf{x} = \{R|\mathbf{v}\}\mathbf{x} = R\mathbf{x} + \mathbf{v}. \tag{A.19}$$

Generically, given two elements $g_1 = \{R_1|\mathbf{v}_1\}$ and $g_2 = \{R_2|\mathbf{v}_2\}$ the multiplication is defined as

$$g_1 \cdot g_2 = \{R_1 R_2 \mid R_1\mathbf{v}_2 + \mathbf{v}_1\}. \tag{A.20}$$

Although the space group consists of symmetries of the crystal, once the lattice points are atoms with orbitals, these symmetries also act on the quantum mechanical states. Due to translational symmetries in the space group, these states will form bands and it is enough to restrict to the Brillouin zone in momentum space. Given a Bloch function at momentum $\mathbf{k}$ and position $\mathbf{x}$, [194]

$$\Psi_{\mathbf{k}}(\mathbf{x}) = \exp(i\mathbf{k}\cdot\mathbf{x})u_{\mathbf{k}}(\mathbf{x}) \tag{A.21}$$

with $u_{\mathbf{k}}(\mathbf{x}+\mathbf{t}_i) = u_{\mathbf{k}}(\mathbf{x})$, the action of a space group element on $\Psi_{\mathbf{k}}$ is given by

$$\{R|\mathbf{v}\}\Psi_{\mathbf{k}}(\mathbf{x}) = \Psi_{\mathbf{k}}(R^{-1}(\mathbf{x}-\mathbf{v})) = \Psi_{R\mathbf{k}}(\mathbf{x}-\mathbf{v}). \tag{A.22}$$

The action of the point group (i.e. elements R) on the momentum vectors $\mathbf{k}$ is thus conjugate to its action on the lattice vectors $\mathbf{x}$. Taking g to be a pure translation, we get the familiar result;

$$\{e|\mathbf{t}_i\}\Psi_{\mathbf{k}}(\mathbf{r}) = \Psi_{\mathbf{k}}(\mathbf{r}-\mathbf{t}_i) = \exp(-i\mathbf{k}\cdot\mathbf{t}_i)\Psi_{\mathbf{k}}(\mathbf{r}). \tag{A.23}$$

In fact, this shows that only a particular momentum vectors are to be considered. Momentum space is defined by a set of reciprocal lattice vectors $\mathbf{g}_i$ such that $\mathbf{g}_i\cdot\mathbf{t}_j = 2\pi\delta_{ij}$. Periodicity of the exponential in A.23 then shows that Bloch functions at $\mathbf{k}$ are the same as those on $\mathbf{k}+\mathbf{g}_i$. Consequently, we only need to consider the unit cell spanned by the vectors $\mathbf{g}_i$, which is the (first) Brillouin zone.

Quantum mechanically, translational symmetry means that the Hamiltonian H commutes with $T_{\mathbf{t}_i}$, the operator generating translations along $\mathbf{t}_i$. These operators are thus simultaneously diagonalizable. In fact, the eigenvalues of $T_{\mathbf{t}_i}$ are immaterial phases given in A.23. However, the important thing is to realise that due to translational symmetry $\mathbf{k}$ becomes a good quantum number. Thus we have a continuum of states labelled by $\mathbf{k}$, which form the electronic bands. The point group symmetries relates various pieces of different bands and organize them accordingly as we will embark on below. In general, these symmetries act as

$$\Gamma_{\mathbf{k}}(R)H(R\cdot k)\Gamma_{\mathbf{k}}^{-1}(R) = H(k) \tag{A.24}$$

where $\Gamma_{\mathbf{k}}$ is a representation of the stabilizer $G_{\mathbf{k}} \subset G$ of momentum $\mathbf{k}$. This representation is formed by the bands at $\mathbf{k}$. There are two things to note here. First of all, because of this action, it is enough to know the bandstructure only on part of the Brillouin zone to fully determine it, since various momenta are related by symmetry. The momenta that are not related to each other by any symmetry form the fundamental domain Ω and will mostly focus on this region in the BZ. The second thing to note is that the representations have a continuous label $\mathbf{k}$ and when varying $\mathbf{k}$ over the BZ, representations could change abruptly. Let us now argue that this will actually be smooth. Let $\alpha : [0,1] \to BZ \simeq \mathbf{T}^d$ be a path from

$\alpha(0) = \mathbf{k}_0$ to $\alpha(1) = \mathbf{k}_1$ such that the stabilizer groups $G_{\mathbf{k}_i}$ at $\mathbf{k}_i$ for $i = 0, 1$ are different from the one at $\alpha(t)$ for $t \in (0, 1)$, which we denote by $\widetilde{G}$ and take to be independent of t for simplicity. It is clear that $\widetilde{G}$ is a subgroup of $G_{\mathbf{k}_i}$. With smoothness we then mean that the representation $\Gamma_{\alpha(t)}$ for $t \in (0, 1)$ induces a representation $\Gamma_{\mathbf{k}_0}$ at $\mathbf{k}_0$ in the $t \to 0$ limit and similarly for $t \to 1$. Since $\widetilde{G}$ is a subgroup of $G_{\mathbf{k}_i}$, this can always be done and so the representations are smooth throughout the Brillouin zone.

For symmorphic space groups, determining the representations at each $\mathbf{k}$ is rather straightforward. They are just representations of finite groups that have been studied since the beginning of group theory. For non-symmorphic symmetries, this situation is a bit different. To see this, suppose $G_{\mathbf{k}}$ contains some non-symmorphic elements $g_i = \{R_i|\mathbf{w}_i\}$ with $\mathbf{w}_i$ fractional lattice translations such that $R_i\mathbf{k} = \mathbf{k}$ for all R_i present in the elements g_i of $G_{\mathbf{k}}$. From the multiplication rule (A.20), it is then clear that a representation $\Gamma_{\mathbf{k}}$ of $G_{\mathbf{k}}$ has to satisfy,

$$\Gamma_{\mathbf{k}}(R_i)\Gamma_{\mathbf{k}}(R_j) = \exp\left(-i\mathbf{g}_i \cdot \mathbf{w}_j\right)\Gamma_{\mathbf{k}}(R_iR_j) \tag{A.25}$$

with $\mathbf{g}_i$ defined throught $R_i^{-1}\mathbf{k} = \mathbf{k} + \mathbf{g}_i$. Representations that satisfy these constraints are called projective representations and so the bands will sit in these representations rather than the ordinary ones. The projectiveness of these representations is measured by the function $c(R_i, R_j) = \mathbf{g}_i \cdot \mathbf{w}_j$ and is commonly referred to as a group 2-cocycle.

The recipe for determining the representation the electronic bands transform under is now clear. We first determine all fixed points under the action of G on the Brillouin zone and then determine the various representations that each stabilizer group has including possible group 2-cocycles. Since these stabilizer groups are always discrete, this is straightforward, but still a rather cumbersome computation for non-symmorphic space groups. Let us therefore consider a simple example to see all this machinery in action.

Nonsymmorphic space group: p2gg

As a concrete example, consider the wallpaper group $p2gg$. This is a two-dimensional space group of a crystal with two orthogonal lattice directions and hence the Brillouin zone has the topology of a $\mathbf{T}^2$. We parametrise this torus by the square $-\pi \leq k_{x,y} \leq \pi$ and identify opposite edges. The associated point group is generated by two elements; one reflection t_x in the k_x-direction and an inversion σ. Modulo lattice translations, this wallpaper group has the following elements,

$$\mathcal{G}/\mathbf{Z}^2 \simeq G = \left\{\{e|00\}, \{\sigma|00\}, \{t_x|\tfrac{1}{2}\tfrac{1}{2}\}, \{t_y|\tfrac{1}{2}\tfrac{1}{2}\}\right\}, \tag{A.26}$$

$\mathcal{C}_i^n$	Stabilizer group
$\Gamma = (0,0)$	$\mathbf{Z}_2 \times \mathbf{Z}_2 = \{1, \sigma, t_x, t_y\}$
$X = (\pi,0)$	$\mathbf{Z}_2 \times \mathbf{Z}_2 = \{1, \sigma, t_x, t_y\}$
$M = (\pi,\pi)$	$\mathbf{Z}_2 \times \mathbf{Z}_2 = \{1, \sigma, t_x, t_y\}$
$Y = (0,\pi)$	$\mathbf{Z}_2 \times \mathbf{Z}_2 = \{1, \sigma, t_x, t_y\}$
$l_1 = (\alpha,0)$	$\mathbf{Z}_2 = \{1, t_y\}$
$l_2 = (\alpha,\pi)$	$\mathbf{Z}_2 = \{1, t_y\}$
$l_3 = (0,\alpha)$	$\mathbf{Z}_2 = \{1, t_x\}$
$l_4 = (\pi,\alpha)$	$\mathbf{Z}_2 = \{1, t_x\}$

Table A.1: The high symmetry locations for $p2gg$. The same structure is also valid $p2mm$ and $p2gm$. The corresponding fundamental domain Ω is given by the first quadrant of the first Brillouin zone, i.e. $0 \leq k_{x,y} \leq \pi$.

where we denoted the identity element by e. Using the elements σ, t_x, and $t_y = t_x\sigma$, we find that there are four fixed points, Γ, X, M, and Y, which all have stabilizer group G. There are also four lines that are held fixed by reflections in the two axes. These lines connect the four high symmetry points and form the boundary of the fundamental domain Ω. These results are summarised in table A.1.

The non-symmorphic elements do not enhance the representations at Γ, because $\mathbf{g}_i = 0$ for all elements R_i. There could however, be projective representations at X, Y, and M. First, consider the high symmetry point X, and consider the phase factor,

$$\phi(R_i, R_j) = \exp\left(-i\mathbf{g}_i \cdot \mathbf{w}_j\right), \tag{A.27}$$

In this case, all ϕ's are unity except for $\phi(t_x,t_x) = \phi(t_x,t_y) = \phi(\sigma,t_x) = \phi(\sigma,t_y) = -1$. This can easily be seen by noting that $g_e = 0$, $g_\sigma = -g_1$, $g_{t_x} = -g_1$, and $g_{t_y} = 0$, with $g_1 = (2\pi, 0)$. This information is enough to determine the representations at X, using the standard theory of projective representations. This is most easily done by lifting the group elements in G_0 to elements in a bigger group $\widetilde{G}$, which is a semi-direct product of G_0 and a cyclic group $\mathbf{Z}_h$ with h the order of the phase ν. In the case at hand $h = 2$, so that we represent the elements G_0 in $\widetilde{G}$ as (g, α) with $\alpha = 0, 1$. Note that only the group elements with $\alpha = 0$ correspond the the physical symmetries. The group 2-cocycle of corresponding to $\widetilde{G}$ is now $hc/(2\pi)$, i.e. the multiplication rule is

$$(g_1, \alpha)(g_2, \beta) = (g_1 g_2, \alpha + \beta + \frac{h}{2\pi} c(g_1, g_2)) \tag{A.28}$$

with the second entry evaluated modulo h. One advantage of this procedure is that we can constraint certain lifted elements. In particular, representations of (e, α)

commute with everything and hence should be proportional to the identity matrix by Schur's lemma. The constant of proportionality is a phase $\exp(2\pi i\alpha/h)$. In our case we know that $h = 2$, so a representation $\Gamma_{\mathbf{k}}(e,1)$ equals minus the identity. From the cocycle structure, one can also deduce various relations between the lifted group elements. For example, we have

$$(t_x,0)^4 = (e,0), \quad (\sigma,0)^2 = (e,0), \quad (t_x,0)(\sigma,0) = (\sigma,0)(t_x,0)^3, \tag{A.29}$$

which are the defining relations of D_4. Together with the constraint $\Gamma_{\mathbf{k}}(e,1) = -\mathbf{1}$, we deduce that bands at X transform in the two dimensional representation of D_4 and are thus doubly degenerate there. Repeating the analysis for Y and M, one easily verifies that the two dimensional representation of D_4 is found also at Y, whereas at M there are four possible irreducible representations of the group $\mathbf{Z}_2 \times \mathbf{Z}_4$. Thus we see that the non-symmorphicity can introduce new degeneracies that where not there in the symmorphic counterpart. These degeneracies where in fact used in [179] as a mechanism to get non-trivial two-dimensional Dirac semi-metals.

Non-symmorphicity is not the only was of introducing additional degeneracies in the band structure. A much more mundane symmetry that does the same job is simply invariance under the reflection of the arrow of time. This may seem like an uncommon symmetry, but actually, many materials have such a symmetry since it acts by flipping the spins of the electrons. For example, paramagnetic materials are time-reversal invariant. To understand this and the relation with other crystal symmetries, let us study time-reversal symmetry in more detail.

Time-reversal symmetry

Let us ignore interaction effects and focus on one-particle states. As the symmetry says, time-reversal symmetry (TRS) T reverses time:

$$T : t \to -t \tag{A.30}$$

In the Lorentz group in d dimensions, this takes the form of a matrix having 1's on the diagonal except for the tt component where it is -1. On the levels of the Poincaré algebra, this has the effect that conjugation of iH with T is

$$T(iH)T^{-1} = -iH. \tag{A.31}$$

This can mean two things. First of all $THT^{-1} = -H$ and $TiT^{-1} = i$, which would make the spectrum unbounded and so is ruled out. The other possibility $TiT^{-1} = -i$ and $THT^{-1} = H$ leads to a bounded spectrum and hence is physically relevant action of T, but makes it an anti-unitary operator that acts anti-linearly. This might be different from the usual symmetries that we consider, but according

to Wigner [227], this is a perfectly fine symmetry of the quantum mechanical theory. The anti-unitary nature of T also has its implications in momentum space. On the translational part of the lattice symmetry, this action is simple. The representations are simple phases of the form $e^{i\mathbf{k}\cdot\mathbf{x}}$ and conjugation with T reverses the sign of the momentum, since it does not act on $\mathbf{x}$ and hence makes T act as an inversion symmetry in momentum space. For the representations of the remaining symmetries, more work is required.

One prime example of this non-trivial action is revealed by studying the action of T on the other generators of the Lorentz group. In particular, by considering the rotation generators, one can show that [228] the square of T is constrained:

$$T^2 = (-1)^{2s} \tag{A.32}$$

with s the spin of the particle. For fermionic systems this means the the time-reversal operator squares to minus one! A priori this appears to be not so important, but it causes the spectrum to be double degenerate at those momenta that are invariant under time-reversal. This degeneracy is called Kramers' degeneracy [229] and to show its existence, we simply consider an normalised energy eigenstate $|\psi\rangle$ and its time-reversal partner $T|\psi\rangle$. The claim of Kramer is that these two states are in fact orthogonal. Indeed, let us assume they are not orthogonal, then $T|\psi\rangle = \alpha|\psi\rangle$ for some $\alpha \in \mathbf{C}$ and

$$-|\psi\rangle = T\alpha|\psi\rangle = T\alpha T^{-1}T|\psi\rangle = \alpha^* T|\psi\rangle = |\alpha|^2|\psi\rangle\,, \tag{A.33}$$

which is impossible and hence the two states $|\psi\rangle$ and $T|\psi\rangle$ must be orthogonal.

Time-reversal symmetry can also be incorporated in the space group $\mathcal{G}$, [194]. The full symmetry group is then called a magnetic space group and there are three different types to distinguish depending on whether T itself is a symmetry or some composite symmetry operator. Let us denote by A the anti-unitary operator by which we want to enlarge our space group. When $A = T$, the time-reversal operator, $M = \mathcal{G} \sqcup A\mathcal{G}$[1] is called a type-II Shubnikov space group. Notice that for this magnetic space group, TRS commutes with all elements of $\mathcal{G}$ and the crystal is non-magnetic. If a system is magnetic, it could still be invariant under an anti-unitary operator, but not under T alone. TRS should then be accompanied by either a rotation or a reflection, allowing the system to be invariant under a type-III or type-IV Shubnikov space group. In the subsequent, we will not consider these space groups but instead focus on the type-II Shubnikov space groups. For more details on the other types we refer to [194, 230].

[1] Here, the symbol $\sqcup$ means that we take the elements of $\mathcal{G}$ together with all elements obtained by multiplying every element of $\mathcal{G}$ by A from the left.

Representation theory

To see what time-reversal symmetry does to the representation theory of the (Shubnikov type-II) space group, we first focus on the action of the time-reversal operator T on the bands, and let it act on $\rho(g)\,|\psi_n\rangle$ (where n is the band index), ignoring any momentum dependence for now. The operator $\rho(g)$ is any unitary operator corresponding to an element g of $\mathcal{G}$ that acts on the states according to some representation ρ of the space group $\mathcal{G}$. Now,

$$\mathcal{T}\rho(g)\,|\psi_n\rangle = \rho^*(g)\mathcal{T}\,|\psi_l\rangle \tag{A.34}$$

with $\mathcal{T}$ a representation of T. Representations of the magnetic space group need to satisfy this relation. It is straightforward to show that these representations have the following properties: 1) the time-reversed representation $\hat{D}(g)$ of a representation $D(g)$ for some element g is equivalent to the complex conjugated representation of g, i.e.

$$\hat{D}(g) = D(g)^* \tag{A.35}$$

Second, and this is what we already saw before, is that time-reversal symmetry can also enhance the state space and double the degeneracy at momenta invariant under time-reversal symmetry.

Consider a general magnetic group $M = \mathcal{G} \sqcup A\mathcal{G}$, and suppose that g is an element of $\mathcal{G}$, the space group. Then in the basis $\{|\psi\rangle\,, A\,|\psi\rangle\}$, the representation of g takes the form

$$D(g) = \begin{pmatrix} \rho(g) & 0 \\ 0 & \rho^*(A^{-1}gA) \end{pmatrix} \tag{A.36}$$

However, for the other half of the elements of M, elements of the form $b = Ag \in A\mathcal{G}$, the representation looks like

$$D(b) = \begin{pmatrix} 0 & \rho(bA) \\ \rho^*(A^{-1}b) & 0 \end{pmatrix} \tag{A.37}$$

These representations are irreducible in the sense as given in [194]. It is important to note that the translational part of the space group again, factors out and is proportional to a block diagonal matrix with each block proportional to the identity matrix. Therefore, we can simply focus on the point group G of $\mathcal{G}$.

Intuitively, TRS is understood as a symmetry that can cause bands to stick together to form Kramers pairs. This can happen in three ways: *a*) Either time-reversal symmetry does nothing to the representation and there are no Kramers pairs, *b*) two unitarily equivalent representations of dimension k form a new (irreducible) representation of dimension $2k$, or *c*) complex conjugate irreducible representations of dimension l form a representation of dimension $2l$. In cases *b*)

and c) there are thus Kramers pairs present. The three cases can be described as follows:

a) In this case $\rho(g)$ is unitarily equivalent to $\rho^*(A^{-1}gA)$, which means that $N\rho^*(A^{-1}gA)N^{-1} = \rho(g)$ for some fixed unitary matrix N and $g \in G$. Moreover, N satisfies $NN^* = +\rho(A^2)$, and then $D(g) = \rho(g)$ and $D(Ag) = \pm\rho(AgA^{-1})N$ [2].

b) In this case $\rho(g)$ is unitarily equivalent to $\rho^*(A^{-1}gA)$, so again we have $\rho(g) = N\rho^*(A^{-1}gA)N^{-1}$ for some fixed unitary matrix N and $g \in G$. However, N satisfies $NN^* = -\rho(A^2)$, and then

$$D(g) = \begin{pmatrix} \rho(g) & 0 \\ 0 & \rho(g) \end{pmatrix}, \quad D(Ag) = \begin{pmatrix} 0 & -\rho(AgA^{-1})N \\ \rho(AgA^{-1})N & 0 \end{pmatrix}. \tag{A.38}$$

c) In this case $\rho(g)$ is not unitarily equivalent to $\bar{\rho}(A^{-1}gA)$. The representations are then given by

$$D(g) = \begin{pmatrix} \rho(g) & 0 \\ 0 & \rho^*(A^{-1}gA) \end{pmatrix}, \quad D(Ag) = \begin{pmatrix} 0 & \rho(AgA) \\ \rho^*(g) & 0 \end{pmatrix}. \tag{A.39}$$

To determine whether we are dealing with type (a), (b) or (c) upon inclusion of TRS we use a test deviced by Herring in 1937 [231] based on the Frobenius-Schur indicator. Given a (projective) irreducible representation $\Gamma_{\mathbf{k}}$ of the stabilizer group at $\mathbf{k}$, we can write this test as

$$\begin{aligned} I(\Gamma_{\mathbf{k}}) &= \frac{1}{\#S_i}\sum_{S_i} e^{-i(\mathbf{k}+S_i^{-1}\mathbf{k})\cdot\mathbf{w}_i}\Gamma_{\mathbf{k}}(g_i^2) \\ &= \frac{1}{\#S_i}\sum_{S_i} e^{-i\mathbf{g}\cdot\tau_i}\Gamma_{\mathbf{k}}(g_i^2). \end{aligned} \tag{A.40}$$

where the sum is over those $S_i = \{g_i|\tau_i\}$ such that $g_i\cdot\mathbf{k} = -\mathbf{k}$ modulo a reciprocal lattice vector $\mathbf{g}$. The fractional translation associated to S_i is denoted by τ_i. Thus when $\mathbf{k} \equiv -\mathbf{k}+\mathbf{g}$ (i.e. at fixed points which are also TRS invariant points), we sum over all elements of $G_{\mathbf{k}}$. The value of $I(\Gamma_{\mathbf{k}})$ determines whether the irreducible representation $D_{\mathbf{k}}$ arrising from $\Gamma_{\mathbf{k}}$ by adding time-reversal symmetry, is of type (a), (b) or (c). The assignment follows from:

$$I(\Gamma_{\mathbf{k}}) = \begin{cases} T^2 & \text{case (a)} \\ -T^2 & \text{case (b)} \\ 0 & \text{case (c)} \end{cases}. \tag{A.41}$$

[2] In this case, the matrix representations of g and Ag for $g \in G$ given in (A.36) and (A.37) can both be made block diagonal and in fact the representation D is reducible. Consequently, ρ and D have the same dimensionality. The $\pm$ appearing for $D(Ag)$ represents to unitary equivalent representations. See [194] for more details.

TRS degeneracies

Now that we know where degeneracies occur, we need to determine which irreducible representations stick together. For cases where (A.41) yields $I = \pm 1$, this is trivial, but for $I = 0$ it is not. Let us assume that we are at a fixed point which has $G_{\mathbf{k}}$ as its stabilizer group and that $I = 0$ for some, possibly projective, irreducible representations of $G_{\mathbf{k}}$. Also we assume the magnetic stabilizer group is given by $M_{\mathbf{k}} = G_{\mathbf{k}} \sqcup AG_{\mathbf{k}}$, with $A = TA_0$. It is important to note that A_0 is not part of $G_{\mathbf{k}}$ and so multiplication is done within the full point group. The TRS reversed representation is given by

$$\hat{\Gamma}(S) = \Gamma(A_0^{-1} S A_0)^*, \tag{A.42}$$

where $S = \{g|\tau\}$ with τ a fractional translation and $A_0 = \{g_0|0\}$. This can be rewritten using

$$\begin{aligned} A_0^{-1} S A_0 &= \{g_0^{-1}|0\}\{g|\tau\}\{g_0|0\} \\ &= \{e|g_0^{-1}\tau - \tau\}\{g_0^{-1} g g_0|\tau\}, \end{aligned} \tag{A.43}$$

where e is the identity element. Thus (A.42) becomes

$$\hat{\Gamma}(S) = \exp(i\mathbf{k} \cdot (g_0^{-1}\tau - \tau))\rho(\{g_0^{-1} g g_0|\tau\})^*. \tag{A.44}$$

Now there are two possible situations. We could have $A_0 = \{e|0\}$ ($M^{\mathbf{k}}$ is a type-II Shubnikov space group), in which case

$$\hat{\Gamma}(S) = \Gamma(\{g|\tau\})^*. \tag{A.45}$$

This situation occurs when $\mathbf{k}$ is also a TRS invariant point. The other option is $g_0 \neq e$ with $g_0 \cdot \mathbf{k} = -\mathbf{k}$ and so

$$\hat{\Gamma}(S) = \exp(-i\mathbf{k} \cdot \tau)\rho(g_0^{-1} g g_0)^* \tag{A.46}$$

where the product $g_0^{-1} g g_0$ should be calculated in the full point group, which might be realised projectively. For example, for $T^2 = -1$ and when $G_{\mathbf{k}}$ consists of a single glide plane (e.g. $p2mg$ or $p2gg$) and A_0 is a reflection in the k_x axis, then the multiplication should be done in the central extension, i.e. in the quaternion group. In this group the reflections anti-commute. On top of that, when $T^2 = -1$, we need to consider the double cover (which we discuss more in the next two chapters) of the quaternion group, which then results in a pairing of two representations where only the eigenvalues of the two-fold rotation are complex conjugate to each other.

Summary

The preceding discussion contained a lot of mathematics and new terminology. All the machinery that we introduced is important in determining the representation content of a given (magnetic) space group. From a more physical point

of view, we have learned two important lessens. First of all, at a given momentum $\mathbf{k}$ the spectrum is arranges itself into unitary irreducible representations of the stabilizer group of $\mathbf{k}$. This highly restricts the possible band structures. Second, time-reversal symmetry and non-symmorpyic symmetry operators introduce additional degeneracies, i.e. cause the states to transform in higher-dimensional unitary irreps. In chapter 5, these two observations are crucial in determining all topological phases living on a particular crystal with or without time-reversal symmetry.

A.4 A brief introduction to K-theory

In this appendix we will discuss the mathematics behind the classification of topological insulators. This requires making certain physical concepts more abstract. We start by discussing the general set-up and review the role of the translational symmetry in this regard. In particular we observe the emergence of a vector bundle structure. This provides the basis for the next section in which we discuss the classification of these bundles using K-theory. Inclusion of the full space group symmetry is then discussed in section A.4.2. There, we will argue for a simple combinatorial way of computing the corresponding equivariant K-theory. At the end of this appendix, we will consider the space group $Pm\bar{3}m$ as an explicit example. Throughout this section, we will focus on symmorphic symmetries.

Historically, the mathematical classifications of gapped free fermion theories[3] protected by symmetry groups, all stem from the work by Hořava in 2005 [232], who noticed a connection between Fermi surfaces and K-theory, which was further elaborated on by Kitaev in 2009 [150]. In particular, Kitaev discussed gapped free fermions in various Altland-Zirnbauer (AZ) classes with discrete translational symmetry. Nonetheless, this study failed to rigorously include the full crystal symmetry in its analysis. From the K-theory side, Freed and Moore attempted to fill this hiatus in 2013 [181]. They pointed out what type of mathematical objects could classify topological phases in any AZ class, in the presence of arbitrary space group symmetry.

A.4.1 Set-up

We are interested in the topological properties of class A massive fermions on a d-dimensional lattice. These systems have a particular space group symmetry $\mathcal{G}$.

[3] This is the high-energy terminology for an insulator for which interactions are ignored. Putting such gapped free fermions on a lattice results in a non-interacting band insulator.

The dynamics of massive free fermions or insulator are governed by a gapped Hamiltonian H. Let E be the eigenvalues of H and $|\psi\rangle$ its eigenstates. We say that a Hamiltonian is gapped if there exists a range $|E| < \Delta$ for some $\Delta > 0$ such that H does not have an eigenstate χ with eigenvalue α within this range in the infinite volume limit. As these gapped free fermions live on a lattice in d dimensions, H respects the lattice symmetry, i.e. $\Gamma(g)H = H\Gamma(g)$ with $\Gamma(g)$ a representation of the space group. Let us first consider the discrete translations in $\mathcal{G}$. A lattice Λ is a subset of Euclidean space. It is isomorphic to $\mathbf{Z}^d$ and is spanned by orthogonal basis vectors $\mathbf{t}_i$, $i = 1, \ldots, d$. The discrete translation symmetry

$$T_{\mathbf{n}} : \mathbf{x} \mapsto \mathbf{x} + n_i \mathbf{t}_i \tag{A.47}$$

with $\mathbf{n} = (n_1, \ldots, n_d)$ in $\mathbf{Z}^d$ and $\mathbf{x}$ a lattice vector, constrain the fermions to form a representation of this symmetry. The representations are simple phases labelled by a d-dimensional momentum vector $\mathbf{k}$. More precisely, the representations are defined by

$$\Gamma_{\mathbf{k}}(\{e|\mathbf{v}\}) = \exp(-i\mathbf{x} \cdot \mathbf{k}), \tag{A.48}$$

where we used Seitz notation to represent the discrete translation. This is basically a discrete Fourier transformation. The nature of these representations allows for a simple description of fermions in momentum space, because $k_i \sim k_i + g_i$ with $\{g_i\}$ a basis of momentum space such that $g_i \cdot g_j = 2\pi\delta_{ij}$. In momentum space, the fermions thus live on a d-dimensional torus; the Brillouin zone $\mathcal{M}$. The Brillouin zone is in fact the space of characters of the form given in (A.48) and we will use k as a parameterization. For each $\mathbf{k}$ vector we have a Hamiltonian $H(\mathbf{k})$ and Hilbert space $\mathcal{H}(\mathbf{k})$. The Hamiltonian $H(\mathbf{k})$ is related to the second quantized gapped Hamiltonian H as

$$H = \sum_{\mathbf{k},i,j} H_{ij}(\mathbf{k}) c^\dagger_{i,\mathbf{k}} c_{j,\mathbf{k}}. \tag{A.49}$$

As we saw already in section A.3, besides discrete translational symmetry, lattices may also have reflection, rotation and (in $3d$) inversion symmetries. The form of the space group as given in (A.15) and (A.16) means that $\mathcal{G}$ sits in the short exact sequence

$$1 \to \mathbf{Z}^d \to \mathcal{G} \to G \to 1, \tag{A.50}$$

where G contains all symmetries beside translations, i.e it is the point group, $G \simeq \mathcal{G}/\mathbf{Z}^d$. Interestingly, from a mathematics point of view, symmorphicity is now the statement that this exact sequence is split or not. Furthermore, we showed A.3 how these symmetries act on $\mathcal{M}$ and that the Hilbert spaces for each momenta decompose in unitary irreducible representations of the stabilizer group.

The data $H(\mathbf{k})$, $\mathcal{H}(\mathbf{k})$ and $\mathcal{M}$ can be conveniently packaged in terms of a Hilbert bundle:

$$\begin{array}{ccc} \mathcal{H} & \longrightarrow & \mathcal{E} \circlearrowleft H \\ & & \downarrow \\ & & \mathcal{M} \end{array}$$

The fibres of this bundle are the Hilbert spaces $\mathcal{H}$, which due to the gapped nature of the system, splits into a direct sum $\mathcal{E} = \mathcal{E}_c \oplus \mathcal{E}_v$, with $\mathcal{E}_c$ the conduction band and $\mathcal{E}_v$ the valance band. For an insulator the valance band is completely filled and the fermions, i.e electrons, in those states can have non-trivial behavior. Notice that $\mathcal{E}_v$ is a finite rank vector bundle. For topological phases, the non-trivial behavior originates from the topology of $\mathcal{E}_v$. For example as we saw in section 4.1, the quantization of the Hall conductivity σ_{xy} may seen to be due to the topology of $\mathcal{E}_v$ using the TKNN invariant [141, 183]. A topologically trivial insulator is then one for which $\mathcal{E}_v$ is topologically trivial. In contrast, for non-trivial topological insulators, the vector bundle $\mathcal{E}_v$ is non-trivial. The different topological types of vector bundles can be enumerated under a suitable notion of equivalence. This enumeration is a classification of vector bundles and thus of topological phases.

The classification of finite rank vector bundles as a mathematical pursuit was initiated in the late 50s and early 60s by Grothendieck and Atiyah with the development of K-theory. Since then, this theory has been generalized in several directions. The basic idea of this work can be readily understood by considering a space X which consists of a single point, i.e. $X = \{x\}$. Vector bundles over x are vector spaces of a particular rank n. Suppose V_n and $V_{n'}$ are two vector spaces of rank n and n', respectively. In order to classify these vector spaces, we need a notion that compares them. In K-theory, the notion of bundle isomorphisms is used. Specifically, in the present example V_n is isomorphic to $V_{n'}$ if and only if $n = n'$. Different vector bundles over X are thus classified by their rank, which is a non-negative integer. Vector bundles can be added using the so-called internal Whitney sum, giving the set of isomorphism classes, Vect(X) the structure of an Abelian monoid. Using the bundle isomorphism, the monoid is isomorphic to $\mathbf{N}$. The resulting set does not form a group (it does not contain inverses), complicating further analysis. Fortunately, however, Vect(X) may be converted to a group using the Grothendieck completion. This construction takes two copies of Vect(X) and subjects it to the following equivalence relation

$$\begin{aligned} (m, n) \quad &\sim \quad (m', n') \\ \Leftrightarrow \text{there exists } p \text{ such} \quad &\text{that} \quad m + n' + p = n + m' + p. \end{aligned} \tag{A.51}$$

Let us denote the equivalence classes by $[(m, n)]$. The essential new feature is now that we can take inverses; $[(n, m)]$ is the inverse of $[(m, n)]$. Consequently, elements in the Grothendieck completion are denoted by formal differences, $m - n$.

For the case at hand, $\mathbf{N}$ is converted to $\mathbf{Z}$ by the Grothendieck completion. The K-theory of X is then said to be $\mathbf{Z}$ and is denoted as $K^0(X) = \mathbf{Z}$. Although we discussed only the zero-dimensional case, for general compact base manifolds X, a similar statement has been verified [233] and is encapsulated in the following proposition.

Proposition A.4.1. *Every element in $K^0(X)$ can be written as $[E]-[\Theta_n]$, where E is a vector bundle over X and Θ_n is a trivial vector bundle of rank n over X. Moreover, $[E]-[\Theta_n] = [F]-[\Theta_m]$ if and only if there exists an integer q such that $E \oplus \Theta_{m+q} \simeq F \oplus \Theta_{n+q}$. In particular, for $n = m$, $[E] = [F]$ in $K^0(X)$ if an only if $E \oplus \Theta_q \simeq F \oplus \Theta_q$ for some q.*

From a physics point of view, the proposition is easily interpreted. In section A.4.1 we discussed how free fermion systems naturally acquire the structure of a Hilbert bundle. The Hilbert bundle $\mathcal{H}$ can have a topology measured for example by the TKNN invariant. Adding a trivial vector bundle Θ_m to $\mathcal{H}$ should not change, for example, the conduction properties of the electrons. We thus want to regard $\mathcal{H}$ and $\mathcal{H}' = \mathcal{H} \oplus \Theta_m$ as being topologically equivalent. Indeed, in K-theory we see that the trivial piece can be subtracted, i.e. $[\mathcal{H}] = [\mathcal{H}']-[\Theta_m]$. From a physical point of view, it is not immediately clear what a trivial vector bundle will be. As we will see in chapter 5, a trivial vector bundle is not one that has only trivial representations and trivial Chern numbers. In fact, it is a vector bundle $\mathcal{E}$ that consists of particle-hole symmetric bands. The hole bands then describe the negative integers in the K-theory classification and by particle-hole symmetry we then mean there are as many holes as electrons, so that $\mathcal{E} \simeq [0]$ in $K^0(X)$. Although in the absence of additional space group symmetries this definition of a trivial vector bundles might seem a bit too much, in the presence of such symmetries we are required to use this definition.

A.4.2 Equivariant K-theory

The final ingredient in our discussion is the point group symmetry of the lattice. In momentum space, the action of G on $\mathcal{M}$ is defined as

$$g \cdot \mathbf{k} = D(g)\mathbf{k} \tag{A.52}$$

for $\mathbf{k}$ in $\mathcal{M}$ and g in G, the point group. $D(g)$ is a fixed d-dimensional representation acting by matrix multiplication on $\mathbf{k}$. This is simple the vector representation of G. The action of g on $\mathcal{M}$ lifts to an action on the Hilbert spaces $\mathcal{H}(\mathbf{k})$, which we denote by

$$g * |\psi_{\mathbf{k}}\rangle = \Gamma_k(g)\,|\psi_{\mathbf{k}}\rangle\,. \tag{A.53}$$

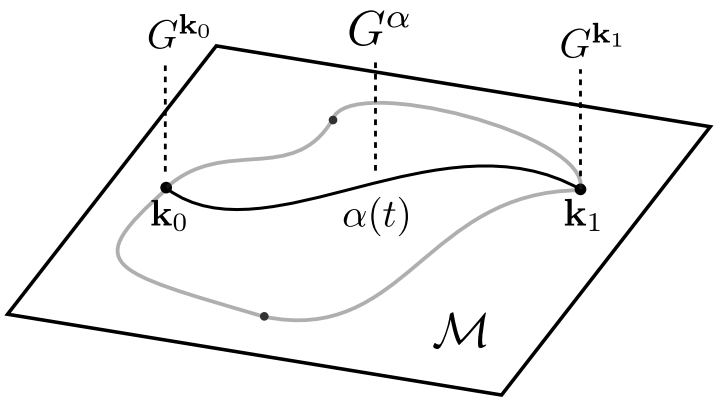

Figure A.1: Representations of G^α along α induce representations of $G^{\mathbf{k}_i}$ at $\mathbf{k}_i$. The shaded paths indicate possible other fixed point sets in $\mathcal{M}$.

Furthermore, $H(\mathbf{k})$ and $\Gamma_{\mathbf{k}}$ commute in a particular way with each other as we saw in equation (A.24), which, for clarity, we repeat here,

$$\Gamma_{\mathbf{k}}(R)H(R\cdot\mathbf{k})\Gamma_{\mathbf{k}}^{-1}(R) = H(\mathbf{k}). \tag{A.54}$$

For generic momenta, the states will form a trivial representation, because equation (A.54) is not a commutation relation. Nevertheless, for a subset S of $\mathcal{M}$ which is held pointwise fixed by a subgroup G_S, we have $[H(g\cdot\mathbf{k}), \rho_{\mathbf{k}}(g)] = 0$. The states with $\mathbf{k}$ in S can then form non-trivial representations. This extra data provides the Hilbert bundle with an equivariant structure in the sense discussed by Segal in [234]. This means that with the projection $p : \mathcal{E} \to \mathcal{M}$ defined as $p(|\psi_{\mathbf{k}}\rangle) = \mathbf{k}$, we have

$$p(g * |\psi_{\mathbf{k}}\rangle) = p(\rho_k(g)\,|\psi_{g\cdot\mathbf{k}}\rangle) = g\cdot\mathbf{k} = g\cdot p(|\psi_{\mathbf{k}}\rangle), \tag{A.55}$$

which shows that p respects the action of G. Furthermore, the action of g provides a homomorphism between the fibres, i.e. vector spaces, at k and $g\cdot k$. With these properties and the action of G on $\mathcal{M}$ and $\mathcal{E}$, as well as relation (A.54), we can choose the representation of the filled states, i.e. $\mathcal{E}_v$, which is relevant for classifying topological phases in class A. Let us make this concrete. Consider a point $\mathbf{k}_0$ in $\mathcal{M}$ and its stabilizer group $G_{\mathbf{k}_0}$, which leaves $\mathbf{k}_0$ pointwise fixed. The fibre $\mathcal{E}_{\mathbf{k}_0}$ at $\mathbf{k}_0$ is a vector space of eigenstates of $H(\mathbf{k}_0)$. These states form a representation of $G_{\mathbf{k}_0}$ and hence so is $\mathcal{E}_{\mathbf{k}_0}$. Let $\Gamma_{\mathbf{k}_0}$ be a representation of $G_{\mathbf{k}_0}$. Now consider variations of $\mathbf{k}_0$. We do this by choosing a path $\alpha(t)$ in $\mathcal{M}$ such that $\alpha(0) = \mathbf{k}_0$ and $\alpha(1) = \mathbf{k}_1$ for some $\mathbf{k}_1$ in $\mathcal{M}$, as shown in Figure A.1. Along α a subgroup G^α of $G^{\mathbf{k}}$ is preserved. Without loss of generality we can choose this situation instead of the reverse case with $G^{\mathbf{k}}$ being a subgroup of G^α and we can assume G^α to be independent of t. At α, the states form a representation of G^α, which we denote

by $\widetilde{\rho}_\alpha$. Taking the limit $t \to 0$, $\widetilde{\rho}_\alpha$ induces the representation $\rho_{\mathbf{k}_0}$, meaning that $\rho_{\mathbf{k}_0}|_{G^\alpha} = \rho_\alpha$. This constraints the representations that can be induced at $\mathbf{k}_0$ given a representation along α. Similar arguments hold when taking the limit $t \to 1$. Finding the constraints between all fixed points in this way, results in a finite set of gluing conditions between fibres at different $\mathbf{k}$. These conditions signify the fact that we cannot just pick any number of representation at the fixed points and be guaranteed that we obtain a representation of $\mathcal{E}_v$.

The constraints can be understood more clearly when considering the representation rings of the various fixed points in $\mathcal{M}$. Consider the example discussed above, with $\mathbf{k}_0$ and $\mathbf{k}_1$ connected by a a path α. The stabilizer groups are $G^{\mathbf{k}_0}, G^{\mathbf{k}_1}$ and G^α respectively. Denote by $R(G^{\mathbf{k}_0})$, $R(G^{\mathbf{k}_1})$, and $R(G^\alpha)$ the representation rings over $\mathbf{Z}$ of the stabilizer groups. These rings are constructed by assigning to each irrep of the stabilizer group a copy of $\mathbf{Z}$. We denote the dimensions of the representation rings by d_0, d_1 and d_α, respectively. The constraints are then maps $\phi_{0,1}$ in

$$\mathbf{Z}^{d_0} \xrightarrow{\phi_0} \mathbf{Z}^{d_\alpha} \xleftarrow{\phi_1} \mathbf{Z}^{d_1}, \tag{A.56}$$

which can be represented by the following matrices,

$$A^{\mathbf{k}}_{ij} = \begin{cases} 1 & \rho^i_{\mathbf{k}}|_{G^\alpha} = \rho^j_\alpha \\ 0 & \rho^i_{\mathbf{k}}|_{G^\alpha} \neq \rho^j_\alpha \end{cases} \tag{A.57}$$

with $\mathbf{k} = \mathbf{k}_{0,1}$.

The task of finding the constraints between all fixed points can be simplified using the fact that $g : \mathcal{E}_k \to \mathcal{E}_{g\cdot k}$ is a homomorphism. We can use this homomorphism to focus on just the fundamental domain Ω of the action of G. This domain only includes points k that are not related to each other by an element of G, and hence knowing the constraints in that region is enough to know all constraints in all of $\mathcal{M}$.

Imposing these relations on the elements in the representation rings at each fixed point in Ω, gives us a set of independent integers that specify the representation of $\mathcal{E}$ and in particular of $\mathcal{E}_v$. In the above, we did not specify the type of representation, and thus the same arguments also hold for projective representations. These representations occur when the group extension in (A.50) is not split, i.e. for nonsymmorphic crystals. The integers discussed above thus fix the representation of $\mathcal{E}_v$ for both split and non-split extensions in (A.50). However, they do not fix the characteristic classes of $\mathcal{E}_v$. For the complex vector bundles discussed above, the Chern character is the most important one and results in an integer once integrated over an even dimensional submanifold of the base manifold $\mathcal{M}$. Below in section A.4.2 we discuss how these are constrained by space group symmetry.

In summary, to fix the topology and representation of the G-equivariant bundle $\mathcal{E} \to \mathcal{M}$, one specifies the Chern numbers and the set of independent integers in each representation ring associated to each fixed point.

The point of view we have taken in the above discussion is in fact an easy way of understanding the classification of G-equivariant vector bundles. The integers and Chern numbers discussed there are the only integers that need to be specified to fix an equivalence class in K-theory. In fact, the K-theory of $\mathcal{M}$ given an action of G computes Abelian invariants of G-equivariant bundles over $\mathcal{M}$. These are the representation of the bundle and the Chern numbers. The K-theory is $K^0_G(\mathcal{M})$. In terms of cyrstal symmetries, this is true for both symmorphic and nonsymmorphic crystals. In conclusion, topological phases in class A protected by space group $\mathcal{G}$ are classified by

$$\mathrm{TopPh}^d_{\mathcal{G}} = K^0_G(\mathbf{T}^d). \tag{A.58}$$

A similar conclusion was found in [181]. For class AIII we can use the same type of K-theory, but now K^0 is replaced with a different K-theory group, namely K^{-1}. Since we will not discuss class AIII at all in this dissertation we will not give a definition of K^{-1} here, but rather refer to [181] for details.

A big flaw of K-theory is that the K-theory groups are notoriously hard to compute. Only in simple cases could these objects be computed for general space group. Therefore, in chapter 5 we will develop a simple and intuitive way of thinking about these K-theory groups and how they can be computed using simple physical arguments. In chapter 6, we will then do the K-theory computations to indeed check that these arguments are correct.

Relations between K-theory and de Rham cohomology

Before going into actual examples, we briefly discuss some interesting results relating K-theory to de Rham cohomology. These results help us to check the arguments we made above and in the main text. Details can be found in [233,235,236].

To make the connection with de Rham cohomology we use the Chern character. The Chern character assigns an even dimensional form to a vector bundle $\mathcal{E}$ as

$$\mathrm{Ch}(\mathcal{E}) = \sum_{n=0}^{\infty} \frac{1}{n!} \mathrm{Tr} \left(\frac{i\mathcal{F}_{\mathcal{E}}}{2\pi} \right)^n \tag{A.59}$$

where $\mathcal{F}_{\mathcal{E}}$ is the Berry curvature two-form of the bundle $\mathcal{E}$. The n-th Chern character is given by

$$\mathrm{Ch}_n(\mathcal{E}) = \frac{1}{n!} \mathrm{Tr} \left(\frac{i\mathcal{F}_{\mathcal{E}}}{2\pi} \right)^n . \tag{A.60}$$

From the K-theory perspective, the Chern character provides a (ring) homomorphism

$$\begin{aligned} \mathrm{Ch} : K^0(\mathcal{M}) \quad &\to \quad H^{\mathrm{even}}_{dR}(\mathcal{M};\mathbf{Q}) = \bigoplus_{n=0}^{\infty} H^{2n}_{dR}(\mathcal{M};\mathbf{Q}), \\ \mathrm{Ch} \quad &: \quad [E-\Theta_m] \mapsto \mathrm{Ch}([E]) \end{aligned} \tag{A.61}$$

where $H^{2j}_{dR}(\mathcal{M};\mathbf{Q})$ is the $2j$-th de Rahm cohomology of $\mathcal{M}$ over the rational $\mathbf{Q}$. Forgetting about torsion in $K^0(\mathcal{M})$, this becomes an isomorphism $K^0(\mathcal{M})\otimes\mathbf{Q} \simeq H^{\mathrm{even}}_{dR}(\mathcal{M})$. For the K-theory, $K^{-1}(\mathcal{M})$, a similar statement holds. In fact,

$$\mathrm{Ch} : K^{-1}(\mathcal{M}) \to H^{\mathrm{odd}}_{dR}(\mathcal{M};\mathbf{Q}) \tag{A.62}$$

is a group homomorphism and

$$H^{\mathrm{odd}}_{dR}(\mathcal{M};\mathbf{Q}) = \bigoplus_{n=0}^{\infty} H^{2n+1}_{dR}(\mathcal{M};\mathbf{Q}). \tag{A.63}$$

These odd-dimensional cohomology classes are generated by odd-dimensional forms of the form $\mathrm{Tr}((f^{-1}df)^{2n+1}))$ with $f : \mathcal{M} \to \mathcal{E}$ a smooth function on $\mathcal{M}$. In contrast to the Chern characters, they can be understood as winding numbers once integrated. A similar isomorphism as for $K^0(\mathcal{M})$ also exists in this case:

$$K^*(\mathcal{M})\otimes\mathbf{Q} \simeq H^*_{dR}(\mathcal{M};\mathbf{Q}). \tag{A.64}$$

The purpose of this isomorphism is to translate information hidden in the K-theory of $\mathcal{M}$ to a more familiar form in terms of the cohomology of $\mathcal{M}$. The Chern characters in (A.60) give an accurate account for this information, which is most easily seen by integrating them. In doing so, the characters Ch_n become topological invaraints, called Chern numbers c_n. These Chern numbers can only take integer values and account for various topological properties of gapped free fermion systems. An example of a physical observable related to Chern numbers is the TKNN invariant. This invariant is directly proportional to the first Chern number and is related to the Hall conductivity by

$$\sigma_{xy} = \frac{e^2}{h}\int_{\mathbf{T}^2} \mathrm{Ch}_1(\mathcal{E}) = \frac{e^2}{h} c_1. \tag{A.65}$$

Here the integration is over the full Brillouin zone $\mathcal{M} = \mathbf{T}^2$. The winding numbers obtained from integrating odd forms in H^{odd}_{dR} also capture information about the topological phase, but then for those in class AIII. We note that they are related to electric and magnetoelectric polarizability [237], but will not discuss them here.

In the present context of electrons within a crystal lattice, we will mostly be interested in $\mathcal{M} = \mathbf{T}^2$ or $\mathbf{T}^3$, and hence we will only be concerned with the zeroth

and first Chern number. In the equivariant picture sketched above, we already saw how the zeroth Chern number, which is responsible for the representations, is constrained by space group symmetry. We will now see how these contrains affect the first Chern number.

Chern numbers and crystal symmetry

Chern numbers can only be defined on even dimensional fixed submanifolds of $\mathbf{T}^3$. In the case at hand, these are the bounding planes P in Ω. These are planes in the fundamental domain, but to integrate the Chern character, we need a submanifold $\mathcal{N}$ in $\mathbf{T}^3$. Denote by C_g the centralizer of the symmetry g that leaves P invariant. This submanifold $\mathcal{N}$ is then obtained by acting with C_g on P. In other words, C_g still has a non-trivial action on the submanifold. When the Chern characters are integrated, the action of C_g needs to be taken into account. The action of C_g can be such that it inverts the orientation of $\mathcal{N}$. Thus when unfolding P, $\mathcal{N}$ will consist of patches U_- and U_+ with different orientations, indicated by the subscript. More precisely, the submanifold $\mathcal{N}$ is a $|C_g|$-fold cover of P and whenever orientation reversing elements are in C_g, $|C_g|$ is even. Suppose g^* is the orientation reversing element. The submanifold $\mathcal{N}$ will then contain an equal number of patches U_+ and $U_- = g^*U_+$. The integral of the Chern character over $\mathcal{N}$ will therefore vanish. Thus, whenever there are orientation reversing elements in C_g, the Chern numbers on planes fixed by g will be zero.

To be a bit more explicit, consider $\mathcal{N}$ to be two dimensional, i.e. $\mathcal{N} \simeq \mathbf{T}^2$. This two-torus is held fixed by $G^{\mathcal{N}} \simeq \mathbf{Z}_2 = \langle g \rangle$ and has centralizer C_g. In the fundamental domain we denote it as the subset P, thus $\mathcal{N}$ is a $|C_g|$-fold cover of P. For topological phases in real materials, this is the only case of interest. Let $\mathcal{F}_\mathcal{E} = F_{xy}\, dk_x \wedge dk_y$ be the Berry curvature of a vector bundle $\mathcal{E}$. Suppose h is an element of C_g, then h acts on $\mathcal{F}_\mathcal{E}$ as

$$F_{xy}(D(h)\mathbf{k}) = \det(D(h))F_{xy}(\mathbf{k}) \tag{A.66}$$

with D a fixed representation, as in equation (A.52). The Chern number is given by

$$\begin{aligned} c_1 &= \int_\mathcal{N} F_{xy}(k_x, k_y)\, d^2k \\ &= \sum_{h \in C_g} \det(D(h)) \int_P F_{xy}(k_x, k_y)\, d^2k. \end{aligned} \tag{A.67}$$

The sum will tell us whether c_1 vanishes or not. The centralizer can either be $\mathbf{Z}_n$ or D_n with $n = 2$, 3, 4, or 6, or it can be trivial. When it is one of the cyclic groups, then c_1 does not vanish, but when C_g contains reflections, half of the terms in the sum in (A.67) have negative determinant, ensuring that $c_1 = 0$.

$[g]$	$\mathcal{M}^g$	C_g
$[1]$	$\mathbf{T}^3$	G
$[tr^2tr^2]$	$\{(0,0,k_z),(\pi,\pi,k_z),(0,\pi,k_z),$ $(\pi,0,k_z)\}$	$\mathbf{Z}_2 \times D_4$
$[r^3tr]$	$\{(0,k_y,-k_y),(\pi,k_y,-k_y)\}$	$\mathbf{Z}_2^3$
$[Itrt]$	$\{(0,0,0),(0,\pi,\pi),(\pi,0,0),$ $(\pi,\pi,\pi)\}$	$\mathbf{Z}_2 \times \mathbf{Z}_4$
$[Itr^2t]$	$\{(0,k_y,k_z),(\pi,k_y,k_z)\}$	$\mathbf{Z}_2 \times D_4$
$[tI]$	$\{(k_x,-k_x,k_z)\}$	$\mathbf{Z}_2^3$
$[Itr^3]$	$\{(0,0,0),(\pi,\pi,\pi)\}$	$\mathbf{Z}_6$
$[rtr^3t]$	$\{(k_x,-k_x,k_x)\}$	$\mathbf{Z}_6$
$[r^2t]$	$\{(0,0,k_z),(\pi,\pi,k_z)\}$	$\mathbf{Z}_2 \times \mathbf{Z}_4$
$[I]$	$\{$ 8 pnts$\}$	G

Table A.2: Fixed point sets $\mathcal{M}^g$ for each conjugacy class $[g]$ of G and their centralizers C_g. The set $\{8$ pnts$\}$ equals $\{(0,0,0),(\pi,0,0),(0,\pi,0),(0,0,\pi),(\pi,\pi,0),(\pi,0,\pi),(0,\pi,\pi),(\pi,\pi,\pi)\}$.

The maps relating K-theory to ordinary cohomology are useful when considering the following result by Segal [236],

$$K_G^{-n}(\mathcal{M}) \otimes \mathbf{C} = \bigoplus_{[g]} K^{-n}(\mathcal{M}^g)^{C_g} \otimes \mathbf{C}. \tag{A.68}$$

with $\mathcal{M}$ compact and G finite. The sum is over representatives of conjugacy classes of G. The centralizer of g is denoted by C_g and $\mathcal{M}^g$ is the fixed point set of g. This formula relates G-equivariant K-theory (tensored with $\mathbf{C}$) to the ordinary K-theory of the fixed points $\mathcal{M}^g$. To deal with the C_g acting on $K^{-n}(\mathcal{M}^g)$ we compose this formula with the Chern character Ch as discussed above. The summand on the right hand side then amounts to counting invariant forms on $\mathcal{M}^g$.

Example: Octahedral group

Let us now see how the formula by Segal works. In this formula, we need to compute the fixed point manifolds associated with representatives of the conjugacy classes of G. This information is collected in table A.2. From this table, the K-theory group (modulo torsion) can be found straightforwardly. The only thing that we need to take into account, is the action of C_g on $\mathcal{M}^g$. Let us start with the Chern numbers. For [1], $[Itr^2t]$ and $[tI]$ no Chern numbers are possible, because the centralizer contains a reflection. The K-theory is then,

$$K^0(\mathbf{T}^3)^G \otimes \mathbf{C} \oplus K^0(\mathbf{T}^2 \amalg \mathbf{T}^2)^{\mathbf{Z}_2 \times D_4} \otimes \mathbf{C} \oplus K^0(\mathbf{T}^2)^{\mathbf{Z}_2^3} \otimes \mathbf{C} \simeq \mathbf{C}^4$$

Similarly, for the one-dimensional fixed point sets we get eight copies of $\mathbf{C}$, because for $[tr^2tr^2]$ two circles are related by the action of $C_{tr^2tr^2} = \mathbf{Z}_2 \times D_4$. Finally, the zero-dimensional fixed point sets give $\mathbf{C}^{10}$ following the same reasoning as before. Adding these results all up, we obtain

$$K_G^0(\mathbf{T}^3) \otimes \mathbf{C} \simeq \mathbf{C}^{22}. \tag{A.69}$$

Time-reversal symmetry

So far, we discussed topological insulators in class A and how they are classified using K-theory. For systems in class AII, the classification is still done using K-theory, but dressed with additional information. On the representation side, this dressing causes states to become degenerate and moreover the fermionic nature of the electrons has to be taken into account (for class AII). This means that we have to consider the double cover of G and decompose $\mathcal{E}_v$ in terms of irreducible (fermionic) representations of that group. This could also be done for class A, but for AII this is required.

These modifications to K-theory are not too exciting; the real challenge of time-reversal symmetric topological insulators in class AII lies, however, in the Chern-like invariants. These invariants, as we saw in chapters 5 and 6, are $\mathbf{Z}_2$-valued instead of $\mathbf{Z}$-valued. From the pure K-theory perspective, the computation of the corresponding K-theory groups is even harder than in class A. In fact, there is very little literature on this subject tailored towards our set-up. In chapter 6, we embarked on this endeavour and computed the K-theories for certain simple space groups. A bit more detail on the relevant K-theory groups can be found in the next appendix.

A.5 Freed & Moore K-theory and twists

In order to illustrate our approach to computing these K-theory groups, let us first rigorously define the notions used in chapter 6. While doing this, we also connect the technical mathematical language of Freed & Moore [181] to our more concrete setting. To motivate this, first consider a $2+1$-dimensional square crystal and a finite classical symmetry group G consisting of a time-reversing symmetry T and a spatial symmetry R of rotation by π. To account for the fact that R acts unitarily and T acts antiunitarily, we define a homomorphism $\phi : G \to \mathbf{Z}_2$ by $\phi(R) = 1$ and $\phi(T) = -1$. Although the classical group is $G = \mathbf{Z}_2 \times \mathbf{Z}_2$, we know that for fermions, we have $T^2 = R^2 = -1$ on the quantum level. Hence we are not interested in modules over the group algebra of G, but in modules over a

twisted group algebra. To implement this fact mathematically, we twist the group G by a group 2-cocycle $\tau \in Z^2(G, U(1))$, where $U(1)$ is the circle group seen as a G-module by $Te^{i\theta} = e^{-i\theta}$ and $Re^{i\theta} = e^{i\theta}$. This cocycle is given by

$$\tau(T,T) = -1, \quad \tau(R,R) = -1, \quad \tau(T,R) = \tau(R,T) = 1. \tag{A.70}$$

We extend this definition to a cocycle on all of G by the cocycle relation and demanding that $\tau(g,1) = \tau(1,g) = 1$ for all $g \in G$. On the quantum level of twisted representations, we want to impose equations such as $T \cdot T = \tau(T,T)$ instead of the equations holding in G.

To implement this in a more general setting, suppose that we are given a finite classical symmetry group G consisting of point group symmetries and (possibly) time-reversal symmetry. Let $\phi : G \to \mathbf{Z}_2$ be a homomorphism determining whether a group element acts unitarily or antiunitarily. Consider a group 2-cocycle $\tau \in Z^2(G, U(1)_\phi)$, where $U(1)_\phi$ is the G-module $g \cdot e^{i\theta} := e^{\phi(g)i\theta}$. By the one-to-one correspondence between group extensions and group cohomology, the data of τ is equivalent to what is called a ϕ-twisted extension in Freed & Moore [181]. This is a group extension

$$1 \to U(1) \to G^\tau \xrightarrow{\pi} G \to 1 \tag{A.71}$$

such that $e^{i\theta}g = ge^{\phi(\pi(g))i\theta}$ for all $g \in G^\tau$. In fact, two such ϕ-twisted extensions are isomorphic if and only if the corresponding group 2-cocycles are cohomologous. Therefore only the cohomology class $[\tau] \in H^2(G, U(1)_\phi)$ of the cocycle is relevant for the theory.

Now we can define how to twist representations of G by ϕ and τ. Indeed, a (ϕ,τ)-projective action of G is a map $\rho : G \to GL_{\mathbf{R}}(V)$ into the real linear automorphisms of a complex vector space V such that $\rho(g)$ is complex linear if $\phi(g) = 1$, complex antilinear if $\phi(g) = -1$ and

$$\rho(g)\rho(h) = \tau(g,h)\rho(gh). \tag{A.72}$$

Note in particular that if τ is nontrivial, ρ is not a homomorphism of groups. Via the correspondence between group cocycles τ and extensions, such projective actions are exactly the same as (ϕ,τ)-twisted representations in the sense of Freed and Moore [181]. These are defined as genuine homomorphisms $\rho^\tau : G^\tau \to GL_{\mathbf{R}}(V)$ into the real linear automorphisms of a complex vector space V such that $\rho^\tau(g)$ is complex linear if $\phi^\tau(g) = 1$, complex antilinear if $\phi^\tau(g) = -1$ and $\rho^\tau(z)$ is just multiplication by z if z is in the circle subgroup $U(1) \subseteq G^\tau$. Therefore we will use (ϕ,τ)-projective actions and (ϕ,τ)-twisted representations interchangeably.

The twist τ can also be used to twist the group algebra as follows. We define the twisted group algebra ${}^\phi\mathbf{C}^\tau G$ to be the $2\cdot\#G$-dimensional algebra over $\mathbf{R}$ generated

by the symbols x_g for every $g \in G$ and a formal imaginary unit i with defining relations

$$x_g x_h = \tau(g,h) x_{gh}, \quad i^2 = -1, \quad x_g i = \phi(g) i x_g. \tag{A.73}$$

If no confusion can arise we usually just write g for the symbol x_g. Modules over the twisted group algebra are clearly equivalent to projective actions with cocycle τ and hence equivalent to (ϕ, τ)-twisted representations.

For example, suppose we consider time-reversal symmetry T and n-fold rotation R in a system of spinful fermions. Then the symmetry group is $G = \mathbf{Z}_n \times \mathbf{Z}_2$ and ϕ is projection on the second factor. It can be shown using basic techniques in group cohomology that

$$H^2(G, U(1)_\phi) = \begin{cases} \mathbf{Z}_2^2 \text{ if } n \text{ is even,} \\ \mathbf{Z}_2 \text{ if } n \text{ is odd.} \end{cases} \tag{A.74}$$

For n even, the two $\mathbf{Z}_2$'s correspond exactly to the choices of signs in $R^n = \pm 1$ and $T^2 = \pm 1$. For example, if $n = 2$, a representative τ of the cohomology class that assumes for both signs the negative is given in equation (A.70). For n odd however, the sign of R does not influence the isomorphism class of the twist. This is not very surprising from a representation-theoretic perspective. Indeed, if we redefine $S := -R$ in the group algebra ${}^\phi\mathbf{C}^\tau G$ then we get the group algebra with the twist chosen such that $S^n = -1$ and T has the same square as before. Note that this would not work for even n; we could have defined $S := iR$, but then S would not commute with T. However, if there would have been no time-reversal symmetry, this argument would have worked and the sign of R^n does not matter for the cohomology class. This simply resonates the fact that $H^2(\mathbf{Z}_n, U(1)) = 0$ in case of trivial ϕ. Conclusively, assuming that $R^n = -1$ in class A would not influence the classification of topological insulators and assuming that $R^n = 1$ in class AII would not influence the classification in case n is odd.

The group cocycle τ can be used as a twisting for the Freed-Moore K-theory groups. The G-equivariant K-theory of the Brillouin zone torus twisted by τ then classifies topological phases protected by the twisted symmetry group (G, ϕ, τ). In the abstract language of Freed and Moore, to twist a G-space X means that we consider the following ϕ-twisted extension of the action groupoid (or orbifold) $X/\!\!/G$. The line bundle is picked trivial and the cocycle on $X/\!\!/G$ is picked equal to the cocycle τ at every $x \in X$, see also [208, section 2]. Twisted equivariant bundles are then the bundle-theoretic analogue of (ϕ, τ)-twisted representations of G in the same sense that Atiyah & Segal's complex equivariant vector bundles are the bundle-theoretic analogue of ordinary group representations of G. More concretely, we define a (ϕ, τ)-twisted equivariant vector bundle over a G-space X to be a

complex vector bundle E over X together with a family $\{\rho(g) : E \to E : g \in G\}$ of maps such that

(i) $\rho(g)$ covers the action of g on the base space;

(ii) $\rho(g)$ is complex linear if $\phi(g) = 1$ and conjugate linear if $\phi(g) = -1$;

(iii) $\rho(g)\rho(h) = \tau(g,h)\rho(gh)$.

The K-theory classifying such bundles is simply the Grothendieck completion of the monoid of isomorphism classes of such bundles. Written out in full, the resulting abelian group

$$^{\phi}K_G^{\tau}(X)$$

is called the (ϕ,τ)-twisted G-equivariant K-theory of X. Twisted equivariant K-theory of this form can be expanded to a contravariant functor from a category of sufficiently nice G-spaces to the category of abelian groups. By mimicking the technique of Segal [215], it can be shown that this theory extends to a $\mathbf{Z}$-graded additive generalized equivariant cohomology theory in the sense of Bredon [209]. One can also show that the twisted equivariant K-theory above is equivalent to the K-theory of Freed & Moore (with our specific form of the twist τ) under the correspondences described above c.f. [208]. The fact that Freed & Moore's K-theory satisfies the axioms desired for a cohomology theory of this kind also follows from [208]. Hence we can use the equivariant form of the usual cohomology axioms (suspension axiom, homotopy invariance, etc.) freely. The associated reduced cohomology theory is called reduced twisted equivariant K-theory. For a pointed G-space (X,x), where $x \in X$ is a point that is completely fixed under the action, the reduced K-theory is defined as the kernel of the map given by restricting to the fiber over the base point:

$$^{\phi}\tilde{K}_G^{\tau+p}(X) := \ker\left(^{\phi}K_G^{\tau+p}(X) \to^{\phi} K_G^{\tau+p}(x)\right). \tag{A.75}$$

If $Y \subseteq X$ is a subspace closed under the G-action, then the relative twisted equivariant K-theory of the pair (X,Y) is defined as

$$^{\phi}K_G^{\tau+p}(X,Y) := {}^{\phi}\tilde{K}_G^{\tau+p}(X/Y) \tag{A.76}$$

It should also be noted that that the K-theory twisted by a cocycle τ' cohomologous to τ is isomorphic to the K-theory twisted by τ.

Finally we remark on how to formally construct the necessary τ for classifying class AII crystalline topological insulator. We do this by considering the double cover group sketched in Section 6.4.1. Before we can do this, we first have to sketch the relation between double cover groups and twists τ. In order to show this, suppose we have a group of the form $G = G_0 \times \mathbf{Z}_2^T$ with ϕ projection onto the second factor

and $G_0 \hookrightarrow O(d)$ a point group. As described using group extensions in Section 6.4.1, we start with the class in $H^2(O(d), \mathbf{Z}_2)$ corresponding to the Pin$_-$-double cover of $O(d)$. Restricting the class to the subgroup $G_0 \subseteq O(d)$ then gives a class $[\tau_1] \in H^2(G_0, \mathbf{Z}_2)$, which exactly corresponds to the double cover group $\widehat{G}_0$. To get the right square of time-reversal, we then take the class $[\tau_2] \in H^2(\mathbf{Z}_2^T, \mathbf{Z}_2) = \mathbf{Z}_2$ to be trivial in class AI and nontrivial in class AII. Next, in order to construct the desired total double cover group which covers G instead of G_0, we now combine $[\tau_1]$ and $[\tau_2]$. To do this we pull the classes back along the two projection maps $p_1 : G \to G_0$ and $p_2 : G \to \mathbf{Z}_2^T$ and then take their product:

$$[\tau'] = p_1^*([\tau_1]) \cdot p_2^*([\tau_2]) \in H^2(G, \mathbf{Z}_2). \tag{A.77}$$

Note that this product is not the cup product, but simply the product on the level of the coefficients $\mathbf{Z}_2$. Finally, we get our desired twist $[\tau] \in H^2(G, U(1)_\phi)$ by extending the coefficients to $U(1)$. More precisely, we consider the map $H^2(G, \mathbf{Z}_2) \to H^2(G, U(1)_\phi)$ induced by the G-module injection $\mathbf{Z}_2 \hookrightarrow U(1)_\phi$.

More generally, we could have taken group cocycles $\tau \in Z^2(G, C(X, U(1)_\phi))$ that vary over the Brillouin zone X to account for nonsymmorphic crystal structures. These more general twists can be used as a ϕ-twisted extension of the action groupoid $X/\!\!/G$ in the Freed-Moore framework by picking the line bundle to be trivial and the cocycle to be equal to τ, now varying over space. This construction results in a well-defined K-theory group that classifies nonsymmorphic crystalline topological insulators. However, we can no longer define the relative K-theory of (X, Y) to be the reduced K-theory of the quotient if τ varies along X^{p-1}. For a definition of relative K-theory that holds in a more general setting, see [208].

A.5.1 Higher twisted representation rings and the K-theory of a point

Assume we are given a finite group G, a homomorphism $\phi : G \to \mathbf{Z}_2$ and a group 2-cocycle with values in the G-module $g \cdot e^{i\theta} = e^{i\phi(g)\theta}$. The basic building blocks of K-theory from which spectral sequences can be built are the higher degree K-theory groups of a point ${}^\phi K_G^{\tau - q}(\mathrm{pt})$. It follows from the last section that for $q = 0$, the group ${}^\phi K_G^\tau(\mathrm{pt})$ is the Grothendieck completion of the monoid of isomorphism classes of modules over the group algebra ${}^\phi \mathbf{C}^\tau G$ twisted by τ. This is what is called the twisted representation ring of degree $q = 0$ in the main text. Remark that due to the twist τ, these abelian groups do not have a ring structure, but we will nevertheless refer to them as twisted representation rings in analogy with the nontwisted case.

In higher degrees, the twisted equivariant K-theory of a point has a similar con-

crete description in terms of representation theory and Clifford algebras. This is expressed by using a generalized version of the Atiyah-Bott-Shapiro isomorphism [238]. Heuristically, this theorem asserts that going down a degree in K-theory (i.e. taking a suspension) corresponds to adding a Clifford algebra element on the algebraic level, at least for the K-theory of a point. More explicitly, let $Cl_{p,q}$ for the real Clifford algebra of signature (p,q). Then $Cl_{p,q}$ is an algebra over the real numbers with has a natural $\mathbf{Z}_2$-grading such that the standard generators $\gamma_1, \ldots, \gamma_{p+q} \in Cl_{p,q}$ are odd. If we then take group elements to be even, we can give the tensor product ${}^{\phi}\mathbf{C}^{\tau}G \otimes_{\mathbf{R}} Cl_{0,q}$ the structure of a $\mathbf{Z}_2$-graded algebra as well. The (ϕ,τ)-twisted equivariant K-theory of a point can then be described by the isomorphism

$$ {}^{\phi}K_G^{\tau-q}(\mathrm{pt}) \cong {}^{\phi}R^{\tau-q}(G) := \frac{\{\mathbf{Z}_2\text{-graded modules over } {}^{\phi}\mathbf{C}^{\tau}G \otimes_{\mathbf{R}} Cl_{0,q}\}}{\{\text{modules that extend to a } {}^{\phi}\mathbf{C}^{\tau}G \otimes_{\mathbf{R}} Cl_{1,q}\text{-module}\}}, \tag{A.78} $$

and we call ${}^{\phi}R^{\tau-q}(G)$ the (ϕ,τ)-twisted (higher) representation ring of G in degree $-q$. This fact follows from the discussion in [208, §3.5]. This way of computing the complex and real equivariant K-theory of a point has been known for a long time, see the final section of [239]. Also see Donovan-Karoubi [240, §6.15] for a precise version of such a statement for a certain type of twisted equivariant K-theory of more general spaces. We again stress that the twisted higher representation rings as defined above are not rings themselves, because the tensor product of two (ϕ,τ)-twisted representations is a $(\phi,2\tau)$-twisted representation. However, they are modules over the $(\phi,1)$-twisted representation ring. We could in theory make them into genuine rings by summing over all possible twists τ, but this would not be a very natural thing to do from the perspective of physics. Namely, using the language of Section 6.4.1, the product of two fermionic representations will be a bosonic one.

To illustrate the definition of the twisted representation ring, we provide a few examples. First of all, if ϕ and τ are trivial, it can be shown that the higher representation rings are equal to the representation ring of the group in even degree and vanish in odd degree, i.e. it gives the complex equivariant K-theory of a point as expected. For certain simple groups like the time-reversal group $G = \mathbf{Z}_2 = \{1, T\}$ (with $\phi(T) = -1$), the twisted representation rings are also readily computed using basic Clifford algebra theory. They are simply the real (respectively quaternionic) K-theory of a point for a trivial (respectively nontrivial) twist τ. This results in the relevant representation rings for both class AI with trivial twist τ_0 and class AII with twist τ_1, as was summarized in Table 6.1. If we just take the real group algebra instead of the twisted group algebra, we get the equivariant KR-theory of a point as can be shown by comparing with the results in [239]. It is also

worth noting that the higher twisted representation ring defined by (A.78) indeed equals the Grothendieck group of the monoid consisting of isomorphism classes of (ϕ, τ)-twisted representations of G in case $q = 0$.

The higher representation rings of the twisted group algebra in general can be computed by decomposing the algebra into a direct sum of matrix rings over $\mathbf{R}, \mathbf{C}$ and $\mathbf{H}$. Since the twisted group algebra is semisimple, this can always be done. If the number of real, complex and quaternionic matrix rings occurring in this decomposition are $n_{\mathbf{R}}, n_{\mathbf{C}}$ and $n_{\mathbf{C}}$ respectively, then

$$ {}^{\phi}R^{\tau-q}(G) = K^{-q}(\mathrm{pt})^{n_{\mathbf{C}}} \oplus KR^{-q}(\mathrm{pt})^{n_{\mathbf{R}}} \oplus KR^{-q-4}(\mathrm{pt})^{n_{\mathbf{H}}}. \tag{A.79} $$

This follows because the representation rings preserve direct sums and are independent of Morita equivalence. Therefore, to determine the representation rings, we only need to make an analogous twisted representation theory to the theory of real representations of finite groups. Such a theory already exists in the physics literature and is described in section 6.4.1.

A.5.2 Construction of the spectral sequence

In this appendix some details on the existence of the spectral sequence will be outlined. For an introduction to the theory used in this section and throughout the chapter 6, such as spectral sequences in general and the Atiyah-Hirzebruch spectral sequence for (nonequivariant) cohomology theories such as ordinary K-theory, we refer the reader to [241]. The construction of the spectral sequence for the type of K-theory we are concerned with can be done using standard methods already described for general equivariant cohomology theories by Bredon [209].

As before, let G be a finite group, $\phi : G \to \mathbf{Z}_2$ a homomorphism and $\tau \in Z^2(G, U(1)_\phi)$ a group cocycle. We now start with a finite G-CW complex $X^0 \subseteq \cdots \subseteq X^d = X$ and construct the Atiyah-Hirzebruch spectral sequence with respect to this G-CW-structure. In order to make sure that the reduced K-theory of X is defined, we have to assume that there is at least one point $0 \in X^0$ that is fixed by the whole group G. Note that this is always the case in practice; if X is the Brillouin zone torus then the point $k = 0$ is fixed by all symmetries. As stated in [209], the first page $E_1^{p,-q}$ of the spectral sequence is given by the relative K-theory groups

$$ E_1^{p,-q} = {}^{\phi}K_G^{\tau+p-q}(X^p, X^{p-1}). \tag{A.80} $$

Let us now show that this is the group of Bredon equivariant cochains with a particular coefficient functor. Indeed first note that since τ is constant in space,

the relative K-theory equals reduced K-theory of the quotient:

$$
\begin{aligned}
{}^{\phi}K_G^{\tau+p-q}(X^p, X^{p-1}) &= {}^{\phi}\widetilde{K}_G^{\tau+p-q}(X^p/X^{p-1}) && \text{(A.81)}\\
&\cong {}^{\phi}\widetilde{K}_G^{\tau+p-q}\left(\bigvee_{\sigma}\bigvee_{gH_\sigma} S^p_{gH_\sigma}\right). && \text{(A.82)}
\end{aligned}
$$

Here the first wedge product is over all equivariant p-cells σ of X, which look like $S^p_\sigma \times G/H_\sigma$, where $H_\sigma \subseteq G$ is the stabilizer of the cell σ. The second wedge product is over all ordinary cells $S^p_{gH_\sigma}$ contained in the equivariant cell σ, i.e. over all cosets gH_σ of the stabilizer group. The appearance of the wedge sums is a consequence of the quotient X^p/X^{p-1}. For example, if $X = S^2$ is the sphere of figure 6.1 and $p = 2$, then X^p/X^{p-1} is the space that results from pinching ℓ and $T\ell$ to a point, i.e. $S^2 \vee S^2$.

Now by additivity and the suspension axiom,

$$
\begin{aligned}
{}^{\phi}K_G^{\tau+p-q}(X^p, X^{p-1}) &= {}^{\phi}\widetilde{K}_G^{\tau+p-q}\left(\bigvee_{\sigma}\bigvee_{gH_\sigma} S^p_{gH_\sigma}\right) && \text{(A.83)}\\
&\cong \bigoplus_{\sigma\ p\text{-cell}} {}^{\phi}\widetilde{K}_G^{\tau+p-q}\left(\bigvee_{gH_\sigma} S^p_{gH_\sigma}\right) && \text{(A.84)}\\
&= \bigoplus_{\sigma\ p\text{-cell}} {}^{\phi}\widetilde{K}_G^{\tau+p-q}(\Sigma^p(G/H_\sigma \sqcup \mathrm{pt})) && \text{(A.85)}\\
&\cong \bigoplus_{\sigma\ p\text{-cell}} {}^{\phi}\widetilde{K}_G^{\tau-q}(G/H_\sigma \sqcup \mathrm{pt}) && \text{(A.86)}\\
&\cong \bigoplus_{\sigma\ p\text{-cell}} {}^{\phi}K_G^{\tau-q}(G/H_\sigma). && \text{(A.87)}
\end{aligned}
$$

Here $\Sigma^p Y$ denotes the pth reduced suspension of the pointed G-space Y and $\sqcup$pt is the disjoint union with an extra added basepoint. Similarly to nontwisted equivariant K-theory we can then make use of the isomorphism

$$
{}^{\phi}K_G^{\tau-q}(G/H) \cong {}^{\phi}K_H^{\tau-q}(\mathrm{pt}) \qquad \text{(A.88)}
$$

induced by restricting bundles over G/H to the fiber lying over the trivial coset H. Note that on the right hand side, we have to restrict the twisting data ϕ, τ to H, but this is omitted in the notation.

The first page of the spectral sequence can now be rewritten as a group of Bredon

equivariant cochains

$$\bigoplus_{\sigma\ p\text{-cell}} {}^{\phi}K_G^{\tau-q}(G/H_\sigma) \cong \bigoplus_{\sigma\ p\text{-cell}} {}^{\phi}K_{H_\sigma}^{\tau-q}(\mathrm{pt}) \tag{A.89}$$

$$\cong \bigoplus_{\sigma\ p\text{-cell}} {}^{\phi}R^{\tau-q}(H_\sigma) \tag{A.90}$$

$$\cong C_G^p(X, {}^{\phi}\mathcal{R}_G^{\tau-q}), \tag{A.91}$$

where the coefficients ${}^{\phi}\mathcal{R}_G^{\tau-q}$ form a functor from the orbit category of G to the category of abelian groups. Topologically, this functor is just the restriction of the twisted equivariant K-theory functor to the orbit category, but an algebraic desciption is more enlightening. It sends the orbit space G/G_σ to the twisted representation ring ${}^{\phi}R^{\tau-q}(G_\sigma)$ defined in the previous section:

$${}^{\phi}\mathcal{R}_G^{\tau-q}(G/G_\sigma) = {}^{\phi}R^{\tau-q}(G_\sigma). \tag{A.92}$$

Thus although our cochains appear to have coefficients in a functor, once evaluated for specific cells in the CW complex of X, the coefficients are just the degree $-q$ twisted representation ring of the stabilizer group of that cell. However, its action on morphisms is more complicated to describe algebraically. Quotient maps $G/H \to G/K$ are sent to restrictions of representations ${}^{\phi}R^{\tau-q}(K) \to {}^{\phi}R^{\tau-q}(H)$ as expected, but conjugation maps $G/H \to G/gHg^{-1}$ can yield nontrivial results similar to the action of T as described around equation (6.16). As stated in the main text, it can be shown that the first differential is precisely the cellular Bredon differential d

$$(df)(\sigma) = \sum_{\mu \in C^p(X)} [\mu : \sigma] f(\mu)|_{G_\sigma}, \tag{A.93}$$

see for example Bredon's work [209].

Summarizing, there exists a spectral sequence $E_r^{p,-q}$ associated to a finite pointed G-CW-complex X converging to twisted equivariant K-theory:

$$E_r^{p,-q} \implies {}^{\phi}K_G^{\tau+p-q}(X) \tag{A.94}$$

such that the second page $E_2^{p,q}$ is Bredon cohomology of degree p with coefficient functor ${}^{\phi}\mathcal{R}_G^{\tau-q}$. To derive explicit computational tools from this fact, recall from the basic theory of spectral sequences that this means that there is a filtration F^p of ${}^{\phi}K_G^{\tau}(X)$

$$0 = F^{d+1} \subseteq F^d \subseteq \cdots \subseteq F^1 \subseteq F^0 = {}^{\phi}K_G^{\tau}(X) \tag{A.95}$$

such that the final page $E_\infty^{p,-p}$ forms the associated graded space, i.e.

$$E_\infty^{p,-p} \cong \frac{F^p}{F^{p+1}}. \tag{A.96}$$

If $d = 2$, this results in the short exact sequences (6.6) and (6.7), where $F = F^1$.

For computations for nonsymmorphic crystals, we would need to generalize these methods to include twisting data for K-theory that varies over X. Since τ is no longer constant in this setting, most arguments given in this section fail. First of all, the relative K-theory of (X^p, X^{p-1}) no longer seems to be equal to the K-theory of the quotient X^p/X^{p-1} if τ varies along X^{p-1}, so we have to preserve the information of the values of τ over X^{p-1}. Moreover, it is not clear how to compute the twisted equivariant K-theory of a sphere for nonconstant twist, since there is no obvious generalization of the isomorphism (A.78) here. Ignoring these mathematical difficulties for the moment and assuming we have some kind of spectral sequence, we should at least arrive at a point where the coefficient functors ${}^{\phi}\mathcal{R}_G^{\tau-q}$ are no longer constant. In particular, a Bredon cochain of say degree 1 could map different points of a single 1-cell into different twisted representation rings. The second page is no longer ordinary Bredon cohomology and therefore it is not clear how to generalize this section to that setting.

Summary & Outlook

The research presented in this dissertation is twofold. On the one hand, we discussed, in part I, the AdS/CFT correspondence and deviations from it and on the other hand, in part II, we focussed on the classification of topological insulators. In the beginning of each part, we mentioned several motivations for studying these topics and in this final piece of the dissertation, we want to reflect back on these motivations and discuss to what extend we have answered some of the questions that we raised. We will do so for each part separately and discuss various future directions afterwards. We already did this in each chapter to some extent, but here we will mention some additional future directions and a possible symbiosis of parts one and two.

Summary

High-energy theory

In the first part of the dissertation we considered departures from the usual and well-known examples of AdS/CFT. We considered (asymptotically) AdS spacetimes with a specific boundary topology and asked what constraints a CFT needs to satisfy in order to describe the gravitational physics in the bulk. In particular, we focussed on Einstein gravity and its bulk phase structure. The first and simplest constraint is that for semi-classical bulk, i.e. Einstein gravity, we need a large number of degrees of freedom. A second constraint follows from the existence of black hole solutions in the bulk. These objects have an entropy that obeys a Cardy type formula and in order to properly describe the bulk physics, the field theory has to have a density of states that grows in a particular way. In two dimensions, this implies a particular constraint on the spectrum. In higher dimensions, we showed that similar arguments can be given, but are subtly different. For the field theories we considered (which live on d-dimensional tori), the vacuum energy is

rather non-universal, which prevents a direct application of the arguments in two dimensions. However, by demanding a certain form of the vacuum energy and using modular invariance in higher dimensions, we could derive a constraint on the spectrum, analogous to the one that already existed in $d = 2$.

We have thus succeeded in finding a few constraints that CFTs need to obey in order to be holographic as advertised in chapter 1. However, these only form a few constraints of a much larger set that is expected to exist. Such constraints would take more refined information in the bulk into account, such as a large gap to higher-spin particles. In our analysis, the most interesting constraint is the one on the form of the vacuum energy. Since the vacuum energy on tori is rather arbitrary, this constraint means there should be a mechanism in holographic CFTs enforcing it. Most likely this is a strong coupling effect, but it is unclear how that works in detail and it would be extremely interesting to study this further.

In chapter 1, we also mentioned that our constraints could help finding new examples of holographic CFTs. This is an extremely difficult taks, but for the few features we wanted to reproduce in the bulk, we managed to give an infinite set of such CFTs. We achieved this by generalising the known constructions of symmetric product orbifolds to higher dimensions. In two dimensions this was rather successful, but in $d > 2$ the seed theory from which the symmetric product orbifold theory is constructed already needs to have the special form of the vacuum energy. It is therefore unclear whether we are in some sense already putting the answer in. A more refined study of these theories would be needed to confirm this.

In chapter 3, we considered a deformation of the usual AdS/CFT dictionary. We put a hard cutoff wall inside AdS and put Dirichlet boundary conditions there. This is one, out of many, generalisations of the AdS/CFT dictionary at finite cutoff and is the one studied in this chapter. As a result, given a radial slicing of the bulk metric, equality of the gravitational partition function and the field theory generating functional is now not demanded at asymptotic infinity, but at some finite $r = r_c$. By studying the dependence on r_c, we were able to write down an explicit deformation of the field theory dual to these boundary conditions. This deformation takes the form of a flow equation and generalises the known $T\bar{T}$ deformation in two dimensions to higher dimensions, but makes crucial use of large N to achieve a similar factorisation property.

We study the flow equation and derive a formula for the deformed spectrum that we then match with a gravitational computation, i.e the energy of black holes in AdS with a finite radial extent. Moreover, we show that the deformation can also be seen as coupling to a fluctuating, but random, metric using a Hubbard-Stratonovich transformation. Remarkably, this point of view gives one of the

Hamilton equations in the bulk. The important lesson here is that the T^2 deformation of chapter 3 could potentially be viewed as coupling the CFT to gravity. This makes sense, since gravity is not decoupled at finite r. In two dimensions this was shown to be the case [103], but it would be interesting to establish similar results in higher dimensions. Of course, this would require going beyond the leading order in N results we found.

The energy levels of the deformed theory also give rise to a different density of states. For positive coupling constant of the deforming operator, the UV is cut out, so there is no asymptotic region anymore, but for negative values there is and we find a super-Hagedorn density of states at asymptotically large energies. It is intriguing to note that this matches precisely with that of the semi-classical quantisation of $(d-1)$-branes! This was to be expected, but the non-trivial result here is that this could indicate that for negative values of the coupling, the deformation moves the radial slice out of the AdS throat. For example, one could potentially see the D3-branes popping up when moving out of the AdS_5 throat. It would be extremely interesting to make this more precise in the future.

Classification of topological insulators

The second part of this dissertation was devoted to an entirely different subject in theoretical physics: the classification of topological insulators. In chapter 4 we mentioned that for a full understanding of topological insulators a classification is crucial. In this dissertation we achieved this classification (modulo some subtlety mentioned below) on arbitrary crystals and with or without time-reversal symmetry. We have given an intuitive and simple algorithm to count how many topological insulators there are in class A and AII given any crystal symmetry. We can summarise this algorithm as follows.

We focussed on the crystal symmetries and argued that the number of bands carrying a particular eigenvalue under the symmetry operators are topological invariants. However, not all of these invariants are independent, since there are relation between eigenvalues (or rather, representations) arising from continuity of the band structure. Modulo global invariants such as Chern numbers and FKM invariants, this is the full classification. To incorporate the global invariants in the classification, some more work is needed. For the Chern numbers this is rather straightforward as they only exist on two dimensional slices of the Brillouin zone and are zero whenever a reflection acts within that slice. The difficult part is the incorporation of the FKM invariant in class AII. The key insight, presented in chapter 5, is to view the FKM invariant as the presence or absence of vortex-anti vortex pairs protected by time-reversal symmetry. This allowed us to study the effects of crystal symmetries on the FKM invariant in a clear and systematic

way. In fact, we argued that crystal symmetry forces vortices to be frozen at high-symmetry points and lines, giving rise to a whole zoo of $\mathbf{Z}_2$ invariants. Some of these invariants were known already but we also proposed an entirely new invariant.

Besides giving an algorithm to count topological insulators, we also mentioned in chapter 4 that it is worthless without a proper check. Luckily, the classification of topological insulators can be translated to a rigorous question in mathematics, providing us with the necessary check.

For class A we could check our results in two dimensions against known complex K-theory computations and found perfect agreement. In three dimensions, there was a slight disagreement due to exotic topologies like $\mathbf{RP}^2$. For class AII, the situation is more complicated. A direct check with all our results was not possible, since not much literature on the corresponding K-theory groups exists. In order to check our results, we thus had to compute the K-theory groups ourselves. In 6, we used the Atiyah-Hirzebruch spectral sequence to compute twisted equivariant K-theory groups for certain simple cases. Already in those simple cases, the computations were rather non-trivial, but in the end we showed that indeed they given the same classification as the heuristic arguments given in chapter 5.

Outlook

Let us now mention some future directions that can help to give a better understanding of quantum gravity and the wild world of topological phases. We already discussed some of them briefly in the above, but here we would like to be a bit more specific and find possible bridges between parts one and two.

Symbiosis

Although this dissertation contains two seemingly different topics in theoretical physics, there is actually some overlap. Not directly, but rather between string theory and topological phases. In string theory, D-brane charges are classified by K-theory in exactly the same way as is the case for topological insulators. There should therefore also be a construction within string theory that could also host the topological phases we discussed in this dissertation. Indeed, for example in [242], a construction of two parallel D-branes was proposed that can, host fermions with a mass given by their separation. In light of our studies, it would be worthwhile to see how crystal symmetries can be included in that setup. Time-reversal symmetry can already be implemented in a straightforward way by using O-planes, but for crystal symmetry, a particular translational symmetry breaking deformation has

to be turned on. This, however, is rather difficult to implement and a better way to see the effects of additional (discrete) symmetries, is by putting the system on an orbifold so that on the common dimensions there is a discrete group G acting. The K-theory will then become G-equivariant K-theory and the fermions feel this additional symmetry G. Doing this for G a space group is challenging, but as we have seen, interesting invariants appear already when forgetting about translational symmetry, so it is probably enough to restrict to G being a point group.

It is not only interesting to see these topological phases appearing in string theory and how they can be constructed, but also because this construction might help to find strongly coupled versions of the topological phases we have found in our analysis. As is known in cases without crystal symmetry [243], interactions can cause some values of the invariants to be unprotected, resulting in a reduction from $\mathbf{Z}$ to $\mathbf{Z}_8$. It would be interesting to see how the various $\mathbf{Z}_2$ invariants we found, survive interactions.

One interesting way to study strongly coupled versions of topological insulators is by using the stringy constructions and taking a suitable large N limit. This might allow us to study them using holography. It would be interesting, for example, to see what the topological phases mean in the bulk and how the topological features on the boundary manifest themselves in gravity. For the quantum Hall states, some work in this direction was already done in, for example, [244].

Boundary physics

In our classification of topological insulators, we found many new topological phases, but never really embarked on a crucial question, namely what happens at the edges? In [3] we discussed this question in the case of an interface between two topological phases and found that there could be massless boundary modes at the interface, purely on the basis of representation theory. This analysis was rather abstract and it would be interesting to have a more hands-on description of the boundary modes. This might also shed some light on how time-reversal symmetry impacts the presence of boundary modes and how our newly proposed invariant has its imprints on the boundary.

From a high-energy point of view, the study of edge physics can be understood using an anomaly inflow mechanism. This says that even though the boundary theory cannot live on its own on a closed manifold, it can live on the boundary of some manifold. The anomalies of the boundary theory are in this way cancelled by the anomalies of the bulk theory. It would be interesting to understand this mechanism in a more general sense, including interactions and additional (discrete)

symmetries for example. By studying these systems as systems of intersecting D-branes one could maybe try to understand the boundary theory at strong coupling with the aid of holography.

Studying the edge physics would be the precursor to something much more important, which we touched upon before as well, namely trying to understand all incarnations of topology in band insulators. From a theoretical point of view, this dissertation has made a big step in that direction, but experimentally there are still many challenges ahead and one of them is measuring the new invariant that we found. A simple set of materials one could start with to measure it, is by using layered materials. These materials are effectively two dimensional and could therefore be a host material for our new invariant, when, for instance, there is two-fold rotation acting within the layers.

Non-critical string theory and $T\bar{T}$

In chapter 3, we mostly focussed on the case in which $\lambda > 0$ and found a connection with holography. However, the $\lambda < 0$ theory is also a very interesting theory to consider. It has the advantage that the deformed spectrum is much better behaved and does not complexify for most states. As a result, one might wonder whether this theory admits a non-perturbative definition. Remarkable, this can indeed be done in two (equivalent) ways. One uses a coupling of the CFT to a flat space version of Jackiw-Teitelboim gravity [103], whereas the other uses a coupling to a two dimensional string theory, which is work in progress with Herman Verlinde and Nele Callebaut.

The connection with string theory can be most easily understood as follows. Consider the deformed energy levels

$$E_n(\lambda, L) = \frac{L}{4\lambda}\left(1 - \sqrt{1 - 8M_n\frac{\lambda}{L^2} + 64\pi^2 P_n^2\frac{\lambda^2}{L^4}}\right), \tag{A.97}$$

of a two dimensional CFT on a cylinder with circumference L and states with (dimensionless) energy M_n and momentum P_n. This is a generalisation of 3.78 at $d = 2$ and no charge to non-zero momentum. Upon rewriting A.97 as

$$\left(E_n - \frac{L}{4\lambda}\right)^2 = \frac{L^2}{(4\lambda)^2} - 2\frac{M_n}{4\lambda} + \frac{4\pi^2 P_n^2}{L^2}, \tag{A.98}$$

we see that this is nothing but the Virasoro condition on the string spectrum for a string with $\alpha' = -4\lambda > 0$ on a cylinder! More precisely, it turns out that it is a non-critical string theory[4] with a constant B-field and in the winding one sector.

[4] When the seed CFT has $c = 24$ it is in fact critical string theory.

The B-field results in the shift on the right hand side of (A.98). The oscillator piece is now captured by the undeformed theory. The beauty of this proposal lies in the natural appearance of the non-perturbative definition of the Hilbert space in terms of a BRST cohomology, which was not present in the proposal by Dubovsky et al. [103]. Moreover, in this prescription, treatment of the negative M_n states is similar to the treatment of the tachyon in bosonic string theory.

The relation with string theory also brings about some cute properties of the $T\bar{T}$ theory. For example, in the old days of string theory, there can only be on-shell observables in target space, making it hard to define local operators in the $T\bar{T}$ theory. However, since 1995 [245], we know that string theory also hosts non-perturbative objects that could potentially help defining such local operators in the target space. Furthermore, the appearance of a non-local phase factor in the S-matrix of the $T\bar{T}$ deformed theory on Minkowski space [98] is a consequence of the non-commutativity of the target space coordinates. A detailed analysis of all these claims is an interesting future direction that helps understand not only the $T\bar{T}$ theory for $\lambda < 0$, but might also shed some light on the holographic interpretation.

Irrelevant deformations in quantum mechanics

Besides a more thorough understanding of the two dimensional case, another fruitful research direction is to generalize the techniques in chapter 3 to general dilaton gravities in two dimensions. By deforming the putative dual quantum mechanics in a particular way, one can then understand how one can flow inside the two dimensional bulk. In particular, an interesting set up to consider is dilaton gravities that have a de Sitter region deep in the bulk and an anti-de Sitter region asymptotically [246]. By flowing from asymptotic infinity to the dS_2 region, one might have a controllable way to understand holography for dS_2, which was one of the goals we set out in the beginning of this dissertation. See [247] for similar ideas. General dilaton gravities also arise from a spherical reduction of, say, four dimensional Einstein-Maxwell theory to two dimensions and therefore, understanding how to flow in two dimensions, might also help to understand flowing outwards, so from AdS_2 to AdS_{d+1}. A more careful analysis of this is work in progress with Edgar Shaghoulian.

Holoception

Finally, we mention a rather radical, but extremely interesting idea. From the proposal of Dubovsky et al. [103] and the Hubbard-Stratonovich transformation in section 3.4, it is clear that a non-perturbative description of the $T\bar{T}$ theory is one in which we couple the CFT to gravity. This means that we again have a theory of

gravity to which we can apply the holographic principle. More precisely, consider AdS_2 slices of AdS_3, so that at finite cutoff in AdS_3, the $T\bar{T}$ theory lives on AdS_2. This theory on AdS_2 again contains gravity and once we understand how to apply the techniques in chapter 3 to that case, we can relate that $T\bar{T}$ theory on AdS_2 (at finite cutoff) to the physics of a quantum mechanics theory. In some sense, this is doing holography within holography and gives rise to a description of AdS_3 bulk physics using a quantum mechanical theory deformed by the generalisation of the T^2 deformation of chapter 3 to $d = 1$. In order to make this more precise, one would have to show that the $T\bar{T}$ theory on AdS_2 is the same as coupling the $T\bar{T}$ theory to Jackiw-Teitelboim gravity and not its flat space version, since for flat space we do not really know how to do holography. Moreover, the factorisation property of Zamolodchikov still needs to hold, which should indeed be the case, since AdS_2 is still a symmetric space. One can take this idea even further and say that the cascade extends to higher dimensions as well and so will always reduce AdS_{d+1} physics at finite cutoff to a special quantum mechanics theory. Similar ideas were actually pursued before already, for instance in [248, 249].

Bibliography

[1] A. Belin, J. de Boer, J. Kruthoff, B. Michel, E. Shaghoulian, and M. Shyani, "Universality of sparse $d > 2$ conformal field theory at large N," *JHEP* **03** (2017) 067, arXiv:1610.06186 [hep-th].

[2] T. Hartman, J. Kruthoff, E. Shaghoulian, and A. Tajdini, "Holography at finite cutoff with a T^2 deformation," *JHEP* **03** (2019) 004, arXiv:1807.11401 [hep-th].

[3] J. Kruthoff, J. de Boer, J. van Wezel, C. L. Kane, and R.-J. Slager, "Topological Classification of Crystalline Insulators through Band Structure Combinatorics," *Phys. Rev. X* **7** (Dec, 2017) 041069. https://link.aps.org/doi/10.1103/PhysRevX.7.041069.

[4] J. Kruthoff, J. de Boer, and J. van Wezel, "Topology in time-reversal symmetric crystals," arXiv:1711.04769 [cond-mat.str-el].

[5] L. Stehouwer, J. de Boer, J. Kruthoff, and H. Posthuma, "Classification of crystalline topological insulators through K-theory," arXiv:1811.02592 [cond-mat.mes-hall].

[6] A. Belin, J. de Boer, and J. Kruthoff, "Comments on a state-operator correspondence for the torus," *SciPost Phys.* **5** (2018) 060, arXiv:1802.00006 [hep-th].

[7] **LIGO Scientific Collaboration and Virgo Collaboration** Collaboration, "Observation of Gravitational Waves from a Binary Black Hole Merger," *Phys. Rev. Lett.* **116** (Feb, 2016) 061102. https://link.aps.org/doi/10.1103/PhysRevLett.116.061102.

[8] N. Arkani-Hamed, L. Motl, A. Nicolis, and C. Vafa, "The string landscape, black holes and gravity as the weakest force," *Journal of High Energy Physics* **2007** no. 06, (Jun, 2007) 060–060. https://doi.org/10.1088%2F1126-6708%2F2007%2F06%2F060.

[9] G. 't Hooft, "Dimensional reduction in quantum gravity," *Conf. Proc.* **C930308** (1993) 284–296, arXiv:gr-qc/9310026 [gr-qc].

[10] J. D. Bekenstein, "Black Holes and Entropy," *Phys. Rev. D* **7** (Apr, 1973) 2333–2346. https://link.aps.org/doi/10.1103/PhysRevD.7.2333.

[11] S. W. Hawking, "Particle creation by black holes," *Communications in Mathematical Physics* **43** no. 3, (Aug, 1975) 199–220. https://doi.org/10.1007/BF02345020.

[12] J. M. Maldacena, "The Large N limit of superconformal field theories and supergravity," *Int.J.Theor.Phys.* **38** (1999) 1113–1133, arXiv:hep-th/9711200 [hep-th].

[13] A. G. Riess, A. V. Filippenko, P. Challis, A. Clocchiatti, A. Diercks, P. M. Garnavich, R. L. Gilliland, C. J. Hogan, S. Jha, R. P. Kirshner, B. Leibundgut, M. M. Phillips, D. Reiss, B. P. Schmidt, R. A. Schommer, R. C. Smith, J. Spyromilio, C. Stubbs, N. B. Suntzeff, and J. Tonry, "Observational Evidence from Supernovae for an Accelerating Universe and a Cosmological Constant," *The Astronomical Journal* **116** no. 3, (Sep, 1998) 1009–1038. https://doi.org/10.1086%2F300499.

[14] S. Perlmutter, G. Aldering, G. Goldhaber, R. A. Knop, P. Nugent, P. G. Castro, S. Deustua, S. Fabbro, A. Goobar, D. E. Groom, I. M. Hook, A. G. Kim, M. Y. Kim, J. C. Lee, N. J. Nunes, R. Pain, C. R. Pennypacker, R. Quimby, C. Lidman, R. S. Ellis, M. Irwin, R. G. McMahon, P. Ruiz-Lapuente, N. Walton, B. Schaefer, B. J. Boyle, A. V. Filippenko, T. Matheson, A. S. Fruchter, N. Panagia, H. J. M. Newberg, W. J. Couch, and T. S. C. Project, "Measurements of Ω and Λ from 42 High-Redshift Supernovae," *The Astrophysical Journal* **517** no. 2, (Jun, 1999) 565–586. https://doi.org/10.1086%2F307221.

[15] A. Strominger, "The dS/CFT correspondence," *Journal of High Energy Physics* **2001** no. 10, (Oct, 2001) 034–034. https://doi.org/10.1088%2F1126-6708%2F2001%2F10%2F034.

[16] D. Anninos, T. Hartman, and A. Strominger, "Higher spin realization of the DS/CFT correspondence," *Classical and Quantum Gravity* **34** no. 1, (Dec, 2016) 015009. https://doi.org/10.1088%2F1361-6382%2F34%2F1%2F015009.

[17] L. McGough, M. Mezei, and H. Verlinde, "Moving the CFT into the bulk with $T\overline{T}$," *JHEP* **04** (2018) 010, arXiv:1611.03470 [hep-th].

[18] J. D. Brown and M. Henneaux, "Central Charges in the Canonical

Realization of Asymptotic Symmetries: An Example from Three-Dimensional Gravity," *Commun. Math. Phys.* **104** (1986) 207–226.

[19] M. Bañados, C. Teitelboim, and J. Zanelli, "Black hole in three-dimensional spacetime," *Phys. Rev. Lett.* **69** (Sep, 1992) 1849–1851. https://link.aps.org/doi/10.1103/PhysRevLett.69.1849.

[20] M. Bañados, M. Henneaux, C. Teitelboim, and J. Zanelli, "Geometry of the 2+1 black hole," *Phys. Rev. D* **48** (Aug, 1993) 1506–1525. https://link.aps.org/doi/10.1103/PhysRevD.48.1506.

[21] J. W. York, "Role of Conformal Three-Geometry in the Dynamics of Gravitation," *Phys. Rev. Lett.* **28** (Apr, 1972) 1082–1085. https://link.aps.org/doi/10.1103/PhysRevLett.28.1082.

[22] G. W. Gibbons and S. W. Hawking, "Action integrals and partition functions in quantum gravity," *Phys. Rev. D* **15** (May, 1977) 2752–2756. https://link.aps.org/doi/10.1103/PhysRevD.15.2752.

[23] V. Balasubramanian and P. Kraus, "A Stress tensor for Anti-de Sitter gravity," *Commun.Math.Phys.* **208** (1999) 413–428, arXiv:hep-th/9902121 [hep-th].

[24] T. Hartman, C. A. Keller, and B. Stoica, "Universal Spectrum of 2d Conformal Field Theory in the Large c Limit," *JHEP* **09** (2014) 118, arXiv:1405.5137 [hep-th].

[25] S. W. Hawking and D. N. Page, "Thermodynamics of black holes in anti-de Sitter space," *Communications in Mathematical Physics* **87** no. 4, (Dec, 1983) 577–588. https://doi.org/10.1007/BF01208266.

[26] J. L. Cardy, "Operator Content of Two-Dimensional Conformally Invariant Theories," *Nucl. Phys.* **B270** (1986) 186–204.

[27] L. Susskind and E. Witten, "The Holographic bound in anti-de Sitter space," arXiv:hep-th/9805114 [hep-th].

[28] X. O. Camanho, J. D. Edelstein, J. Maldacena, and A. Zhiboedov, "Causality Constraints on Corrections to the Graviton Three-Point Coupling," *JHEP* **02** (2016) 020, arXiv:1407.5597 [hep-th].

[29] A. L. Fitzpatrick, J. Kaplan, and M. T. Walters, "Virasoro Conformal Blocks and Thermality from Classical Background Fields," *JHEP* **11** (2015) 200, arXiv:1501.05315 [hep-th].

[30] A. L. Fitzpatrick, J. Kaplan, M. T. Walters, and J. Wang, "Hawking from

Catalan," *JHEP* **05** (2016) 069, arXiv:1510.00014 [hep-th].

[31] A. L. Fitzpatrick and J. Kaplan, "Conformal Blocks Beyond the Semi-Classical Limit," *JHEP* **05** (2016) 075, arXiv:1512.03052 [hep-th].

[32] A. L. Fitzpatrick and J. Kaplan, "A Quantum Correction To Chaos," *JHEP* **05** (2016) 070, arXiv:1601.06164 [hep-th].

[33] A. L. Fitzpatrick, J. Kaplan, D. Li, and J. Wang, "On information loss in AdS_3/CFT_2," *JHEP* **05** (2016) 109, arXiv:1603.08925 [hep-th].

[34] H. Chen, A. L. Fitzpatrick, J. Kaplan, D. Li, and J. Wang, "Degenerate Operators and the $1/c$ Expansion: Lorentzian Resummations, High Order Computations, and Super-Virasoro Blocks," arXiv:1606.02659 [hep-th].

[35] A. Liam Fitzpatrick and J. Kaplan, "On the Late-Time Behavior of Virasoro Blocks and a Classification of Semiclassical Saddles," arXiv:1609.07153 [hep-th].

[36] D. A. Roberts and D. Stanford, "Two-dimensional conformal field theory and the butterfly effect," *Phys. Rev. Lett.* **115** no. 13, (2015) 131603, arXiv:1412.5123 [hep-th].

[37] T. Hartman, "Entanglement Entropy at Large Central Charge," arXiv:1303.6955 [hep-th].

[38] C. T. Asplund, A. Bernamonti, F. Galli, and T. Hartman, "Holographic Entanglement Entropy from 2d CFT: Heavy States and Local Quenches," *JHEP* **02** (2015) 171, arXiv:1410.1392 [hep-th].

[39] C. T. Asplund, A. Bernamonti, F. Galli, and T. Hartman, "Entanglement Scrambling in 2d Conformal Field Theory," *JHEP* **09** (2015) 110, arXiv:1506.03772 [hep-th].

[40] E. Perlmutter, "Bounding the Space of Holographic CFTs with Chaos," *JHEP* **10** (2016) 069, arXiv:1602.08272 [hep-th].

[41] T. Anous, T. Hartman, A. Rovai, and J. Sonner, "Black Hole Collapse in the 1/c Expansion," *JHEP* **07** (2016) 123, arXiv:1603.04856 [hep-th].

[42] P. Kovtun and A. Ritz, "Black holes and universality classes of critical points," *Phys. Rev. Lett.* **100** (2008) 171606, arXiv:0801.2785 [hep-th].

[43] I. Heemskerk, J. Penedones, J. Polchinski, and J. Sully, "Holography from Conformal Field Theory," *JHEP* **10** (2009) 079, arXiv:0907.0151 [hep-th].

[44] S. El-Showk and K. Papadodimas, "Emergent Spacetime and Holographic CFTs," *JHEP* **10** (2012) 106, arXiv:1101.4163 [hep-th].

[45] Z. Komargodski and A. Zhiboedov, "Convexity and Liberation at Large Spin," *JHEP* **11** (2013) 140, arXiv:1212.4103 [hep-th].

[46] A. L. Fitzpatrick, J. Kaplan, D. Poland, and D. Simmons-Duffin, "The Analytic Bootstrap and AdS Superhorizon Locality," *JHEP* **12** (2013) 004, arXiv:1212.3616 [hep-th].

[47] A. L. Fitzpatrick and J. Kaplan, "AdS Field Theory from Conformal Field Theory," *JHEP* **02** (2013) 054, arXiv:1208.0337 [hep-th].

[48] A. L. Fitzpatrick, J. Kaplan, and M. T. Walters, "Universality of Long-Distance AdS Physics from the CFT Bootstrap," *JHEP* **08** (2014) 145, arXiv:1403.6829 [hep-th].

[49] A. L. Fitzpatrick, J. Kaplan, M. T. Walters, and J. Wang, "Eikonalization of Conformal Blocks," *JHEP* **09** (2015) 019, arXiv:1504.01737 [hep-th].

[50] T. Hartman, S. Jain, and S. Kundu, "Causality Constraints in Conformal Field Theory," *JHEP* **05** (2016) 099, arXiv:1509.00014 [hep-th].

[51] J. Maldacena, D. Simmons-Duffin, and A. Zhiboedov, "Looking for a bulk point," arXiv:1509.03612 [hep-th].

[52] L. F. Alday, A. Bissi, and T. Lukowski, "Lessons from crossing symmetry at large N," *JHEP* **06** (2015) 074, arXiv:1410.4717 [hep-th].

[53] N. Benjamin, M. C. N. Cheng, S. Kachru, G. W. Moore, and N. M. Paquette, "Elliptic Genera and 3d Gravity," *Annales Henri Poincare* **17** no. 10, (2016) 2623–2662, arXiv:1503.04800 [hep-th].

[54] E. Shaghoulian, "Modular forms and a generalized Cardy formula in higher dimensions," *Phys. Rev.* **D93** no. 12, (2016) 126005, arXiv:1508.02728 [hep-th].

[55] E. Shaghoulian, "Black hole microstates in AdS," *Phys. Rev.* **D94** no. 10, (2016) 104044, arXiv:1512.06855 [hep-th].

[56] L. J. Dixon, D. Friedan, E. J. Martinec, and S. H. Shenker, "The Conformal Field Theory of Orbifolds," *Nucl. Phys.* **B282** (1987) 13–73.

[57] R. Dijkgraaf, G. W. Moore, E. P. Verlinde, and H. L. Verlinde, "Elliptic genera of symmetric products and second quantized strings," *Commun. Math. Phys.* **185** (1997) 197–209, arXiv:hep-th/9608096 [hep-th].

[58] P. Bantay, "Characters and modular properties of permutation orbifolds," *Phys. Lett.* **B419** (1998) 175–178, arXiv:hep-th/9708120 [hep-th].

[59] P. Bantay, "Symmetric products, permutation orbifolds and discrete torsion," *Lett. Math. Phys.* **63** (2003) 209–218, arXiv:hep-th/0004025 [hep-th].

[60] O. Lunin and S. D. Mathur, "Correlation functions for M^N/S_N orbifolds," *Commun. Math. Phys.* **219** (2001) 399–442, arXiv:hep-th/0006196 [hep-th].

[61] A. Pakman, L. Rastelli, and S. S. Razamat, "Diagrams for Symmetric Product Orbifolds," *JHEP* **10** (2009) 034, arXiv:0905.3448 [hep-th].

[62] C. A. Keller, "Phase transitions in symmetric orbifold CFTs and universality," *JHEP* **03** (2011) 114, arXiv:1101.4937 [hep-th].

[63] J. de Boer, "Six-dimensional supergravity on $S^3 \times AdS_3$ and 2-D conformal field theory," *Nucl. Phys.* **B548** (1999) 139–166, arXiv:hep-th/9806104 [hep-th].

[64] R. Dijkgraaf, "Instanton strings and hyperKahler geometry," *Nucl. Phys.* **B543** (1999) 545–571, arXiv:hep-th/9810210 [hep-th].

[65] N. Seiberg and E. Witten, "The D1 / D5 system and singular CFT," *JHEP* **04** (1999) 017, arXiv:hep-th/9903224 [hep-th].

[66] S. M. Trott, "A pair of generators for the unimodular group," *Canad. Math. Bull.* **5** (1962) .

[67] R. C. Myers, "Stress tensors and Casimir energies in the AdS / CFT correspondence," *Phys.Rev.* **D60** (1999) 046002, arXiv:hep-th/9903203 [hep-th].

[68] G. T. Horowitz and R. C. Myers, "The AdS / CFT correspondence and a new positive energy conjecture for general relativity," *Phys. Rev.* **D59** (1998) 026005, arXiv:hep-th/9808079 [hep-th].

[69] A. Belin, C. A. Keller, and A. Maloney, "Permutation Orbifolds in the large N Limit," arXiv:1509.01256 [hep-th].

[70] F. M. Haehl and M. Rangamani, "Permutation orbifolds and holography," *JHEP* **03** (2015) 163, arXiv:1412.2759 [hep-th].

[71] A. Belin, C. A. Keller, and A. Maloney, "String Universality for Permutation Orbifolds," *Phys. Rev.* **D91** no. 10, (2015) 106005, arXiv:1412.7159 [hep-th].

[72] N. Benjamin, S. Kachru, C. A. Keller, and N. M. Paquette, "Emergent space-time and the supersymmetric index," *JHEP* **05** (2016) 158, arXiv:1512.00010 [hep-th].

[73] P. H. Ginsparg, "APPLIED CONFORMAL FIELD THEORY," in *Les Houches Summer School in Theoretical Physics: Fields, Strings, Critical Phenomena Les Houches, France, June 28-August 5, 1988*, pp. 1–168. 1988. arXiv:hep-th/9108028 [hep-th]. https://inspirehep.net/record/265020/files/arXiv:hep-th_9108028.pdf.

[74] P. J. Cameron, *Oligomorphic permutation groups*, vol. 152 of *London Mathematical Society Lecture Note Series*. Cambridge University Press, Cambridge, 1990. http://dx.doi.org/10.1017/CBO9780511549809.

[75] P. J. Cameron, "Oligomorphic permutation groups," in *Perspectives in mathematical sciences. II*, vol. 8 of *Stat. Sci. Interdiscip. Res.*, pp. 37–61. World Sci. Publ., Hackensack, NJ, 2009. http://dx.doi.org/10.1142/9789814273657_0003.

[76] P. J. Cameron, "Transitivity of permutation groups on unordered sets," *Math. Z.* **148** no. 2, (1976) 127–139.

[77] D. Goldfeld, *Automorphic Forms and L-Functions for the Group GL(n,R)*. Cambridge Studies in Advanced Mathematics. Cambridge University Press, 2006. https://books.google.nl/books?id=QOHckFMXObMC.

[78] M. J. Park, C. Fang, B. A. Bernevig, and M. J. Gilbert, "Modular Anomalies in (2+1) and (3+1)-D Edge Theories," arXiv:1604.00407 [cond-mat.str-el].

[79] J. L. Cardy, "Operator content and modular properties of higher dimensional conformal field theories," *Nucl. Phys.* **B366** (1991) 403–419.

[80] S. Hellerman, "A Universal Inequality for CFT and Quantum Gravity," *JHEP* **08** (2011) 130, arXiv:0902.2790 [hep-th].

[81] S. Hellerman and C. Schmidt-Colinet, "Bounds for State Degeneracies in 2D Conformal Field Theory," *JHEP* **08** (2011) 127, arXiv:1007.0756 [hep-th].

[82] D. Friedan and C. A. Keller, "Constraints on 2d CFT partition functions," *JHEP* **10** (2013) 180, arXiv:1307.6562 [hep-th].

[83] J. D. Qualls and A. D. Shapere, "Bounds on Operator Dimensions in 2D Conformal Field Theories," *JHEP* **05** (2014) 091, arXiv:1312.0038 [hep-th].

[84] J. D. Qualls, "Universal Bounds in Even-Spin CFTs," *JHEP* **12** (2015) 001, arXiv:1412.0383 [hep-th].

[85] N. Benjamin, E. Dyer, A. L. Fitzpatrick, and S. Kachru, "Universal Bounds on Charged States in 2d CFT and 3d Gravity," *JHEP* **08** (2016) 041, arXiv:1603.09745 [hep-th].

[86] S. Collier, Y.-H. Lin, and X. Yin, "Modular Bootstrap Revisited," arXiv:1608.06241 [hep-th].

[87] L.-Y. Hung, R. C. Myers, M. Smolkin, and A. Yale, "Holographic Calculations of Renyi Entropy," *JHEP* **1112** (2011) 047, arXiv:1110.1084 [hep-th].

[88] L.-Y. Hung, R. C. Myers, and M. Smolkin, "Twist operators in higher dimensions," *JHEP* **1410** (2014) 178, arXiv:1407.6429 [hep-th].

[89] J. de Boer, E. Verlinde, and H. Verlinde, "On the holographic renormalization group," *Journal of High Energy Physics* **2000** no. 08, (2000) 003. http://stacks.iop.org/1126-6708/2000/i=08/a=003.

[90] M. Bianchi, D. Z. Freedman, and K. Skenderis, "Holographic renormalization," *Nucl. Phys.* **B631** (2002) 159–194, arXiv:hep-th/0112119 [hep-th].

[91] I. Heemskerk and J. Polchinski, "Holographic and Wilsonian Renormalization Groups," *JHEP* **06** (2011) 031, arXiv:1010.1264 [hep-th].

[92] T. Faulkner, H. Liu, and M. Rangamani, "Integrating out geometry: Holographic Wilsonian RG and the membrane paradigm," *JHEP* **08** (2011) 051, arXiv:1010.4036 [hep-th].

[93] V. Balasubramanian, M. Guica, and A. Lawrence, "Holographic Interpretations of the Renormalization Group," *JHEP* **01** (2013) 115, arXiv:1211.1729 [hep-th].

[94] S.-S. Lee, "Quantum Renormalization Group and Holography," *JHEP* **01** (2014) 076, arXiv:1305.3908 [hep-th].

[95] A. B. Zamolodchikov, "Expectation value of composite field T anti-T in two-dimensional quantum field theory," arXiv:hep-th/0401146 [hep-th].

[96] F. Smirnov and A. Zamolodchikov, "On space of integrable quantum field theories," *Nuclear Physics B* **915** (2017) 363 – 383, http:

//www.sciencedirect.com/science/article/pii/S0550321316304126.

[97] A. CavagliÃă, S. Negro, I. M. SzÃľcsÃľnyi, and R. Tateo, "$T\bar{T}$-deformed 2D Quantum Field Theories," *JHEP* **10** (2016) 112, arXiv:1608.05534 [hep-th].

[98] S. Dubovsky, V. Gorbenko, and M. Mirbabayi, "Asymptotic fragility, near AdS_2 holography and $T\overline{T}$," *JHEP* **09** (2017) 136, arXiv:1706.06604 [hep-th].

[99] V. Shyam, "Background independent holographic dual to $T\bar{T}$ deformed CFT with large central charge in 2 dimensions," *JHEP* **10** (2017) 108, arXiv:1707.08118 [hep-th].

[100] P. Kraus, J. Liu, and D. Marolf, "Cutoff AdS_3 versus the $T\bar{T}$ deformation," arXiv:1801.02714 [hep-th].

[101] J. Cardy, "The $T\overline{T}$ deformation of quantum field theory as a stochastic process," arXiv:1801.06895 [hep-th].

[102] O. Aharony and T. Vaknin, "The TT* deformation at large central charge," arXiv:1803.00100 [hep-th].

[103] S. Dubovsky, V. Gorbenko, and G. HernÃąndez-Chifflet, "$T\bar{T}$ Partition Function from Topological Gravity," arXiv:1805.07386 [hep-th].

[104] W. Donnelly and V. Shyam, "Entanglement entropy and $T\overline{T}$ deformation," arXiv:1806.07444 [hep-th].

[105] G. Bonelli, N. Doroud, and M. Zhu, "$T\bar{T}$-deformations in closed form," *JHEP* **06** (2018) 149, arXiv:1804.10967 [hep-th].

[106] B. Chen, L. Chen, and P.-x. Hao, "Entanglement Entropy in $T\overline{T}$-Deformed CFT," arXiv:1807.08293 [hep-th].

[107] D. Marolf and M. Rangamani, "Causality and the AdS Dirichlet problem," *JHEP* **04** (2012) 035, arXiv:1201.1233 [hep-th].

[108] T. Andrade, W. R. Kelly, D. Marolf, and J. E. Santos, "On the stability of gravity with Dirichlet walls," *Class. Quant. Grav.* **32** no. 23, (2015) 235006, arXiv:1504.07580 [gr-qc].

[109] J. Cardy, "Quantum Quenches to a Critical Point in One Dimension: some further results," *J. Stat. Mech.* **1602** no. 2, (2016) 023103, arXiv:1507.07266 [cond-mat.stat-mech].

[110] M. J. Duff, T. Inami, C. N. Pope, E. Sezgin, and K. S. Stelle, "Semiclassical

Quantization of the Supermembrane," *Nucl. Phys.* **B297** (1988) 515–538.

[111] S. Fubini, A. J. Hanson, and R. Jackiw, "New approach to field theory," *Phys. Rev.* **D7** (1973) 1732–1760.

[112] A. Strumia and G. Venturi, "Are Hadrons Strings?," *Lett. Nuovo Cim.* **13** (1975) 337.

[113] E. Alvarez and T. Ortin, "Asymptotic density of states of p-branes," *Mod. Phys. Lett.* **A7** (1992) 2889–2894.

[114] G. Giribet, "$T\bar{T}$-deformations, AdS/CFT and correlation functions," *JHEP* **02** (2018) 114, arXiv:1711.02716 [hep-th].

[115] A. Giveon, N. Itzhaki, and D. Kutasov, "A solvable irrelevant deformation of AdS_3/CFT_2," *JHEP* **12** (2017) 155, arXiv:1707.05800 [hep-th].

[116] A. Giveon, N. Itzhaki, and D. Kutasov, "$T\overline{T}$ and LST," *JHEP* **07** (2017) 122, arXiv:1701.05576 [hep-th].

[117] M. Asrat, A. Giveon, N. Itzhaki, and D. Kutasov, "Holography Beyond AdS," *Nucl. Phys.* **B932** (2018) 241–253, arXiv:1711.02690 [hep-th].

[118] S. Chakraborty, A. Giveon, N. Itzhaki, and D. Kutasov, "Entanglement Beyond AdS," arXiv:1805.06286 [hep-th].

[119] S. de Haro, K. Skenderis, and S. N. Solodukhin, "Holographic Reconstruction of Spacetime and Renormalization in the AdS/CFT Correspondence," *Communications in Mathematical Physics* **217** no. 3, (Mar, 2001) 595–622. https://doi.org/10.1007/s002200100381.

[120] D. Martelli and W. Mueck, "Holographic renormalization and Ward identities with the Hamilton-Jacobi method," *Nucl. Phys.* **B654** (2003) 248–276, arXiv:hep-th/0205061 [hep-th].

[121] E. Mintun and J. Polchinski, "Higher Spin Holography, RG, and the Light Cone," arXiv:1411.3151 [hep-th].

[122] M. Caselle, D. Fioravanti, F. Gliozzi, and R. Tateo, "Quantisation of the effective string with TBA," *JHEP* **07** (2013) 071, arXiv:1305.1278 [hep-th].

[123] M. Taylor, "TT deformations in general dimensions," arXiv:1805.10287 [hep-th].

[124] I. G. Avramidi and G. Esposito, "Lack of strong ellipticity in Euclidean quantum gravity," *Class. Quant. Grav.* **15** (1998) 1141–1152,

arXiv:hep-th/9708163 [hep-th].

[125] G. Mandal and P. Nayak, "Revisiting AdS/CFT at a finite radial cut-off," *JHEP* **12** (2016) 125, arXiv:1608.00411 [hep-th].

[126] V. Balasubramanian and P. Kraus, "A Stress Tensor for Anti-de Sitter Gravity," *Communications in Mathematical Physics* **208** no. 2, (Dec, 1999) 413–428. https://doi.org/10.1007/s002200050764.

[127] M. Henningson and K. Skenderis, "The holographic Weyl anomaly," *Journal of High Energy Physics* **1998** no. 07, (1998) 023. http://stacks.iop.org/1126-6708/1998/i=07/a=023.

[128] E. Shaghoulian, "Emergent gravity from Eguchi-Kawai reduction," *JHEP* **03** (2017) 011, arXiv:1611.04189 [hep-th].

[129] D. Brattan, J. Camps, R. Loganayagam, and M. Rangamani, "CFT dual of the AdS Dirichlet problem: fluid/gravity on cut-off surfaces," *Journal of High Energy Physics* **2011** no. 12, (Dec, 2011) 90. https://doi.org/10.1007/JHEP12(2011)090.

[130] A. Bzowski, P. McFadden, and K. Skenderis, "Implications of conformal invariance in momentum space," *Journal of High Energy Physics* **2014** no. 3, (Mar, 2014) 111. https://doi.org/10.1007/JHEP03(2014)111.

[131] W. Mück and K. S. Viswanathan, "Conformal field theory correlators from classical field theory on anti–de Sitter space: Vector and spinor fields," *Phys. Rev. D* **58** (Oct, 1998) 106006. https://link.aps.org/doi/10.1103/PhysRevD.58.106006.

[132] W. Mueck and K. S. Viswanathan, "The Graviton in the AdS-CFT correspondence: Solution via the Dirichlet boundary value problem," arXiv:hep-th/9810151 [hep-th].

[133] K. Jensen, "Chaos in AdS_2 Holography," *Phys. Rev. Lett.* **117** no. 11, (2016) 111601, arXiv:1605.06098 [hep-th].

[134] J. Maldacena, D. Stanford, and Z. Yang, "Conformal symmetry and its breaking in two dimensional Nearly Anti-de-Sitter space," *PTEP* **2016** no. 12, (2016) 12C104, arXiv:1606.01857 [hep-th].

[135] J. Engelsöy, T. G. Mertens, and H. Verlinde, "An investigation of AdS_2 backreaction and holography," *JHEP* **07** (2016) 139, arXiv:1606.03438 [hep-th].

[136] J. M. Maldacena, "Non-Gaussian features of primordial fluctuations in

single field inflationary models," *JHEP* **05** (2003) 013, arXiv:astro-ph/0210603 [astro-ph].

[137] L. D. Landau, "On the theory of phase transitions," *Zh. Eksp. Teor. Fiz.* **7** (1937) 19–32. [Ukr. J. Phys.53,25(2008)].

[138] K. v. Klitzing, G. Dorda, and M. Pepper, "New Method for High-Accuracy Determination of the Fine-Structure Constant Based on Quantized Hall Resistance," *Phys. Rev. Lett.* **45** (Aug, 1980) 494–497. https://link.aps.org/doi/10.1103/PhysRevLett.45.494.

[139] T. Ando, Y. Matsumoto, and Y. Uemura, "Theory of Hall Effect in a Two-Dimensional Electron System," *Journal of the Physical Society of Japan* **39** no. 2, (1975) 279–288, https://doi.org/10.1143/JPSJ.39.279. https://doi.org/10.1143/JPSJ.39.279.

[140] H. Aoki and T. Ando, "Effect of localization on the hall conductivity in the two-dimensional system in strong magnetic fields," *Solid State Communications* **38** no. 11, (1981) 1079 – 1082. http://www.sciencedirect.com/science/article/pii/0038109881900211.

[141] D. J. Thouless, M. Kohmoto, M. P. Nightingale, and M. den Nijs, "Quantized Hall Conductance in a Two-Dimensional Periodic Potential," *Phys. Rev. Lett.* **49** (Aug, 1982) 405–408. http://link.aps.org/doi/10.1103/PhysRevLett.49.405.

[142] H. Aoki and T. Ando, "Quantum Hall Effect: From the Winding Number to the Flow Diagram," in *High Magnetic Fields in Semiconductor Physics*, G. Landwehr, ed., pp. 45–48. Springer Berlin Heidelberg, Berlin, Heidelberg, 1987.

[143] X.-L. Qi, Y.-S. Wu, and S.-C. Zhang, "Topological quantization of the spin Hall effect in two-dimensional paramagnetic semiconductors," *Phys. Rev. B* **74** (Aug, 2006) 085308. https://link.aps.org/doi/10.1103/PhysRevB.74.085308.

[144] R. Jackiw and C. Rebbi, "Solitons with fermion number $\frac{1}{2}$," *Phys. Rev. D* **13** (Jun, 1976) 3398–3409. https://link.aps.org/doi/10.1103/PhysRevD.13.3398.

[145] G. V. Dunne, "Aspects of Chern-Simons theory," in *Topological Aspects of Low-dimensional Systems: Proceedings, Les Houches Summer School of Theoretical Physics, Session 69: Les Houches, France, July 7-31 1998*. 1998. arXiv:hep-th/9902115 [hep-th].

[146] A. P. Schnyder, S. Ryu, A. Furusaki, and A. W. W. Ludwig, "Classification of topological insulators and superconductors in three spatial dimensions," *Phys. Rev. B* **78** (Nov, 2008) 195125. https://link.aps.org/doi/10.1103/PhysRevB.78.195125.

[147] D. Tong, "Lectures on the Quantum Hall Effect," 2016. arXiv:1606.06687 [hep-th].

[148] F. J. Dyson, "The Threefold Way. Algebraic Structure of Symmetry Groups and Ensembles in Quantum Mechanics," *Journal of Mathematical Physics* **3** no. 6, (1962) 1199–1215, https://doi.org/10.1063/1.1703863. https://doi.org/10.1063/1.1703863.

[149] A. Altland and M. R. Zirnbauer, "Nonstandard symmetry classes in mesoscopic normal-superconducting hybrid structures," *Physical Review B* **55** no. 2, (1997) 1142.

[150] A. Kitaev, "Periodic table for topological insulators and superconductors," *AIP Conference Proceedings* **1134** no. 1, (2009) 22–30. http://scitation.aip.org/content/aip/proceeding/aipcp/10.1063/1.3149495;jsessionid=SQkiPEQz8V-aPjnkBpe3PaSG.x-aip-live-06.

[151] S. Ryu, A. P. Schnyder, A. Furusaki, and A. W. W. Ludwig, "Topological insulators and superconductors: tenfold way and dimensional hierarchy," *New Journal of Physics* **12** no. 6, (2010) 065010. http://stacks.iop.org/1367-2630/12/i=6/a=065010.

[152] A. Altland and M. R. Zirnbauer, "Nonstandard symmetry classes in mesoscopic normal-superconducting hybrid structures," *Phys. Rev. B* **55** (Jan, 1997) 1142–1161. http://link.aps.org/doi/10.1103/PhysRevB.55.1142.

[153] L. Fu, C. L. Kane, and E. J. Mele, "Topological Insulators in Three Dimensions," *Phys. Rev. Lett.* **98** (Mar, 2007) 106803. http://link.aps.org/doi/10.1103/PhysRevLett.98.106803.

[154] J. E. Moore and L. Balents, "Topological invariants of time-reversal-invariant band structures," *Phys. Rev. B* **75** (Mar, 2007) 121306. http://link.aps.org/doi/10.1103/PhysRevB.75.121306.

[155] R.-J. Slager, A. Mesaros, V. Juricic, and J. Zaanen, "The space group classification of topological band-insulators," *Nat Phys* **9** no. 2, (02, 2013) 98–102. http://dx.doi.org/10.1038/nphys2513.

[156] Y. Ran, Y. Zhang, and A. Vishwanath, "One-dimensional topologically

protected modes in topological insulators with lattice dislocations," *Nat Phys* **5** no. 4, (04, 2009) 298–303. http://dx.doi.org/10.1038/nphys1220.

[157] J. C. Y. Teo and C. L. Kane, "Topological defects and gapless modes in insulators and superconductors," *Phys. Rev. B* **82** (Sep, 2010) 115120. http://link.aps.org/doi/10.1103/PhysRevB.82.115120.

[158] V. Juričić, A. Mesaros, R.-J. Slager, and J. Zaanen, "Universal Probes of Two-Dimensional Topological Insulators: Dislocation and π Flux," *Phys. Rev. Lett.* **108** (Mar, 2012) 106403. http://link.aps.org/doi/10.1103/PhysRevLett.108.106403.

[159] R.-J. Slager, A. Mesaros, V. Juričić, and J. Zaanen, "Interplay between electronic topology and crystal symmetry: Dislocation-line modes in topological band insulators," *Phys. Rev. B* **90** (Dec, 2014) 241403. http://link.aps.org/doi/10.1103/PhysRevB.90.241403.

[160] R.-J. Slager, L. Rademaker, J. Zaanen, and L. Balents, "Impurity-bound states and Green's function zeros as local signatures of topology," *Phys. Rev. B* **92** (Aug, 2015) 085126. http://link.aps.org/doi/10.1103/PhysRevB.92.085126.

[161] R.-J. Slager, V. Juričić, V. Lahtinen, and J. Zaanen, "Self-organized pseudo-graphene on grain boundaries in topological band insulators," *Phys. Rev. B* **93** (Jun, 2016) 245406. http://link.aps.org/doi/10.1103/PhysRevB.93.245406.

[162] L. Fu, "Topological Crystalline Insulators," *Phys. Rev. Lett.* **106** (Mar, 2011) 106802. http://link.aps.org/doi/10.1103/PhysRevLett.106.106802.

[163] C. Fang, M. J. Gilbert, and B. A. Bernevig, "Bulk topological invariants in noninteracting point group symmetric insulators," *Phys. Rev. B* **86** (Sep, 2012) 115112. http://link.aps.org/doi/10.1103/PhysRevB.86.115112.

[164] A. Alexandradinata and B. A. Bernevig, "Berry-phase description of topological crystalline insulators," *Phys. Rev. B* **93** (May, 2016) 205104. http://link.aps.org/doi/10.1103/PhysRevB.93.205104.

[165] Z. Wang, A. Alexandradinata, R. J. Cava, and B. A. Bernevig, "Hourglass fermions," *Nature* **532** no. 7598, (04, 2016) 189–194. http://dx.doi.org/10.1038/nature17410.

[166] B. Bradlyn, J. Cano, Z. Wang, M. G. Vergniory, C. Felser, R. J. Cava, and

B. A. Bernevig, "Beyond Dirac and Weyl fermions: Unconventional quasiparticles in conventional crystals," *Science* **353** no. 6299, (2016) . http://science.sciencemag.org/content/353/6299/aaf5037.

[167] J. C. Y. Teo and T. L. Hughes, "Existence of Majorana-Fermion Bound States on Disclinations and the Classification of Topological Crystalline Superconductors in Two Dimensions," *Phys. Rev. Lett.* **111** (Jul, 2013) 047006. https://link.aps.org/doi/10.1103/PhysRevLett.111.047006.

[168] C.-K. Chiu, H. Yao, and S. Ryu, "Classification of topological insulators and superconductors in the presence of reflection symmetry," *Phys. Rev. B* **88** (Aug, 2013) 075142. https://link.aps.org/doi/10.1103/PhysRevB.88.075142.

[169] T. Morimoto and A. Furusaki, "Topological classification with additional symmetries from Clifford algebras," *Phys. Rev. B* **88** (Sep, 2013) 125129. https://link.aps.org/doi/10.1103/PhysRevB.88.125129.

[170] K. Shiozaki and M. Sato, "Topology of crystalline insulators and superconductors," *Phys. Rev. B* **90** (Oct, 2014) 165114. https://link.aps.org/doi/10.1103/PhysRevB.90.165114.

[171] C.-X. Liu, R.-X. Zhang, and B. K. VanLeeuwen, "Topological nonsymmorphic crystalline insulators," *Phys. Rev. B* **90** (Aug, 2014) 085304. https://link.aps.org/doi/10.1103/PhysRevB.90.085304.

[172] K. Shiozaki, M. Sato, and K. Gomi, "Topology of nonsymmorphic crystalline insulators and superconductors," *Phys. Rev. B* **93** (May, 2016) 195413. https://link.aps.org/doi/10.1103/PhysRevB.93.195413.

[173] X. Wan, A. M. Turner, A. Vishwanath, and S. Y. Savrasov, "Topological semimetal and Fermi-arc surface states in the electronic structure of pyrochlore iridates," *Phys. Rev. B* **83** (May, 2011) 205101. http://link.aps.org/doi/10.1103/PhysRevB.83.205101.

[174] S.-Y. Xu, I. Belopolski, D. S. Sanchez, C. Zhang, G. Chang, C. Guo, G. Bian, Z. Yuan, H. Lu, T.-R. Chang, P. P. Shibayev, M. L. Prokopovych, N. Alidoust, H. Zheng, C.-C. Lee, S.-M. Huang, R. Sankar, F. Chou, C.-H. Hsu, H.-T. Jeng, A. Bansil, T. Neupert, V. N. Strocov, H. Lin, S. Jia, and M. Z. Hasan, "Experimental discovery of a topological Weyl semimetal state in TaP," *Science Advances* **1** no. 10, (2015) . http://advances.sciencemag.org/content/1/10/e1501092.

[175] B. Q. Lv, H. M. Weng, B. B. Fu, X. P. Wang, H. Miao, J. Ma, P. Richard, X. C. Huang, L. X. Zhao, G. F. Chen, Z. Fang, X. Dai, T. Qian, and

H. Ding, "Experimental Discovery of Weyl Semimetal TaAs," *Phys. Rev. X* **5** (Jul, 2015) 031013. http://link.aps.org/doi/10.1103/PhysRevX.5.031013.

[176] B. Q. Lv, N. Xu, H. M. Weng, J. Z. Ma, P. Richard, X. C. Huang, L. X. Zhao, G. F. Chen, C. E. Matt, F. Bisti, V. N. Strocov, J. Mesot, Z. Fang, X. Dai, T. Qian, M. Shi, and H. Ding, "Observation of Weyl nodes in TaAs," *Nat Phys* **11** no. 9, (09, 2015) 724–727. http://dx.doi.org/10.1038/nphys3426.

[177] S. M. Young, S. Zaheer, J. C. Y. Teo, C. L. Kane, E. J. Mele, and A. M. Rappe, "Dirac Semimetal in Three Dimensions," *Phys. Rev. Lett.* **108** (Apr, 2012) 140405. http://link.aps.org/doi/10.1103/PhysRevLett.108.140405.

[178] C. Fang, M. J. Gilbert, X. Dai, and B. A. Bernevig, "Multi-Weyl Topological Semimetals Stabilized by Point Group Symmetry," *Phys. Rev. Lett.* **108** (Jun, 2012) 266802. http://link.aps.org/doi/10.1103/PhysRevLett.108.266802.

[179] S. M. Young and C. L. Kane, "Dirac Semimetals in Two Dimensions," *Phys. Rev. Lett.* **115** (Sep, 2015) 126803. http://link.aps.org/doi/10.1103/PhysRevLett.115.126803.

[180] T. Hahn, *The 17 plane groups (two-dimensional space groups)*, pp. 92–109. Springer Netherlands, Dordrecht, 2002.

[181] D. S. Freed and G. W. Moore, "Twisted Equivariant Matter," *Annales Henri Poincaré* **14** no. 8, (2013) 1927–2023. http://dx.doi.org/10.1007/s00023-013-0236-x.

[182] L. P. Bouckaert, R. Smoluchowski, and E. Wigner, "Theory of Brillouin Zones and Symmetry Properties of Wave Functions in Crystals," *Phys. Rev.* **50** (Jul, 1936) 58–67. http://link.aps.org/doi/10.1103/PhysRev.50.58.

[183] J. E. Avron and R. Seiler, "Quantization of the Hall Conductance for General, Multiparticle Schrödinger Hamiltonians," *Phys. Rev. Lett.* **54** (Jan, 1985) 259–262. http://link.aps.org/doi/10.1103/PhysRevLett.54.259.

[184] A. Alexandradinata, C. Fang, M. J. Gilbert, and B. A. Bernevig, "Spin-Orbit-Free Topological Insulators without Time-Reversal Symmetry," *Phys. Rev. Lett.* **113** (Sep, 2014) 116403. https://link.aps.org/doi/10.1103/PhysRevLett.113.116403.

[185] L. Fu and C. L. Kane, "Time reversal polarization and a Z_2 adiabatic spin pump," *Phys. Rev. B* **74** (Nov, 2006) 195312. https://link.aps.org/doi/10.1103/PhysRevB.74.195312.

[186] C. L. Kane and E. J. Mele, "Quantum Spin Hall Effect in Graphene," *Phys. Rev. Lett.* **95** (Nov, 2005) 226801. https://link.aps.org/doi/10.1103/PhysRevLett.95.226801.

[187] A. Lau, J. van den Brink, and C. Ortix, "Topological mirror insulators in one dimension," *Phys. Rev. B* **94** (Oct, 2016) 165164. https://link.aps.org/doi/10.1103/PhysRevB.94.165164.

[188] G. De Nittis and K. Gomi, "Classification of "Quaternionic" Bloch-Bundles," *Communications in Mathematical Physics* **339** no. 1, (2015) 1–55. http://dx.doi.org/10.1007/s00220-015-2390-0.

[189] L. Fu, C. L. Kane, and E. J. Mele, "Topological Insulators in Three Dimensions," *Phys. Rev. Lett.* **98** (Mar, 2007) 106803. https://link.aps.org/doi/10.1103/PhysRevLett.98.106803.

[190] R. Roy, "$\mathbf{Z}_2$ classification of quantum spin Hall systems: An approach using time-reversal invariance," *Physical Review B* **79** no. 19, (2009) 195321.

[191] S.-S. Lee and S. Ryu, "Many-Body Generalization of the Z_2 Topological Invariant for the Quantum Spin Hall Effect," *Phys. Rev. Lett.* **100** (May, 2008) 186807. https://link.aps.org/doi/10.1103/PhysRevLett.100.186807.

[192] V. Juričić, A. Mesaros, R.-J. Slager, and J. Zaanen, "Universal Probes of Two-Dimensional Topological Insulators: Dislocation and π Flux," *Phys. Rev. Lett.* **108** (2012) 106403. https://link.aps.org/doi/10.1103/PhysRevLett.108.106403.

[193] C. Fang, M. J. Gilbert, and B. A. Bernevig, "Bulk Topological Invariants in Noninteracting Point Group Symmetric Insulators," *Phys. Rev. B* **86** (2012) 115112.

[194] C. Bradley and A. Cracknell, *The mathematical theory of symmetry in solids: representation theory for point groups and space groups*. Clarendon Press, 1972. https://books.google.nl/books?id=OKXvAAAAMAAJ.

[195] W. Lück and R. Stamm, "Computations of K-and L-theory of cocompact planar groups," *K-theory* **21** no. 3, (2000) 249–292.

[196] M. Yang, *Crossed products by finite groups acting on low dimensional complexes and applications*. Phd thesis, University of Saskatchewan, 1997.

http://hdl.handle.net/10388/etd-10212004-000606.

[197] N. Phillips, *Equivariant K-theory for proper actions*. Longman Scientific & Technical, Essex, 1989.

[198] J. C. Y. Teo, L. Fu, and C. L. Kane, "Surface states and topological invariants in three-dimensional topological insulators: Application to $Bi_{1-x}Sb_x$," *Phys. Rev. B* **78** (Jul, 2008) 045426. http://link.aps.org/doi/10.1103/PhysRevB.78.045426.

[199] L. Fu and C. L. Kane, "Topological insulators with inversion symmetry," *Phys. Rev. B* **76** (Jul, 2007) 045302. https://link.aps.org/doi/10.1103/PhysRevB.76.045302.

[200] P. Hořava, "Stability of Fermi Surfaces and K-Theory," *Phys. Rev. Lett.* **95** (Jun, 2005) 016405. https://link.aps.org/doi/10.1103/PhysRevLett.95.016405.

[201] K. Shiozaki, M. Sato, and K. Gomi, "Atiyah-Hirzebruch Spectral Sequence in Band Topology: General Formalism and Topological Invariants for 230 Space Groups," arXiv:1802.06694 [cond-mat.str-el].

[202] K. Shiozaki, C. Z. Xiong, and K. Gomi, "Generalized homology and Atiyah-Hirzebruch spectral sequence in crystalline symmetry protected topological phenomena," arXiv:1810.00801 [cond-mat.str-el].

[203] C.-K. Chiu, H. Yao, and S. Ryu, "Classification of topological insulators and superconductors in the presence of reflection symmetry," *Phys. Rev. B* **88** (Aug, 2013) 075142. https://link.aps.org/doi/10.1103/PhysRevB.88.075142.

[204] M. F. Atiyah, "K-theory and reality," *The Quarterly Journal of Mathematics* **17** no. 1, (1966) 367–386.

[205] W. Lück and B. Oliver, "Chern characters for the equivariant K-theory of proper G-CW-complexes," in *Cohomological methods in homotopy theory*, pp. 217–247. Springer, 2001.

[206] F. Hirzebruch and T. Höfer, "On the Euler number of an orbifold," *Mathematische Annalen* **286** no. 1-3, (1990) 255–260.

[207] A. Adem and Y.-b. Ruan, "Twisted orbifold K theory," *Commun. Math. Phys.* **237** (2003) 533–556, arXiv:math/0107168 [math-at].

[208] K. Gomi, "Freed-Moore K-theory," *arXiv preprint arXiv:1705.09134* (2017) .

[209] G. E. Bredon, *Equivariant cohomology theories*, vol. 34. Springer, 2006.

[210] A. Hatcher, "Algebraic topology. 2002," *Cambridge UP, Cambridge* **606** no. 9, (2002) .

[211] A. Lau, J. van den Brink, and C. Ortix, "Topological mirror insulators in one dimension," *Phys. Rev. B* **94** (Oct, 2016) 165164. https://link.aps.org/doi/10.1103/PhysRevB.94.165164.

[212] L. Fu, "Topological Crystalline Insulators," *Phys. Rev. Lett.* **106** (Mar, 2011) 106802. https://link.aps.org/doi/10.1103/PhysRevLett.106.106802.

[213] C. Dwyer, "Twisted equivariant K-theory for proper actions of discrete groups," *K-Theory* **38** no. 2, (2008) 95–111.

[214] N. Bárcenas, J. Espinoza, B. Uribe, and M. Velásquez, "Segal's spectral sequence in twisted equivariant K-theory for proper and discrete actions," *Proceedings of the Edinburgh Mathematical Society* (2018) 1–30.

[215] G. Segal, "Equivariant K-theory," *Publications mathématiques de l'IHÉS* **34** no. 1, (1968) 129–151.

[216] E. A. McAlister, *Noncommutative CW-complexes arising from crystallographic groups and their K-theory*. PhD thesis, University of Colorado, 2005.

[217] J.-H. Cho, "A Survey on equivariant K-theory of representation spheres," *Trends in Mathematics* **4** no. 1, (2001) 84–89.

[218] M. Atiyah and G. Segal, "Twisted K-theory," *arXiv preprint math/0407054* (2004) .

[219] J. F. Adams and S. Priddy, "Uniqueness of BSO," in *Mathematical Proceedings of the Cambridge Philosophical Society*, vol. 80, pp. 475–509, Cambridge University Press. 1976.

[220] K. Gomi and G. C. Thiang, "Crystallographic T-duality," arXiv:1806.11385 [hep-th].

[221] E. Witten, "D-branes and K theory," *JHEP* **12** (1998) 019, arXiv:hep-th/9810188 [hep-th].

[222] M. F. Atiyah and G. B. Segal, "The Index of Elliptic Operators: II," *Annals of Mathematics* **87** no. 3, (1968) 531–545. http://www.jstor.org/stable/1970716.

[223] J. Distler, D. S. Freed, and G. W. Moore, "Orientifold Precis," arXiv:0906.0795 [hep-th].

[224] G. W. Moore, "Quantum symmetries and K-theory." http://www.physics.rutgers.edu/~gmoore/PiTP-LecturesA.pdf, 2015.

[225] R. Emparan, C. V. Johnson, and R. C. Myers, "Surface terms as counterterms in the AdS / CFT correspondence," *Phys. Rev.* **D60** (1999) 104001, arXiv:hep-th/9903238 [hep-th].

[226] T. Chatterji, *Neutron Scattering from Magnetic Materials*. Elsevier Science, 2005. https://books.google.com/books?id=ehBFD7mWCs8C.

[227] E. Wigner, "Ueber die Operation der Zeitumkehr in der Quantenmechanik," *Nachrichten von der Gesellschaft der Wissenschaften zu Göttingen, Mathematisch-Physikalische Klasse* **1932** (1932) 546–559. http://eudml.org/doc/59401.

[228] S. Weinberg, *The Quantum Theory of Fields*, vol. 1. Cambridge University Press, 1995.

[229] H. Kramers *Proc. of Koninklijke Akademie van Wetenschappen* (1930) 959–972.

[230] H. Watanabe, H. C. Po, and A. Vishwanath, "Structure and topology of band structures in the 1651 magnetic space groups," *Science Advances* **4** no. 8, (2018) , http://advances.sciencemag.org/content/4/8/eaat8685.full.pdf. http://advances.sciencemag.org/content/4/8/eaat8685.

[231] C. Herring, "Effect of Time-Reversal Symmetry on Energy Bands of Crystals," *Phys. Rev.* **52** (Aug, 1937) 361–365. https://link.aps.org/doi/10.1103/PhysRev.52.361.

[232] P. Hořava, "Stability of Fermi Surfaces and K Theory," *Phys. Rev. Lett.* **95** (Jun, 2005) 016405. http://link.aps.org/doi/10.1103/PhysRevLett.95.016405.

[233] M. Karoubi, *K-theory: An introduction*. Springer-Verlag Berlin Heidelberg New York, 1978.

[234] G. Segal, "Equivariant K-theory," *Publications Mathématiques de l'IHÉS* **34** (1968) 129–151.

[235] E. Park, *Complex Topological K-Theory*. Cambridge University Press, Cambridge, 2008.

[236] F. Hirzebruch and T. Höfer, "On the Euler number of an orbifold," *Mathematische Annalen* **286** no. 1, (1990) 255–260. http://dx.doi.org/10.1007/BF01453575.

[237] X.-L. Qi, T. L. Hughes, and S.-C. Zhang, "Topological field theory of time-reversal invariant insulators," *Phys. Rev. B* **78** (Nov, 2008) 195424. http://link.aps.org/doi/10.1103/PhysRevB.78.195424.

[238] M. F. Atiyah, R. Bott, and A. Shapiro, "Clifford modules," *Topology* **3** (1964) 3–38.

[239] M. F. Atiyah and G. B. Segal, "Equivariant K-theory and completion," *J. Differential Geometry* **3** no. 1-18, (1969) 9.

[240] P. Donovan and M. Karoubi, "Graded Brauer groups and K-theory with local coefficients," *Publications Mathématiques de l'Institut des Hautes Études Scientifiques* **38** no. 1, (1970) 5–25.

[241] P. J. Hilton, *General cohomology theory and K-theory*, vol. 1. Cambridge University Press, 1971.

[242] S. Ryu and T. Takayanagi, "Topological Insulators and Superconductors from String Theory," *Phys. Rev.* **D82** (2010) 086014, arXiv:1007.4234 [hep-th].

[243] T. Morimoto, A. Furusaki, and C. Mudry, "Breakdown of the topological classification $\mathbb{Z}$ for gapped phases of noninteracting fermions by quartic interactions," *Phys. Rev.* **B92** no. 12, (2015) 125104, arXiv:1505.06341 [cond-mat.str-el].

[244] O. Bergman, N. Jokela, G. Lifschytz, and M. Lippert, "Quantum Hall Effect in a Holographic Model," *JHEP* **10** (2010) 063, arXiv:1003.4965 [hep-th].

[245] J. Polchinski, "Dirichlet Branes and Ramond-Ramond Charges," *Phys. Rev. Lett.* **75** (Dec, 1995) 4724–4727. https://link.aps.org/doi/10.1103/PhysRevLett.75.4724.

[246] D. Anninos and D. M. Hofman, "Infrared Realization of dS_2 in AdS_2," *Class. Quant. Grav.* **35** no. 8, (2018) 085003, arXiv:1703.04622 [hep-th].

[247] V. Gorbenko, E. Silverstein, and G. Torroba, "dS/dS and $T\bar{T}$," *JHEP* **03** (2019) 085, arXiv:1811.07965 [hep-th].

[248] J. de Boer and S. N. Solodukhin, "A Holographic reduction of Minkowski

space-time," *Nucl. Phys.* **B665** (2003) 545–593, arXiv:hep-th/0303006 [hep-th].

[249] B. Freivogel, Y. Sekino, L. Susskind, and C.-P. Yeh, "A Holographic framework for eternal inflation," *Phys. Rev.* **D74** (2006) 086003, arXiv:hep-th/0606204 [hep-th].

Samenvatting

Onderzoek in de theoretische natuurkunde kun je je voorstellen als een groot magisch kasteel. Er is een stevig fundament, gevormd door allerlei wetten en principes in de natuurkunde, zoals die van Newton of de stromingsleer. Door de jaren heen zijn die wetten niet een alleen maar een steviger fundament geworden, ze zijn ook gemoderniseerd. Bijvoorbeeld, door de komst van de kwantummechanica en de algemene relativiteitstheorie van Einstein.

Op het fundament zijn ook verschillende kamers gebouwd. Deze kamers stellen verder onderzoek in een bepaalde richting voor, zoals de studie naar zwarte gaten of de geleidingseigenschappen van exotische materialen. Soms bevinden zich er ook deuren in deze kamers, die leiden naar andere onderzoeksvelden en zo een aaneengesloten web van kennis vormen. In de theoretische natuurkunde zijn deze deuren zeer waardevol en zorgen vaak voor interessante en nieuwe inzichten. De snaartheorie (één van de hipste theorieën van dit moment) werd bijvoorbeeld gevonden door onderzoeken naar een andere theorie, namelijk de theorie die nu in Genève bij het CERN getest wordt. Het openen van die deuren kan dus een volledig nieuw onderzoeksgebied tot gevolg hebben en kan een volledig nieuwe zijvleugel aan het gebouw der theoretische fysica betekenen.

Kwantumzwaartekracht

Een erg belangrijke en praktisch volledig onontgonnen zijvleugel is eentje die je zowel vanuit de zwaartekracht kamer als de kwantummechanica kamer binnen kunt gaan. Deze zijvleugel is een symbiose van twee zeer succesvolle theorieën, namelijk die van het allerkleintste (kwantummechanica) en het allergrootste (zwaartekracht). We noemen dit onderzoeksgebied dan ook wel de kwantumzwaartekracht.

In de kwantumzwaartekracht is men bezig met het begrijpen van de kwantummechanische structuur van zwaartekracht. Dit betekent dat men de fundamentele bouwstenen probeert te vinden van de ruimtetijd waarin we nu leven. Een mooi voorbeeld van een belangrijk vraagstuk in de kwantumzwaartekracht is die over de structuur van zwarte gaten. Zwarte gaten zijn exotische objecten in ons universum, die zo zwaar zijn dat zelfs licht niet aan ze kan ontsnappen (vandaar ook de naam). Recentelijk is er een prachtige foto van zo'n zwart gat gemaakt, waar we veel van kunnen leren en dat is nodig, want we weten eigenlijk niet zo veel over zwarte gaten. Wat we wel weten is bijvoorbeeld dat zwarte gaten een bepaalde temperatuur hebben en uit een groot aantal fundamentele bouwstenen opgebouwd moet zijn, maar wat die bouwstenen precies zijn en wat er aan de binnenkant van zo'n zwart gat gebeurt, is nog een groot raadsel.

Het vraagstuk over zwarte gaten is slechts een van vele vraagstukken in de kwantumzwaartekracht waar wetenschappers zich nu al meer dan een halve eeuw het hoofd over breken. Dit is niet omdat we niet slim genoeg zijn, maar omdat het gewoon heel erg moeilijk is. Er zijn nog geen concrete experimenten gedaan, waardoor de theoretisch fysicus geen helpende hand heeft, zoals bijna altijd wel het geval was in het verleden. Onderzoek in de kwantumzwaartekracht is daarom voornamelijk van theoretische aard en gaat uit van een aantal basis principes om een voorspelling te kunnen doen over wat zo'n theorie van kwantumzwaartekracht precies zou kunnen zijn.

Één mogelijke theorie van kwantumzwaartekracht die sinds de jaren 70 is voorgesteld is de snaartheorie. De snaartheorie is een theorie die succesvol de theorie van het allerkleinste (de kwantummechanica) en de theorie van het allergrootste (zwaartekracht, de algemene relativiteitstheorie van Einstein) samenvoegt. Dit is een ingewikkelde theorie, waar op dit moment veel onderzoek naar wordt verricht en waar veel lessen over kwantumzwaartekracht uit getrokken worden. Een van de belangrijkste lessen die we geleerd hebben in de afgelopen 20 jaar is dat kwantumzwaartekracht zich het beste laat beschrijven door een hologram.

Dit klinkt natuurlijk best wel vreemd en dat is het ook. Je kunt je afvragen waarom zou kwantumzwaartekracht zich op die manier laten beschrijven. Een hologram is een tweedimensionale voorstelling van iets in drie dimensies en dus mis je dan niet informatie om de volledig driedimensionale ruimte te reconstrueren? Dit zijn allemaal valide vragen, en een volledig antwoord is er nog niet. Het is inmiddels echter al wel duidelijk dat het hologram geen informatie mist, maar het op een ingewikkelde en speciale manier verpakt en daarvoor speciale eigenschappen moet hebben.

Een paar van die speciale eigenschappen zijn onderzocht in dit proefschrift. In

het bijzonder is er een heel basale vereiste van het hologram onderzocht, namelijk de eis dat de wetten van Newton of de algemene relativiteitstheorie van Einstein gereconstrueerd kunnen worden. Hieruit is gebleken dat de hologrammen nog specialer en ingewikkelder moeten zijn dan we al dachten. Dit is eigenlijk het gevolg van het verpakken van iets driedimensionaals in iets tweedimensionaals, maar reflecteert ook hoe ingewikkeld en rijk kwantumzwaartekracht is.

Met dit onderzoek zijn we een klein stapje dichterbij een beter begrip van kwantumzwaartekracht gekomen, maar er is nog veel onderzoek nodig om het hologram in zijn volledigheid te begrijpen. Een ding is zeker, er staat ons nog veel prachtige en verbazingwekkende natuurkunde te wachten in onze ontdekkingsreis door de kamer van de kwantumzwaartekracht.

Topologische fasen

Ondertussen zijn wetenschappers ook begonnen aan een ontdekkingsreis door een heel ander deel van het kasteel. In dit deel van het kasteel bevinden zich de kamers die te maken hebben met materialen en hun eigenschappen, zoals hoe ze een elektrisch stroompje kunnen geleiden. Een zeer rijke kamer in dit deel van het kasteel is de kamer over topologische fasen.

Topologische fase (een fase is een bepaalde toestand waarin een materiaal zich kan bevinden, zoals water in de vorm van ijs of waterdamp) zijn fasen van exotische materialen die buitengewone geleidingseigenschappen hebben. In gewone materialen gaat het elektrisch stroompje door de binnenkant van het materiaal, maar dit is niet zo voor topologische fasen. In deze materialen gaat het stroompje alléén via de buitenkant. Het zijn dus niet zulke goede geleiders, zoals bijvoorbeeld koper of goud, maar wat ze geleiden doen ze op een subtiele en elegante manier.

Dit is niet het enige bijzondere aan topologische fasen. Topologische fase geleiden een stroompje namelijk alleen op een stapsgewijze manier. Hiermee bedoelen we dat de mate van geleiding alleen maar aangeven kan worden met een geheel getal, zoals 3 of 27 (maar negatieve gehele getallen, want dan gaat het stroompje de andere kant op). Eigenlijk is het een beetje alsof je de geleiding een cijfer geeft om aan te geven hoe goed die geleiding is en daarvoor alleen maar gehele getallen, die niet perse tussen 0 en 10 liggen, mag gebruiken. Deze stapsgewijze geleiding wordt ook wel een gekwantiseerde geleiding genoemd.

Een gekwantiseerde geleiding is natuurlijk iets heel bijzonders, omdat normaal gesproken de geleiding elke mogelijke waarde aannemen. Er moet dus een speciaal mechanisme aanwezig zijn in het materiaal wat hiervoor kan zorgen en andere waarden dan gehele getallen verbiedt. Het blijkt dat dat mechanisme te maken

heeft met een verborgen eigenschap van een topologische fase.

Om dit te begrijpen moeten we eerst uitleggen wat *topologie* nu precies betekent. Kort gezegd betekent topologie de robuste vorm van een object. Bijvoorbeeld, een mandarijn is bolvormig en heeft geen gaten. We zeggen dan dat de mandarijn de topologie van een bol heeft. Met robust bedoelen we dan dat als je de mandarijn zachtjes indrukt, de bolvormigheid niet verandert. Druk je te hard, dan vervorm je de mandarijn zodanig dat ie scheurt of er gaten in komen. Je hebt dan de topologie van de mandarijn veranderd. Zit er na het drukken bijvoorbeeld een enkel gat in, dan lijkt de mandarijn meer op een donut dan iets bolvormigs. Een donut heeft dan ook een andere topologie. In het algemeen kun je door het tellen van het aantal gaten er achter komen met welke topologie je te maken hebt. Geen gaten is de topologie van een bol, één gat die van een donut en bijvoorbeeld drie gaten die van een krakeling. Dit is natuurlijk een versimpeling van hoe we er als natuurkundigen tegen aan kijken, maar bevat wel de essentie van wat topologie is.

Topologie betekent dus een soort van stapsgewijsheid; alleen gehele getallen bepalen de topologie. Dit lijkt heel veel op de stapsgewijze geleiding in topologische fasen waar we het eerder over hadden. Het blijkt dat deze twee stapsgewijsheden aan elkaar gerelateerd zijn en in het bijzonder dat er een verborgen topologie is die de stapsgewijsheid van de geleiding kan verklaren. Bovendien verklaart het ook waarom de geleiding zo robust is, want daarvoor moet je de topologie veranderen en dat gaat niet zo eenvoudig. Dit verband tussen topologie en geleiding werd begin jaren 80 gevonden door de vier wetenschappers Thouless, Kohmoto, Nightingale en den Nijs en heeft aangezet tot een heel nieuwe onderzoeksgebied in de theoretische natuurkunde.

Inmiddels is de studie naar topologische fasen uitgegroeid tot een groot onderzoeksgebied, waarin veel interessante en verassende resultaten gevonden zijn. Het mooie aan dit onderzoeksgebied is ook dat, in tegenstelling tot de kwantumzwaartekracht, veel experimenten gedaan zijn. De helpende hand van het experiment was hier dus zeker aanwezig en heeft tot zeer interessant theoretisch onderzoek geleidt.

Een mooi voorbeeld van zo'n theoretisch onderzoek is het tellen van het aantal topologische fasen dat in de natuur aanwezig kan zijn. Dit noemen we ook wel het classificeren van topologische fasen en in feite betekent het dat we alle topologische fasen met dezelfde waarde voor de geleiding bij elkaar groeperen, dus alle topologische fasen met geleidingswaarde 1 gaan in een (denkbeeldig) bakje, alle fasen met geleidingswaarde 2 in een ander bakje, enzovoort. Dit geeft inzicht in welke soorten topologie er zijn en hoe die door andere eigenschappen van het materiaal tevoorschijn kunnen komen.

Het onderzoek in dit proefschrift gaat over het tellen van topologische fasen. Wij hebben laten zien dat deze telling op een heel eenvoudige en intuïtieve manier gedaan kan worden. Aan de hand van een aantal bekende eigenschappen van een materiaal hebben wij laten zien dat je met een paar simpele stappen het aantal mogelijke topologische fasen in dat materiaal kunt bepalen. Voorheen werd dit op een vrij omslachtige en heuristische manier gedaan, maar wij hebben aangetoond dat dit veel simpeler kan. Als gevolg van onze telling hebben we ook een volledig nieuw soort topologie voorspelt, die mogelijk via experimenten gezien zou kunnen worden.

Acknowledgements

Jan, it has been an incredible journey together! As two down-to-earth Dutchmen, I felt we were the perfect match. We worked on many different things together and throughout I learned not only an enormous amount of insights, fascinating physics and mathematics from you, but also about academia in general. Your guidance and advice pushed to greater heights, which started already in 2014, when I did my master project with you. I always enjoyed those moments you would randomly come in the office and talk about some idea you had. I am grateful for all the opportunities and freedom you gave me.

Jasper, I am equally indebted to you. You guided me throughout and showed me how I should manoeuvre through the condensed matter community. I had a wonderful time when we were thinking about the classification of topological insulators. Thank you for sharing your profound insights and the freedom and opportunities you gave me.

Diego, the way you think about physics inspires me a lot. Thank you for your guidance and teaching me all those insights from which I hope to get some more in the future.

Dionysios, the enthusiasm you have when talking about physics is so contagious that it motivated me to think about the big questions in physics in a different and exciting way.

This dissertation would not be possible without all the fantastic collaborators I worked with. Thank you, Robert-Jan, Charles, Amir, Tom, Luuk, Hessel, Milind and Ben. I am especially indebted to Alex and Edgar. Alex, bro, I will never forget those nights at the UvA when we were working on my first physics project. Thank you for everything you taught me and your advice on many things. Edgar, I had a lot of fun working with you. You pushed me further as a scientist. I learned a great deal of physics from you and I am glad you always listened to my random ideas.

Gerben, Lars, Manus, Jaco and Vincent, it meant a lot for me to being able to discuss physics or things in live with you. It was and is a lot more fun with you guys. I would also like to thank Jan-Pieter, Erik, Alejandra, Vladimir, Miranda, Jay, Sagar, Greg, Antonio, Evita, Beatrix, Eva, Fernando, Daniel, Fotis, Diego, Irfan, Laurens, Nabil, Jans and Ana for the discussions, advice and fun times at the theory corridor.

Feike, Frank, Janna, Fenna, Guido, Willem, Stefanie and Bram, you were always there for me when I needed that distraction the most. I loved being together with you guys, either when cooking and drinking together or just when discussing things in live. I will never forget those nights at the Buurvrouw, where we would always go for *een kleintje met de jas aan*. I am sure we will have plenty more of those nights, but can we please stop playing *toepen*?

Gerben, Nick and Pieter, our time at the KNSM-Laan was simply fantastic. It was always nice to come home and relax with you guys. *En dóóór*.

I would also like to thank my cousin Coen. You always made sure I wasn't forgetting about my *beun* mentality. Welding the sous vide apparatus at ROC Twente was simply fantastic!

Willem Vos and Jeroen Spandaw, you have been there since the beginning and sparked my interest in (theoretical) physics. Thank you for all those times we spent together and the advice you gave.

José, Richard and Julia, you have always been there for me. Thank you for your unwavering support and helping with whatever I wanted to do.

Nahima, my love. I know you are getting sick of all those late night Skype calls, but in Stanford we won't have that problem anymore. By the time I defend this dissertation, we will be married and I can't wait to spend the rest of my live with you.